



**HAL**  
open science

# Analysis of the Dynamics of Metabolic Shifts in *Yarrowia lipolytica*

Rana Sagnak

► **To cite this version:**

Rana Sagnak. Analysis of the Dynamics of Metabolic Shifts in *Yarrowia lipolytica*. Biochemistry [q-bio.BM]. INSA de Toulouse, 2019. English. NNT : 2019ISAT0041 . tel-03523281

**HAL Id: tel-03523281**

**<https://theses.hal.science/tel-03523281>**

Submitted on 12 Jan 2022

**HAL** is a multi-disciplinary open access archive for the deposit and dissemination of scientific research documents, whether they are published or not. The documents may come from teaching and research institutions in France or abroad, or from public or private research centers.

L'archive ouverte pluridisciplinaire **HAL**, est destinée au dépôt et à la diffusion de documents scientifiques de niveau recherche, publiés ou non, émanant des établissements d'enseignement et de recherche français ou étrangers, des laboratoires publics ou privés.



# THÈSE

En vue de l'obtention du

## DOCTORAT DE L'UNIVERSITÉ DE TOULOUSE

Délivré par :

Institut National des Sciences Appliquées de Toulouse (INSA de Toulouse)

---

**Présentée et soutenue par :**

**Rana SAGNAK**

**le** lundi 18 novembre 2019

**Titre :**

Analyse des dynamiques des bascules métaboliques chez *Yarrowia lipolytica*

---

**École doctorale et discipline ou spécialité :**

ED SEVAB : Ingénieries microbienne et enzymatique

**Unité de recherche :**

TBI - Toulouse Biotechnology Institute, Bio & Chemical Engineering

**Directeur/trice(s) de Thèse :**

Stéphane GUILLOUET et Carole MOLINA-JOUVE

**Jury :**

Mme Elke NEVOIGT, Rapporteur

M. Pau FERRER, Rapporteur

Mme Caroline REMOND, Examinatrice

Mme Florence BORDES, Examinatrice

M. Stéphane GUILLOUET, Directeur de thèse

Mme Carole MOLINA-JOUVE, Directrice de thèse



**Nom:** SAGNAK

**Prénom:** Rana

**Titre:** Analyse des dynamiques des bascules métaboliques chez *Yarrowia lipolytica*

**Année:** 2019

**Lieu:** INSA Toulouse

---

## Résumé

La demande en composés lipidiques est en forte croissance avec de nombreuses applications industrielles en chimie, santé et biocarburants ; de nouvelles ressources en lipides sont aujourd'hui indispensables en intégrant des systèmes de production aux impacts environnementaux réduits. La voie microbienne répond à ces exigences. Ces travaux de recherche se focalisent sur l'amélioration du contenu lipidique et la modification du profil des acides gras d'une levure oléagineuse *Yarrowia lipolytica* selon des approches d'ingénierie biochimique et métabolique. La stratégie expérimentale est basée sur la modulation des flux de carbone en amont et en aval de la voie de synthèse des acides gras (AG), et examine les réponses de la levure *Y. lipolytica* à ces modulations en termes d'accumulation de lipides, de profil des acides gras, et de formation de co-métabolites (acide citrique). Le comportement dynamique d'une souche mutante de *Y. lipolytica* JMY3501, favorisant l'orientation du flux de carbone vers la synthèse de triacylglycérol (TAG) et inactivée par la mobilisation et la dégradation de TAG, a été caractérisé ; la modulation du shift du métabolisme oxydatif à l'accumulation de lipides et la production d'acide citrique sur glucose, en absence et en présence d'inhibiteurs du système d'enzyme acide synthase (FAS) ont été quantifiées. Les résultats ont montré que le métabolisme des lipides et la formation de produits de la souche *Y. lipolytica* JMY3501 peuvent être altérés de manière significative en ciblant l'activité de l'enzyme FAS. Indépendamment du domaine catalytique de ce système enzymatique (étapes initiales ou de terminaison), lors des ajouts séquencés de composés inhibiteurs, le profil des acides gras a été modifié et l'accumulation d'acides gras à chaîne courte et moyenne a été favorisée sans affecter la survie cellulaire. Il a également été révélé que des ajouts d'inhibiteur contrôlant les flux de carbone de la voie de synthèse des acides gras peuvent affecter les caractéristiques morphologiques des cellules de levure d'une manière dépendante de la dose. Enfin, la souche mutante de *Y. lipolytica* CR62 présentant une mutation sur le domaine KS de FAS, a permis l'obtention d'une amélioration significative de la production d'acides gras de longueur de chaîne moyenne. Cette souche a accumulé jusqu'à 16 % d'acide gras à 14 atomes de carbone. Ce travail de recherche a démontré que la levure oléagineuse *Y. lipolytica* offre de nouvelles opportunités pour la production d'acides gras spécifiques lorsque les ingénieries biochimiques et métaboliques combinent.

---

**Mots clés :** *Yarrowia lipolytica*, fermentation, bascule métabolique, lipide, acide citrique

## Abstract

The demand for lipid compounds is growing rapidly with many industrial applications in chemistry, health and biofuels; new lipid resources are now essential by integrating production systems with reduced environmental impacts. The microbial route meets these requirements. This research focuses on the enhancement of lipid content and modification of fatty acid profile of an oleaginous yeast *Yarrowia lipolytica* together with biochemical and metabolic engineering strategies. The experimental strategy was based on the directed modulation of the carbon fluxes up- and down-ward of the fatty acid (FA) synthesis pathway and investigating the responses of the yeast *Y. lipolytica* to these modulations in terms of lipid accumulation, FA profile and formation of co-metabolites (citric acid). The dynamic behavior of a mutant strain of *Y. lipolytica* JMY3501 which has the ability to pull the carbon flow into triacylglycerol (TAG) synthesis and inactivated for the TAG mobilization and degradation, was characterized for the modulation of the metabolic shift from oxidative metabolism to lipid accumulation and citric acid production on glucose, and further pulsed with known inhibitors of fatty acid synthase enzyme system (FAS). The results showed that lipid metabolism and product formation of *Y. lipolytica* JMY3501 engineered strain was significantly altered by the targeted FAS enzyme activity. Regardless on the catalytic domain of this enzyme system (initial or termination steps) inhibitor pulses modified the FA profile and favored the accumulation of short and medium chain length fatty acids without affecting cell survival. However, dependent on the catalytic domain, the inhibitor pulses controlled the carbon fluxes of up- and down-ward of the FA synthesis pathway; and affected the morphological features of the yeast cells in dose-dependent manner. Finally, we demonstrated in a mutant strain of *Y. lipolytica* CR62, which has been engineered in the KS domain of the FAS, a significant increase in the amount of medium chain length fatty acids. The strain accumulated up to 16 % of C14 fatty acid. This research demonstrated that oleaginous yeast *Y. lipolytica* with combined engineering efforts presented novel opportunities for the production of designed and/or high value fatty acids.

---

**Key words:** *Yarrowia lipolytica*, fermentation, metabolic shift, lipid, citric acid

## ACKNOWLEDGEMENTS

*This thesis was supported by a doctoral fellowship granted through the project ProBio3 “Biocatalytic production of lipidic bioproducts from renewable resources and industrial by-products: BioJet Fuel Application” sponsored by French National Institute for Agricultural Research, INRA.*

*This thesis research was carried out in the Processes and Biological Systems Engineering Laboratory (Laboratoire d’Ingénierie des Systèmes Biologiques et des Procédés) LISBP, in Institut National des Sciences Appliquées, INSA Toulouse. Therefore, I would like to thank the director of LISBP Prof. MOLINA-JOUVE for having me welcomed in her laboratory and I also would like to thank to SEVAB (Sciences Ecologiques, Vétérinaires, Agronomiques et Bioingénieries) doctoral school director Prof. MARANGES.*

*I would like to extend my sincere gratitude to my supervisor Prof. Stéphane GUILLOUET for his inspiration, expertise and enthusiasm. His mission for producing high-quality work and dedicated help kept me constantly engaged with my research and has enabled me to complete the task.*

*I would like to extend my sincere gratitude to my supervisor Prof. Carole MOLINA-JOUVE for her advice, constructive comments and extended discussions. Her kindness and support have always kept me going ahead.*

*This work would not have been possible without their continuous encouragement, patience and motivation, their suggestion and immense knowledge on this interesting topic. Their constant guidance helped me all the time of my research and writing of this thesis. I am deeply grateful for the freedom and support that has been granted to me in all my work, and for their trust in me and the successful completion of this dissertation. It was a great pleasure and honor working with them.*

*I would like to thank to Dr. France THEVENIEAU who gave me much valuable advice in the early stages of this research and Dr. Jean-Marc NICAUD all for his valuable suggestions and discussions during my thesis committee meetings.*

*These acknowledgments would not be complete without expressing my gratitude to all the members of the Fermentation Advances and Microbial Engineering (FAME) team.*

*I am immensely grateful to Dr. Nathalie GORRET for the opportunity to learn a new and unique skill, that of flow cytometry. I greatly appreciated for her invested time, hearth warming support, providing interesting and valuable feedback.*

*I thank to Xavier CAMELEYRE and Eric LOMBARD for their technical advices, suggestions and for their availability during my experiments set up and/or run.*

*I would like thank to following people for their technical support and all their answers to my questions in English. I thank to Florence LERAY for the development of my analytical protocols, her engineering skills and all the help during my analysis. I thank to Julie LESAGE for her unlimited help and I thank to Sandrine COCHOT and Marine CAYUELA for their technical supports during my experimental work. I thank to Philippe COPILLET for his cooperation and for lab material logistics.*

*My deep appreciation goes to all my research lab colleagues' and I would like to thank each and every one of them. It was fantastic to have the opportunity to work with all of you: Arnaud, Alexis, Asma, Aurore C., Aurore M., Carlos, Céline, Chainese, Cuong, Damien, Estelle, Elodie B., Elodie G., Florence, Hazar, Jan, Jillian, Julie B., Julie M., Lannig, Lucie, Marine C., Marine D., Maud, Mégane, Melodie, Nicolas, Olivier, Ulysse, Rafael, Tuan, Sandrine, Sandy, Susana, Xiaomin, and Yannick.*

*It was also a great sharing in or outside of the laboratory with my lab mates during my studies: Agustina, Ceren, Cléa, Claudio, Debora, Ines, Jian, JJ, Luce, Maja, Marion, Ran and Rosie.*

*I would like to thank to Dr. Micheal O'Donohue for introducing me to this exciting field of science.*

*My heartfelt regard and thanks goes to my lovely parents, to my brothers, to my sister in laws and my friends for their love, encouragement and unconditional support that they extended to me during my studies.*

*A special thank due to Yannick, who has given me all the encouragement, love, moral support that I needed in every step of my studies throughout these challenging years.*

*Thank you!*

## Table of Contents

<b>Résumé .....</b>	<b>ii</b>
<b>Abstract.....</b>	<b>iii</b>
<b>ACKNOWLEDGEMENTS.....</b>	<b>iv</b>
<b>Figures.....</b>	<b>x</b>
<b>Tables .....</b>	<b>xii</b>
<b>Abbreviations.....</b>	<b>xiii</b>
<b>INTRODUCTION.....</b>	<b>2</b>
<b>CHAPTER 1. STATE-OF-THE-ART .....</b>	<b>4</b>
<b>1.1. Oleaginous Microorganisms.....</b>	<b>4</b>
1.1.1. Oleaginous Yeast.....	5
1.1.1.1. Oleaginous yeast of major interest: <i>Yarrowia lipolytica</i> .....	5
<b>1.2. Classification of Fatty Acids Based on Their Chain Length.....</b>	<b>6</b>
<b>1.3. Lipid Metabolism in Yeast.....</b>	<b>7</b>
1.3.1. Lipid Synthesis and Citrate Metabolism: General Considerations .....	7
1.3.2. Intracellular Lipid Accumulation.....	9
1.3.2.1. <i>De novo</i> Lipid Synthesis .....	10
1.3.2.1.1. Fatty Acid Synthesis .....	10
1.3.2.1.2. Triacylglycerol Synthesis.....	12
1.3.2.2. <i>Ex-novo</i> Lipid Synthesis .....	14
<b>1.4. Key Enzymes of Intermediary Metabolisms.....</b>	<b>14</b>
1.4.1. NAD <sup>+</sup> -dependent: Isocitrate Dehydrogenase .....	14
1.4.2. Malic Enzyme .....	15
1.4.3. Malate Dehydrogenase.....	17
1.4.4. ATP Citrate Lyase .....	18
1.4.5. Acetyl-CoA Carboxylase .....	20
<b>1.5. Fatty Acid Synthase Enzyme System .....</b>	<b>22</b>
1.5.1. Fatty Acid Synthase inhibitions with small molecules .....	25

1.5.1.1. Triclosan .....	26
1.5.1.2. Orlistat .....	26
1.5.1.3. Cerulenin .....	27
<b>1.6. Conclusion .....</b>	<b>29</b>
<b>CHAPTER 2. MATERIALS &amp; METHODS .....</b>	<b>30</b>
<b>2.1. Microorganisms .....</b>	<b>30</b>
2.1.1. Cryopreservation of the strains .....	30
<b>2.2. Media and Growth Conditions.....</b>	<b>31</b>
2.2.1. Medium compositions for shake flask cultures .....	31
2.2.2. Medium composition of initial fed-batch cultures .....	32
<b>2.3. Pre-Cultures .....</b>	<b>32</b>
2.3.1. Preparation of working plates.....	32
2.3.2. Preparation of inoculums .....	32
<b>2.4. Bioreactor.....</b>	<b>33</b>
2.4.1. General description of bioreactor.....	33
2.4.2. Culture design and strategy .....	35
<b>2.5. Inhibitory Molecules.....</b>	<b>36</b>
<b>2.6. Analytical Methods.....</b>	<b>37</b>
2.6.1. Determination of biomass concentration .....	37
2.6.2. Determination of extracellular metabolites .....	37
2.6.2.1. Determination of glucose concentration by YSI .....	38
2.6.2.2. Determination of organic acids and glucose concentrations by HPLC.....	38
2.6.2.3. Determination of ammonium ion concentration .....	39
2.6.3. Determination of intracellular metabolites .....	40
2.6.3.1. Extraction and quantification of total lipid content .....	40
2.6.3.2. Identification and quantification of lipid content and composition .....	41
2.6.3.3. Calculations of lipid accumulation and fatty acid profile .....	43
2.6.3.4. Observation of lipid accumulation.....	44
2.6.4. Cell viability and cell morphology assessments by flow cytometer .....	45
<b>2.7. Data Treatment.....</b>	<b>47</b>
2.7.1. Mass balances for a state variable A for batch cultures .....	47

2.7.2. Mass balances for a state variable <i>A</i> for fed-batch cultures .....	48
2.7.3. Data Smoothing .....	49
2.7.4. Gas analysis .....	49
2.7.5. Ratio of N/C .....	50
<b>CHAPTER 3. RESULTS AND DISCUSSIONS.....</b>	<b>51</b>
<b>3.1. Screening Strategy of Inhibitory Molecules.....</b>	<b>51</b>
3.1.1. Impact of different solvent usage .....	51
3.1.2. Preliminary screening with triclosan as a model inhibitory molecule .....	55
3.1.2.1. Triclosan dissolved in Dimethyl Sulfoxide .....	55
3.1.2.2. Triclosan dissolved in Ethanol .....	59
3.1.3. Conclusions.....	65
<b>3.2. Strain Characterization of <i>Yarrowia lipolytica</i>.....</b>	<b>66</b>
3.2.1. Modulation of the metabolic shift from oxidative metabolism to lipid accumulation and citric acid production in <i>Yarrowia lipolytica</i> .....	66
3.2.2. Fed-batch culture of <i>Y. lipolytica</i> JMY3501 under nitrogen limitation with solvent pulses .....	83
3.2.3. Conclusions.....	88
<b>3.3. Fed-batch cultures of <i>Yarrowia lipolytica</i> under nitrogen limitation with cerulenin pulses.....</b>	<b>89</b>
3.3.1. Fed-batch culture of <i>Yarrowia lipolytica</i> JMY3501 under nitrogen limitation with cerulenin pulses .....	89
3.3.1.1. Fed-batch culture of <i>Yarrowia lipolytica</i> JMY3501 under nitrogen limitation with high dosage of cerulenin pulses .....	90
3.3.1.2. Fed-batch culture of <i>Yarrowia lipolytica</i> JMY3501 under nitrogen limitation with middle dosage of cerulenin pulses .....	93
3.3.1.3. A single cerulenin pulse .....	96
3.3.2. Cell Viability and Morphology .....	114
3.3.2.1. Cell Viability .....	114
3.3.2.1.1. Reference Culture .....	114
3.3.2.1.2. High dosage of cerulenin pulses .....	115
3.3.2.1.3. Middle dosage of cerulenin pulses .....	117

3.3.2.2. Cell Morphology .....	118
<b>3.4. Fed-batch culture of <i>Yarrowia lipolytica</i> JMY3501 under nitrogen limitation with Orlistat .....</b>	<b>121</b>
3.4.1. Orlistat pulses .....	121
3.4.2. Cell Viability and Cell Morphology .....	127
<b>CHAPTER 4. CONCLUSION AND PERSPECTIVES .....</b>	<b>131</b>
<b>CHAPTER 5. REFERENCES .....</b>	<b>136</b>
<b>ANNEX-1. PUBLISHED MANUSCRIPT .....</b>	<b>150</b>
<b>ANNEX-2. RESUME EN FRANÇAIS .....</b>	<b>156</b>

## Figures

Figure 1.1. Overview of the main metabolic pathway of lipid metabolism in <i>Y. lipolytica</i> on glucose as carbon source (Adapted from Tai and Stephanopoulos, 2013). .....	8
Figure 1.2. Fatty Acid Synthesis.....	12
Figure 1.3. TAG synthesis.....	13
Figure 1.4. Type I FAS .....	24
Figure 1.5. Reaction scheme of yeast fatty acid synthesis and specific domain inhibition with small molecules .....	25
Figure 1.6. Structure of triclosan.....	26
Figure 1.7. Structure of orlistat.....	27
Figure 1.8. Structure of cerulenin .....	27
Figure 2.1. General Design for fed-batch cultures .....	34
Figure 2.2. Gas chromatograph of standard FAMES solution .....	42
Figure 2.3. Box plot .....	47
Figure 3.1. Cumulative solvent concentration (M) by number of pulses .....	52
Figure 3.2. The effect of solvent pulses on <i>Yarrowia lipolytica</i> W29.....	53
Figure 3.3. Total Fatty Acid Composition (% w/w) of <i>Y. lipolytica</i> W29 under nitrogen deficiency conditions with and without ethanol pulses .....	54
Figure 3.4. Variation of state variables versus time during triclosan pulses at different concentrations .....	57
Figure 3.5. The composition of Total Fatty Acid % with triclosan pulses .....	58
Figure 3.6. Short and long term triclosan pulse impact on saturated / unsaturated FA ratio.....	59
Figure 3.7. Variation of state variables versus time during triclosan pulses at different concentrations	61
Figure 3.8. Impact of different triclosan pulse ratios (Ethanol) on the Total Fatty Acid %.....	63
Figure 3.9. Short and long term triclosan pulse impact on Saturated / Unsaturated FA ratio .....	64
Figure 3.10. Schematic representation of the strain JMY3501 construction. ....	66
Figure 3.11. Ethanol doses per pulse ( $\text{gEtOH}\cdot\text{g}^{-1}\text{DCW}$ ).....	83
Figure 3.12. Fed-batch culture of <i>Y. lipolytica</i> JMY3501 under nitrogen limitation with solvent pulses. ....	84

Figure 3.13. Impact of solvent pulses on fatty acid composition (% w/w) during lipid accumulation phase for fed-batch cultures of <i>Y. lipolytica</i> JMY3501 under nitrogen limitation. ....	86
Figure 3.14. Specific rates of state variables .....	87
Figure 3.15. Ethanol doses per pulse ( $g_{EtOH} \cdot g^{-1}_{DCW}$ ).....	90
Figure 3.16. Fed-batch culture of <i>Y. lipolytica</i> JMY3501 for fed-batch cultures under nitrogen limitation with high dose of Cerulenin pulses. ....	91
Figure 3.17. Specific rates of state variables .....	92
Figure 3.18. Fed-batch culture of <i>Y. lipolytica</i> JMY3501 for fed-batch cultures under nitrogen limitation with middle dose of Cerulenin pulses.....	94
Figure 3.19. Specific rates of state variables .....	95
Figure 3.20. Cell viability assessment of <i>Y. lipolytica</i> JMY3501 with solvent pulses .....	115
Figure 3.21. Cell viability assessment of <i>Y. lipolytica</i> JMY3501 with high dosage Cerulenin pulses .	116
Figure 3.22. Cell viability assessment of <i>Y. lipolytica</i> JMY3501 with middle dosage cerulenin pulses .....	117
Figure 3.23. Cell size distribution of <i>Y. lipolytica</i> JMY3501 with Cerulenin pulses.....	118
Figure 3.24. Distribution of cell length of <i>Y. lipolytica</i> JMY3501 with Cerulenin pulses.....	119
Figure 3.25. Distribution of cell granularity of <i>Y. lipolytica</i> JMY3501 with Cerulenin pulses.....	120
Figure 3.26. Fed-batch culture of <i>Y. lipolytica</i> JMY3501 for fed-batch cultures under nitrogen limitation with Orlistat pulses. ....	122
Figure 3.27. Specific rates of state variables .....	124
Figure 3.28. Impact of Orlistat pulses on fatty acid composition (% w/w) during lipid accumulation phase for fed-batch cultures of <i>Y. lipolytica</i> JMY3501 under nitrogen limitation. ....	126
Figure 3.29. Cell viability assessment of <i>Y. lipolytica</i> JMY3501 with Orlistat pulses.....	127
Figure 3.30. Distribution of cell size of <i>Y. lipolytica</i> JMY3501 with Orlistat pulses.....	128
Figure 3.31. Distribution of cell length of <i>Y. lipolytica</i> JMY3501 with Orlistat pulses.....	129
Figure 3.32. Distribution of cell granularity of <i>Y. lipolytica</i> JMY3501 with Orlistat pulses .....	130

## Tables

Table 1.1. Lipid content and major fatty acids of oleaginous microorganisms.....	4
<b>Table 1.2.</b> Nomenclature of fatty acids.....	7
<b>Table 1.3.</b> Malic Enzyme.....	16
Table 1.4. ATP Citrate Lyase.....	20
Table 1.5. Acetyl-CoA Carboxylase.....	22
Table 1.6. Genes and Enzymes of Type II Fatty Acid Synthases.....	23
Table 1.7. Genes and Enzymes of Type I Yeast Fatty Acid Synthase.....	24
Table 2.1. YPD medium.....	30
Table 2.2. Medium Composition .....	31
Table 2.3. Trace Elements .....	31
Table 2.4. Vitamins .....	31
Table 2.5. Stock Glucose Solution .....	32
Table 2.6. Mineral Salts .....	32
Table 2.7. Solubility of Inhibitory Molecules .....	37
Table 2.8. Retention time of the target compounds .....	39
Table 2.9. Required equipment and solutions of NH <sub>4</sub> <sup>+</sup> measurements.....	40
Table 2.10. Operating conditions of Gas Chromatograph.....	41
Table 2.11. Oven Temperature Program .....	42
Table 2.12. Proportion of fatty acid profile in the catalytic biomass of <i>Y. lipolytica</i> .....	44
Table 2.13. Parameters of Microscopy.....	45
<b>Table 2.14.</b> Calculations of the volumetric and specific rates of state variables for fed-batch culture..	48
Table 3.1. Triclosan Doses .....	55
Table 3.2. Triclosan Doses .....	60
Table 3.3. Fatty acid composition of <i>Y. lipolytica</i> JMY3501 mutant strain with and without solvent pulses ( <i>n. m. not measured</i> ).....	88
Table 3.4. Comparison of <i>Y. lipolytica</i> JMY3501 mutant strain performances with and without solvent pulses.....	88

## Abbreviations

<b>AC (AT):</b> Ac(et)yltransferase	<b>LPA:</b> Lysophosphatidic acid
<b>ACC:</b> Acetyl-CoA Carboxylase	<b>KR:</b> Ketoacyl Reductase
<b>ACP:</b> Acyl Carrier Protein	<b>KS:</b> Ketoacyl Synthase
<b>ACL:</b> ATP Citrate Lyase	<b>MDH:</b> Malate dehydrogenase
<b>AMP:</b> Adenosine monophosphate	<b>ME:</b> Malic Enzyme
<b>ATP:</b> Adenosine triphosphate	<b>MPT:</b> Malonyl/Palmitoyl-Transacylase
<b>DAG:</b> Diacylglycerol	<b>NAD:</b> Nicotinamide adenine dinucleotide
<b>DCW:</b> Dry cell weight	<b>NADPH:</b> Nicotinamide adenine dinucleotide phosphate
<b>DH:</b> Dehydratase	<b>OAA:</b> Oxaloacetate
<b>DH:</b> $\beta$ -ketoacyl-ACP dehydratase	<b>PA:</b> Phosphatidic acid
<b>DPA:</b> Docosapentaenoic acid	<b>PAP:</b> PA-phosphohydrolase
<b>DHA:</b> Docosahexaenoic acid	<b>PDAT:</b> Phospholipid: DAG acyltransferase
<b>DHAP:</b> Dihydroxyacetone phosphate	<b>PDH:</b> Pyruvate Dehydrogenase
<b>DMSO:</b> Dimethyl sulfoxide	<b>PL:</b> Glycerol phospholipids
<b>EPA:</b> Eicosapentaenoic acid	<b>PPP:</b> Pentose phosphate pathway
<b>ER:</b> Endoplasmic reticulum	<b>PPT:</b> Phosphopantetheine Transferase
<b>EtOH:</b> Ethanol	<b>PUFA:</b> Polyunsaturated fatty acid
<b>FA:</b> Fatty acid	<b>RQ:</b> Respiratory quotient
<b>FAME:</b> Fatty acid methyl esters	<b>SE:</b> Sterol esters
<b>FAS:</b> Fatty acid synthase	<b>SCO:</b> Single Cell Oils
<b>FSC:</b> Forward scatter	<b>SSC:</b> Side scatter
<b>G3P:</b> Glycerol-3-phosphate	<b>TAG:</b> Triacylglycerols
<b>ICDH:</b> Isocitrate dehydrogenase	<b>TCA:</b> Tricarboxylic acid cycle
<b>IMP:</b> Inosine 5'-monophosphate	<b>TFA:</b> Total fatty acid
<b>LB:</b> Lipid bodies	
<b>LD:</b> Lipid droplets	



# INTRODUCTION

---

Fats (solid at room temperature) and oils (liquid at room temperature) are mainly composed of triacylglycerol which consists of three long-chain fatty acids esterified to glycerol molecule. Fatty acids and their derivatives are molecules that are of major interest in many industrial sectors such as food, pharmaceutical, oleochemical and biofuels. Apart from animal and plant derived origin of these molecules (Metzger and Bornscheuer, 2006), microbial production has been the focus of current research efforts in the academic and private sector due to growing markets demand on low-cost, environmentally friendly, sustainable and high-quality alternatives.

The production of fats and oils with microorganisms for industrial and nutritional applications has several advantages compared to mechanical and chemical production from edible and non-edible sources such as palm, soybean, physic nut, castor, rapeseed *etc.* They are not competitive with food, require much smaller area for production, are easy to scale up and independent from seasonal and climate conditions as well (Sawangkeaw and Ngamprasertsith, 2013; Thevenieau and Nicaud, 2013).

*Yarrowia lipolytica*, with special physiological features and the acceptance of its generally recognized as safe status, is an excellent example of a microorganism with multiple biotechnological applications (Bankar et al., 2009; Gonçalves et al., 2013; Harzevili, 2014; Liu et al., 2015).

Moreover, thanks to the development of various molecular and genetic tools (Barth and Gaillardin, 1997; Madzak, 2018), *Y. lipolytica* is recognized as a model organism for numerous academic studies such as degradation of hydrocarbons (Fickers et al., 2005a; Thevenieau et al., 2007), secretion of proteins (proteases, lipases) (Fickers et al., 2011; Madzak, 2015; Madzak C., 2013; Vandermies and Fickers, 2019), secretion of organic acids (isocitric, a-ketoglutaric, citric acid) (Moeller et al., 2007; Papanikolaou et al., 2002), stress response and dimorphism (Morales-Vargas et al., 2012; Ruiz-Herrera and Sentandreu, 2002; Shi et al., 2017; Timoumi et al., 2018).

Furthermore, *Y. lipolytica* is considered advantageous host for the development of platforms to produce lipid-based chemicals due to its capability to synthesize and accumulate lipids more than 20 % of its dry cell weight (Beopoulos et al., 2009a; Carsanba et al., 2018; Xie, 2017).

In this context, these works focused on the study of lipid metabolism of *Y. lipolytica* aiming to answer whether the dynamics of metabolic carbon fluxes up and down-ward of the fatty acid synthesis pathway control the metabolic shift of the lipid metabolism and to what extent lipid accumulation, fatty acid composition and citric acid formation are impacted.

To achieve this aim, the strategy is developed for the modulation of specific enzymes involved in the lipid metabolism by using specific inhibitors at moderate concentration. The idea behind in this strategy is to identify what are the genetic targets or the key enzymes that should be targeted in order to construct a mutant strain potentially leading to the accumulation of short chain length fatty acids.

In this regard, this document has been organized in the following way.

The first chapter dedicated to the lipid metabolism of oleaginous yeast *Y. lipolytica* focuses particularly to the *de novo* fatty acid synthesis pathway. The research efforts are presented to improve lipid production of oleaginous yeasts including gene over-expressions and deletions of key enzymes that draw the carbon flux from central carbon metabolism towards fatty acid synthesis. Moreover, for the synthesis of fatty acids an essential enzymatic complex the fatty acid synthase (FAS) and its known inhibitors of this enzyme system are reviewed.

The experimental strategy is developed based on the directed modulation of the carbon fluxes up- and down-ward of the FA synthesis pathway through biochemical engineering and metabolic engineering approaches. The second chapter describes the strains and growth conditions, the culture design and strategy of the experiments and further details the analytical instruments and the softwares used in this thesis.

In the third chapter, the results are reported in sections based on the screening strategy of inhibitory molecules, the strain characterization of *Y. lipolytica* and the investigations of the two inhibitory molecules impact on the lipid metabolism and on the physiology of this yeast.

Finally, the last chapter draws a conclusion from the obtained results and proposes potential follow-up studies.

# CHAPTER 1. STATE-OF-THE-ART

## 1.1. Oleaginous Microorganisms

A small number of microorganisms (bacteria, fungi, yeast and algae) have the potential to accumulate lipids above 20 % of their dry cell weight: they are named oleaginous microorganisms (Ageitos et al., 2011; Beopoulos et al., 2009a; Meng et al., 2009).

It was also reported by C. Ratledge (Ratledge, 2004) that the ability of an organism to accumulate significant amount of lipids in other words the reason for oleaginity character, is based on :

- (i) The ability to produce a continuous supply of acetyl-CoA directly in the cytosol of the cell as a necessary precursor for fatty acid synthase (FAS),
- (ii) The ability to produce a sufficient supply of NADPH as the essential reduced cofactor used in fatty acid biosynthesis.

Lipid accumulation in an oleaginous microorganism is known to take place under nutrient limitation (the most studied being nitrogen) with an excess of carbon sources (Ratledge and Wynn, 2002). Lipid content in terms of mass and composition as a function of the oleaginous microorganisms are shown in Table 1.1.

**Table 1.1.** Lipid content and major fatty acids of oleaginous microorganisms

Oleaginous Microorganisms	Lipid content(%dry weight)	Major FA (% w/w, Cx:y)	References
<b>Bacteria</b>			
<i>Arthrobacter sp.</i>	>40	-	(Meng et al., 2009)
<i>Acinetobacter calcoaceticus</i>	27–38	-	(Meng et al., 2009)
<i>Rhodococcus opacus</i>	24–25	25 C18:1 30 C16:0	(Meng et al., 2009) (Kurosawa et al., 2013)
<i>Bacillus alcalophilus</i>	18–24	-	(Meng et al., 2009)
<b>Fungi</b>			
<i>Aspergillus oryzae</i>	40	30 C18:1	(Muniraj et al., 2013)
<i>Mortierella isabellina</i>	43	-	(Meng et al., 2009)
<i>Humicola lanuginosa</i>	3	-	(Meng et al., 2009)
<i>Mortierella alpina</i>	40	-	(Kosa and Ragauskas, 2011)
<b>Yeast</b>			
<i>Cryptococcus curvatus</i>	69	48 C18:1	(Iassonova et al., 2008)
<i>Cryptococcus albidus</i>	65	73 C18:1	(Beopoulos et al., 2011)

Table 1.1. continues

<i>Lipomyces starkeyi</i>	63	51 C18:1	(Beopoulos et al., 2009b)
<i>Rhodotorula glutinis</i>	72	47 C18:1	(Beopoulos et al., 2011)
<i>Yarrowia lipolytica</i>	36	51 C18:2	(Beopoulos et al., 2009b)
<i>Thrichosporon pullulans</i>	62	-	(Zhu et al., 2008)
<b>Algae</b>			
<i>Botryococcus braunii</i>	25-75	-	(Meng et al., 2009)
<i>Cylindrotheca sp.</i>	16-37	-	(Meng et al., 2009)
<i>Nitzschia sp.</i>	45-47	-	(Meng et al., 2009)
<i>Schizochytrium limanicum</i>	50	56 C16:0	(Ratledge and Wynn, 2002)
<i>Aurantiochytrium mangrovei</i>	73	45 C16:0 40 C22:5n-6	(Chaung et al., 2012)

### 1.1.1. Oleaginous Yeast

Among all the oleaginous microorganisms, yeasts have been known as the best candidates for lipid production because of their ability to accumulate triacylglycerol as cellular storage lipids up to 70 % of their dry cell weight (Ratledge, 2002) and their accessible molecular tools (Fickers et al., 2005a).

Many yeast species such as *Cryptococcus curvatus*, *Lipomyces starkeyi*, *Rhodotorula glutinis*, *Rhodospiridium toruloides*, *Thrichosporon pullulans* and *Y. lipolytica* can synthesize and store large quantities of lipid when cultivated under optimal conditions. The majority of these lipids are usually triacylglycerols (TAG) and sterol esters (SE). Depending on yeast species, the cultivation mode and also the environmental conditions influence the lipid content. The yeast's duplication times are usually less than 1 h and their cultures are more easily scaled up than algae since light is needed for autotrophic microalgae for cultivation process and required specific attention (Ageitos et al., 2011; Li et al., 2008).

#### 1.1.1.1. Oleaginous yeast of major interest: *Yarrowia lipolytica*

The ascomycetous yeast *Y. lipolytica* was formerly known as *Candida lipolytica*, *Endomycopsis lipolytica* and *Saccharomycopsis lipolytica* (Barth and Gaillardin, 1997; Papanikolaou and Aggelis, 2010). Through the oleaginous yeast *Y. lipolytica* is the only one with a developed genetic tools and complete genome sequence (Beopoulos et al., 2009b; Nicaud, 2012). *Y. lipolytica* has been found to be a great model organism for the understanding of many aspects of yeast metabolism such as protein expression and secretion (Kabani et al., 2000; Madzak et al., 2004), dimorphism (Kawasse et al., 2003; Perez-Campo and Dominguez, 2001; Ruiz-Herrera and Sentandreu, 2002; Timoumi et al., 2017a, 2017b,

2016), degradation of hydrophobic substrates (Fickers et al., 2005a; Thevenieau et al., 2007) and single-cell oil production (Beopoulos et al., 2008; Papanikolaou and Aggelis, 2011a).

*Y. lipolytica* is often found in environments rich in hydrophobic substrates such as alkanes, fatty acids and oils and its strains are most commonly isolated from dairy products, soil, sewage and oil-polluted environments (Barth and Gaillardin, 1997; Thevenieau et al., 2007). Being able to assimilate efficiently wide range of fatty substances as carbon sources and store lipids as TAG and SE in specifically developed organelles with special key enzymes, this yeast is the most common target model for studying the metabolism implicated in the lipid accumulation process (Ledesma-Amaro et al., 2016, 2015; Ml'ickov'á et al., 2004a; Papanikolaou et al., 2013).

## **1.2. Classification of Fatty Acids Based on Their Chain Length**

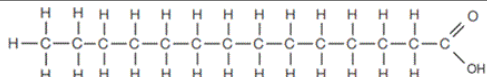
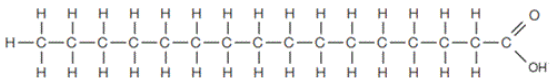
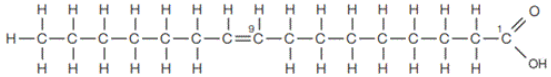
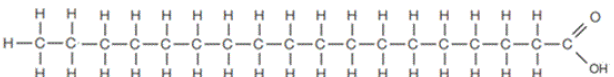
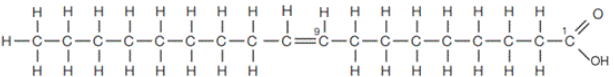
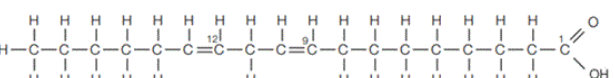
Lipids belong to a diverse family of compounds and defined simply -with a physical property- on the basis of their relative insolubility in water and solubility in non-polar solvents. Based on their diverse molecular structures, lipids are categorized into eight classes which are fatty acids, glycerolipids, glycerophospholipids, sterols, sphingolipids, prenol lipids, glycolipids (saccharolipids) and polyketides (Fahy et al., 2011, 2005; Klug and Daum, 2014).

Fatty acids are the key constituents of lipids and consist of hydrocarbon chain of different lengths and degrees of unsaturation with a terminal carboxylic acid group. The hydrocarbon chain of fatty acid is either saturated or unsaturated. Saturated fatty acids have no double bonds between the carbon atoms, whereas unsaturated fatty acids have one (monounsaturated) or more double bonds (polyunsaturated). Saturated fatty acids have the ability to pack their molecules together tightly to form ordered rigid structures whereas, the presence of one or more double bonds bends the hydrocarbon chain causing the molecule to take up more space thus prevents close packing as tightly as saturated fatty acids (Harvey R. A.; Ferrier D. R., 2011).

A simplified nomenclature of these compounds defines by their total number of carbon atoms and number of any double bonds for example, the notation C16:0 denotes a 16 carbon atoms without any double bonds, whereas C18:2 signifies that there are two double bonds (Table 1.2). Fatty acids based on their carbon chain length could be classified as:

- ◆ Short Chain Length Fatty Acids (SCFA): contain less than 12 carbon atoms such as C8:0 and C10:0,
- ◆ Medium Chain Length Fatty Acids (MCFA): contain less than 16 carbon atoms such as C12:0 and C14:0,
- ◆ Long Chain Length Fatty Acids (LCFA): contain 16 or 18 carbon atoms such as C16:1, C18:0 and C18:2,
- ◆ Very Long Chain Length Fatty Acids (VLCFA): contain more than 18 carbon atoms such as C20:0 and C24:0.

**Table 1.2.** Nomenclature of fatty acids

Shorthand	Systematic name	Common name	Structure
C14:0	Tetradecanoic	Myristic	
C16:0	Hexadecanoic	Palmitic	
C16:1	c-9-Hexadecenoic	Palmitoleic	
C18:0	Octadecanoic	Stearic	
C18:1	c-9-Octadecenoic	Oleic	
C18:2	c-9,c-12-Octadecadienoic	Linoleic	

## 1.3. Lipid Metabolism in Yeast

### 1.3.1. Lipid Synthesis and Citrate Metabolism: General Considerations

Lipid biosynthesis in all yeasts is a cytosolic process with acetyl-CoA as the basic precursor unit (Evans and Ratledge, 1985). Figure 1.1 presents the main metabolic pathway of *Y. lipolytica* lipid metabolism on glucose as carbon source.

Lipid accumulation in an oleaginous microorganism on glucose starts when a mineral nutrient becomes limiting in the cultivation medium with carbon excess. Even though different nutrients can be limiting, generally nitrogen is used for this purpose because it is easy to control and has a great effect on lipid accumulation. When non-oleaginous yeasts are

cultivated in the same nitrogen limiting medium, carbon excess sources are converted into various polysaccharides such as glycogen, glucans and mannans (Beopoulos et al., 2009a; Ratledge and Wynn, 2002).

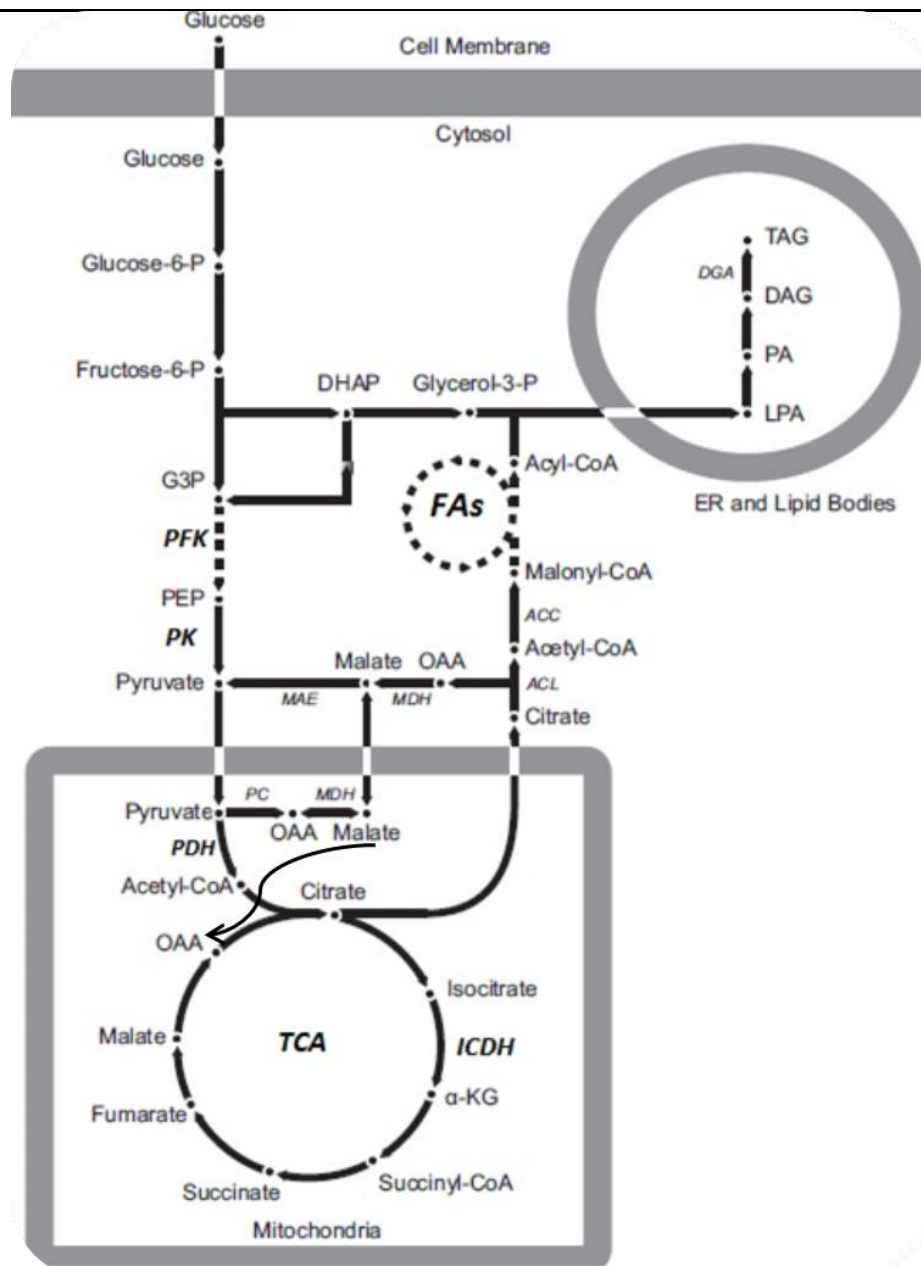


Figure 1.1. Overview of the main metabolic pathway of lipid metabolism in *Y. lipolytica* on glucose as carbon source (Adapted from Tai and Stephanopoulos, 2013).

After nitrogen depletion or limitation in the culture medium, the intracellular concentration of various different metabolites channeled towards lipid synthesis. These chain reactions start with the increased activity of the adenosine monophosphate-deaminase (AMP deaminase) which catalyzes the transformation of AMP in IMP (inosine 5'-monophosphate) and ammonia (Eq.1.1).



This increased level of AMP deaminase, decreases the cellular content of AMP including mitochondrial AMP concentration and increases cellular ammonium concentration as an intracellular source of nitrogen. The diminished content of mitochondrial AMP inhibits isocitrate dehydrogenase (ICDH) which is responsible for the conversion of isocitric acid to  $\alpha$ -ketoglutaric (2-Oxoglutarate) acid (Eq.1.2).

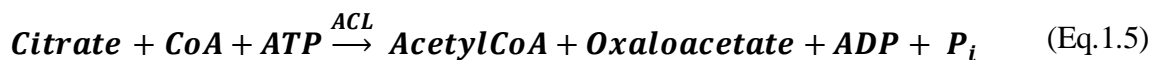


ICDH activity strictly depends on AMP (Evans and Ratledge, 1985) and it was reported by (Botham and Ratledge, 1979) that tricarboxylic acid cycle (TCA) could be interrupted by inactivation of the  $NAD^+$ -dependent ICDH (ICDH: $NAD^+$  dependent).

Since isocitrate cannot be channeled further through the TCA cycle, the accumulated isocitrate equilibrates with citrate via the activation of aconitase (Eq.1.3).



The accumulated citrate is then transported out of mitochondria to cytosol via the citrate/malate translocase system (Eq.1.4) and is cleaved by ATP Citrate Lyase (ACL) in the cytosol to give Oxaloacetate (OAA) and Acetyl-CoA (Eq.1.5).



The cytosolic OAA is transformed by Malate dehydrogenase (MDH) to Malate and transported back to mitochondria to complete the citrate/malate translocase system (Eq.1.6) (Fig.1).



### 1.3.2. Intracellular Lipid Accumulation

Lipids are important compounds that are stored by all living cells to provide energy. In all types of eukaryotic cells, stored lipids are found in the cell in special organelles usually called lipid bodies (LB) or lipid droplets (LD) (Zweytick et al., 2000). As mentioned before, oleaginous yeasts store significant lipid quantities (20-70 % DCW) in lipid bodies and are mostly composed of TAGs and SEs. The LB of *Y. lipolytica* is composed mostly of TAG (95 %), with SE being much less abundant (5 %) (Dulermo and Nicaud, 2011).

In oleaginous yeast lipid accumulation occurs via two different ways:

(i) The *de novo* lipid synthesis provides precursors for fatty acid synthesis such as Acetyl-CoA and Malonyl-CoA (Beopoulos et al., 2011).

(ii) The *ex-novo* accumulation pathway via the incorporation of hydrophobic substrates (uptake of exogenous FA, oils and TAG substrates from the culture medium).

### 1.3.2.1. *De novo* Lipid Synthesis

#### 1.3.2.1.1. Fatty Acid Synthesis

The fatty acid synthesis requires a continuous supply of Acetyl-CoA. This requirement is supplied by the  $\beta$ -oxidation pathway or cytosolic Acetyl-CoA which is provided from the citrate cleavage by ACL. The main provision of Acetyl-CoA for FA synthesis is considered to come via ACL (Beopoulos et al., 2009a; Ratledge and Wynn, 2002).

Fatty acid chain elongation also requires in each cycle two molecules of NADPH. The supplier of NADPH is considered to be mostly the pentose phosphate pathway (PPP) in the cytoplasm through glucose-6-dehydrogenase and 6-phosphogluconate dehydrogenase (Tehlivets et al., 2007) and to a lesser extent the Malic Enzyme (ME) (Eq.1.7).



Then pyruvate may be converted back to Acetyl-CoA or Oxaloacetate by Pyruvate Dehydrogenase (PDH, EC 1.2.4.1) and Pyruvate Carboxylase (PC, EC 6.4.1.1), respectively (Eq.1.8).



*De novo* FA synthesis is carried out in the cytosol and requires two soluble enzyme systems; Acetyl-CoA Carboxylase (ACC, EC 6.4.1.2) (Eq.1.9) and Fatty Acid Synthase (FAS) (Eq.1.10) (Gill and Ratledge, 1973). The cytosolic Acetyl-CoA is converted into Malonyl-CoA provided by biotin-dependent ACC as a starting step of FA synthesis in the cytosol (Eq.1.9) (Kosa and Ragauskas, 2011).

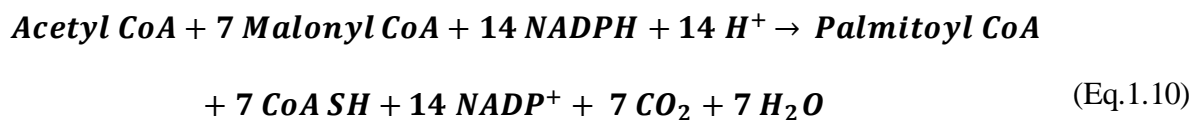


The fatty acid chain elongation grows through the addition of Malonyl-CoA and Acetyl-CoA as the first two carbon atoms of *de novo* fatty acid synthesis. Once Malonyl-CoA is synthesized, it reacts with existing prote in called acyl-carrier protein (ACP) to form Malonyl-ACP and with the same manner Acetyl-CoA also reacts with ACP to form Acetyl-ACP.

These two molecules start the first FA elongation cycle and involve a sequence of four chain reactions (Liang and Jiang, 2013; Ratledge and Wynn, 2002; Rossi et al., 2011; Tehlivets et al., 2007) (Figure 1.2).

- *Condensation*: to form  $\beta$ -ketoacyl-ACP by the enzyme  $\beta$ -ketoacyl-ACP synthetase (KS),
- *Reduction*:  $\beta$ -ketoacyl-ACP is reduced to 3-hydroxyacyl-ACP by the enzyme of  $\beta$ -ketoacyl-ACP reductase (KR),
- *Dehydration*: 3-hydroxyacyl-ACP is dehydrated to form 2,3-trans-enoyl-ACP by the enzyme  $\beta$ -ketoacyl-ACP dehydratase (DH),
- *A second reduction* to give the final two carbon elongated fatty acyl chain by enoyl-ACP reductase (ER) to form butyryl-ACP.

These chain reactions are repeated seven times and yield to palmitoyl-ACP which hydrolysis produces Palmitic acid (C16:0) and can be summarized as follows (Eq.1.10):



In oleaginous yeast FAs culminates in the formation of C16 or C18 saturated fatty acids. The most frequently found fatty acids are C16:0 (palmitic acid), C16:1 (palmitoleic acid), C18:1 (oleic acid), C18:2 (linoleic) (Ratledge, 2004).

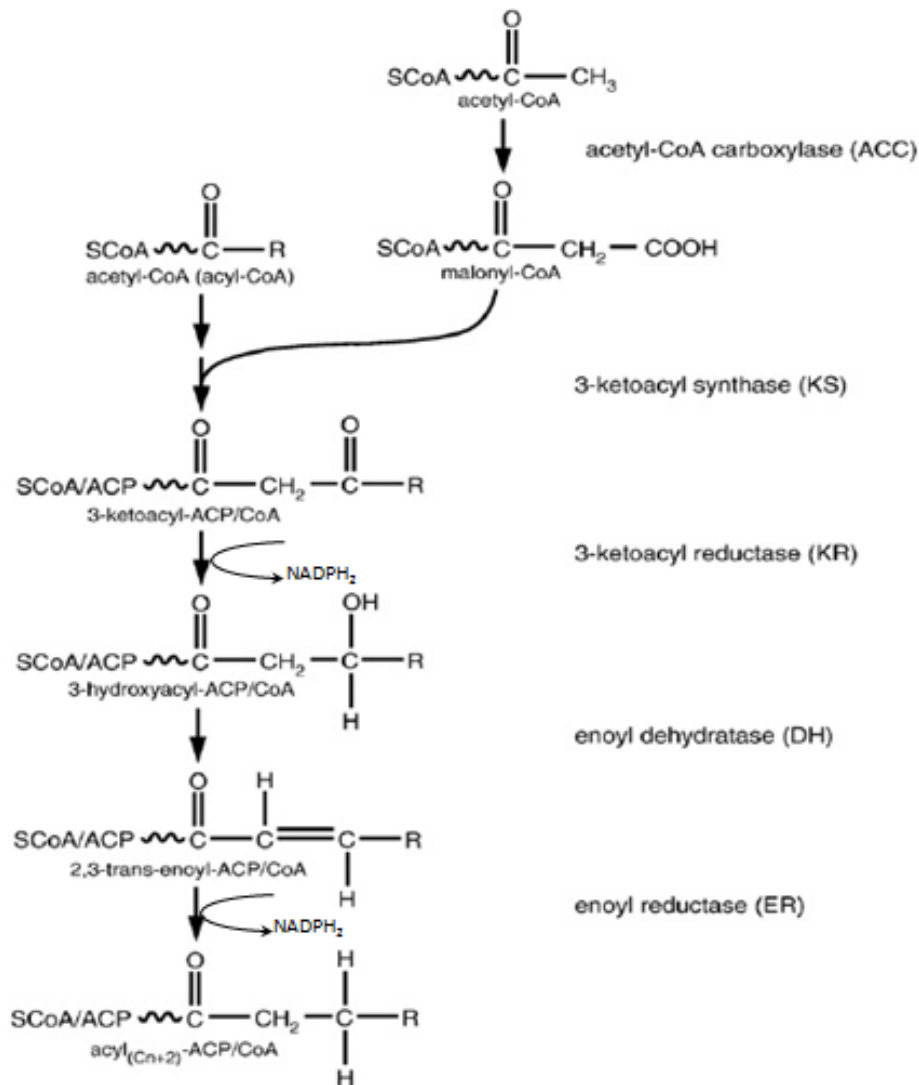


Figure 1.2. Fatty Acid Synthesis

(Adapted from Tehlivets et al., 2007)

---

### 1.3.2.1.2. Triacylglycerol Synthesis

Triacylglycerols (TAG) consist of three fatty acid chains esterified to a glycerol backbone. Triacylglycerol synthesis is an efficient form to store fatty acids and play an essential role in energy storage and energy balance in eukaryotic cells (Ageitos et al., 2011; Athenstaedt and Daum, 2006; Rajakumari et al., 2008; Sorger and Daum, 2003).

TAG synthesis generally follows the Kennedy pathway which occurs in the endoplasmic reticulum (ER) and requires acyl-CoA and glycerol-3-phosphate (G3P). It is reported that G3P can be produced either from glycerol via glycerol kinase (*GUT1*) in the cytosol or can be synthesized from dihydroxyacetone phosphate (DHAP) by G3P-dehydrogenase (*GPD1*) which is a reversible reaction catalyzed by an isoform of G3P dehydrogenase (*GUT2*)

(Beopoulos et al., 2009a; Rossi et al., 2011) (Figure 1.3). Deletion of *GUT2* gene redirected carbon flux toward TAG assembly, with a 3-fold increase in lipid accumulation (Beopoulos et al., 2008).

The first step of TAG biosynthesis starts with the acylation of G3P by the G3P-acyltransferase (SCT1) to form lysophosphatidic acid (LPA) at the sn-1 position. LPA can also be formed by reduction of acyl-DHAP by an NADPH-dependent acyl-DHAP reductase (AYR1) (Beopoulos et al., 2011; Rossi et al., 2010).

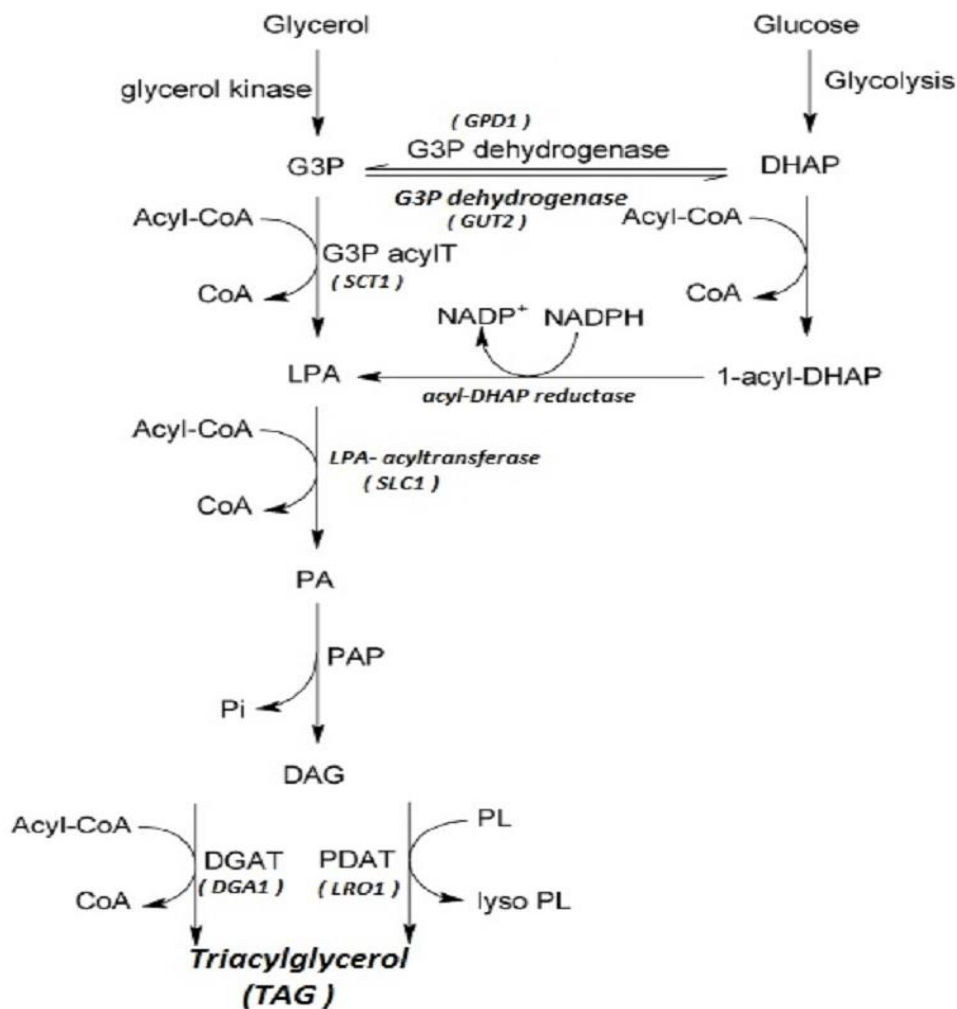


Figure 1.3. TAG synthesis

(Adapted from Czabany et al., 2007)

The further acylation of LPA is catalyzed by LPA-acyltransferase (SLC1) to generate phosphatidic acid (PA) at the sn-2 position. This is followed by PA dephosphorylation via the PA-phosphohydrolase (PAP) which releases the diacylglycerol (DAG) (Beopoulos et al., 2009a).

In the last step of *de novo* synthesis of TAG, the synthesized DAGs can follow different ways, either by using diverse acyl donors, acyl-CoA dependent such as DGA1 with acyl-CoA as an acyl donor or with acyl-CoA independent phospholipid:DAG acyltransferase (PDAT) e.g. LRO1 with glycerol phospholipids (PL) as an acyl donor (Dulermo and Nicaud, 2011).

### **1.3.2.2. *Ex-novo* Lipid Synthesis**

The lipid accumulation performed from hydrophobic substances (such as TAGs, alkanes, free fatty acids) as the sole carbon sources from the culture medium in an unchanged or modified form within the cell, is named as *ex novo* lipid synthesis (Beopoulos et al., 2009b).

The common yeast species as *Candida rugosa*, *Pichia jadinii*, *Torulopsis colliculosa* and *Y. lipolytica*, which are specific for degradation of hydrophobic substrate, are more efficient in *ex novo* lipid accumulation pathway (Beopoulos et al., 2011).

To increase the substrate transfer at the cell, *Y. lipolytica* secretes extra-cellular emulsifiers (surfactants such as liposan) which reduce hydrophobic droplets size and also secretes extra-cellular lipases (called Lip2p, encoded by the gene LIP2) for the hydrolysis of external long chain TAG (Fickers et al., 2005b). These reduced-size HSs and released FAs proceed to enter the cell with different transport/export mechanisms and once enter the cell, they will be either degraded for growth needs (degradation) or will act as a new substrate for the production of new fatty acids (modification) or will be stored in the lipid bodies as TAG (storage) (Aggelis and Sourdis, 1997; Beopoulos and Nicaud, 2012; Papanikolaou and Aggelis, 2011a).

## **1.4. Key Enzymes of Intermediary Metabolisms**

### **1.4.1. NAD<sup>+</sup>-dependent: Isocitrate Dehydrogenase**

NAD<sup>+</sup>-dependent: isocitrate dehydrogenase (NAD<sup>+</sup>: ICDH, EC 1.1.1.42) was found in numerous yeasts. NAD<sup>+</sup>: ICDH activity in oleaginous yeasts is absolutely dependent on AMP and inhibited by adenosine triphosphate (ATP). It shows that the ATP/AMP ratio is the main regulatory parameter controlling the TCA cycle and also regulates the amount of lipid accumulated by yeasts during the nitrogen limitation (Botham and Ratledge, 1979; Evans et al., 1981; Evans and Ratledge, 1985).

### 1.4.2. Malic Enzyme

Malic enzyme (EC 1.1.1.40) is found in most of the oleaginous microorganism which was considered to be a major source of NADPH for *de novo* lipid biosynthesis (Wynn et al., 1999; Wynn and Ratledge, 1997). Without ME activity, fatty acid biosynthesis is still functional but cells only produced essential lipids (phospholipids) by using other NADPH sources (Ratledge and Wynn, 2002). Thus, malic enzyme was regarded as a key enzyme involved in lipid accumulation.

Malic enzyme in oleaginous fungus *Mucor circinelloides* CBS 108.16 identified by Song et al. (2001) contains at least six isoforms (I, II, III, IV, V, VI) encoded by five different genes (Song et al., 2001), whereas *Mortirella alpina* contains at least seven isoforms (A,B, C, D, E, F, G) (Zhang and Ratledge, 2008). In *M. circinelloides* isoforms III and IV and in *M. alpina* isoforms D and E were reported that encoded in only one gene whereas isoforms III and D were present before nitrogen exhaustion and active in growth phase while isoforms IV and E appeared after nitrogen exhaustion from the medium and showed to be associated with lipid accumulation (Song et al., 2001; Zhang et al., 2007).

Zhang *et al.*, (2007) showed that lipid content increased substantially when both genes encoding the ME isoforms were expressed in *M. circinelloides* under the control of a constitutive promoter (glyceraldehyde-3-phosphate dehydrogenase, *gpd1*). Transformed cells in *M. circinelloides* with isoforms from *M. alpina* (D and E) and isoforms from *M. circinelloides* (III and IV) caused 3 and 2 fold increases in ME activity and also 2.5 and 2.4 fold increases in the amount of lipid content in the transformed cells compared to 12 % lipid content in wild type strain, respectively **Table 1.3**. Increased ME activity not only led to an increase in lipid content but also in the uptake of glucose and higher biomass concentration; and even in the unsaturated fatty acid production including  $\gamma$ -linoleic acid (18:3 n-6) (Zhang et al., 2007). Rodriguez-Frometa *et al.*, (2013) overexpressed the gene (*malA*) coding the isoforms III and IV under the control of a promoter of *M. circinelloides* resulting in a 15.8 fold increases in ME activity compared to control strain, however no increase was observed in lipid accumulation **Table 1.3** (Rodríguez-Frómata et al., 2013).

The malic enzyme activity was examined by Holdsworth *et al.*, (1988) in four different oleaginous yeasts *Candida curvata* D, *Trichosporon cutaneum* 40 and two strains of *Rhodospiridium toruloides* CBS14 and ATCC26217 that were cultivated on different nutrient availability in batch culture. *C. curvata* D showed the highest ME activity when the cells were

cultivated on nitrogen limited medium compared to *T. cutaneum* 40 and two strains of *R. toruloides* CBS14 and ATCC26217; 111, 34, 37 and 18 nmol.mg protein<sup>-1</sup>, respectively. Similar trend was also observed with small decreases in ME activity by carbon-starvation 85, 35, 20 and 25 nmol.mg protein<sup>-1</sup>, respectively. However there was a loss of activity when all yeasts were cultivated on exogenous lipid source (triolein) and activity of ME was undetectable in *C. curvata* D and *R. toruloides* ATCC26217 (Holdsworth et al., 1988).

Zhang *et al.*, (2013) cloned the ME gene from *Y. lipolytica* (that contains only one ME gene (MAE1, YALIOE18634 g) located in mitochondria, into pET28a vector and expressed in *E. coli* BL21 (DE3) for protein expression and purified the recombinant protein (YIME) to determine its biochemical characteristics. YIME activity showed that *Y. lipolytica* mostly had a higher affinity for NAD<sup>+</sup> (Km = 0.63 mM) than for NADP<sup>+</sup> (Km = 3.9 mM) and most of the intermediates of TCA cycle except succinate acid inhibited the malic enzyme activity. Furthermore, to figure out if ME was the main provider of NADPH for fatty acid biosynthesis in *Y. lipolytica*, from *M. alpina*, NADP<sup>+</sup>-dependent ME gene (*mce2*) was cloned in vector PINA1312 and expressed in *Y. lipolytica* (*Y. lipolytica* / PINA1312-*mce2*). The ME activity was increased from 1 to 350 nmol.mg<sup>-1</sup>.min<sup>-1</sup> in mutant strain while no significant increase was occurred in lipid content and FA profiles in *Y. lipolytica* **Table 1.3** (Zhang et al., 2013).

**Table 1.3.** Malic Enzyme

Microorganism	Gene Overexpression	Activity	Lipid Content	References
<i>Mucor circinelloides</i>	<i>Mortirella alpina</i> isoforms D & E + <i>gpd11</i> promoter	3 fold increase	2.5 fold increase	(Zhang and Ratledge, 2008)
	<i>Mucor circinelloides</i> isoforms III & IV ( <i>malA</i> gene)	2 fold increase	2.4 fold increase	(Zhang et al., 2007)
	<i>malA</i> gene + control promoter	15.8 fold increase	No increase	(Rodríguez- Frómeta et al., 2013)
<i>Y. lipolytica</i>	<i>Mortirella alpina</i> <i>mce2</i> + vector PINA1312	350 nmol/mg.min	No increase	(Zhang et al., 2013)

Ochoa-Estopier and Guillouet, (2014) reported that during D-stat of *Y. lipolytica*, the significant increase in malic enzyme specific activity was obtained when the specific lipid accumulation rate was strongly increased. The lipid accumulation rate exhibited its highest specific rate with the maximal amount of ME activity at 180 h approximately 80 mU.mg

protein<sup>-1</sup>. The results suggested the importance of ME activity to sustain high lipid accumulation rate.

These observations suggest the idea that required continuous supply of NADPH supplied by malic enzyme is the rate limiting step of fatty acid biosynthesis and lipid accumulation in oleaginous fungus *M. circinelloides* and *M. alpina* (Rodríguez-Frómata et al., 2013); on the other hand, for oleaginous yeast *Y. lipolytica*, it is still debated whether pentose phosphate pathway (PPP) or ME is the main provider of NADPH for lipid biosynthesis.

Similar results were reported by Liu *et al.*, (2013) for an oleaginous yeast *T. cutaneum* 2.1374 that under limited nitrogen conditions: NADP<sup>+</sup> dependent ME was confirmed to be the major source of NADPH where the activity of malic enzyme was detected to be highest in lipid accumulation phase compared to cell in growth phase approximately 8 U.mg protein<sup>-1</sup> to 5 U.mg protein<sup>-1</sup>, respectively (Z. Liu et al., 2013).

The malic enzyme activity is dependent on the presence of divalent metal ions (Mg<sup>+2</sup> or Mn<sup>+2</sup>) which helps the catalytic activity and also plays a role in structural stability. Replacement of this essential ion by other metal ions (Fe<sup>+2</sup>, Cu<sup>+2</sup>, Zn<sup>+2</sup>) automatically alters the geometry of the enzyme active site (Chang and Tong, 2003). Zhang *et al.*, (2013) also suggesting that metal ion is completely required due to the effects of different concentrations of MgCl<sub>2</sub> on ME activity that the maximum activity of ME was found at 6 mM (Zhang et al., 2013). However oxaloacetate, tartronic acid, 1-methylenecyclopropane trans-2,3-dicarboxylic acid, malonic acid and glutaric acid were showed to cause a complete inhibition in ME activity at 10 mM (Savitha et al., 1997). The effects of AMP, ADP and ATP also reported to inhibit ME activity at 10 mM and no effect was observed at 3 mM (Savitha et al., 1997). Furthermore, sesamol, a nonoil component of sesame seed oil and most likely its derivatives such as catechol-like compounds caused a 98 % inhibition of ME activity at 5.7 mM sesamol for *M. circinelloides in vivo* and a decrease in the lipid content in the cell from 24 to 2 % thus limiting the supply of NADPH (Wynn et al., 1997).

### **1.4.3. Malate Dehydrogenase**

In *Y. lipolytica*, Malate dehydrogenase (MDH) is encoded by two genes and exists in the form of 3 iso-enzymes, whereas in *Saccharomyces cerevisiae* MDH is encoded in three genes *MDH1* (mitochondrial, YKL085W), *MDH2* (cytosol, Y0L126C) and *MDH3* (peroxisomal, YDL378C) (Kabran et al., 2012).

Mitochondrial MDH (mMDH) in *Y. lipolytica* is encoded by *YIMDH1* gene (YALI0D16753g) while cytosolic and peroxisomal MDH are encoded by *YIMDH2* gene (YALI0E14190g) (Kabran et al., 2012). mMDH, which is involved in tricarboxylic acid cycle, catalyzes the reaction of malate to OAA with using cofactor NADH. Cytosolic OAA, which is generated by citrate cleavage enzyme (ACL), is converted to malate using NAD<sup>+</sup> as a cofactor by cytosolic MDH (cMDH). Peroxisomal MDH (pMDH) is involved in the reoxidation of NADH generated during the fatty acid  $\beta$ -oxidation (Kurita, 2003). Mitochondrial and cytosolic isoforms of MDH play a significant role in the malate/citrate translocase system to balance reducing equivalents between the mitochondria and cytosol across the mitochondrial membranes in the form of malate/oxaloacetate rather than as NAD/NADH (Minárik et al., 2002).

Ochoa-Estopier and Guillouet, (2014) reported that at the onset of lipid accumulation the specific activity of MDHs showed a weak induction of its synthesis and a decrease during the citric acid production using D-stat cultivation system of *Y. lipolytica* where N/C ratio linearly decreased. Which was in good agreement with prior work of Mullinax *et al.*, (1982) that increased concentration of citrate inhibits the cMDH activity on both directions of the reaction and inhibits the mMDH activity in the NADH  $\rightarrow$  NAD<sup>+</sup> direction and increases in the reverse direction of the reaction (Mullinax et al., 1982).

Gelpi *et al.*, (1992) also reported that citrate inhibits the reduction of OAA under all conditions, malate oxidation perturbs only at low malate and NAD<sup>+</sup> concentrations however, citrate attempts to enhance the activity of MDH at high malate and NAD<sup>+</sup> concentrations 10 mmol/L and 5 mmol/L, respectively (Gelpi et al., 1992).

#### **1.4.4. ATP Citrate Lyase**

ATP Citrate Lyase (ACL, EC 2.3.3.8), an enzyme so far only found in oleaginous microorganisms, is absent from the majority of non-oleaginous yeasts (Boulton and Ratledge, 1981a; Ratledge, 2004; Ratledge and Wynn, 2002). Besides, it has also been reported that while its presence in oleaginous yeasts accounted for their ability to accumulate significant amount of lipids, it does not mean that it is the only key enzyme to extend the lipid accumulation (Ratledge, 2002).

ACL enzyme activity in *Y. lipolytica* is encoded by two genes: *ACL1* and *ACL2* (X. Y. Liu et al., 2013) and requires ammonium ion for its activation (Beopoulos et al., 2011). This

enzyme activity is strongly dependent on the changes in energy charge: a weak inhibition (22 %) was occurred with AMP while a strong inhibition (60 %) caused by ADP (Pfitzner et al., 1987). However, while ACL activity was strongly inhibited in *Aspergillus niger* by palmitoyl-CoA, 5  $\mu$ M causing 87 % inhibition reported by Pfitzner et al., (1987), it was also showed by Adams et al., (2002) that the only compounds found to inhibit the activity of this enzymes in *A. nidulans* are malonyl-CoA and ADP accumulation, 70 % for 0.4 mM and 82 % for 2 mM, respectively.

It was also reported that ACL activity was inhibited by oleyl-CoA, 3  $\mu$ M caused 50 % inhibition that could reversed by adding bovine serum albumin (1 mg.ml<sup>-1</sup>) and by long-chain fatty acyl-CoA esters from *Lipomyces starkeyi*; it suggests that this enzyme may be a limiting step for lipid biosynthesis. Its role is also important to regulate the lipid formation in oleaginous yeast grown in continuous cultures (Boulton and Ratledge, 1981b).

Ochoa-Estopier and Guillouet, (2014) reported that in *Y. lipolytica*, ACL specific activity was maximal during the lipid accumulation however sharply decreased with the onset of the citric acid excretion. This strong decrease in ACL specific activity, where the specific lipid accumulation rate was the highest, could reveal that ACL was not the limiting step for the lipid accumulation (Ochoa-Estopier and Guillouet, 2014): other enzyme activities could be also responsible for to ensure lipid accumulation (Ratledge, 2004).

However the overexpression of ACL activity could benefit the level of cytosolic acetyl-CoA and thus enhanced *de novo* fatty acid synthesis considering the fact that ACL is required to cleave citrate to acetyl-CoA and OAA in the cytosol. Tang et al., (2013) introduced this enzyme in to *S. cerevisiae*, since ACL does not exist in non-oleaginous yeast. The maximal activity of ACL was obtained in stationary phase and increased level of saturated fatty acids composition detected compared to wild type strain C14:0, C16:0 and C18:0; 20 %, 14 % and 27 %, respectively (Tang et al., 2013).

Tamano et al., (2013) also reported that 1.7-fold increase in fatty acids and 1.9-fold increases in triglycerides were observed in the ATP-citrate lyase-enhanced expression strain in oleaginous fungi *Aspergillus oryzae* where *tefl* promoters of both *A. oryzae* and *Aspergillus nidulans* were used to make the enhanced expression strain.

It has been also showed that lipid content and ACL activity were reduced and caused a rise in citric acid production after (i) the deletion of some of the ACL genes (*ACL1*) in *Y.*

*lipolytica* and (ii) increased the copy number of *ICL1* gene encoding isocitrate lyase (ICL) (X. Y. Liu et al., 2013).

While the activity of ACL in *A. nidulas* was dependent on carbon sources (Adams et al., 2002), *A. niger* was not affected by the changes or the type of carbon or nitrogen sources (Pfitzner et al., 1987). It was also reported by Papanikolaou and Aggelis, (2002) that ACL activity was inactive in the presence of excess glucose and causing low level of lipid accumulation in *Y. lipolytica*.

**Table 1.4.** ATP Citrate Lyase

Microorganism	Gene Overexpression	Lipid Content	References
<i>Saccharomyces cerevisiae</i>	<i>acl</i> fragment from <i>musmusculus</i>	20 % increased C14:0, 14 % increased C16:0, 27 % increased C18:0	(Tang et al., 2013)
<i>Aspergillus oryzae</i>	<i>Aspergillus oryzae tef1</i> (from <i>A. oryzae</i> + <i>A. nidulans</i> )	1.7 fold increase FA and 1.9 fold increase TG	(Tamano et al., 2013)

#### 1.4.5. Acetyl-CoA Carboxylase

Acetyl-CoA Carboxylase (ACC, EC 6.4.1.2) is the first committed enzyme involved in the cytoplasmic fatty acid synthesis catalyzing the carboxylation of Acetyl-CoA to Malonyl-CoA.

ACC was found in all kingdoms of life with the exception of Archaea (Cronan and Waldrop, 2002). The active sites of ACC are located in a single protein for eukaryotic cells (type I ACC) while it is consisted of four subunits for bacteria (type II ACC) (Soriano et al., 2006). In *Y. lipolytica*, ACC is encoded by the *ACC1* gene and is known as YALI0C11407g (Beopoulos et al., 2009a) while in *Escherichia coli* ACC encoded by four subunits *AccA*, *AccB*, *AccC*, *AccD*; carboxyl transferase  $\alpha$ , biotin carboxyl carrier protein (BCCP), biotin carboxylase and carboxyl transferase  $\beta$ , respectively (Davis et al., 2000; Soriano et al., 2006).

Kamiryo et al., (1979) reported that the content of this enzyme decreased in cells that grown on fatty acids compared to glucose. ACC is inhibited by low concentrations of long chain acyl-CoA while is activated by citrate and  $Mg^{+2}$  (Gill and Ratledge, 1973; Ratledge and Wynn, 2002).

Estopier, (2012) reported that even after the citric acid excretion in the medium, ACC maintained its activity and its maximal specific activity (approx. 20 mU.mg protein<sup>-1</sup>) was found during lipid accumulation in *Y. lipolytica*. Botham and Ratledge, (1979) showed that

ACC activity was above 150 nmol h<sup>-1</sup> .mg protein<sup>-1</sup> where citrate was up to 10 mM. The ACC maximal activity in *Candida 107* was found at 1 mM citrate but the enzyme activity was unaffected for *Candida utilis*. However in both yeasts ACC activity was inhibited by Fructose 1,6-biphosphate while this enzyme activity was enhanced in *S. cerevisiae* by this molecule (Botham and Ratledge, 1979).

ACC enzyme activity completely abolished with the addition of fungicide 10 µg/ml Soraphen A even if the medium was supplemented with C16-18 fatty acids in *A. nidulans*; on the other hand 5-fold increase was observed in ACC enzyme activity using potassium nitrate (60 mM) than ammonium tartrate (30 mM) as a sole nitrogen source (Morrice et al., 1998). Morrice et al., (1998) also showed that ACC enzyme activity and transcription of *AccA* gene which has 63 % identity at the amino acid level to the *S. cerevisiae ACC1* gene in *A. nidulans* were higher in medium containing potassium nitrate (4.9-fold) than ammonium tartrate. Besides, ACC was suggested as an essential enzyme by the disruption of *AccA* gene leading to a lethal event for *A. Nidulans* (Morrice et al., 1998).

To enhance the fatty acid synthesis Davis et al., (2000) overexpressed in *E. coli* the genes ACC encoding the four subunits of *E. coli* with a periplasmic enzyme Thioesterase I encoded by the *tesA* gene; but the mutant protein called 'TesA blocks the export of the enzyme to the cellular periplasm where it cleaves the long chain acyl-ACP in the cytosol. These conditions led to a six fold increase in the rate of fatty acids synthesis with an increase in free fatty acid production from 1.03 to 6.69 nmol.

It was also recently showed that gram negative oleaginous bacterium *Acinetobacter calcoaceticus* was used as a donor for overexpression ACC including four subunits in *E. coli* resulted in a threefold enhancement in intracellular fatty acid content 177.66 mg/g with a 1.82 % molar yield (Meng et al., 2011).

Zha et al., (2009) reported that overexpression of *Corynebacterium glutamicum* ACC in *E. coli* resulted in a threefold increase in cellular Malonyl-CoA concentration. Lu et al., (2008) reached a 20-fold increase in total fatty acid production in *E. coli* introducing four genotypic alterations; which were (i) blocking fatty acid degradation, (ii) heterologous expression of a plant thioesterase, (iii) overexpression of ACC to increase the supply of Malonyl-CoA, (iv) over-expression of an endogenous thioesterase.

Plasmid based overexpression of endogenous *ACC1* gene in *S. cerevisiae* led to a 58 % increase in lipid content from 4.3 % to 6.8 % and an increase in total fatty acid production

from 42.7 mg. L<sup>-1</sup> to 63.2 mg. L<sup>-1</sup> was observed by Runguphan and Keasling, (2014). Similarly a 40 % increase in the total fatty acid content of a non-oleaginous yeast *Hansenula polymorpha* was achieved by overexpressing *ACC1* gene from an oleaginous fungus *Mucor rouxii* (Ruenwai et al., 2009).

In *Y. lipolytica*, Tai and Stephanopoulos, (2013) reported that overexpression of *ACC1* increased the lipid content twofold from 8.8 % to 17.9 % and the strain further combined with *DGAI* (diacylglycerol acyltransferase) was able to accumulate up to 62 % of its dry cell weight and reported almost 5-fold greater than the control strain. Similarly, total lipid production increased when *ACC1* and *DGAI* genes are overexpressed in *R. toruloides* (Zhang et al., 2016).

**Table 1.5.** Acetyl-CoA Carboxylase

Microorganism	Gene Deletion	Gene Overexpression	Lipid Content	References
<i>Acinetobacter calcoaceticus</i>	-	4 subunits of ACC in <i>E. coli</i>	3 fold increase in FA	(Meng et al., 2011)
<i>Escherichia coli</i>	-	4 subunits of ACC <i>E. coli</i>	6 fold increase in FA	(Davis et al., 2000)
<i>Escherichia coli</i>	-	<i>Corynebacterium glutamicum</i> ACC	3 fold increase in Malonyl-CoA	(Zha et al., 2009)
<i>Escherichia coli</i>	<i>fadD</i> gene	thioesterase <i>Cinnamomum camp horum</i> + ACC	20 fold increase FA	(Lu et al., 2008)
<i>Saccharomyces cerevisiae</i>	-	<i>ACC1</i> <i>S. cerevisiae</i>	6.8 % increase	(Runguphan and Keasling, 2014)
<i>Y. lipolytica</i>	-	ACC	2 fold increase lipid content	(Tai and Stephanopoulos, 2013)
<i>Hansenula polymorpha</i>	-	ACC1 <i>Mucor rouxii</i>	40 % increase TFA	(Ruenwai et al., 2009)

## 1.5. Fatty Acid Synthase Enzyme System

Fatty acid synthases have been classified into two types based on the organization of their catalytic units. Type I FAS, present in eukaryotic cytoplasm, are large multifunctional proteins that carry out all enzymatic steps essential for *de novo* fatty acid synthesis (Leibundgut et al., 2008). In contrast to type I FAS, type II FAS system, possess in most bacteria but also in mitochondria or in chloroplasts of eukaryotic cells (Leibundgut et al.,

2008; Tehlivets et al., 2007), are small independent proteins which are encoded by a series of separate genes (Table 1.6) (Heath et al., 2001; Schweizer and Hofmann, 2004).

Type I FAS systems are represented as discrete functional domains on a single polypeptide chain ( $\alpha$ ) or on two different polypeptide chains ( $\alpha$ ) and ( $\beta$ ). According to their domain organizations of the multifunctional proteins and their subunit stoichiometry, type I FASs are divided into two subgroups; microbial type I FAS (type 1a) (EC2.3.1.86) and animal type IFAS (type 1b) (EC2.3.1.85) (Lomakin et al., 2007; Schweizer and Hofmann, 2004). The 540 kDa dimeric, X-shaped animal type I FAS forming  $\alpha_2$  dimers with a domain sequence of KS-AT-DH-ER-KR-ACP-TE (Table 1.7); however microbial type I FAS is organized as either  $\alpha_6\beta_6$  dodecamers for fungal FAS or  $\alpha_6$  hexamers for bacterial type I FAS (Leibundgut et al., 2008).

In yeasts, the FAS is a member of type I FAS family, barrel-shaped structure yeast FAS contains six copies of eight independent functional domains with a sequence of AT-ER-DH-MPT/ACP-KR-KS-PPT in an  $\alpha_6\beta_6$  dodecamer complex of 2.6 MDa (Fig.1.4B).

**Table 1.6.** Genes and Enzymes of Type II Fatty Acid Synthases

Gene	Protein	Enzyme activity
<i>accABCD</i>	AccABCD	Acetyl-CoA carboxylase
<i>accA</i>	AccA	Acetyl-CoA carboxylase, Carboxyltransferase subunit $\alpha$ -subunit
<i>accB</i>	AccB	Acetyl-CoA carboxylase, carboxy biotin carrier protein
<i>accC</i>	AccC	Acetyl-CoA carboxylase, Biotin carboxylase
<i>accD</i>	AccD	Acetyl-CoA carboxylase, Carboxyltransferase $\beta$ -subunit
<i>acpP</i>	ACP	Acyl carrier protein (ACP)
<i>fabA</i>	FabA	$\beta$ -Hydroxy decanoyl-ACP dehydratase
<i>fabD</i>	FabD	Malonyl-CoA: ACP transacylase
<i>fabB</i>	FabB	$\beta$ -Ketoacyl-ACP synthase I
<i>fabF</i>	FabF	$\beta$ -Ketoacyl-ACP synthase II
<i>fabH</i>	FabH	$\beta$ -Ketoacyl-ACP synthase III
<i>fabG</i>	FabG	$\beta$ -Ketoacyl-ACP reductase
<i>fabI</i>	FabI	trans-2-Enoyl-ACP reductase I
<i>fabK</i>	FabK	trans-2-Enoyl-ACP reductase II
<i>fabL</i>	FabL	trans-2-Enoyl-ACP reductase III
<i>fabZ</i>	FabZ	$\beta$ -Hydroxyacyl-ACP dehydratase
<i>fadR</i>	FadR	Transcriptional activator/repressor
<i>farR</i>	FarR	Transcriptional activator/repressor

Yeast FAS is encoded by *FAS1* ( $\beta$ -subunit, 230kDa) and *FAS2* ( $\alpha$ -subunit, 210kDa) genes (Table 1.7) (Tehlivets et al., 2007). The rate limiting step for the synthesis of long chain fatty

acids is the specificity of initial condensing enzymes from the fatty acid synthase (FAS) complex (Ratledge and Wynn, 2002).

**Table 1.7.** Genes and Enzymes of Type I Yeast Fatty Acid Synthase

Gene	Enzyme
	AC (AT) <i>Ac(et)yltransferase</i>
<i>FAS1</i> ( $\beta$ subunit)	<i>ER</i> <i>Enoyl reductase</i>
	<i>DH</i> <i>Dehydratase</i>
	<i>MPT</i> <i>Malonyl/Palmitoyl-Transacylase</i>
	ACP <i>Acyl Carrier Protein</i>
<i>FAS2</i> ( $\alpha$ subunit)	<i>KR</i> <i>Ketoacyl Reductase</i>
	<i>KS</i> <i>Ketoacyl Synthase</i>
	<i>PPT</i> <i>Phosphopantetheine Transferase</i>

In contrast to animal type I FAS, yeast FAS contains MPT domain which transfers malonyl moieties used for chain elongation from CoA to ACP and back transfers saturated fatty acids from ACP to CoA, in addition, yeast FAS contain PPT domain in  $\alpha$  subunit for cofactor attachment to ACP (Figure 1.5) (Jenni et al., 2006; Leibundgut et al., 2008; Tehlivets et al., 2007).

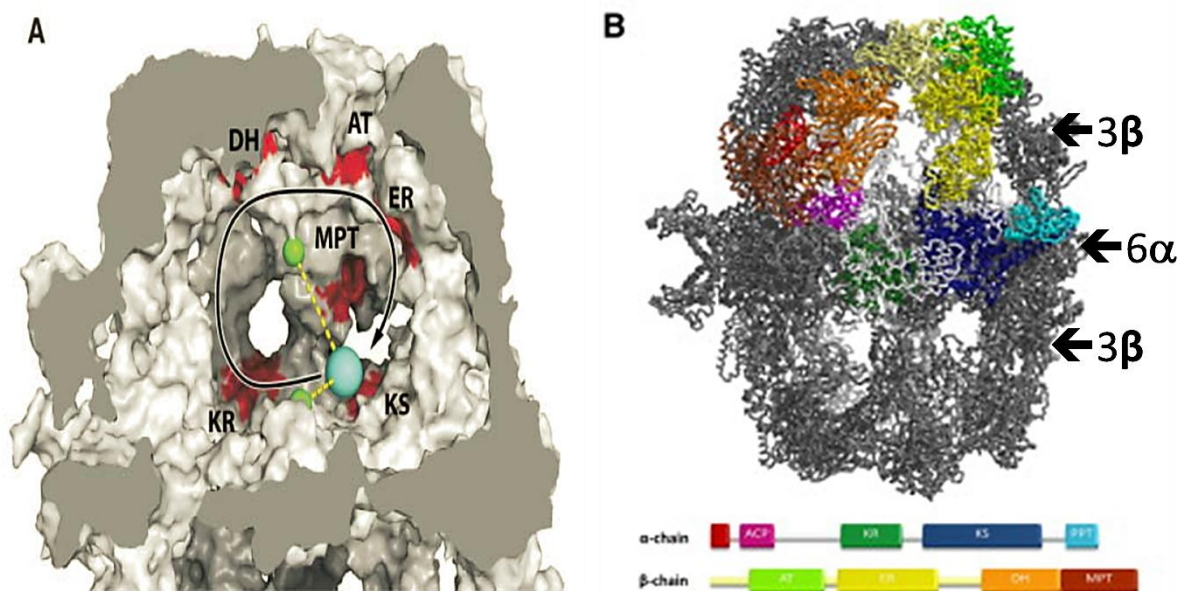


Figure 1.4. Type I FAS

(A) Multimeric options for the auto-activation of the *Saccharomyces cerevisiae* FAS Type I Megasyntase (adapted from Johansson et al., 2009),

(B) Structure of fungal fatty acid synthase and implication for iterative substrate shuttling (adapted from Jenni et al., 2007).

### 1.5.1. Fatty Acid Synthase inhibitions with small molecules

Inhibition of fatty acid synthesis pathway has been extensively studied for the development of clinical drugs in order to treat obesity, diabetes, cancer and bacterial infections. Several antibiotic compounds such as thiolactomycin, platensimycin, ECGC, TOFA, C75, quercetin, cerulenin, triclosan and orlistat have been shown to specifically target the different domain of type I and/or type II fatty acid synthase enzyme system and reviewed in (Flavin et al., 2010; Heath et al., 2001; Lupu and Menendez, 2006; Price et al., 2001; Wright and Reynolds, 2007).

The reaction scheme of yeast fatty acid synthesis and specific domain inhibition of fatty acid synthase enzyme system with the small molecules of Cerulenin, Triclosan and Orlistat are shown in Figure 1.5.

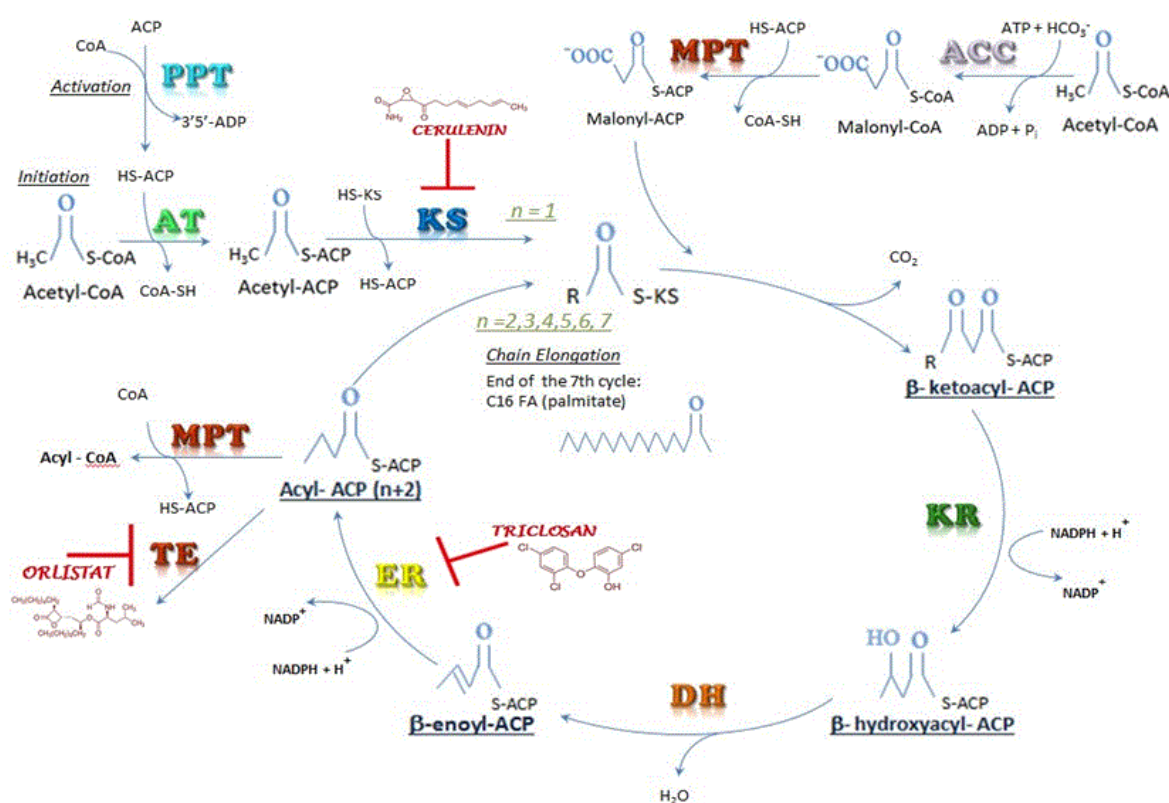


**Figure 1.5. Reaction scheme of yeast fatty acid synthesis and specific domain inhibition with small molecules**

(PPT: Phosphopantetheine Transferase; AT: ac(et)yltransferase; ACC: Acetyl-CoA Carboxylase; MPT: Malonyl/Palmitoyl-Transacylase; KS: Ketoacyl Synthase; KR: Ketoacyl Reductase; DH: Dehydratase; ER: Enoyl reductase)

### 1.5.1.1. Triclosan

Triclosan (2,4,4'-Trichloro-2'-hydroxydiphenyl ether) belongs to the class of organic compounds known as diphenyl ether which are aromatic compounds containing two benzene rings linked to each other through an ether group with a molecular formula of  $C_{12}H_7Cl_3O_2$  (Figure 1.6).

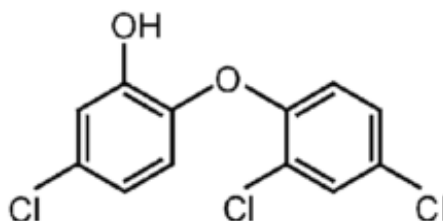


Figure 1.6. Structure of triclosan

Triclosan broadly used as antibacterial and antifungal agent in personal and household products such as soaps, toothpastes, fabrics and plastics.

It was shown that triclosan blocks lipid synthesis of *E. coli* by targeting the gene *fabI* encodes enoyl-acyl carrier reductase (FabI ; ER) that 92 % inhibition on lipid synthesis was obtained with  $0.24 \mu\text{g.ml}^{-1}$  triclosan concentration whereas  $0.15 \mu\text{g.ml}^{-1}$  was sufficient to stop the growth rate by 50 % and  $8 \mu\text{g.ml}^{-1}$  for the lysis of *E. coli* K12 strain AG100 where the triclosan resistant mutant AGT11 showed only 2 % inhibition on lipid synthesis with  $0.24 \mu\text{g.ml}^{-1}$  concentration, 50 % inhibition on the growth with  $13 \mu\text{g.ml}^{-1}$  and 75 % inhibition on the lipid synthesis with  $26 \mu\text{g.ml}^{-1}$  however no lysis was obtained with the concentration of  $256 \mu\text{g.ml}^{-1}$  (McMurry et al., 1998).

It was also shown that triclosan and triclosan analogs inhibited enoyl-acyl carrier protein reductase (*fabI* ; *ER*) component of the type II fatty acid synthase system purified from *E. coli* (Heath et al., 1998).

### 1.5.1.2. Orlistat

Orlistat is a saturated derivative of a naturally occurring lipase inhibitor, lipstatin, produced by *Streptomyces toxytricini* (Weibel et al., 1987) and has a structure of N-Formyl-L-leucine-(1S)-1-(((2S,3S)-3-hexyl-4-oxo-2-oxetanyl)methyl) dodecyl ester with a molecular formula of  $C_{29}H_{53}NO_5$ .

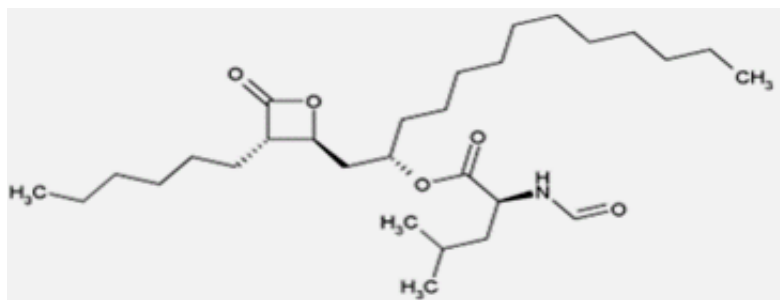


**Figure 1.7. Structure of orlistat**

Orlistat, also known as tetrahyrolipstatin, is a poor water soluble substance and originally designed to treat obesity but has also been shown to inhibit thioesterase (TE) domain of human FAS protein (FASN) which catalyzes the termination step of fatty acid synthesis by hydrolyzing the thioester bond between palmitate and acyl carrier protein to release the end-product palmitate from the ACP (Fako et al., 2014; Kridel et al., 2004; Pemble et al., 2007).

### 1.5.1.3. Cerulenin

Cerulenin has a structure of (2R,3S)-2,3-epoxy-4-oxo-7,10-trans,trans-dodecadienamide with a molecular formula of  $C_{12}H_{17}NO_3$  and first isolated from the culture broth of the fungus *Cephalosporium caerulens* and originally developed as an antifungal antibiotic (Omura, 1976).

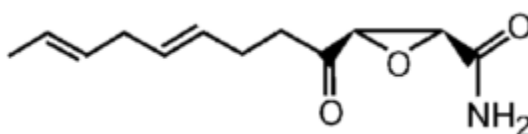


**Figure 1.8. Structure of cerulenin**

Cerulenin was reported as an irreversible inhibitor of type II fatty acid synthase enzyme system (type II FAS) and specifically inhibits the activity of  $\beta$ -ketoacyl-acyl carrier protein synthases I and II (FabB and FabF) (D'agnolo et al., 1973; Price et al., 2001).

The elongation of fatty acids in *Bacillus subtilis* catalyzed by type II FAS via a repeated cycle of condensation (FabF that catalyzes the condensation of malonyl-CoA with acyl-ACP), reduction (FabG), dehydration (FabZ) and a second reduction (enoyl-ACP reductases; FabI and FabL). It was shown that 3-fold decrease in the proportions of unsaturated fatty acids (from 10 % to 3.4 %) and 2-fold increase in the ratio of short-chain length FA (C13-C15) to long-chain length FA (C16 or longer) by inhibiting the condensing enzyme FabF (KS) in *B. subtilis* with the antibiotic cerulenin at the concentration of  $2.5 \mu\text{g}\cdot\text{ml}^{-1}$  (Porrini et al., 2014).

It has been also shown that during the first 40 min. after the addition of cerulenin (100  $\mu\text{g}.\text{ml}^{-1}$ ) the growth and lipid synthesis of *E. coli* was inhibited more than 90 % but the inhibitory effects of cerulenin on growth reversed with 100  $\mu\text{g}.\text{ml}^{-1}$  supplementation of palmitic and oleic acids (Goldberg et al., 1973).

Polyunsaturated fatty acid producing (PUFA) bacteria *Shewanella marinintestina* cultured in a medium containing 5  $\mu\text{g}.\text{ml}^{-1}$  cerulenin increased the level of eicosapentaenoic acid (EPA, C20:5) and another PUFA producing bacteria *Moritella marina* increased docosahexaenoic acid (DHA, C22:6n-3) content from 5.9 % to 19.4 % when cultured in a medium containing 0.5  $\mu\text{g}$  cerulenin. $\text{ml}^{-1}$ . When cerulenin concentration increased up to 2.5  $\mu\text{g}.\text{ml}^{-1}$  *M. marina* increased the level of dodecanoic (C12:0), tetradecenoic (C14:1) and tetradecanoic (C14:0) acids and decreased the level of octadecenoic (C18:1) and hexadecenoic (C16:1) acids and no significant modification was obtained in the level of decanoic acid (C16:0) (Morita et al., 2005).

It has been also shown that cerulenin is a potent inhibitor of type I fatty acid synthase enzyme system (type I FAS) and irreversibly inhibits the activity of  $\beta$ -ketoacyl synthases (KS, condensing enzyme) which was shown for various microorganisms such as *Euglena gracilis*, *Corynebacterium diphtheria*, *Mycobacterium phlei* and from rat liver (Vance et al., 1972). The irreversible inhibition of cerulenin for *E. coli* was associated with 1 mol of cerulenin per mole of the enzyme when inhibition approached 100 % (D'agnolo et al., 1973) and it was reported for *S. cerevisiae* that 3 moles of cerulenin were bound to 1 mol of the enzyme by binding covalently to the cysteine residue of the condensing reaction domain of yeast fatty acid synthetase (Funabashi et al., 1989; Kawaguchi et al., 1982).

Oleaginous microalgae *Aurantiochytrium mangrovei* treated with cerulenin dissolved in ethanol and added to the culture at a concentration of 1, 5 and 25  $\mu\text{M}$ ; increased concentration of cerulenin in the medium decreased the percentage of C14:0 from 4 % to 3.7 % and C16:0 from 42 % to 35 % and 3 % increases was obtained both in polyunsaturated fatty acids: DHA and docosapentaenoic acid (DPA C22:5n-6) (Chaung et al., 2012).

Another DHA and DPA producing microalgae *Schizochytrium sp.* was treated with 0.5 to 200  $\mu\text{M}$  cerulenin concentrations prior to incubation with  $^{14}\text{C}$ -labeled acetate. The incorporation of labeled acetate into DHA and DPA required higher concentrations than 5  $\mu\text{M}$  cerulenin, whereas short chain fatty acids (C14:0 and C16:0) were blocked at lower concentrations (Hauvermale et al., 2006).

## 1.6. Conclusion

In this chapter, the *de novo* fatty acid synthesis pathway and the key enzymes involved in fatty acid synthesis of the oleaginous microorganism were reviewed. Through the literature search, the regulation of the key enzymes involved in the *de novo* fatty acid synthesis at the level of gene expressions and deletions and the impact of such regulations on fatty acid metabolism and lipid accumulation for oleaginous yeasts were reported. Moreover known inhibitors of these key enzymes, their impact on the enzyme activity, on the lipid metabolism and on the fatty acid content and composition are presented.

In the literature there are listed inhibitors targeting the fatty acid biosynthesis enzyme system and specifically used in medical sciences. Based on the literature search, three small inhibitory molecules were chosen in order to target different catalytic domains of FAS enzyme system aiming to modify the synthesis of fatty acids for the oleaginous yeast *Y. lipolytica*.

The iterative elongation of fatty acid chains through reaction cycle of FAS was focused to control on three different catalytic domains:

- (i) on the condensation step by ketoacyl synthase (KS) with the inhibitory molecule Cerulenin,
- (ii) on the second reduction step by enoyl reductase (ER) with inhibitory molecule Triclosan,
- (iii) on the termination step with the inhibitory molecule Orlistat.

The idea was to use little amount of these inhibitors without affecting the cell viability of yeast *Y. lipolytica* in order to identify enzymatic reactions within the FA biosynthesis pathway that have the control on the elongation of fatty acids and on the carbon chain length.

# CHAPTER 2. MATERIALS & METHODS

---

## 2.1. Microorganisms

The strains used in these studies were *Y. lipolytica*W29, *Y. lipolytica* JMY3501 and *Y. lipolytica* CR62. The W29 strain was obtained from the ATCC collection. In the frame of the ProBio3 project, the JMY3501 was provided by the team BimLip, MICALIS, INRA (France) and the CR62 obtained from the CIMES team, Laboratoire d'Ingénierie des Systèmes Biologiques et des Procédés (Toulouse, France). The genotypes of JMY3501 and CR62 were as follows:

Strain JMY3501: MATa ura3-302 leu2-270 xpr2-322  $\Delta$ tg14  $\Delta$ pox1-6 + LEU2ex Tef-yIDGA2 + URA3ex Tef-GPD1

Strain CR62: MATa URA3-302 Leu2-270 xpr2-322  $\Delta$ tg14  $\Delta$ phd1  $\Delta$ mfe1 +LEU2ex TEF-yIDGA2 + URA3ex-Tef-GPD1 + URA3ex- $\Delta$ FAS2 + LEU2ex TEF-yIFAS2 I1220F

### 2.1.1. Cryopreservation of the strains

The strains were initially stored in freezer (-80 °C) from an earlier culture. For this study, new glycerol stock cultures were prepared according to the following procedure:

- \* A drop from an initially stock strain was streaked onto an YPD/agar plate and cultivated for 48 hours at 30°C.
- \* An isolated colony from the plate was picked and inoculated to 5 ml YPD medium Table 2.1 in a sterile tube under laminar flow hood and incubated for 17 hours at 28 °C and 111 rpm. At the end of incubation a biomass concentration of 0.8 g<sub>DCW</sub>. L<sup>-1</sup> was obtained.

---

**Table 2.1.** YPD medium

Component	Concentration g.L <sup>-1</sup>
Yeast extract	10
Bactopeptone	10
Glucose	10
Agar	20 (only used for the YPD/agar plates)

- \* 4 ml culture were transferred into a 500 ml sterile baffled shake flask containing 15 ml of YPD medium and incubated for 8 hours at 28 °C and 111 rpm. At the end of incubation a biomass concentration of 2 g<sub>DCW</sub>. L<sup>-1</sup> was obtained.
- \* 14 ml culture were removed from the shake flask and supplemented with 35 ml of YPD medium under laminar flow hood and incubated for 17 hours at 28 °C and 111 rpm.

\* After 17 hours, this cell suspension was stored in cryotubes in freezer (-80 °C) on YPD medium with the addition of pure sterile glycerol as a cryoprotectant to reach a final glycerol concentration of 30 % (v.v<sup>-1</sup>).

## 2.2. Media and Growth Conditions

### 2.2.1. Medium compositions for shake flask cultures

The mineral salt composition of two different synthetic media (for growth and nitrogen limited medium), for pre- and flask cultures are listed in Table 2.2. The solutions pH was adjusted to 5.6 and was sterilized at 121 °C for 20 minutes.

**Table 2.2.**Medium Composition

Component	Concentration g. L <sup>-1</sup>	Component	Concentration g. L <sup>-1</sup>
<i>Pre-cultures</i>		<i>Nitrogen Limited Cultures</i>	
(NH <sub>4</sub> ) <sub>2</sub> SO <sub>4</sub>	1	(NH <sub>4</sub> ) <sub>2</sub> SO <sub>4</sub>	0.3
KH <sub>2</sub> PO <sub>4</sub>	6	KH <sub>2</sub> PO <sub>4</sub>	6
MgSO <sub>4</sub>	2	MgSO <sub>4</sub>	2

The trace element solutions were prepared separately and filtered through 20 µm porosity of polyamide sterile membrane under laminar flow hood and all solutions were stored at 4 °C. Only the pH of FeSO<sub>4</sub>.7H<sub>2</sub>O solution adjusted to 2 using 37 % HCl. The concentrations of each trace element are listed in Table 2.3.

**Table 2.3.**Trace Elements

Component	Concentration g. L <sup>-1</sup>	Component	Concentration g. L <sup>-1</sup>
EDTA	0.03750	Na <sub>2</sub> MoO <sub>4</sub> .2H <sub>2</sub> O	0.00005
ZnSO <sub>4</sub> . 7H <sub>2</sub> O	0.02810	CaCl <sub>2</sub> .2H <sub>2</sub> O	0.01250
MnCl <sub>2</sub> . 4H <sub>2</sub> O	0.00250	FeSO <sub>4</sub> .7H <sub>2</sub> O	0.00875
CoCl <sub>2</sub> .6H <sub>2</sub> O	0.00075	H <sub>3</sub> BO <sub>3</sub>	0.00250
CuSO <sub>4</sub> .5H <sub>2</sub> O	0.00075		

The vitamin solution was filtered through 20 µm porosity of polyamide sterile membrane under laminar flow hood, pH of the solution was adjusted to 6.5 using 5 M NaOH before filtration and stored at 4 °C. The composition of the solution is listed in Table 2.4

**Table 2.4.**Vitamins

Component	Concentration g. L <sup>-1</sup>	Component	Concentration g.L <sup>-1</sup>
D- Biotin	0.00025	Thiamine	0.001
D-L pantothenic acid	0.001	Pyridoxine	0.001
Nicotinic acid	0.001	Para- amino benzoic acid	0.0002
Myo- inositol	0.00625		

The concentrated glucose solution was prepared from cerelese monohydrate to reach a stock glucose concentration of 700 g. L<sup>-1</sup>. The solution was sterilized at 121 °C for 20 min. and used for pre-cultures for an initial concentration of 20 g. L<sup>-1</sup>.

**Table 2.5.** Stock Glucose Solution

Component	Concentration g. L <sup>-1</sup>
Glucose	700

### 2.2.2. Medium composition of initial fed-batch cultures

The mineral salt composition of two different synthetic media for pre-cultivation and initial fed-batch cultures are listed in Table 2.6. The solutions pH was adjusted to 5.6 and was sterilized at 121 °C for 20 minutes.

**Table 2.6.** Mineral Salts

Component	Concentration g. L <sup>-1</sup>	
	<i>Pre-cultures</i>	<i>Initial Fed-Batch Cultures</i>
(NH <sub>4</sub> ) <sub>2</sub> SO <sub>4</sub>	2.5	0.502
KH <sub>2</sub> PO <sub>4</sub>	6	6
MgSO <sub>4</sub>	2	2

The initial trace elements and vitamin solutions were same as explained in section 2.2.1.

A stock glucose solution was prepared from D-Glucose with a final concentration of 700 g. L<sup>-1</sup>. The solution was sterilized at 121 °C for 20 min. and used for pre-cultures with an initial concentration of 20 g. L<sup>-1</sup>.

## 2.3. Pre-Cultures

### 2.3.1. Preparation of working plates

A drop from a stock strain cryotubes was streaked onto Petri dishes containing YPD medium supplemented with 20 g. L<sup>-1</sup> agar. The culture was cultivated for 48 hours at 28 °C and 72 hours at 30 °C for the strains W29 and JMY3501, respectively. The plates were stored at +4 °C. These cultivated cells were used for inoculation of pre-cultures.

### 2.3.2. Preparation of inoculums

Three sequences of pre-culture were carried out in order to obtain yeast inoculums.

An isolated colony from Petri dish was inoculated to 5 ml YPD liquid medium in a sterile tube under laminar flow hood and was incubated for 12-14 hours at 28 °C at 110 rpm.

After the incubation time, 3 ml YPD culture (Table 2.1) transferred into 0.25 L sterile baffled flask containing 27 ml pre-culture medium of mineral salts Table 2.2 or Table 2.6, trace elements in Table 2.3, vitamins in Table 2.4 and glucose solutions in Table 2.5. The culture was incubated for 10 hours at 28 °C at 110 rpm.

After the second incubation time, 15 ml of cell culture transferred into 1 L sterile baffled flask and containing 135 ml growth medium of mineral salts in Table 2.2 or Table 2.6, trace elements in Table 2.3, vitamins in Table 2.4 and glucose solutions in Table 2.5. The culture incubated for 10 hours at 28 °C at 110 rpm.

3-4 drop of polypropylene glycol (PPG2000) antifoam agent was added to the second and third pre-cultures. The final pre-culture was used to inoculate the culture. Different pre-culture volumes were adjusted according to initial fermentation volume with the amount of 10 % (v.v<sup>-1</sup>) inoculums.

## **2.4. Bioreactor**

### **2.4.1. General description of bioreactor**

Fed-batch experiments were conducted in two different bioreactors.

3 L stirred tank bioreactor with an initial volume of 1.5 L using the BIOSTAT® B. Braun Biotech International (Sartorius AG, Germany).

5 L stirred tank bioreactor with an initial volume of 3 L using the BIOSTAT® B-DCU B. Braun Biotech International (Sartorius AG, Germany).

During the experiments, online acquisition of control parameters such as pH, temperature, partial pressure of dissolved oxygen, stirring rate, airflow rate, relative pressure, addition of acid/base solutions and antifoam agent were monitored and regulated with MFSC/win2.0 software.

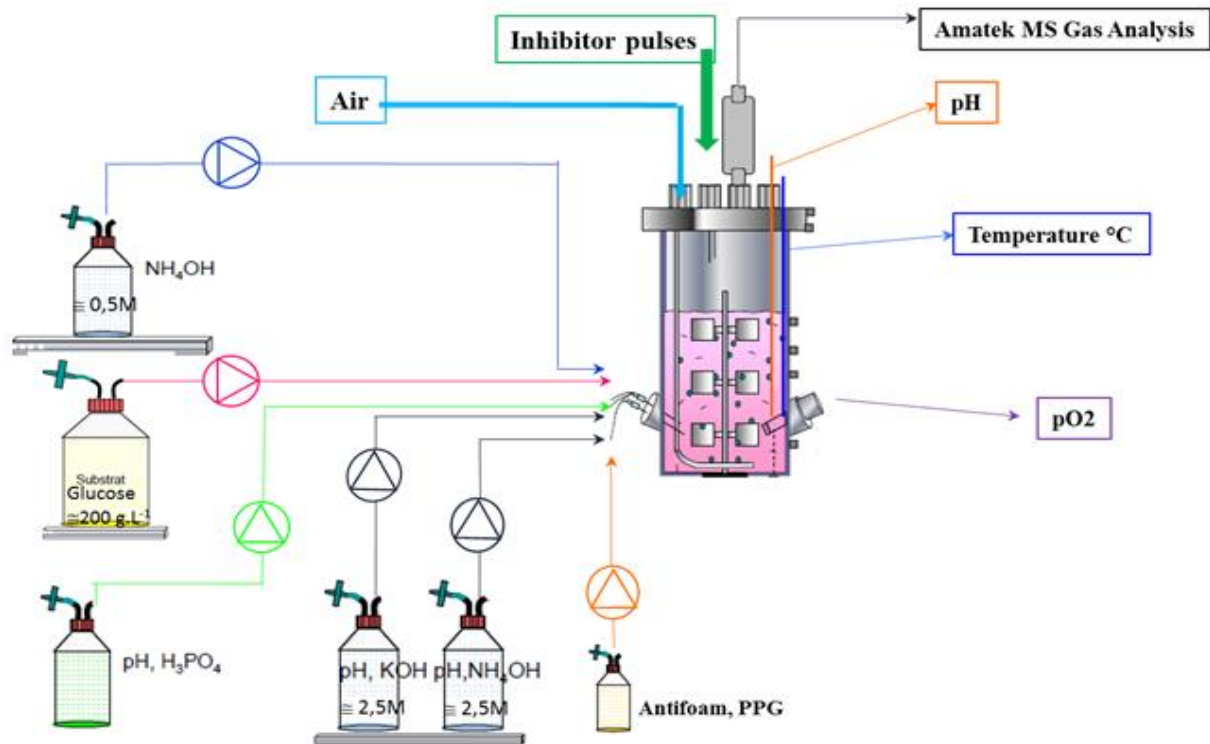


Figure 2.1. General Design for fed-batch cultures

The temperature was controlled at 28 °C with water-jacket. The pH was kept constant at 5.6 with the automatic additions of acid/base solutions and monitored by a pH probe (Mettler-Toledo International Inc.). The relative pressure in the bioreactor was maintained at 300 mbar. Foaming was prevented by addition of polypropylene glycol (PPG) antifoam agent. In order to avoid oxygen limitation, bioreactor was flushed with air and stirred with Rushton turbines to maintain dissolved oxygen above 20 % of saturation and measured with an autoclavable probe (InPro 6000/Optical O<sub>2</sub> sensor Mettler-Toledo International Inc.). Inlet and outlet air were passed through a 0.2 µm sterile polyamide membrane filter and compositions of inlet and outlet gas were analysed with a mass spectrometer (Dycor Proline Process Mass Spectrometer, AMETEK Inc.).

The fed-batch cultures were supplied with sterile feeding solutions (glucose, ammonia, acid/base solutions) via pre-calibrated peristaltic pumps (Watson-Marlow). Concentration of glucose feeding solution was determined precisely from the density of the solution (DE40 Density Meter Mettler-Toledo International Inc.). The mass flow rates of all feeding solutions supplied to bioreactor during the experiment time were determined on-line with 0.1 to 0.01 gram precisions using digital scales (Sartorius AG) and generated data were obtained via LabVIEW data acquisition software (International Instruments Cor.).

Sterile vitamin (Table 2.4) and trace element solutions (Table 2.3) were added to the culture for each 10 g. L<sup>-1</sup> biomass production during fermentation time. Culture volume was estimated by taking into account of mass flow rates of feeding solutions, all pulses and sampling volumes.

#### 2.4.2. Culture design and strategy

The fed-batch culture was divided into three phases according to a feeding strategy.

Growth phase: After the inoculation of bioreactor, a sterile glucose solution at a concentration of 200 g. L<sup>-1</sup> was exponentially fed with a peristaltic pump to maintain constant the specific growth rate ( $\mu_{expo}$ ) at  $0.18 \pm 0.2$  h<sup>-1</sup>. The nitrogen source was supplied by sterile 2.5 M ammonia solution (NH<sub>4</sub>OH) which was also used for pH regulations.

Profile of glucose feeding rate ( $Q_{glc(t)}$ ) was calculated according to equations 2.1.

---


$$Q_{glc} = \frac{\mu_{expo} \cdot X_0 \cdot V_0}{Y_{s,x} \cdot (S_{fed} - S_0)} \exp(\mu_{expo} \cdot t) \quad (\text{Eq.2.1})$$


---

where,

$V_0$  = Initial volume of the reactor (L)

$X_0$  = Initial biomass concentration in the reactor (g. L<sup>-1</sup>)

$S_{fed}$  = Concentration of glucose feeding solution (g. L<sup>-1</sup>)

$S_0$  = Targeted residual glucose concentration in the reactor (g. L<sup>-1</sup>)

$Q_{glc}$  = Glucose feeding flow rate (L. h<sup>-1</sup>)

$Y_{s,x}$  = Biomass yield (g<sub>biomass</sub>·g<sub>glucose</sub><sup>-1</sup>)

Transition phase: When biomass concentration reached approximately 2 g. L<sup>-1</sup>, the pH corrector solution was switched to a sterile 2.5 M potassium hydroxide (KOH) solution.

Limitation phase: When the nitrogen source was depleted in culture medium, 0.3M sterile NH<sub>4</sub>OH solution was fed exponentially to the reactor with a peristaltic pump in order to maintain a constant residual growth rate ( $\mu_{production}$ ) at 0.02 h<sup>-1</sup>. Concomitantly the feeding profile of glucose was modified in order to maintain a constant N/C molar ratio of 0.03 Nmol.Cmol<sup>-1</sup>.

Profile of nitrogen source flow rate ( $Q_{N(t)}^{Lim}$ ) was calculated according to equations 2.2.

---


$$Q_{N(t)} = \frac{\mu_{prod} \cdot x_{(t)}^{Lim} \cdot v_{(t)}^{Lim}}{y_{N,x} \cdot (N_{fed} - N_{(t)})} \exp(\mu_{prod} \cdot t) \quad (\text{Eq.2.2})$$


---

where,

$V_0$  = Initial volume of the reactor (L)

$X_0$  = Initial biomass concentration in the reactor (g. L<sup>-1</sup>)

$S_{fed}$  = Concentration of glucose feeding solution (g. L<sup>-1</sup>)

$S_0$  = Targeted residual glucose concentration in the reactor (g. L<sup>-1</sup>)

$Q_{glc}$  = Glucose feeding flow rate (L. h<sup>-1</sup>)

$Y_{S,x}$  = Biomass yield (g<sub>biomass</sub>·g<sub>glucose</sub><sup>-1</sup>)

$V_{(t)}^{Lim}$  = Volume of the reactor onset of nitrogen limitation phase (L)

$X_{(t)}^{Lim}$  = Biomass concentration in the reactor onset of nitrogen limitation phase (g. L<sup>-1</sup>)

$N_{fed}$  = Concentration of ammoniac solution (M)

$N_{(t)}$  = Residual nitrogen source in the reactor (M)

$Q_{N(t)}$  = Nitrogen source feeding flow rate (L. h<sup>-1</sup>)

$Y_{N,x}$  = Theoretical biomass yield (g<sub>biomass</sub>·mol<sub>Nitrogen</sub><sup>-1</sup>)

## 2.5. Inhibitory Molecules

According to the selected amount of inhibitory molecules on dry cell weight (mg Inhibitor. g<sup>-1</sup><sub>DCW</sub>), the required quantity of the molecule were weighed and dissolved in an organic solvent and aseptically added to the culture. In order to avoid chemical degradation of the compounds in organic solvents and to provide compound stability, the solutions were prepared before the application time. The molecules were dissolved either in dimethyl sulfoxide (DMSO, PanReac AppliChem) or in absolute ethanol (VWR International)

according to culture strategy. The maximum solubility of the molecules provided by manufacturer's instructions for each solvent was shown in Table 2.7. Triclosan was purchased from Sigma-Aldrich; cerulenin and orlistat were provided from EnzoLife Sciences.

<b>Molecule</b>	<b>CAS number</b>	<b>Molecular Weight (g/mole)</b>	<b>Ethanol (mg molecule. 1ml<sup>-1</sup> solvent)</b>	<b>DMSO (mg molecule. 1ml<sup>-1</sup> solvent)</b>
Cerulenin	17397-89-6	223.27	20	25
Orlistat	96829-58-2	495.73	20	10
Triclosan	3380-34-5	289.54	130	Poorly soluble (3.5)

## 2.6. Analytical Methods

### 2.6.1. Determination of biomass concentration

In order to evaluate yeast growth, biomass concentration was measured by a turbidimetric method using a spectrophotometer (Hach-Lange DR3900, UK) at 620 nm ( $OD_{620nm}$ ) with a 2mm path length special optical glass cuvette (Hellma Analytics, Germany).

The dry cell weight (DCW) measurement was determined by a gravimetric method. An accurate volume of the culture (10-15 ml) was harvested and filtered on 0.45  $\mu$ m pore-sized polyamide membranes (Sartorius AG, Göttingen, Germany) which were previously dried and weighed. After the filtration, the membranes were washed with deionized water to eliminate the culture medium and then dried at 60 °C under partial vacuum of 200 mmHg (Heraeus, France) for 48 hours and weighed. The quantification of DCW was determined by the difference in membrane mass before and after the filtration and expressed in  $g_{DCW} \cdot L^{-1}$ .

Correlation between optical density ( $OD_{620nm}$ ) and DCW ( $g_{DCW} \cdot L^{-1}$ ) was found to be 1.77 for *Y. lipolytica* W29 and 2.1 for *Y. lipolytica* JMY3501. The biomass formula used to convert dry cell weight into molar carbon concentration for *Y. lipolytica* W29 was  $CH_{1.744}O_{0.451}N_{0.132}$  for a molecular weight of 24.67  $g \cdot Cmol^{-1}$  with estimation of 8 % ash (Cescut, 2009) and for *Y. lipolytica* JMY3501 was  $CH_{1.770}O_{0.440}N_{0.165}$  with a molecular weight of 26.33  $g \cdot Cmol^{-1}$ .

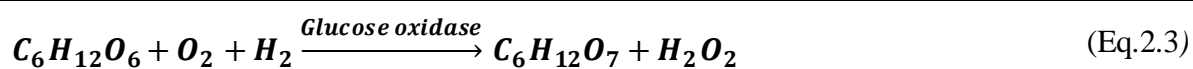
### 2.6.2. Determination of extracellular metabolites

The samples were collected during the experiments and centrifuged at 12000 g. for 4 min. using a micro centrifuge (MiniSpin Eppendorf®, US) with Eppendorf tubes (Sorenson, Bioscience, US). Culture supernatants were separated from the cell pellet and were kept

frozen at -20 °C in order to quantify extracellular metabolites and substrate (glucose) concentrations by high-performance liquid chromatography (HPLC). The determination of glucose concentration from culture supernatants was also performed by YSI method during the experiments.

### 2.6.2.1. Determination of glucose concentration by YSI

Glucose concentration was quantitated by an enzymatic method with an YSI analyzer model 27 A (YSI Life Science, Yellow Springs, Ohio, USA). The principle of the YSI analyzer is based on the detection of hydrogen peroxide ( $H_2O_2$ ) by an immobilized enzyme system. Glucose ( $C_6H_{12}O_6$ ) is oxidized to gluconic acid ( $C_6H_{12}O_7$ ) by glucose oxidase which is immobilized between two membrane layers: polycarbonate layer which limits the diffusion of glucose to immobilized enzyme layer and cellulose acetate layer which permits  $H_2O_2$  to reach platinum electrode (Eq.2.3). The platinum electrode releases an electron flow after the oxidation of  $H_2O_2$ , that is proportional to the  $H_2O_2$  concentration and therefore, to the glucose concentration (Eq.2.4).



After calibration, the glucose concentration was given directly in  $g \cdot L^{-1}$ . The supernatant was diluted using automatic diluter (Microlab 500, Hamilton, US) and/or manually to be in the linear range of the YSI analyzer between 0.1 to 2.5  $g \cdot L^{-1}$ .

### 2.6.2.2. Determination of organic acids and glucose concentrations by HPLC

Substrate (glucose) and extracellular metabolite concentrations such as citric acid, pyruvate, acetate, succinate and other metabolites concentrations were determined by high pressure liquid chromatography (HPLC) (DIONEX Ultimate 3000, California, USA and/or Alliance 2690, Waters, Massachusetts, US). The HPLC system was equipped with an Aminex HPX-87H<sup>+</sup> ion exchange column (300 mm x 7.8 mm) (Bio-Rad, Hercules, CA, US) coupled with a dual detection. Glucose and ethanol were detected with a refractive index detector (IR) and organic acids with a UV detector at 210 nm. The column was operated at 50 °C using a mobile phase of 5 mM  $H_2SO_4$  prepared in ultrapure water. The mobile phase was filtered by

0.20 µm pore-sized membrane filters (Sartorius AG, Göttingen, Germany) before using and run at a flow rate of 0.5 ml.min<sup>-1</sup>. The analysis time was 30-40 min. and injection volume was 20 µL for both standards and samples.

**Table 2.8.** Retention time of the target compounds

<b>Compound</b>	<b>Retention time (min).</b>	<b>Detector</b>
Glucose	11.545	RI
Ethanol	26.864	RI
Citric acid	10.105	UV
Pyruvic acid	11.800	UV
Succinic acid	14.768	UV
Acetic acid	19.070	UV

The calibration curve was obtained by the injection of standard solutions at seven different concentrations. The retention time of the each compound were listed in Table 2.8. The interested metabolites in the culture supernatant were identified by the relative retention time and concentrations were quantified by using the calibration curves of the target compound.

All chemical compounds had the highest analytical grade (Sigma-Aldrich) and ultrapure water was used for the preparation of standard solutions.

### 2.6.2.3. Determination of ammonium ion concentration

The quantification of ammonium ions concentration (NH<sub>4</sub><sup>+</sup>) in the medium was determined using the high performance ammonia ion selective electrode (ISE) following the manufacturer's instructions (Thermo Fisher Scientific, US). All apparatus and solutions required for the measurement of NH<sub>4</sub><sup>+</sup> are listed in Table 2.9.

The principle of the ISE is based on membrane separation techniques. The membrane of the ammonia ISE is hydrophobic and gas permeable. Dissolved ammonia (NH<sub>3</sub>) in the sample diffuses through the membrane until the partial pressure of NH<sub>3</sub> is the same on both sides of the membrane. ISE responds to the partial pressure of dissolved ammonia gas in the sample. The relative amount of NH<sub>3</sub> to NH<sub>4</sub><sup>+</sup> is determined by the addition of ionic strength adjuster (ISA) as a pH adjuster.

10 ml of the culture supernatant were placed in a 50 ml beaker on a magnetic stirrer and stirred at a constant rate (400 rpm). Probe was placed on the surface of the liquid to avoid any air bubbles on the membrane surface. 200 µL of ISA buffer solution was added. Electrode responses were recorded in millivolt (mV) when a stable reading was displayed.

The concentration of  $\text{NH}_4$  was determined with a calibration curve correlating the mV and the  $\text{NH}_4$  concentration in a range of  $10^{-1}$  to  $10^{-5}$  mol.L<sup>-1</sup>  $\text{NH}_4\text{Cl}$ .

**Table 2.9.** Required equipment and solutions of  $\text{NH}_4^+$  measurements

<b>Equipment</b>	
Probe	Thermo Scientific Orion high performance ammonia selective electrode
Voltmeter	Thermo Scientific Orion pH/ISE meter 710A
Membrane	Hydrophobic gas-permeable membrane (Ref:951204,Thermo Scientific)
<b>Solutions</b>	
Ammonia calibration standard	0.1 M ammonia chloride ( $\text{NH}_3\text{Cl}$ ) (Ref:951006)
Electrode filling solution	Thermo Scientific (Ref:951209)
Ionic Strength Adjuster (ISA)	(Ref:951211) 5 mol.L <sup>-1</sup> NaOH, 0.05 mol. L <sup>-1</sup> $\text{Na}_2\text{EDTA}$ , 1 g.L <sup>-1</sup> Methanol

### 2.6.3. Determination of intracellular metabolites

#### 2.6.3.1. Extraction and quantification of total lipid content

The digestion-methylation method based on Browse et al., (1986) has been applied for the extraction of total intracellular lipids which were transesterified to their fatty acid methyl esters (FAMES) with the following steps.

*Sample Preparation:* The samples were collected during the experiments and centrifuged at 3020 g for 5 min or 790 g for 10min. at 4 °C (Centrifuge 5810R, Rotor F-34-6-38, Adapters Reference 5804 775.007 and 5804 776.003, Eppendorf®, US) with Falcon™ 50 ml and/or 15 ml conical centrifuge tubes. Culture supernatants were separated from the cell pellet and were kept at -20 °C in order to quantify extracellular metabolites.

The cell pellets were washed with a 0.9 % NaCl saline solution at 4 °C and centrifuged at 790 g for 10 min at 4 °C (Centrifuge 5810R, Rotor A-4-62, Adapters Reference 5810 763.002 and 5810 755.000 Eppendorf®, US) with Falcon™ 50 ml and/or 15 ml conical centrifuge tubes. Washed cells were kept at -81 °C for at least 8 hours before lyophilisation and freeze-dried for 120 hours.

**Digestion / Methylation:** Approximately 20 mg freeze-dried cells were suspended with 2 ml of 2.5 % (v/v) Methanol / H<sub>2</sub>SO<sub>4</sub> solution containing 1 mg.ml<sup>-1</sup> antioxidant (2,6-di-tert-butyl-4-methylphenol, (BHT)). Tubes were incubated in an agitated water-bath at 85 °C for 120 min. After 120 min., sealed Pyrex tubes were kept at room temperature for the purification step.

**Purification:** 1.5 ml of 5 % NaCl (v/v) solution containing 1 mg.ml<sup>-1</sup> BHT and 2 ml of n-Hexane containing 1 mg.ml<sup>-1</sup> BHT were added and tubes were mixed 2 times for 1 minute with a vortex mixer (Multi Reax shaker, Heidolph, Germany). Samples were centrifuged at 790 g for 10 min at 4 °C (Centrifuge 5810R, Rotor A-4-62, Adapters Reference 5810 755.000, Eppendorf®, US). After centrifugation of the samples, organic phase was collected for the analysis of FAMES in a gas chromatography.

### 2.6.3.2. Identification and quantification of lipid content and composition

Collected organic phase from lipid extraction procedure were analysed in gas chromatography equipped with flame-ionization detector according to following operating conditions as summarized in Table 2.10.

<b>Table 2.10. Operating conditions of Gas Chromatograph</b>	
<b>Parameters</b>	<b>Conditions</b>
Gas Chromatograph	Agilent Hewlett-Packard 6890 Series
Column	Capillary column (CP-Select CB for FAME) Varian CP7419 (L*ID*OD*Film Thickness 50m*0,25mm*0,36mm*0.25µm)
Detector	Flame ionization detector (FID)
Carrier Gas	Nitrogen
Carrier Gas Flow Rate	20 mL.min <sup>-1</sup>
Sample volume	1 µL
Injector Temperature (°C)	270
1. Split ratio	20/1
Oven Temperature (°C)	(Table 2.11)
Detector Temperature (°C)	250
▪ H <sub>2</sub> flow rate ml.min <sup>-1</sup>	40
▪ Air Flow rate ml.min <sup>-1</sup>	450
Data Acquisition Software	Chromeleon

The identification and quantification of fatty acid methyl-esters were based on the comparison of retention times (Figure 2.2) and peak areas of serial dilutions of standard solutions.

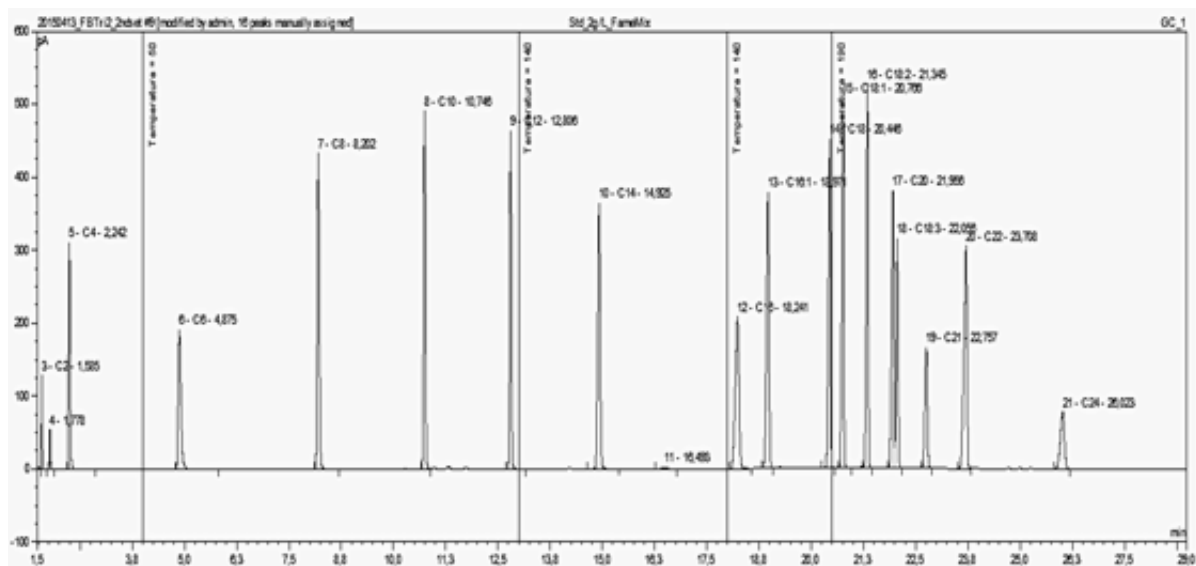


Figure 2.2. Gas chromatograph of standard FAMES solution

All samples and standard solutions were quantified by addition of Methyl heneicosanoate (C21:0) (1 mg.ml<sup>-1</sup> in n-hexane) as an internal standard with an oven temperature program Table 2.11.

Table 2.11. Oven Temperature Program

Number of Gradient	Gradient (°C. min <sup>-1</sup> )	Temperature (°C)	Hold (min)
		50	5
1	10	140	4
2	20	190	9
3	25	275	8

Individual fatty acid methyl esters, including Methyl butyrate (C4:0); Methyl hexanoate (C6:0); Methyl octanoate (C8:0); Methyl decanoate (C10:0); Methyl laurate (C12:0); Methyl myristate (C14:0); Methyl palmitate (C16:0); Methyl palmitoleate (C16:1); Methyl stearate (C18:0); Methyl oleate (C18:1); Methyl linoleate (C18:2); Methyl linolenate (C18:3); Methyl eicosanoate (C20:0); Methyl behenate (C22:0); Methyl tetracosanoate (C24:0) were dissolved in n-hexane. Six different FAMES standard solutions were prepared at concentrations of 0.01, 0.05, 0.25, 0.5, 1 and 2 mg.ml<sup>-1</sup>. The linear range of standard concentration was used to develop a calibration curve for each individual compound by which all unknown concentrations in samples were determined.

All chemical compounds and solvents used in lipid analysis had the highest analytical grade (Sigma-Aldrich).

### 2.6.3.3. Calculations of lipid accumulation and fatty acid profile

#### (i) Total and Accumulated Lipid Content

Total cell mass can be given by equation 2.5.

---

$$X_{\text{Total}} = X_{\text{Catalytic}} + L_{\text{Accumulated}} \quad (\text{Eq.2.5})$$

---

where;

$X_{\text{Total}}$  = Total dry cell weight ( $g_{\text{DCW}}$ ) measured by filtration, contains membrane lipids and accumulated lipids, expressed in grams.

$X_{\text{Catalytic}}$  = Catalytic biomass, corresponds to the biomass without accumulated lipid (only containing membrane lipids), expressed in grams.

$L_{\text{Accumulated}}$  = Accumulated lipid mass, expressed in grams.

In order to differentiate accumulated lipid mass ( $L_{\text{Accumulated}}$ ) within the cells, total lipid mass can be given as in equation 2.6.

---

$$L_{\text{Total}} = L_{\text{Catalytic}} + L_{\text{Accumulated}} \quad (\text{Eq.2.6})$$

---

where;

$L_{\text{Total}}$  = Total lipid mass quantified by GC-FID, expressed in grams.

$L_{\text{Catalytic}}$  = Constitutive lipid mass of catalytic biomass, contains mainly membrane phospholipids, expressed in grams.

During the culture time, ratio of constitutive lipid mass within the cell assumed to be constant ( $k$ ) and can be formulated as in equation 2.7.

---

$$\frac{L_{\text{Catalytic}}}{X_{\text{Catalytic}}} = k \quad (\text{Eq.2.7})$$

---

Equation 2.5 and 2.6 can be reformulated using equation 2.7 and accumulated lipid mass can be found by equation 2.8.

---

$$L_{\text{Accumulated}} = \frac{L_{\text{Total}} - k \cdot X_{\text{Total}}}{(1 - k)} \quad (\text{Eq.2.8})$$

---

#### (ii) Total and Accumulated Fatty Acid Profile

Accumulated fatty acid profile ( $L_{\text{FA,Cn}}^{\text{Acc}}$ ) for a defined Fatty Acid Cn can be formulated as in equation 2.9.

$$L_{FA\_Cn}^{Acc} = L_{FA\_Cn}^{Total} - k \cdot k'_{FA\_Cn} \cdot (X_{Total} - L_{Accumulated}) \quad (\text{Eq.2.9})$$

where,

$k'_{FA\_Cn}$  = Proportion of a defined Fatty Acid (FA\_Cn) in the catalytic biomass (obtained through the growth phase samples and quantified by GC-FID Table 2.12).

$L_{FA\_Cn}^{Total}$  = Total mass of a defined Fatty Acid (FA\_Cn)

**Table 2.12.** Proportion of fatty acid profile in the catalytic biomass of *Y. lipolytica*

k'	C12:0	C14:0	C16:0	C16:1	C18:0	C18:1	C18:2	C18:3	C20:0	C22:0	C24:0
W29	0.0001	0.009	0.08	0.02	0.06	0.54	0.20	-	0.026	0.06	-
JMY3501	0.0023	0.005	0.18	0.18	0.07	0.40	0.28	0.002	0.004	0.004	0.011

**(iii) Mass Percentages of Total and Accumulated Fatty Acid Content and Composition**

The total fatty acids (TFA %) can be expressed relatively to the total biomass as:

$$\% \text{ Total Fatty Acid} = \frac{L_{Total}}{X_{Total}} \cdot 100 \quad (\text{Eq.2.10})$$

Accumulated fatty acids (AFA %) can be expressed relatively to the total biomass as:

$$\% \text{ Accumulated Fatty Acid} = \frac{L_{Accumulated}}{X_{Total}} \cdot 100 \quad (\text{Eq.2.11})$$

Accumulated fatty acid profile (AFA<sub>Cn</sub> %) can be expressed as in equation 2.12.

$$\% \text{ Accumulated Fatty Acid Profile} = \frac{L_{AFA (Cn)}}{\sum L_{AFA}} \cdot 100 \quad (\text{Eq.2.12})$$

**2.6.3.4. Observation of lipid accumulation**

The lipid accumulation was observed by fluorescence microscopy (Olympus®BH-2 RFCA) connected to a Nikon® camera with a NiS-Elements BR v.3.2 software. Cell suspension (1 ml) was stained with 10 µL of Bodipy 493/503 (100 µg.ml<sup>-1</sup> in DMSO) as a lipid droplet marker. The mixture was incubated at 4 °C for 5 min. After 5 min of incubation the mixture was placed into slides and pictures were taken first with normal light and later with fluorescence microscopy as explained in Table 2.13. Photographs were taken during experimental time and reported in annex 1.

**Table 2.13.**Parameters of Microscopy

<b>Parameters</b>	<b>Normal light</b>	<b>Fluorescence</b>
Resolution	1280x1024 Fine-Normal	1280x1024 Fine-Normal
Quality	3840 x 3072 -8bit	3840 x 3072 -8bit
Exposition	1.5 – 30 s	20-30 ms
Contrast	Linear	Improved
Objective	x 40 oil, x100 oil	x 100

#### **2.6.4. Cell viability and cell morphology assessments by flow cytometer**

Flow cytometry provides rapid analysis of multiple characteristics at the single cell level. Characteristics that can be measured by flow cytometry include cell shape and size, cytoplasmic complexity and, by labelling with appropriate fluorochrome, physiological properties of cells such as metabolic activity, membrane integrity and cell viability can be assessed.

Flow cytometer is composed of three main parts: fluidics, optics and electronic systems. The fluidic system of flow cytometer delivers a single cell in a fluid stream to the laser beam for interrogation. Via the effect of hydrodynamic focusing, when a single cell passes through the laser beam, the optical detection system collects the scattered light and emitted fluorescence. Scattered light and fluorescence intensity obtained by optical system are converted to voltage signals by electronic system. The voltage signals can be further analysed as a function of time for morphological characterization of cells including cell size and granularity in two signal directions. Forward scatter (FSC) signal is the amount of light scattered in the forward direction with a small angle ( $0^\circ \pm 13$ ) which is proportional to the size of the cell (shape of the cell). Side scatter (SSC) signal corresponds to the light collected at large angle ( $90^\circ \pm 13$ ) which is proportional to the cell granularity. Duration of the signals (Time of flight) generated by FSC can be also correlated with cell width (length).

Flow cytometry analysis was carried out on a BD Accuri™ C6 (BD Biosciences) equipped with double laser excitations; 488 nm at 20 mW and 640 nm 14.7 mW. Two standard optical filters were used to detect fluorescence emission FL1 (530/30 nm  $\pm$  15) for green light emission at 517 nm and FL4 (>670nm) for red light emission at 660nm.

Slow flow rate (14  $\mu\text{l}\cdot\text{min}^{-1}$ ) was applied to perform the analysis with MiliQ water as sheath fluid with 10  $\mu\text{m}$  core size. Sample volume was set to 20  $\mu\text{l}$  and analysed for 1000 cells. $\mu\text{l}^{-1}$ . The threshold value was defined to 80000 on FSC to eliminate debris and background noise events. Flow Cytometry Size Calibration Kit (F-13838; Molecular probes, Inc.) was used according to manufacturer's instructions to optimize the FSC signals to cell

size. Sample data was generated using CFlow® (Accuri Cytometers, Inc.) and further data analysis was carried out with FlowJo (Tree Star, Inc.) and Sigma Plot (Systat Software Inc.) softwares.

Culture samples were collected during experimental time and centrifuged at 12000 g for 4 min. at 4 °C to pellet the cells. Harvested cell pellets washed twice in McIlvain buffer solution (McIlvaine, 1921) at pH 4 to remove traces of interfering media components from yeast suspension and centrifuged at 12000 g for 4 min. and at 4 °C and re-suspended in 1 ml buffer solution. The McIlvain buffer solution was prepared by mixing 100 mM citric acid ( $C_6H_8O_7$ ,  $H_2O$ ) and 200 mM disodium phosphate ( $Na_2HPO_4$ ,  $12H_2O$ ) and stored at 4 °C after sterilization with 0.2  $\mu m$  membrane filter. Serial dilution was applied with buffer solution to reach a cell suspension relatively  $10^6$  cells. $ml^{-1}$ . Further diluted cell suspensions prepared for untreated control, heat treated and fluorescence staining samples.

Two fluorescence dyes were used for cell viability assessments by dual staining protocol based on Monthéard et al., (2012). 5-cFDA,AM (5-Carboxyfluorescein diacetate, Acetoxymethyl ester) (Molecular probes, Inc.) is a membrane permeable, esterified fluorogenic substrate that once inside the cell undergoes hydrolysis of the diacetate groups into fluorescent carboxyfluorescein by intracellular nonspecific esterases which indicates metabolic activity and cell membrane integrity of the yeast cells. Sytox™ Red Dead Stain(Molecular probes, Inc.) is a high affinity nucleic acid stain that easily penetrates cells with damaged plasma membranes but will not cross intact cell membranes.

A stock solution of cFDA was prepared by dissolving 5 mg cFDA in 500  $\mu l$  dimethyl sulfoxide (DMSO) and 1 ml of Pluronic® F-127 reagent (20 % (w/v) solution in anhydrous DMSO) (Molecular probes, Inc.) and stored in dark at room temperature. Final concentration of dyes in  $10^6$  cells. $ml^{-1}$  cell suspension was 3.3  $\mu g.ml^{-1}$  and 5  $\mu M$  for cFDA and Sytox, respectively. The stained cell suspensions incubated in dark for 10 minutes at 37 C° and after incubation time, samples vortexed vigorously for 5-10 seconds and immediately analysed by flow cytometer.

As a 100 % dead cell control, a culture sample was collected and heat-shocked for 20 minutes at 70 °C. After incubation harvested cells were washed twice in McIlvain buffer and pelleted at 12000 g for 4 min. Cell pellets were re-suspended in buffer solution and further diluted to obtain  $10^6$  cell. $ml^{-1}$ . Cell suspension was double stained with cFDA and Sytox™

Red and re-incubated in dark for 10 minutes at 37 °C. After the incubation time sample analysed in flow cytometer.

Box plots are used to show the distribution of cell population for morphological features of yeast cells in a sample. The shape, the length and the granularity of cells were examined before and after the inhibitor pulses during the time course of the culture. Each box represents a single sample and the box itself represents the 50 % of the data (between the 25<sup>th</sup> and 75<sup>th</sup> percentiles) quantified by flow cytometry as shown in Figure 2.3. The shorter box plots suggest that overall data have a high level of agreement with each other however comparatively taller box plots suggest that the quantified data holds quite different distribution of cell population. Whiskers above and below the box indicate the 90<sup>th</sup> and 10<sup>th</sup> percentiles, respectively. While the mean represents the average value of the overall data set by taking into account of outlier values (the 5<sup>th</sup> and 95<sup>th</sup> percentiles), the median (the 50<sup>th</sup> percentile) is the number that divides the data set into two groups and is not influenced by outliers.

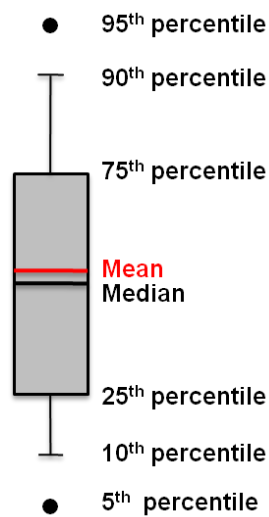


Figure 2.3.Box plot

## 2.7. Data Treatment

### 2.7.1. Mass balances for a state variable A for batch cultures

The mass balance of a state variable A can be expressed using the following statement

$$[\text{Accumulation}]_A = [\text{Inlet}]_A - [\text{Outlet}]_A + [\text{Consumption}]_A - [\text{Production}]_A$$

And can be formulated as in equation 2.13.

$$V_{liq} \cdot \frac{dA}{dt} + A \cdot \frac{dV_{liq}}{dt} = r_A \cdot V_{liq} \quad (\text{Eq.2.13})$$

where,

$V_{liq}$  is the volume of the reactor (L),

$A$  is the concentration of the state variable  $A$  (g.L<sup>-1</sup>),

$r_A$  is the net conversion rate of state variable  $A$

Since the batch reactor is operated without inlet and outlet flow ( $V_{liq} = \text{constant}$ ), the net conversion rate of the state variable  $A$  can be calculated as:

$$\frac{dA}{dt} = r_A \quad (< 0 \text{ } A \text{ is consumed; } > 0 \text{ } A \text{ is produced})$$

Specific conversion rate of state variable  $A$  ( $q_A$ ) can be calculated as:

$$q_A = \frac{r_A}{X}$$

### 2.7.2. Mass balances for a state variable $A$ for fed-batch cultures

The mass balance of a state variable  $A$  can be expressed using the following statement,

$$[\text{Accumulation}]_A = [\text{Inlet}]_A - [\text{Outlet}]_A + [\text{Consumption}]_A - [\text{Production}]_A$$

And can be formulated as in equation 2.14.

$$\frac{dAV_{liq}}{dt} = Q_{in} \cdot A + r_A \cdot V_{liq} \quad (\text{Eq.2.14})$$

The volume of the reactor in fed-batch culture is not constant and the volumetric rate and specific rate of state variables can be calculated as in Table 2.14.

**Table 2.14.** Calculations of the volumetric and specific rates of state variables for fed-batch culture

State Variables	The volumetric rates (g. L <sup>-1</sup> . h <sup>-1</sup> )	The specific rates (g. g <sup>-1</sup> . h <sup>-1</sup> )
Substrate (S)	$r_S = \frac{1}{V_{liq}} (Q_{in} \cdot S_{resc} - \frac{d(V_{liq} \cdot S)}{dt})$	$q_S = \frac{r_S}{X}$
Biomass (X)	$r_X = \frac{1}{V_{liq}} \cdot \frac{d(V_{liq} \cdot X)}{dt}$	$\mu = \frac{r_X}{X}$
Product (P)	$r_P = \frac{1}{V_{liq}} \cdot \frac{d(V_{liq} \cdot P)}{dt}$	$q_P = \frac{r_P}{X}$

### 2.7.3. Data Smoothing

In order to obtain a better understanding of the actual developments of each variable, experimental raw data were processed with smoothing software developed in the laboratory. The measured data obtained in fed-batch cultures for the different variables were converted into cumulative mass to overcome the evolution of volume in the reactor due to the additions or sample withdrawals.

Data smoothing is performed by fitting of the experimental points by polynomials over a sliding window. The smoothing provides a continuity of the values by describing the evolution of the mass of a compound over time. The derivative of the curve obtained by smoothed data was used to determine the reaction rates of the state variables.

From the smoothed data, the specific rates can be calculated as in equation 2.15.

---

$$q_c = \frac{r_c}{\bar{X}} \quad (\text{Eq.2.15})$$

---

$\bar{X}$  = The biomass concentration obtained by data smoothing, expressed as (g)

$r_c$  = The reaction rate of a state variable obtained by data smoothing, expressed as ( $g \cdot h^{-1}$ )

$q_c$  = The specific rate of a state variable, expressed as ( $g \cdot g_{biomass}^{-1} \cdot h^{-1}$ )

### 2.7.4. Gas analysis

Gas analysis determines the O<sub>2</sub>, CO<sub>2</sub>, N<sub>2</sub> and Ar gas compositions of the inlet and outlet gas flows of the reactor. The inlet and outlet gas composition of the reactor was analysed by either a mass spectrometer (Dycor ProLine Process Mass Spectrometer, AMETEK Inc.) or by an acoustic spectroscopy and magneto-acoustic spectroscopy combines a multi sampler (1309 LumaSense Technologies) with a gas analyzer (INNOVA 1313 LumaSense Technologies). The volumetric O<sub>2</sub> consumption rate and the CO<sub>2</sub> production rate were calculated from the differences between the inlet and outlet gas compositions taking into account of the evolution of the aeration rate, the liquid volume in the reactor, the temperature, the humidity and the pressure. The inlet air composition was analysed every 30 min where the outlet gas composition of the reactor was analysed every 3 minutes with a minimum gas flow of 0.5 L. min<sup>-1</sup>.

An important parameter in the fermentation processes is the respiratory quotient which is defined as the ratio of carbon dioxide production rate to the oxygen consumption rate. The precise measurement of gas compositions being fed into and removed from the reactor is an

ideal way of characterizing the physiological state of the culture. During the course of the fermentation gas analysis allow the online determination of the respiratory quotient can be simply approximated as in equation 2.16.

---


$$\mathcal{R}Q = \frac{\% \text{CO}_{2\text{out}} - \% \text{CO}_{2\text{in}}}{\% \text{O}_{2\text{in}} - \% \text{O}_{2\text{out}}} \quad (\text{Eq.2.16})$$


---

### 2.7.5. Ratio of N/C

According to the culture design and feeding strategy of fed-batch cultures rN/rC ratio (Nmol.Cmol<sup>-1</sup>) of the feeding solutions was calculated as in the equation 2.17.

---


$$\frac{rN}{rC} = \left( \frac{(N_i - N_{(i-1)}) \cdot [NH_3]}{\left( \frac{Glc_i - Glc_{(i-1)}}{\rho_{Glc} \frac{[Glc]}{MW_{Glc}^c}} \right)} \right) \quad (\text{Eq.2.17})$$


---

$N_i$ =The mass value of nitrogen feeding solution at  $i^{th}$  time (g)

$N_{(i-1)}$ =The mass value of nitrogen feeding solution at  $(i - 1)^{th}$  time (g)

$[NH_3]$  = The concentration of nitrogen feeding solution (M)

$Glc_i$  =The mass value of glucose feeding solution at  $i^{th}$  time (g)

$Glc_{(i-1)}$ =The mass value of glucose feeding solution at  $(i - 1)^{th}$  time (g)

$[Glc]$  = The concentration of glucose feeding solution (g. L<sup>-1</sup>)

$[\rho_{Glc}]$  = The density of glucose feeding solution (g. cm<sup>-3</sup>)

$MW_{Glc}^c$ = Molecular weight of glucose (g. Cmole<sup>-1</sup>)

## CHAPTER 3. RESULTS AND DISCUSSIONS

---

### 3.1. Screening Strategy of Inhibitory Molecules

#### 3.1.1. Impact of different solvent usage

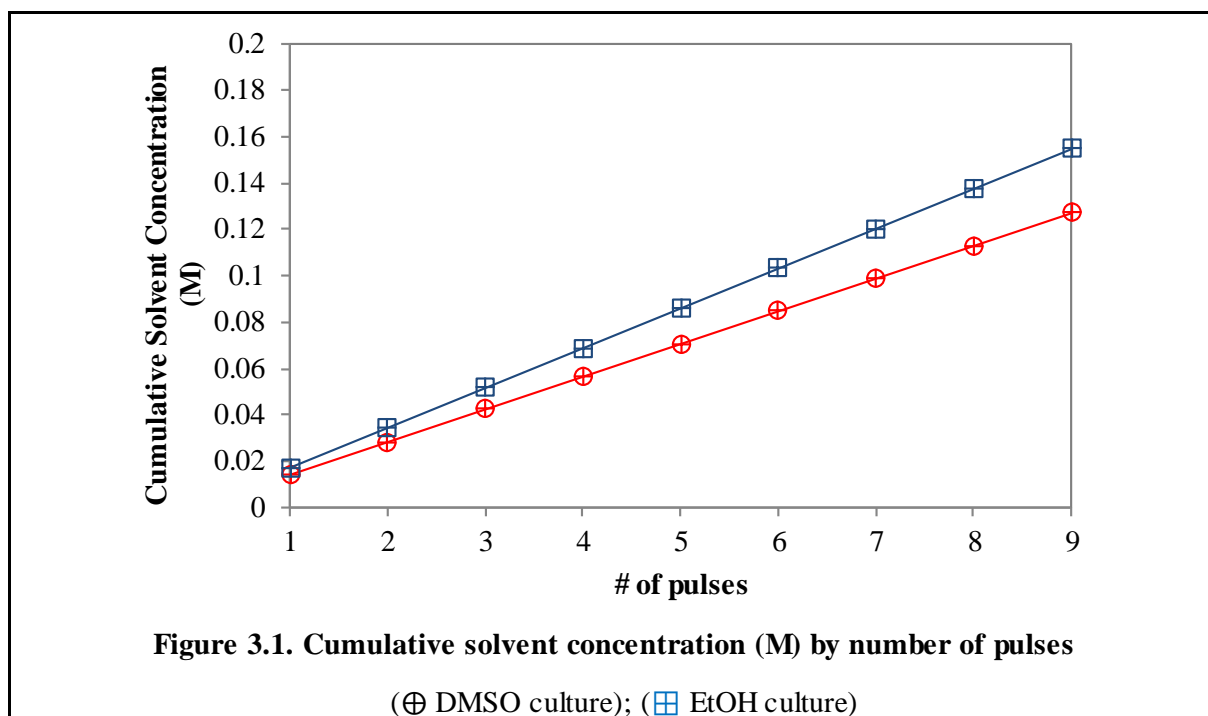
Ethanol (EtOH) and Dimethyl sulfoxide (DMSO) were selected as solvents based on their solubility efficiency on selected inhibitory molecules. The aim of this study was then to first explore the influence of ethanol and dimethyl sulfoxide on the yeast physiology when they were added to culture medium by pulses. *Y. lipolytica* W29 was chosen to identify the solvent pulse impact on fatty acid content and composition under nitrogen deficiency conditions. A reference culture was carried out without any pulse.

Three flask cultures were carried out in 2 L baffled flask with 0.5 L culture mineral medium at pH 5.6 and incubated at 28 °C and 130 rpm. *Y. lipolytica* W29 was grown on glucose as the sole carbon source and  $(\text{NH}_4)_2\text{SO}_4$  as a nitrogen source with an initial N/C molar ratio of  $0.0035 \pm 0.0003 \text{ Nmol. Cmol}^{-1}$ . This amount of nitrogen source allows a production of  $2 \text{ g. L}^{-1}$  biomass.

In order to observe the long term impacts of the solvent utilization on the physiology of *Y. lipolytica* W29, 9 pulses of the selected solvent were added to the culture medium every six hours. The first pulse was added at the deceleration growth phase and followed by 4 more pulses. At the end of 40 hours of the culture, pulses were stopped and re-added at 75 hours and followed by 3 more pulses.

Samples were collected three hours before and after the pulses to observe the influence of the solvent pulses on *Y. lipolytica* lipid metabolism.

DMSO (99.91 %) and EtOH (99.9 %) pulse volumes were less than 0.5 ml. in each pulse and Figure 3.1 shows the expected final solvent concentrations (evaporation of EtOH and DMSO was not determined and assuming no consumption took place) in the flask at the end of each pulses.



As shown in Figure 3.2 (A), first pulses of EtOH and DMSO were added during the deceleration growth phase and no inhibition was observed on the dynamics of growth. However the following DMSO pulses have a negative influence on growth compared to reference culture and reached to 2.3 g. L<sup>-1</sup> biomass concentrations at the end of first 5 pulses. In contrast, EtOH pulses had no impact on the cell growth throughout the culture time that was similar to the reference culture. Both in reference and EtOH pulse cultures, the final biomass concentration reached to 3 g. L<sup>-1</sup> at the end of the culture whereas DMSO long term pulses further inhibited cell growth with a final biomass concentration less than 2 g. L<sup>-1</sup>.

Total glucose consumption correspond to 7.7 and 11.9 g. L<sup>-1</sup> for EtOH and DMSO pulse cultures at the end of short term pulses (Figure 3.2 (B)). The concentration of ethanol in the EtOH pulse culture was determined by HPLC. Contrary to expectations as shown in Figure 3.1, the ethanol concentration in the flask increased when pulses applied, decreased when pulses stopped (between 40 h and 75 h) and re-increased thereafter when pulses re-applied as shown in the Figure 3.2 (B). The observed discrepancy on ethanol concentration could be interpreted as being a result of evaporation of ethanol.

As shown in Figure 3.2 (C), the first five pulses of DMSO pulses had no negative effect on fatty acid synthesis that was similar to reference culture whereas EtOH pulses induced strongly fatty acid synthesis. Total fatty acids (% w/w) in both DMSO and reference cultures were around 20 % g<sub>lip.</sub>·g<sup>-1</sup><sub>DCW</sub> and 26 % g<sub>lip.</sub>·g<sup>-1</sup><sub>DCW</sub> in EtOH culture.

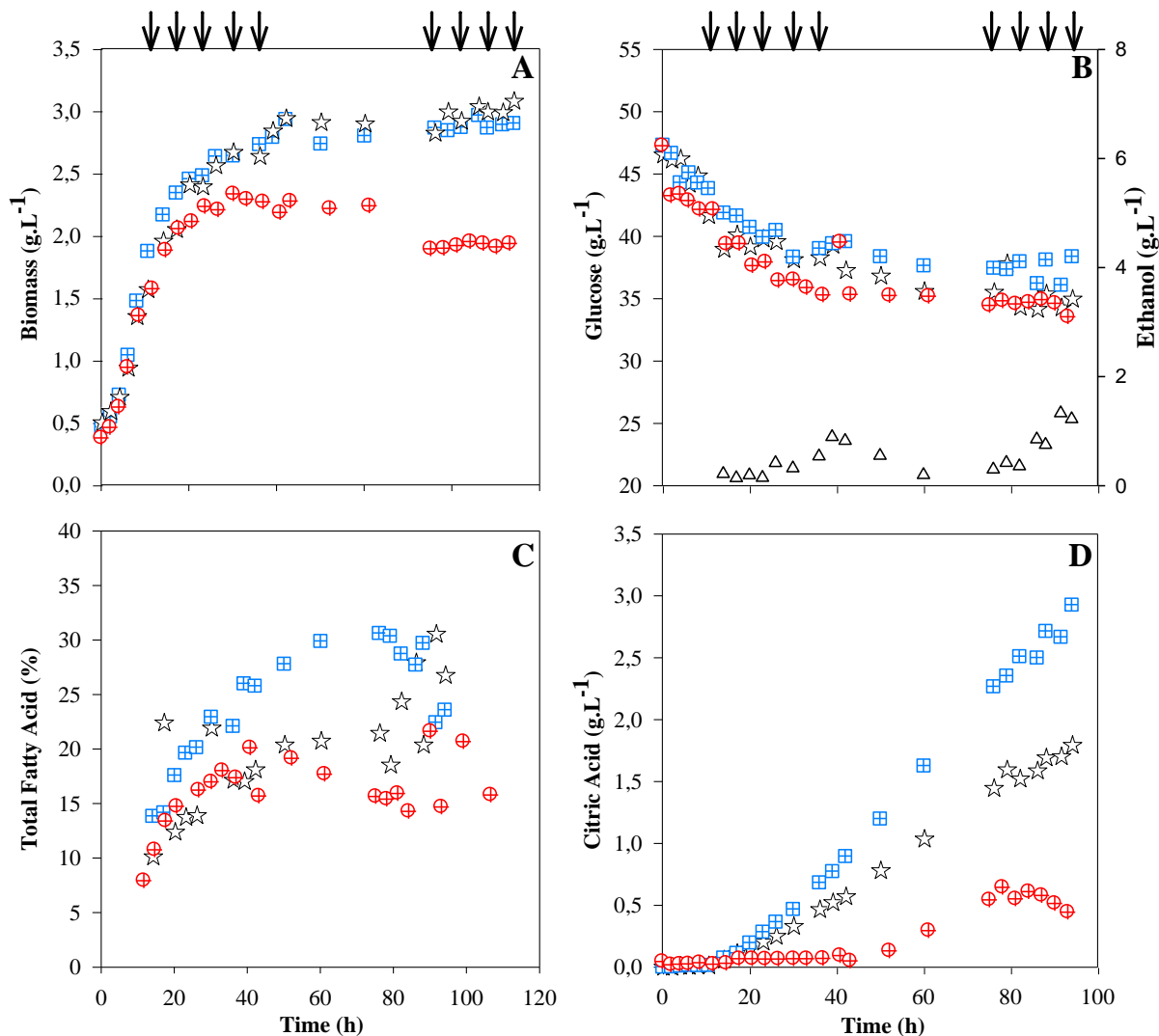


Figure 3.2 The effect of solvent pulses on *Yarrowia lipolytica* W29

(A) Calculated biomass concentrations (g. L<sup>-1</sup>); (B) Glucose and ethanol concentrations (g. L<sup>-1</sup>); (C) Total Fatty Acid content (% w/w); (D) Citric acid concentration (g. L<sup>-1</sup>).

(⊕) DMSO culture; (⊞) EtOH culture and (☆) Reference culture.

Concentration of ethanol in the EtOH culture are shown in the graph B with (△) empty triangles. Pulses were shown in arrows.

Total fatty acids decreased when pulses stopped at 40h in DMSO culture whereas in EtOH culture further increases was observed and total fatty acid content reached up to 31 % (w/w). However fatty acid synthesis ceased with long term pulses in solvent pulse cultures; DMSO pulses had only reached 16 % of total fatty acid where the last 4 pulses of EtOH showed a sharp decrease from 31 % to 24 % in total fatty acid mass percentage at the end of pulses.

As illustrated in Figure 3.2 (D), citric acid secretion was inhibited with the first group of DMSO pulses compared to reference culture. Then, citric acid concentration was increased

when DMSO pulses stopped at 40h. Similarly when pulses restarted approximately at 80h, long term DMSO pulses showed a decrease in citric acid concentration. On the contrary, EtOH pulses induce citric acid secretion compared to reference culture. Final citric acid concentrations of DMSO, EtOH and reference cultures were at 0.3 g. L<sup>-1</sup>, 3 g. L<sup>-1</sup> and 1.8 g. L<sup>-1</sup> respectively.

According to the applied strategy in this work, short term solvent pulses do not have a strong impact in terms of total fatty acid accumulation. EtOH pulses pushed the carbon flux through lipid metabolism in comparison to DMSO pulses. Even though EtOH pulses induced total fatty acid synthesis with short term pulses, no significant modification was observed in the fatty acid composition with short and long term pulses of *Y. lipolytica* W29 under nitrogen deficiency conditions as shown in Figure 3.3.

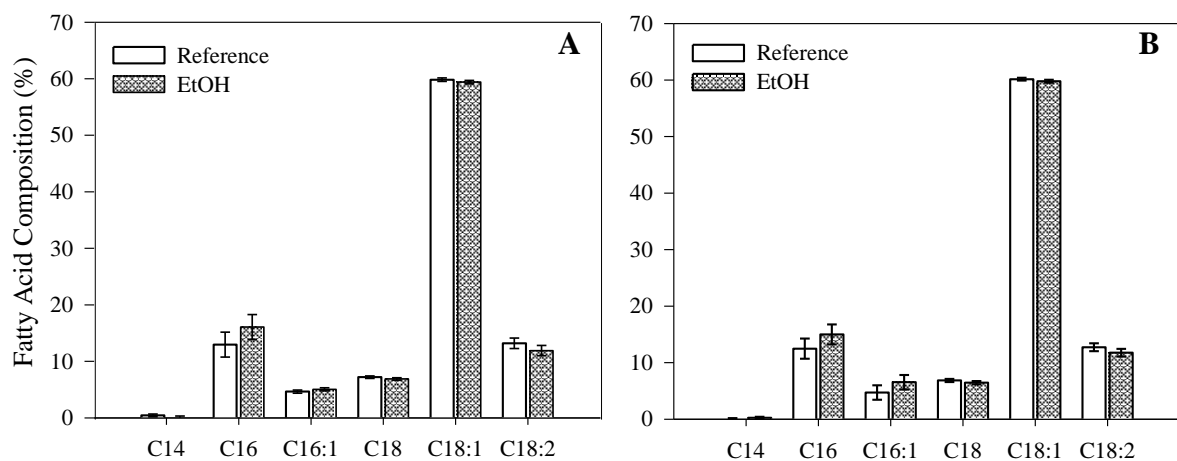


**Figure 3.3. Total Fatty Acid Composition (% w/w) of *Y. lipolytica* W29 under nitrogen deficiency conditions with and without ethanol pulses**

**(A) Short term pulse impact (first five pulse); (B) Long term pulse impact**

### 3.1.2. Preliminary screening with triclosan as a model inhibitory molecule

#### 3.1.2.1. Triclosan dissolved in Dimethyl Sulfoxide

The objective of this study was designed to assess the effect of triclosan pulses on the yeast lipid metabolism and to determine triclosan/dry cell mass ratio ( $\text{mg}_{\text{Triclosan}} \cdot \text{g}^{-1}_{\text{DCW}}$ ) for *Y. lipolytica* W29 under nitrogen deficiency conditions for further investigation in bioreactor.

Six flask cultures were carried out in 2 L baffled flask with 0.5 L culture mineral medium at pH 5.6. and cultivated at 28 °C and 130 rpm. *Y. lipolytica* W29 was grown on glucose as the sole carbon source and  $(\text{NH}_4)_2\text{SO}_4$  as a nitrogen source with an initial N/C molar ratio of  $0.0035 \pm 0.0003 \text{ Nmole} \cdot \text{Cmole}^{-1}$ .

The impact of triclosan inhibition on lipid metabolism of *Y. lipolytica* W29 in terms of citric acid secretion, lipid accumulation and fatty acid content and composition were investigated and compared with control cultures with and without solvent additions.

Four different triclosan/biomass ratios were studied from 2.6 to 15.6  $\text{mg}_{\text{Triclosan}} \cdot \text{g}^{-1}_{\text{DCW}}$  as listed in Table 3.1. Triclosan was dissolved in DMSO and added to the culture medium by pulses according to cell concentrations in the flasks at the pulse time. Solvent pulse volumes were also calculated according to the cell concentration in the solvent culture with an equivalent ratio of the highest triclosan/dry cell weight ratio ( $15.6 \text{ mg}_{\text{Triclosan}} \cdot \text{g}^{-1}_{\text{DCW}}$ ).

Table 3.1. Triclosan Doses

Cultures	$\text{mg}_{\text{Triclosan}} \cdot \text{g}^{-1}_{\text{DCW}}$	$\mu\text{mole}_{\text{Triclosan}} \cdot \text{g}^{-1}_{\text{DCW}}$
Reference Culture	-	-
Solvent Culture	-	-
1	2.6	9
2	6.5	22
3	9.1	31
4	15.6	54

In order to explore the impact of triclosan pulses on the lipid metabolism of *Y. lipolytica* W29; short and long term pulsing strategies were applied. The first pulse was added during the deceleration growth phase and followed by 4 more pulses every six hours to investigate short term pulse impact.

Approximately 40 hours after the culture time, pulses were stopped for all the flask conditions in order to evaluate the reversibility effect of this inhibitory molecule on yeast metabolism. Pulses were restarted at approximately 75 hours, to observe the influence of triclosan long term pulses on the fatty acid content and composition under nitrogen deficiency

conditions of *Y. lipolytica* W29. Samples were collected three hours before and after the pulses.

As depicted in Figure 3.4 (A), before triclosan pulses all the flask cultures exhibited same growth kinetics with a specific growth rate ( $\mu$ ) of  $0.16 \pm 0.01 \text{ h}^{-1}$ . The first pulse of triclosan has no negative impact on the cell growth. Conversely, following pulses considerably decreased cell growth compared to the reference culture. Additionally with long term pulses, increased ratios of triclosan pulses from 2.6 to 15.6  $\text{mg}_{\text{Triclosan}} \cdot \text{g}^{-1}_{\text{DCW}}$  gradually decreased the biomass concentrations from 2.2  $\text{g} \cdot \text{L}^{-1}$  (with 2.6  $\text{mg}_{\text{Triclosan}} \cdot \text{g}^{-1}_{\text{DCW}}$ ) to 1.8  $\text{g} \cdot \text{L}^{-1}$  (with 15.6  $\text{mg}_{\text{Triclosan}} \cdot \text{g}^{-1}_{\text{DCW}}$ ). Among the triclosan doses, 2.6  $\text{mg}_{\text{Triclosan}} \cdot \text{g}^{-1}_{\text{DCW}}$  pulses reached a maximum biomass concentration of 2.41  $\text{g} \cdot \text{L}^{-1}$  at around 60 h which was 17 % less than the reference culture.

Glucose consumption was not influenced by the pulses of triclosan: all the cultures showed a similar consumption trend as the reference culture as shown in Figure 3.4 (B). However compared to the reference culture citric acid formation was affected by triclosan pulses. First of all, triclosan doses performed in this study strongly reduced citric acid production which was less than 0.2  $\text{g} \cdot \text{L}^{-1}$  while the reference culture without any pulses reached a value of 0.6  $\text{g} \cdot \text{L}^{-1}$  at the end of short term pulses as shown in Figure 3.4 (D).

Citric acid secretion was also inhibited with the first group of DMSO pulses until 40 hours. However, when pulses stopped at 40 hours, citric acid secretion was induced and the concentration increased from 0.1 to 0.54  $\text{g} \cdot \text{L}^{-1}$ .

In order to observe long term triclosan pulse impact on citric acid secretion all the pulses restarted at around 80 h. From the triclosan doses performed in this study no citric acid secretion was obtained except in the culture with 2.6  $\text{mg}_{\text{Triclosan}} \cdot \text{g}^{-1}_{\text{DCW}}$  pulses which resulted in 0.37  $\text{g} \cdot \text{L}^{-1}$  citric acid at the end of the culture whereas the reference culture without any pulses reached up to 1.8  $\text{g} \cdot \text{L}^{-1}$  as illustrated in Figure 3.4 (D).

The inhibition of lipid accumulation with triclosan pulses was only observed with 15.6  $\text{mg}_{\text{Triclosan}} \cdot \text{g}^{-1}_{\text{DCW}}$  as shown in Figure 3.4 (C). Total fatty acid percentages in all the other triclosan concentration were around 20 % while the culture at 15.6  $\text{mg}_{\text{Triclosan}} \cdot \text{g}^{-1}_{\text{DCW}}$  pulses had a stronger impact on the fatty acid synthesis and resulted in 13 % (w/w) total fatty acid accumulation. The total fatty acid accumulation was altered with long term pulses: 3 h after the last three pulses there was a strong increase in total fatty acid percentages while 6 h after triclosan pulses loses its impact on the lipid accumulation.

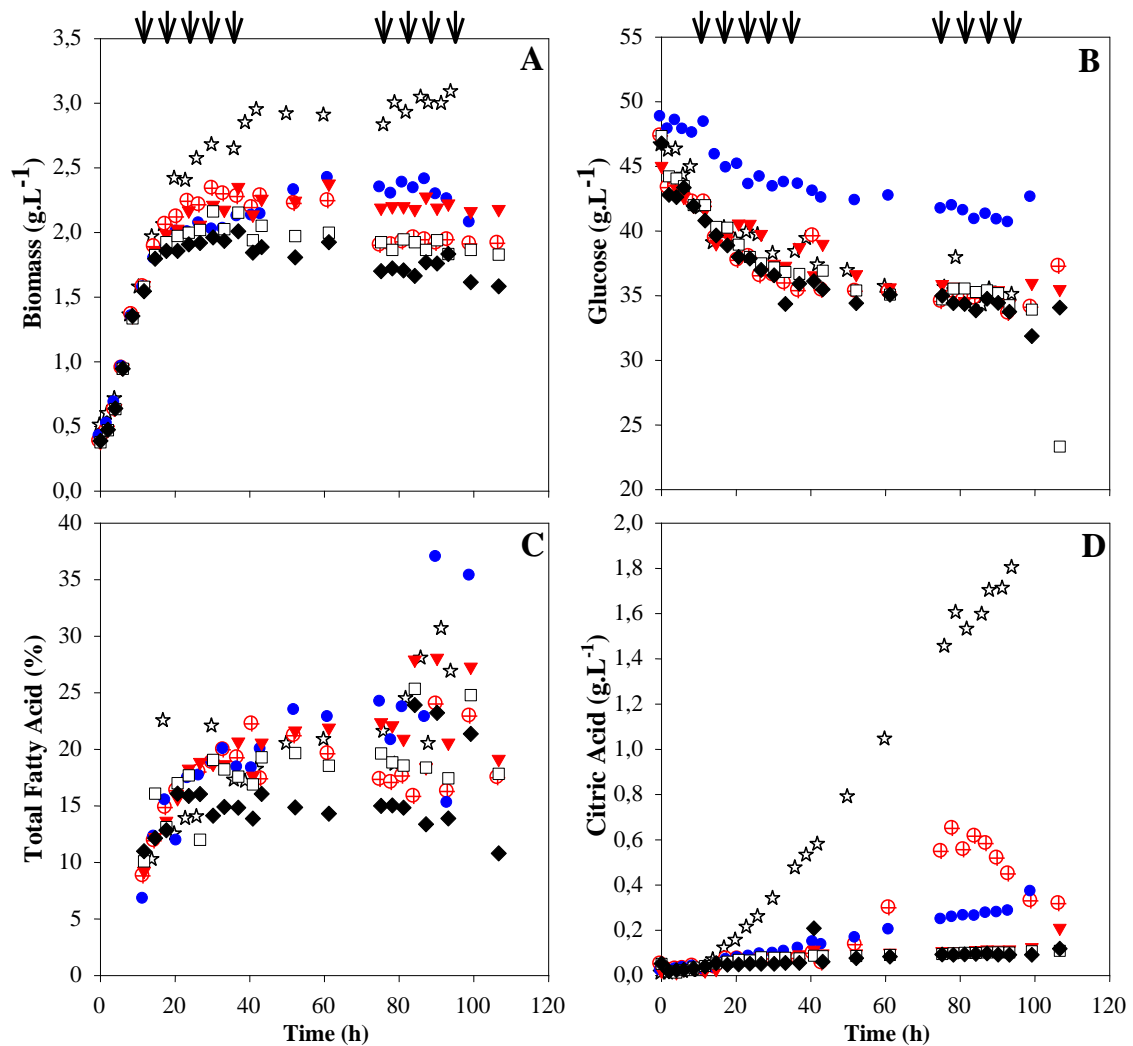


Figure 3.4. Variation of state variables versus time during triclosan pulses at different concentrations

(A) Calculated biomass concentrations ( $\text{g} \cdot \text{L}^{-1}$ ); (B) Glucose concentration ( $\text{g} \cdot \text{L}^{-1}$ ); (C) Total Fatty Acid content (% w/w); (D) Citric acid concentration ( $\text{g} \cdot \text{L}^{-1}$ ).

$\text{mg}_{\text{Triclosan}} \cdot \text{g}^{-1}_{\text{DCW}}$ : (●2.6); (▼6.5); (□9); (◆15.6); (⊕DMSO culture); (★Reference culture).

Pulses were shown in arrows.

On the other hand, slight modifications were observed in the fatty acid composition of *Y. lipolytica* W29 under nitrogen deficiency conditions with different doses of triclosan pulses. Increased triclosan ratios from 2.6 to 15.6  $\text{mg}_{\text{Triclosan}} \cdot \text{g}^{-1}_{\text{DCW}}$  (Figure 3.5A to D) gradually reduced palmitic (C16:0), palmitoleic (C16:1) and stearic acids (C18:0) whereas induced oleic (C18:1) and linoleic acids (C18:2).

Compared to the reference culture and at the end of the first group of different doses of triclosan pulses at 40 h, the fatty acid composition was mostly affected in palmitoleic (C16:1) and stearic acids (C18:0) (Figure 3.5).

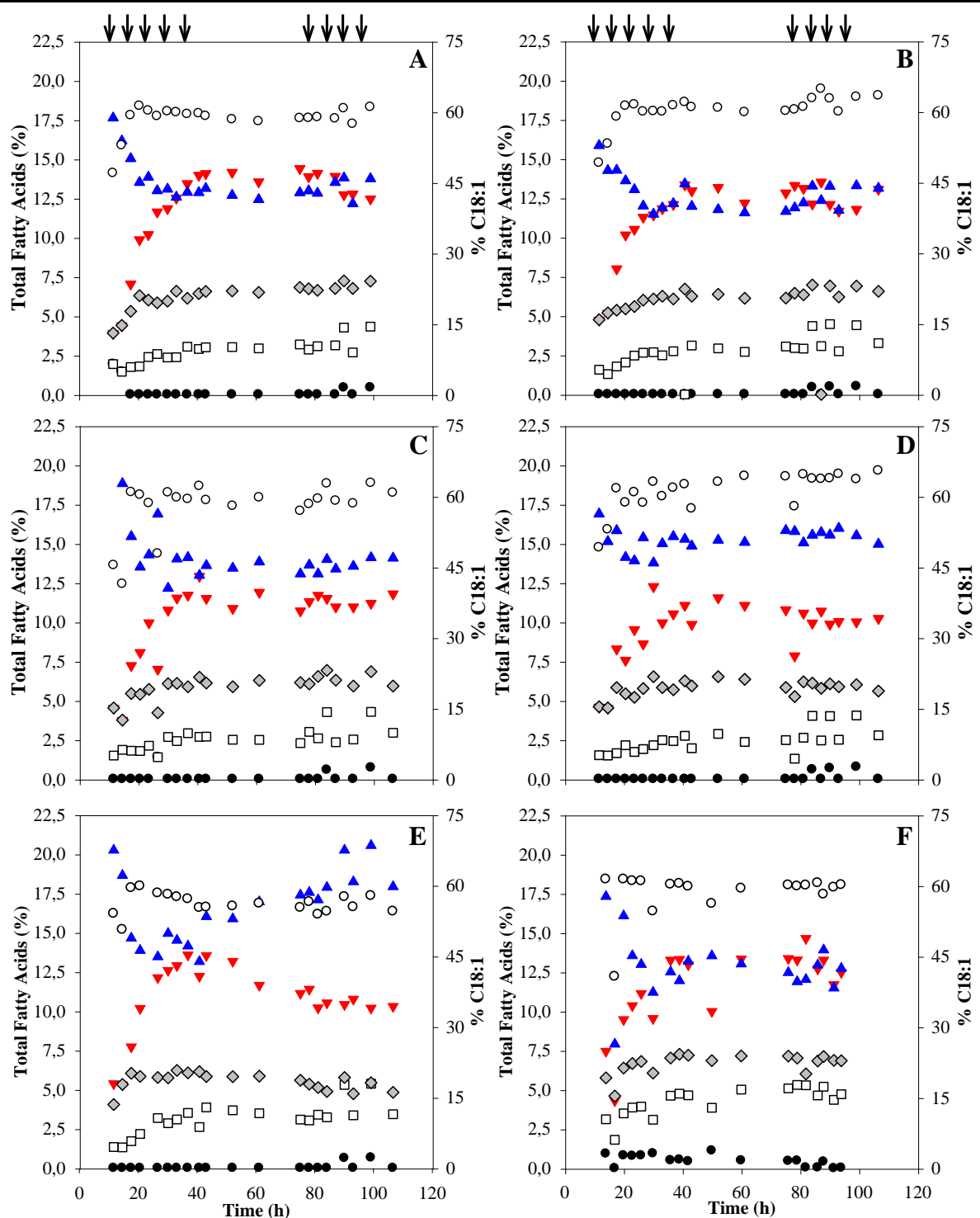


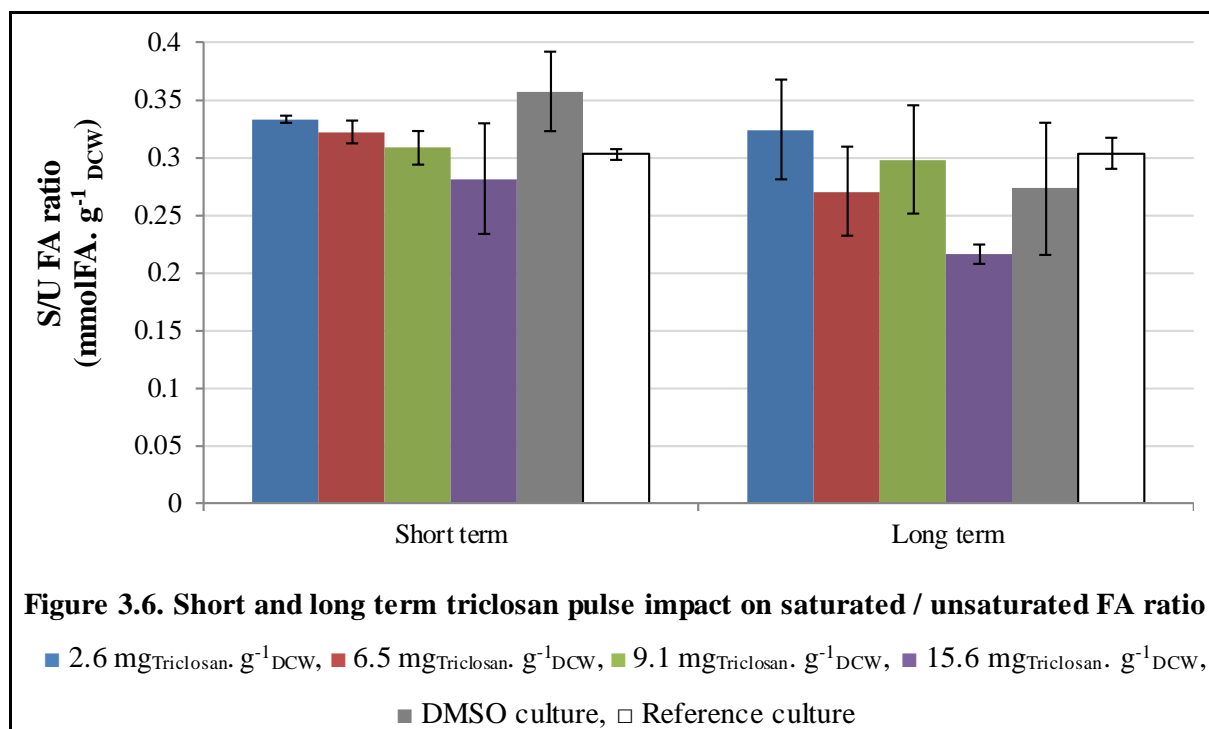
Figure 3.5. The composition of Total Fatty Acid % with triclosan pulses

(A) 2.6 mg Triclosan · g<sup>-1</sup> DCW; (B) 6.5 mg Triclosan · g<sup>-1</sup> DCW; (C) 9 mg Triclosan · g<sup>-1</sup> DCW; (D) 15.6 mg Triclosan · g<sup>-1</sup> DCW; (E) DMSO Culture; (F) Reference Culture.

Total Fatty Acids (% w/w): (● C14:0); (▼ C16:0); (□ C16:1); (◆ C18:0); (○ C18:1); (▲ C18:2). Pulses were shown in arrows.

As reported by Lentini *et al.*, “Saturated/unsaturated fatty acid ratio (S/U) is an indication of the yeast cells’ ability to modify its membrane structure to ensure cellular integrity in

response to stress conditions” (Lentini A, Rogers P, Higgins V, Dawes I, Chandler M, 2003). The S/U fatty acid ratio in reference culture without any pulses remained unchanged 0.3 mmol FA.  $g^{-1}_{DCW}$ . The S/U fatty acid ratio decreased with increased triclosan doses both in short term and long term doses as shown in Figure 3.6.



### 3.1.2.2. Triclosan dissolved in Ethanol

The objective of this study was designed to assess the effect of triclosan pulses on the yeast lipid metabolism and to determine triclosan/dry cell mass ratio (mg<sub>Triclosan</sub>. g<sup>-1</sup><sub>DCW</sub>) for *Y. lipolytica* W29 under nitrogen deficiency conditions.

Six flask cultures were carried out in 2 L baffled flask with 0.5 L culture medium at pH 5.6 and incubated at 28 °C and 130 rpm. *Y. lipolytica* W29 was grown on glucose as the sole carbon source and (NH<sub>4</sub>)<sub>2</sub>SO<sub>4</sub> as a nitrogen source with an initial N/C molar ratio at 0.0035 ± 0.0003 Nmol. Cmol<sup>-1</sup>.

Triclosan powder was dissolved in EtOH (99 %). Triclosan/dry cell weight molar ratios were kept the same as in the previous study in order to compare the impact of different solvent usage with the same inhibitory molecule and the influence of this molecule on yeast lipid metabolism of *Y. lipolytica* W29. Four different doses of triclosan/dry cell weight were performed from 2.6 to 15.6 mg <sub>Triclosan</sub>. g<sup>-1</sup><sub>DCW</sub> as listed in Table 3.2.

Table 3.2. Triclosan Doses

Cultures	mg <sub>Triclosan</sub> · g <sup>-1</sup> <sub>DCW</sub>	μmole <sub>Triclosan</sub> · g <sup>-1</sup> <sub>DCW</sub>
Reference Culture	-	-
Solvent Culture	-	-
1	2.6	9
2	6.5	22
3	9	31
4	15.6	54

Additionally two more cultures were also carried out; first one was a culture where solvent pulses were applied according to the cell concentration in the culture with an equivalent ratio of the highest triclosan/dry cell weight ratio (15.6 mg<sub>Triclosan</sub> · g<sup>-1</sup><sub>DCW</sub>) and a second one was a reference culture without any pulses.

In order to explore the influences of triclosan pulses on citric acid secretion, lipid accumulation and fatty content and composition of *Y. lipolytica* W29, short and long term pulses were applied. The first pulse was added during the deceleration growth phase and followed by 4 more pulses every six hours to investigate short term pulse impact.

Approximately 40 hours after the culture time (~36 h) pulses were stopped in all the flask conditions in order to evaluate the reversibility effect of this inhibitory molecule on yeast metabolism. Pulses were resumed at approximately 75 hours, to observe the impact of triclosan long term pulses on the lipid metabolism of *Y. lipolytica* W29 under nitrogen deficiency conditions. Samples were collected three hours before and after the pulses.

As shown in Figure 3.7 (A), all the cultures exhibited similar growth kinetics before the pulses with a maximum specific growth rate ( $\mu$ ) of  $0.16 \pm 0.007$  h<sup>-1</sup>. The first antibiotic pulse was added during the deceleration phase at around 10 hours. Increasing doses of triclosan pulses showed an impact on the biomass concentration after the second pulse of the antibiotic. Higher was the molar ratio of triclosan pulses; lower was the final biomass concentration from 2.6 to 1.7 g · L<sup>-1</sup> at the end of the culture. Solvent pulses had no impact on the cell growth throughout the culture that was similar to the reference culture without any pulses. At the end of the culture yeast cell concentrations were 2.9 g · L<sup>-1</sup> and 3.1 g · L<sup>-1</sup> for solvent and reference culture, respectively.

Similar glucose consumption trend was observed for all the cultures whereas citric acid production increased with increasing triclosan pulse concentration (Figure 3.7. B and D). Final citric acid concentration for solvent and reference cultures was 2.9 g · L<sup>-1</sup> and 1.8 g · L<sup>-1</sup>, respectively. Compared to the reference culture all the triclosan pulse ratios performed in this

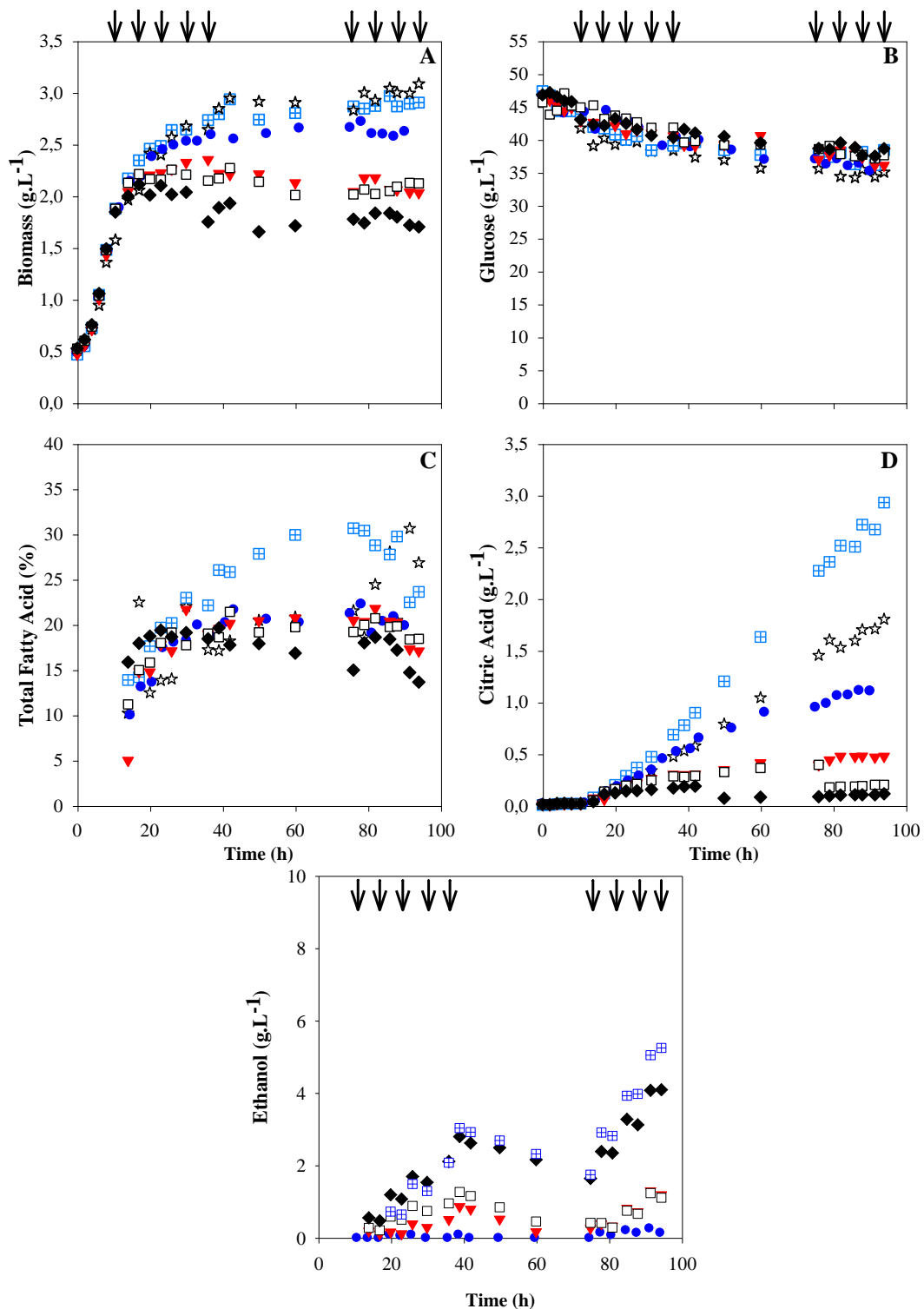


Figure 3.7. Variation of state variables versus time during triclosan pulses at different concentrations  
**(A)** Calculated biomass Concentrations ( $\text{g} \cdot \text{L}^{-1}$ ); **(B)** Glucose concentration ( $\text{g} \cdot \text{L}^{-1}$ ); **(C)** Total Fatty Acid content (% w/w); **(D)** Citric acid concentration ( $\text{g} \cdot \text{L}^{-1}$ ); **(E)** Ethanol concentration ( $\text{g} \cdot \text{L}^{-1}$ ).

$\text{mg Triclosan} \cdot \text{g}^{-1} \text{DCW}$ : (● 2.6); (▼ 6.5); (□ 9); (◆ 15.6); (◻ Ethanol culture); (★ Reference Culture). Pulses were shown in arrows.

study limited the citric acid production. Final citric acid concentration was 1.1, 0.5, 0.2, and 0.1 g.L<sup>-1</sup> for 2.6, 6.5, 9 and 15.6 mg<sub>Triclosan</sub>·g<sup>-1</sup><sub>DCW</sub>, respectively as seen in Figure 3.7.(D).

Among the triclosan doses performed in this study, below 9 mg<sub>Triclosan</sub>·g<sup>-1</sup><sub>DCW</sub> pulse ratios do not inhibit fatty acid accumulation that was around 20 % as shown in Figure 3.7. (C).

At the end of first five pulses at around 40 h total fatty acid content was 0.2, 0.2 and 0.21 g<sub>Lip</sub>·g<sup>-1</sup><sub>DCW</sub> for the triclosan pulse ratios of 2.6, 6.5 and 9 mg<sub>Triclosan</sub>·g<sup>-1</sup><sub>DCW</sub> whereas 0.17 g<sub>Lip</sub>·g<sup>-1</sup><sub>DCW</sub> was found for 15.6 mg<sub>Triclosan</sub>·g<sup>-1</sup><sub>DCW</sub>. At the same time (~40 h) total lipid content was 0.18 and 0.26 g<sub>Lip</sub>·g<sup>-1</sup><sub>DCW</sub> for reference and solvent cultures, respectively.

The ethanol concentrations in each flask with the pulses were shown in Figure 3.7. The evaluation of ethanol concentrations followed the same pattern in each flask that increased with pulses and decreased when pulses stopped and re-increased when pulses re-started. The observed decrease on ethanol concentration in the flask when the pulses stopped could be interpreted as being a result of evaporation of ethanol.

In order to observe long term triclosan pulse impact on lipid accumulation, pulses resumed at around 80 h for all the cultures. Compared to short term pulses 2, 15, 14 and 23 fold decreases were observed in total lipid content with increasing triclosan pulse ratios from 2.6, 6.5, 9, and 15.6 mg<sub>Triclosan</sub>·g<sup>-1</sup><sub>DCW</sub> at the end of long term pulses, respectively.

Figure 3.8 illustrates the analysis of total fatty acid composition of *Y. lipolytica* W29 under nitrogen deficiency conditions over time with the impact of different triclosan pulse ratios from 2.6 to 15.6 mg<sub>Triclosan</sub>·g<sup>-1</sup><sub>DCW</sub> for figures A to D and in the presence and absence of solvent pulses for figures E and F, respectively. No drastic modifications in the fatty acid composition were observed in the different cultures.

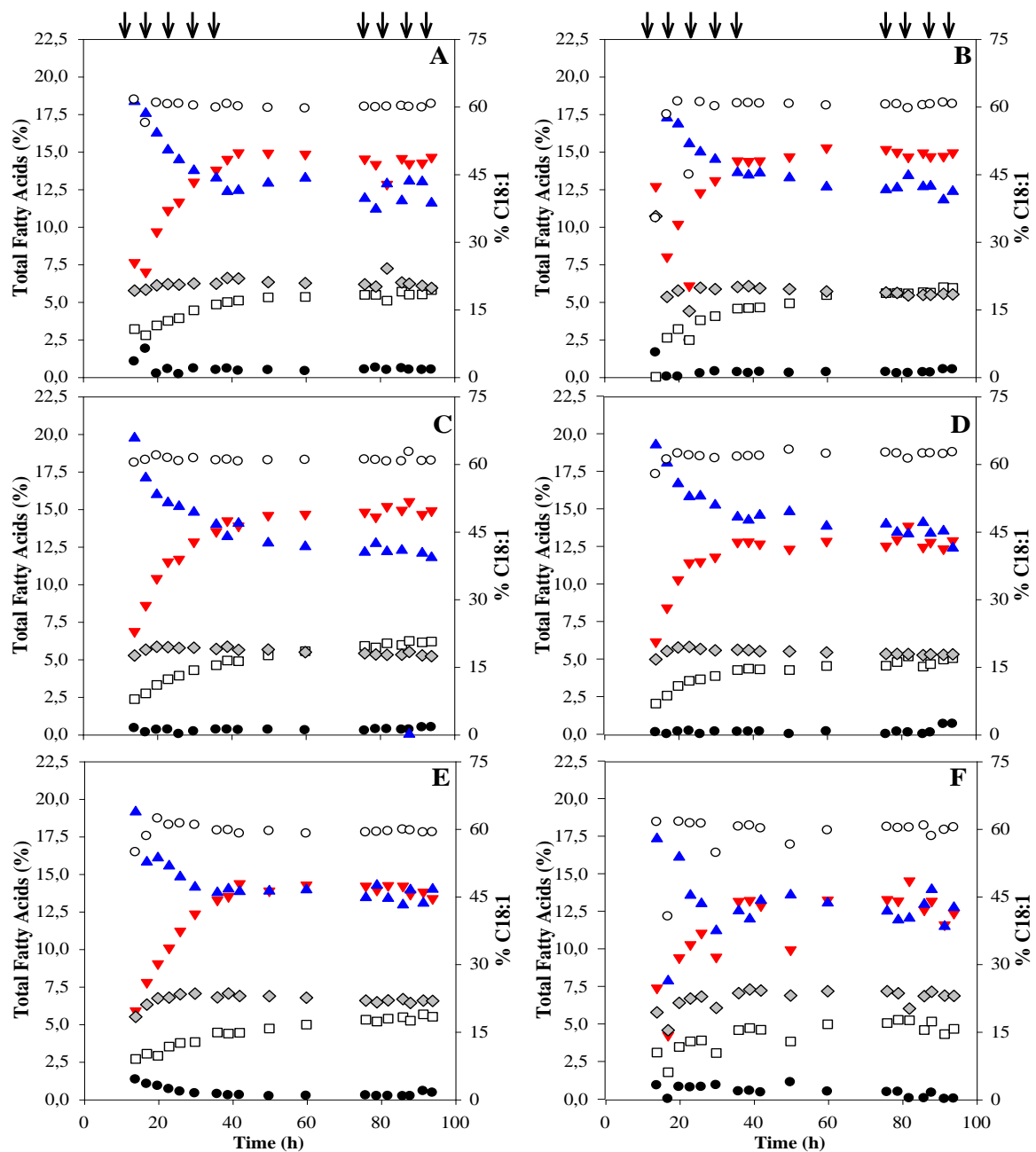
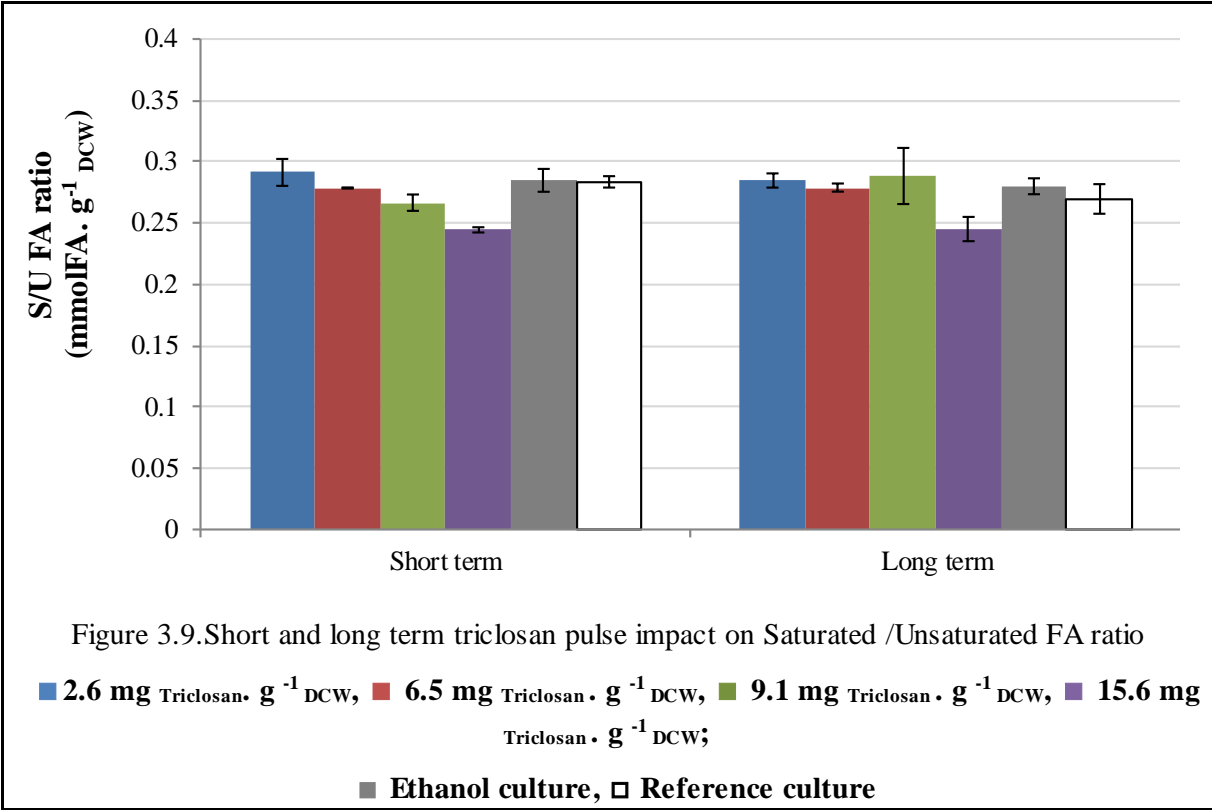


Figure 3.8. Impact of different triclosan pulse ratios(Ethanol) on the Total Fatty Acid %  
**(A) 2.6 mg<sub>Triclosan</sub>·g<sup>-1</sup><sub>DCW</sub>; (B) 6.5 mg<sub>Triclosan</sub>·g<sup>-1</sup><sub>DCW</sub>; (C) 9 mg<sub>Triclosan</sub>·g<sup>-1</sup><sub>DCW</sub>; (D) 15.6 mg<sub>Triclosan</sub>·g<sup>-1</sup><sub>DCW</sub>; (E) Ethanol Culture; (F) Reference Culture.**  
**Total Fatty Acids (% w/w): (● C14:0); (▼ C16:0); (□ C16:1); (◆ C18:0); (○ C18:1); (▲ C18:2). Pulses were shown in arrows.**

Figure 3.9 illustrates the short and long term triclosan pulse impact on the saturated / unsaturated fatty acid ratio (S/U, mmol FA. g<sup>-1</sup><sub>DCW</sub>). The S/U fatty acid ratio remained unchanged in the solvent and the reference culture  $0.28 \pm 0.01$  and  $0.27 \pm 0.01$  mmol FA. g<sup>-1</sup><sub>DCW</sub>, respectively. The saturated to unsaturated fatty acid ratio decreased slightly from 0.29 to 0.24 mmol FA. g<sup>-1</sup><sub>DCW</sub> with increased triclosan doses from 2.6 to 15.6 mg<sub>Triclosan</sub>·g<sup>-1</sup><sub>DCW</sub> at the

end of short term pulses, respectively. No further change was observed on the S/U fatty acid ratio with long term triclosan pulses.



### 3.1.3. Conclusions

This section presented the impacts of triclosan and two different solvents (ethanol and DMSO) on the growth and lipid metabolism of *Y. lipolytica* W29 on glucose under nitrogen deficiency conditions in shake flask cultures.

The results showed that the effects of solvents were very surprising and found to be dependent on the amount and the nature of the solvent. The lipidic metabolism of *Y. lipolytica* W29 was induced by using ethanol as a solvent. More citric acid excretion and more fatty acid accumulation without changing the saturated/unsaturated ratio were observed. On the other hand, DMSO reduced the metabolism by inhibiting citric acid excretion and fatty acid accumulation with a decrease on the saturated/unsaturated fatty acid ratio in the studied range.

In addition, dissolving triclosan in ethanol eliminates the benefits of the effect of ethanol and reduces the citric acid excretion and lipid accumulation without changing the saturated/unsaturated fatty acid ratio. Similarly, dissolving triclosan in DMSO reduces citric acid excretion and lipid accumulation however compensates to some extent for the decrease in the saturated/unsaturated fatty acid ratio.

Therefore, ethanol was chosen as solvent for the following experiments in bioreactor: for its less negative impact on fatty acids, biomass and for its more friendly characteristics in terms of toxicity towards the experimentator.

## 3.2. Strain Characterization of *Yarrowia lipolytica*

### 3.2.1. Modulation of the metabolic shift from oxidative metabolism to lipid accumulation and citric acid production in *Yarrowia lipolytica*

The strain of *Y. lipolytica* JMY3501 has been genetically modified in order to enhance the lipid accumulation. The conditions for obtaining this strain explained in (Lazar et al., 2014) as :

The JMY3501 strain was derived from JMY1233 as shown in Figure 3.10 by deleting a family of six peroxisomal acyl-coenzyme oxidases encoded by the *POX1* to *POX6* genes in *Y. lipolytica*.

The genes encoding acyl-coenzyme A oxidases are involved in the second step of  $\beta$ -oxidation pathway with different substrate specificities and activity levels thus blocking  $\beta$ -oxidation pathway by deleting the genes *POX1* to *POX6* showed no remobilization of lipids and no traces of  $\beta$ -oxidation derivatives revealed after lipid analysis (Beopoulos et al., 2008).

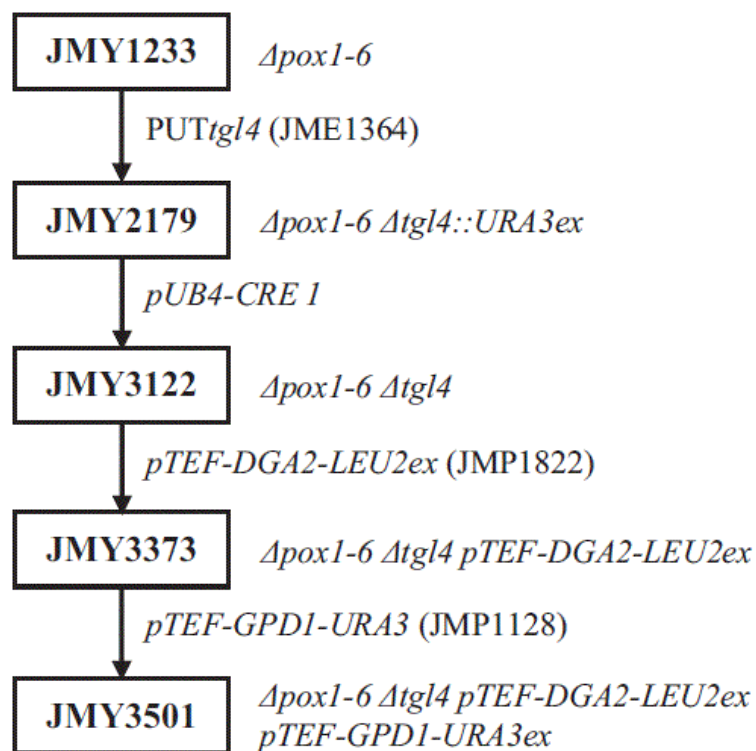


Figure 3.10. Schematic representation of the strain JMY3501 construction.

Adapted from (Lazar et al., 2014)

In *Y. lipolytica*, lipids accumulate in specialized organelles called lipid bodies are composed mostly of triacylglycerols (95 % , TAGs) ((Athenstaedt et al., 2006; Daum et al.,

1998; Dulermo and Nicaud, 2011; Mlčková et al., 2004b). In order to inhibit TAG remobilization, the gene encoding triglyceride lipase attached to the lipid bodies, *TGLA* was inactivated by introducing the disruption cassette *tgl4::URA3ex* from JMP1364 (Dulermo et al., 2013), which generated JMY2179. An excisable auxotrophic marker, *URA3ex*, was then removed from the strain JMY2179 which generated JMY3122.

Finally, to push and pull TAG biosynthesis, the mutant strain of *Y. lipolytica* JMY3501 was then obtained by successively introducing:

(i) *pTEF-DGA2-LEU2ex* from the strain JMP1822 to the strain JMY3122, the gene *yIDGA2*, which encodes the major acyl-CoA: diacylglycerol acyltransferase (Beopoulos et al., 2012);

(ii) *pTEF-GPD1-URA3ex*, from the strain JMP1128, the gene *yIGPD1*, which encodes glycerol-3-phosphate dehydrogenase (Dulermo and Nicaud, 2011) (Dulermo and Nicaud, 2011).

The *DGA2* and *GPD1* gene over-expressions, inactivated TAG remobilization and abolished fatty acid degradation ( $\beta$ -oxidation) leads to increase in lipid accumulation on sucrose (Lazar et al., 2014).

Therefore before determining the inhibitory molecules impact on fatty acid content and profile and to modulate fatty acid carbon chain length, the overproducer strain was optimized for fed-batch cultures in bioreactor in terms of lipid accumulation and citric acid production on glucose.

To evaluate the phenotype of the strain, *Y. lipolytica* JMY3501 was first characterized under nitrogen depletion with glucose as the sole carbon source and further the impact of N/C ratio on the lipid accumulation and citric acid production was determined. This study was published in *Journal of Biotechnology* 265 (2018) 40-45 (Annex):

1 **Title:**

2 **Modulation of the Glycerol Phosphate availability led to concomitant reduction**  
3 **in the citric acid excretion and increase in lipid content and yield in *Yarrowia***  
4 ***lipolytica***

5

6 **Authors:**

7 Rana Sagnak<sup>a</sup>, Sandrine Cochot<sup>a</sup>, Carole Molina-Jouve<sup>a</sup>, Jean-Marc Nicaud<sup>b</sup> and  
8 Stéphane E. Guillouet<sup>a</sup>

9 <sup>a</sup> Université de Toulouse, INSA, UPS, INP, LISBP, 135 Av. de Ranguel F-31077 Toulouse, France

10 INRA, UMR792 Ingénierie des Systèmes Biologiques et des Procédés, F-31400 Toulouse, France

11 CNRS, UMR5504, F-31400 Toulouse, France

12 <sup>b</sup>Micalis Institute, INRA, AgroParisTech, Université Paris-Saclay, 78350 Jouy-en-Josas, France

13

14 **Corresponding author: S. E. Guillouet**

15 e-mail: [stephane.guillouet@insa-toulouse.fr](mailto:stephane.guillouet@insa-toulouse.fr)

16 tel: (33)5 61 55 94 47

17 fax: (33)5 61 55 94 00

18

19 **Abstract**

20 In order to improve TriAcylGlycerol (TAG) lipids accumulation in the yeast *Yarrowia lipolytica*  
21 on glucose, double over-expression of the major acyl-CoA: diacylglycerol acyltransferase  
22 encoding gene (yIDGA2) and of the glycerol-phosphate dehydrogenase encoding gene  
23 (yIGPD1) was carried out. The genes were over-expressed in a strain impaired for the  
24 mobilization of the accumulated lipids, through the deletion of the genes encoding acyl-  
25 coenzyme A oxidases (POX1-6 genes) and the deletion of the very efficient lipase attached  
26 to the lipid bodies, encoded by yITGL4. This metabolic engineering strategy had the objective  
27 of pulling the C-flow into the TAG synthesis by increasing the availability of glycerol-3-  
28 phosphate and its binding to fatty acids for the TAG synthesis.

29 This strain showed a strong improvement in production performances on glucose in terms of  
30 lipid content (increase from 18 to 55 %), lipid yield (increase from 0,035 to 0.14 g g<sup>-1</sup>) and by-  
31 product formation (decrease in citric acid yield from 0.68 to 0.4 g g<sup>-1</sup>).

32 For developing bioprocess for the production of triacylglycerol from renewable carbon  
33 sources as glucose it is of first importance to control the C/N ratio in order to avoid citric acid  
34 excretion during lipid accumulation. Our engineered strain showed a delay in the onset of  
35 citric acid excretion as suggested by the 15 % modulation of the critical C/N ratio.

36

37 **Keywords**

38 *Yarrowia lipolytica*, lipid accumulation, fed-batch, nitrogen limitation, citric acid production,

39 DGA2

40

41

## 42 **1. Introduction**

43 *Yarrowia lipolytica* is one of the most studied "non-conventional" yeasts isolated from oily  
44 environments such as polluted soils, raw poultry or dairy products (Deak, 2001; Lanciotti et  
45 al., 2005; Sinigaglia et al., 1994; Yalcin and Ucar, 2009) classified as generally recognized  
46 as safe (GRAS) by the Food and Drug Administration (FDA, USA). It has become an  
47 important industrial microorganism due to the versatility of its metabolism to produce  
48 metabolites such as heterologous proteins (Madzak, 2015; Madzak et al., 2004; Madzak and  
49 Beckerich, 2013; Nicaud et al., 2002), lipids (Bankar et al., 2009; Beopoulos et al., 2009b;  
50 Papanikolaou et al., 2003) or citric acid (Moeller et al., 2007; Papanikolaou et al., 2002;  
51 Rymowicz et al., 2007).

52 *Y. lipolytica* belongs to the so-called oleaginous yeasts due to its ability to accumulate high  
53 amounts of lipid mainly in the form of triacylglycerol (TAG) (Ratray et al., 1975). *Y. lipolytica*  
54 is indeed able to accumulate lipids up to 43 % of its dry mass on glycerol (Papanikolaou and  
55 Aggelis, 2002) and over 50 %, wt.wt<sup>-1</sup> of total lipids, on fatty acids (Papanikolaou et al.,  
56 2003).

57 *De novo* lipid accumulation in oleaginous yeasts from osidic substrates is triggered by  
58 nutrient imbalance in the culture medium between the carbon source (in excess) and the  
59 nitrogen source in limiting concentration (although other nutrients can be identically made  
60 limiting, such as phosphorous, zinc, iron) (Fontanille et al., 2012; Granger et al., 1993;  
61 Ratledge and Wynn, 2002). Lately, it was demonstrated that double limitation of nitrogen and  
62 magnesium was essential to reach high lipid titres in wild type *Yarrowia* strain (Bellou et al.,  
63 2016). Contrarily *ex-novo* lipid accumulation (i.e. from oily substrates) approximates to a  
64 bioconversion process and therefore is independent to any nutrient imbalance (Papanikolaou  
65 and Aggelis, 2011).

66 Ratledge and Wynn (2002) proposed a general pattern of succession of the metabolic  
67 events that take place upon a N-limitation in oleaginous microorganisms (*Candida 107* and  
68 *C. utilis*, *Rhodotorula glutinis*, *Mucor circinelloides*) leading to lipid accumulation as follows:

69 drop in the adenosine monophosphate (AMP) concentration due to the activation of the AMP  
70 deaminase, inhibition of the isocitrate dehydrogenase (ICDH) by the low AMP content  
71 leading to the accumulation of isocitrate and citrate and then citrate is cleaved by the ATP-  
72 citrate lyase (ACL) into acetyl coenzyme A and oxaloacetate, the acetyl-coA is used for fatty  
73 acid synthesis by the acetyl-coA (ACC). One characteristic that differentiates oleaginous  
74 yeasts from non-oleaginous yeasts is the presence of ATP citrate lyase (ACL) (Holdsworth et  
75 al., 1988; Zhang et al., 2007), several authors have also considered that Acetyl CoA  
76 carboxylase (ACC) (Hasslacher et al., 1993; Waite and Wakil, 1962) and malic enzyme  
77 (Zhang et al., 2007) are essential for lipid accumulation. However over-expression of ME  
78 gene in *Y. lipolytica* did not result in increased lipid accumulation (Beopoulos et al., 2009a).  
79 Tai and Stephanopoulos (2013) reported that *Y. lipolytica* lacks cyto-plasmatic ME and  
80 therefore PPP is the sole source of NADPH as recently verified by Dulermo et al., (2013).

81 Several studies have shown that the metabolic shift in *Y. lipolytica* is related to a nutrient-  
82 limited medium such as nitrogen, phosphorous or magnesium (Anastassiadis et al., 2003;  
83 Bellou et al., 2016; Gill et al., 1977) or to the cultivation conditions such as growth rate,  
84 oxygen availability, pH or temperature (Finogenova et al., 1996; Il'chenko et al., 1998;  
85 Kamzolova et al., 2003; Moeller et al., 2007). One of the parameter that influences the  
86 metabolic shift is the C/N ratio (Anastassiadis et al., 2005; Sattur and Karanth, 1989). It is  
87 commonly observed in oleaginous yeasts a transient citrate excretion during the first step of  
88 lipogenesis (Boulton and Ratledge, 1983; Evans and Ratledge, 1983). However *Y. lipolytica*  
89 when cultivated on glucose as the sole carbon source, mainly produces citric acid upon  
90 nutrient limitation over lipid accumulation only 5-10 % (wt.wt<sup>-1</sup>) of TAG (Papanikolaou et al.,  
91 2006). We previously demonstrated that an accumulation of lipids without citric acid secretion  
92 was possible *Yarrowia lipolytica* wild type strain W29 as long as the C/N rate ratio was  
93 controlled below a value of 47.6 Cmol/Nmol under chemostat conditions (Morin et al., 2011;  
94 Ochoa-Estopier and Guillouet, 2014).

95 In order to improve lipid accumulation in *Yarrowia lipolytica*, a pull and push strategy was  
96 previously tested by overexpressing the acetyl-CoA carboxylase (ACC1) to push the C-flow  
97 into the FA biosynthetic pathway in combination with the over-expression of the  
98 diacylglycerol acyltransferase (DGA1), the final step of the triglyceride (TAG) synthesis  
99 pathway to pull the C-flow into the final product (Tai and Stephanopoulos, 2013). This  
100 strategy led to an increase of total lipid content from 18 to 61 %.

101 We here used a slightly different engineering strategy named as double-pull strategy. In  
102 order to increase the accumulation of lipids by pulling the C-flow into TAG synthesis, the  
103 major acyl-CoA: diacylglycerol acyltransferase encoding gene (yIDGA2) was overexpressed  
104 (Beopoulos et al., 2012) in combination with the overexpression of yIGPD1 to increase the  
105 availability of glycerol-3-phosphate for the TAG synthesis. The genes were overexpressed in  
106 a strain impaired for the mobilization of the accumulated lipids, through the deletion of the  
107 genes encoding acyl-coenzyme A oxidases (POX1-6 genes) (Beopoulos et al., 2008) and the  
108 deletion of the very efficient lipase attached to the lipid bodies, encoded by yITGL4 (Dulermo  
109 et al., 2013). Lately, Lazar and coworkers (2014) improved the lipid content to 30% (w/w) in a  
110 *Yarrowia lipolytica* on sucrose by combining this design with expression of invertase and  
111 hexokinase.

112 We, here, further evaluated the strain on glucose as the sole carbon source in terms of the  
113 dynamics of lipid accumulation and modulation of metabolic shift towards citric acid in fed-  
114 batch cultivations on glucose as the sole carbon source. This study aimed at evaluating the  
115 gain of such a strain in terms of process robustness.

## 116 **2. Materials and Methods**

### 117 2.1. Microorganism, media and growth conditions

118 The strain used in this study was *Y. lipolytica* JMY3501 obtained from the Laboratoire  
119 Microbiologie et Génétique Moléculaire, INRA, (Paris-Grignon., France) in the frame of the  
120 project common "ProBio3". Its genotype was as follows

121 MATa ura3-302 leu2-270 xpr2-322  $\Delta$ tg14  $\Delta$ pox1-6 + LEU2ex Tef-yIDGA2 + URA3ex Tef-  
122 GPD1 (Lazar et al., 2014).

123 The strain was maintained on YPD/glucose agar medium containing  $10\text{g l}^{-1}$  Yeast Extract,  
124  $20\text{g l}^{-1}$  Bactopeptone,  $20\text{g l}^{-1}$  Glucose and  $20\text{g l}^{-1}$  agar. Plates were stored at  $4^{\circ}\text{C}$ . For  
125 preparation of glycerol stocks (for cryopreservation of the cells), pure sterile glycerol was  
126 added to the culture broth to reach a final glycerol concentration of 30 % (v/v). This cell  
127 suspension (glycerol stocks) was then stored at  $-80^{\circ}\text{C}$ .

128 Precultivations were carried out on a 5-ml tube of YPD medium at  $28^{\circ}\text{C}$  for 16 h at 100  
129 rpm. The culture in growth phase was transferred into a 1-l Erlenmeyer flask containing 170  
130 ml of mineral medium at pH 5.6 prepared as follows (all compounds are expressed in  $\text{g l}^{-1}$ ):  
131  $(\text{NH}_4)_2\text{SO}_4$  3.5;  $\text{KH}_2\text{PO}_4$ , 6;  $\text{MgSO}_4$ , 2; EDTA, 0.0375;  $\text{ZnSO}_4 \cdot 7\text{H}_2\text{O}$ , 0.0281;  $\text{MnCl}_2 \cdot 4\text{H}_2\text{O}$ ,  
132 0.0025;  $\text{CoCl}_2 \cdot 6\text{H}_2\text{O}$ , 0.00075;  $\text{CuSO}_4 \cdot 5\text{H}_2\text{O}$ , 0.00075;  $\text{Na}_2\text{MoSO}_4 \cdot 2\text{H}_2\text{O}$ , 0.00005;  
133  $\text{CaCl}_2 \cdot 2\text{H}_2\text{O}$ , 0.0125;  $\text{FeSO}_4 \cdot 7\text{H}_2\text{O}$ , 0.00875;  $\text{H}_3\text{BO}_3$ , 0.0025; D-biotin, 0.00025; D-L-  
134 panthotenic acid, 0.001; nicotinic acid, 0.001; myo-inositol, 0.00625; thiamin, 0.001;  
135 pyridoxine, 0.001; para-aminobenzoic acid, 0.0002. Glucose was added to a final  
136 concentration of  $18\text{ g L}^{-1}$  with chloramphenicol at  $10\text{ mg L}^{-1}$ . After 16 h of growth at  $28^{\circ}\text{C}$  and  
137 100 rpm, 170 ml of the broth were used to inoculate 1.7 l of the same mineral medium in a 3-l  
138 bioreactor.

### 139 2.2. Chemicals used

140 The chemicals glucose, salts, oligo-elements (Carlo Erba) and EDTA (Qbiogène),  
141 orthophosphoric acid were provided by VWR, the vitamins by Sigma. All products had the  
142 highest analytical grade available.

### 143 2.3. Fed-batch cultivation in bioreactor.

144 Fed-batch experiments were performed in a 5-l stirred tank bioreactor with a working volume  
145 of 3 l using the Biostat B-DCU. Braun Biotech International (Sartorius AG, Germany) with the  
146 acquisition software MFCS/win 2.0.

147 The temperature was controlled at  $28^{\circ}\text{C}$  with water jacket. The pH was kept constant at 5.6  
148 with the automatic additions of acid/base solutions and monitored by a pH probe (Mettler-  
149 Toledo International Inc.). The relative pressure in the bioreactor was maintained at  
150 300mbar. Foaming was prevented by addition of polypropylene glycol (PPG) antifoam agent.

151 In order to avoid oxygen limitation, bioreactor was flushed with air and stirred with Rushton  
152 turbines to maintain dissolved oxygen above 20% of saturation and measured with an  
153 autoclavable probe (InPro 6000/Optical O<sub>2</sub> sensor Mettler-Toledo International Inc.). Inlet and  
154 outlet air were passed through a 0.2µm sterile polyamide membrane filter and composition of  
155 inlet and outlet gas were analysed with a mass spectrometer.

156 The fed-batch cultures were supplied with sterile feeding solutions (glucose, ammonia,  
157 acid/base solutions) via pre-calibrated peristaltic pumps (Watson-Marlow). Concentration of  
158 glucose feeding solution was determined precisely from the density of solution (DE40  
159 Density Meter Mettler-Toledo International Inc.). The mass flow rates of all feeding solutions  
160 supplied to bioreactor during the experiment time were determined on-line with 0.1 to 0.01  
161 gram precision using digital scales (Sartorius AG) and generated data was obtained via Lab  
162 VIEW data acquisition software (International Instruments Cor.).

163 Fed-batch cultures were applied following two different procedures depending on the  
164 objective of the strain evaluation: a procedure under Nitrogen depletion and a procedure  
165 under Nitrogen limitation.

#### 166 2.3.1. Fed-batch cultivation under N depleted conditions

167 The fed-batch cultivation was divided into two phases

168 *Growth batch phase:* After the inoculation of bioreactor, a batch phase was applied under  
169 non nutrient limited limitation. Glucose and ammonium sulfate concentrations were set at  
170 100gl<sup>-1</sup> and 5gl<sup>-1</sup>, respectively. The nitrogen concentration was calculated in order to produce  
171 up to 15 gl<sup>-1</sup> of biomass before reaching N-limited conditions. The pH was regulated with 9M  
172 KOH solution.

173 *N-depleted phase:* Growth phase switched naturally to N-depleted production phase when  
174 ammonium was completely exhausted. Glucose was fed by pulses of a 750gl<sup>-1</sup> sterile  
175 glucose solution when residual glucose concentration reached 20gl<sup>-1</sup> in the bioreactor. Pulse  
176 was applied in order to bring the residual glucose concentration back to 100gl<sup>-1</sup>.

#### 177 2.3.2. Fed-batch cultivation under N-limitation conditions

178 The fed-batch culture was divided in five phases according to a feeding strategy.

179 *Growth phase:* After the inoculation of bioreactor, a sterile glucose solution with at a  
180 concentration of  $200\text{g l}^{-1}$  was exponentially fed with a peristaltic pump to maintain constant  
181 the specific growth rate at  $0.18\text{ h}^{-1}$ . The nitrogen source was supplied by sterile 2.5M  
182 ammonia solution which was also used for pH regulation.

183 *Transition phase:* When biomass concentration reached approximately  $10\text{g l}^{-1}$ , the pH  
184 corrector solution was switched to a sterile 2.5M potassium hydroxide (KOH) solution.

185 *N-limited phase:* When the nitrogen source was depleted in the culture medium, 0.3M sterile  
186 ammonia solution was fed exponentially to the reactor with a peristaltic pump in order to  
187 maintain a constant residual growth rate at  $0.04\text{h}^{-1}$ . Concomitantly the feeding profile of  
188 glucose was modified in order to maintain a constant N/C molar ratio above  $0.03\text{ Nmol.Cmol}^{-1}$   
189 <sup>1</sup> in order to induce lipid accumulation without citric acid secretion as demonstrated in Ochoa-  
190 Estopier and Guillouet, 2014.

191 *N/C-decreasing phase:* After 24 hours under N-limited phase, the glucose feeding rate was  
192 accelerated without changing the ammonia feeding profile. Therefore, N-limited condition and  
193 constant specific growth rate were maintained but the N/C was gradually decreased.

194 *N/C-increasing phase:* Once citric acid was detected in the fermentation broth and the critical  
195 N/C ratio determined, the feeding strategy was reversed. The glucose feeding rate was  
196 decelerated without changing the ammonia feeding profile. Therefore, the N/C was gradually  
197 increased without changing the specific growth rate.

## 198 2.5. Off gas analysis

199 The inlet and outlet gas composition in carbon dioxide ( $\text{CO}_2$ ) and oxygen ( $\text{O}_2$ ) were  
200 measured by a fermentation gas monitor system (LumaSense technologies Europe). The  
201 system combines a multipoint sampler 1309 with a gas analyzer (INNOVA1313). Gas  
202 analysis was performed every minute during the whole experiment.  $\text{CO}_2$  production rate  
203 ( $r_{\text{CO}_2}$ ) and  $\text{O}_2$  consumption rate ( $r_{\text{O}_2}$ ) were calculated as described by Poilpre et al., 2002.  
204 The Respiratory Quotient (RQ) was calculated as the molar ratio between  $r_{\text{CO}_2}$  and  $r_{\text{O}_2}$ .

## 205 2.6. Determination of biomass

206 Yeast growth was evaluated by spectrophotometric measurements at 620 nm in a  
207 spectrophotometer (Biochrom Libra S4, UK). Growth rates were determined based on time-  
208 courses of optical density ( $OD_{620nm}$ ).  $OD_{620nm}$  was calibrated against dry cell weight  
209 measurements. The biomass formula used to convert cell dry weight into molar carbon  
210 concentration was  $CH_{1.744}O_{0.451}N_{0.132}$  for a molecular weight of  $24.67g.Cmol^{-1}$  (Ochoa-Estopier  
211 and Guillouet, 2014).

## 212 2.7. Metabolite analysis

213 The culture supernatants were analyzed by High performance Liquid Chromatography  
214 (DIONEX Ultimate 3000, USA) using an Aminex HPX-87H<sup>+</sup> column (Bio-Rad, US) and the  
215 following conditions: a temperature of 50°C with 5mM H<sub>2</sub>SO<sub>4</sub> as eluant (flow rate of 0.5 ml  
216 min<sup>-1</sup>) and a dual detection (IR and UV at 210 nm). Culture supernatant was obtained by  
217 centrifuging (MiniSpin Eppendorf, USA) the fermentation culture in Eppendorf tubes at  
218 13,000 rpm for 3 min. The supernatant was filtered on Minisart filters 0.45 µm pore-sized  
219 diameter polyamide membranes (Sartorius AG, Germany). The metabolites searched for  
220 detections and quantification was glucose, citrate, isocitrate, alpha-ketoglutarate, pyruvate,  
221 malate, succinate, fumarate, lactate and acetate.

222 The quantification of lipids was carried out by digestion as described by Browse et al., 1986.  
223 20 mg of lyophilized cells were added to 1 ml of methanol solution containing 25 ml.L<sup>-1</sup> of  
224 sulfuric acid (95%) and internal standard (C9:0). The mix in sealed tubes was placed in an  
225 80°C bath for 90 minutes. After cooling, 450 µl hexane and 1.5 ml water were added and  
226 vortexed. The lipidic phase was then sampled and the composition was analysed by Gas  
227 Chromatography as mentioned in Cescut et al., 2011. Lipid quantification was also  
228 performed by epifluorescence after staining the cells with Bodipy 493/503 in a Microplate  
229 reader (Synergy HT, Biotek, USA) as follows: the pellets were washed 3 times with PBS  
230 buffer solution (in gl<sup>-1</sup>, NaCl, 8; Na<sub>2</sub>HPO<sub>4</sub>, 1.15; KCl, 0.2; KH<sub>2</sub>PO<sub>4</sub>, 0.2; pH at 6.9-7.1) at 4°C  
231 and resuspended in the same buffer solution to a  $OD_{620nm}$  of 0.5; 1 ml of the cell suspension  
232 was mixed with 10µl of Bodipy 493/503 (100µg.ml<sup>-1</sup> in DMSO) and incubated 5 min at 4°C;  
233 the mixture was then centrifuged 3 min at 13,000 rpm and re-suspended into 1 ml PBS buffer

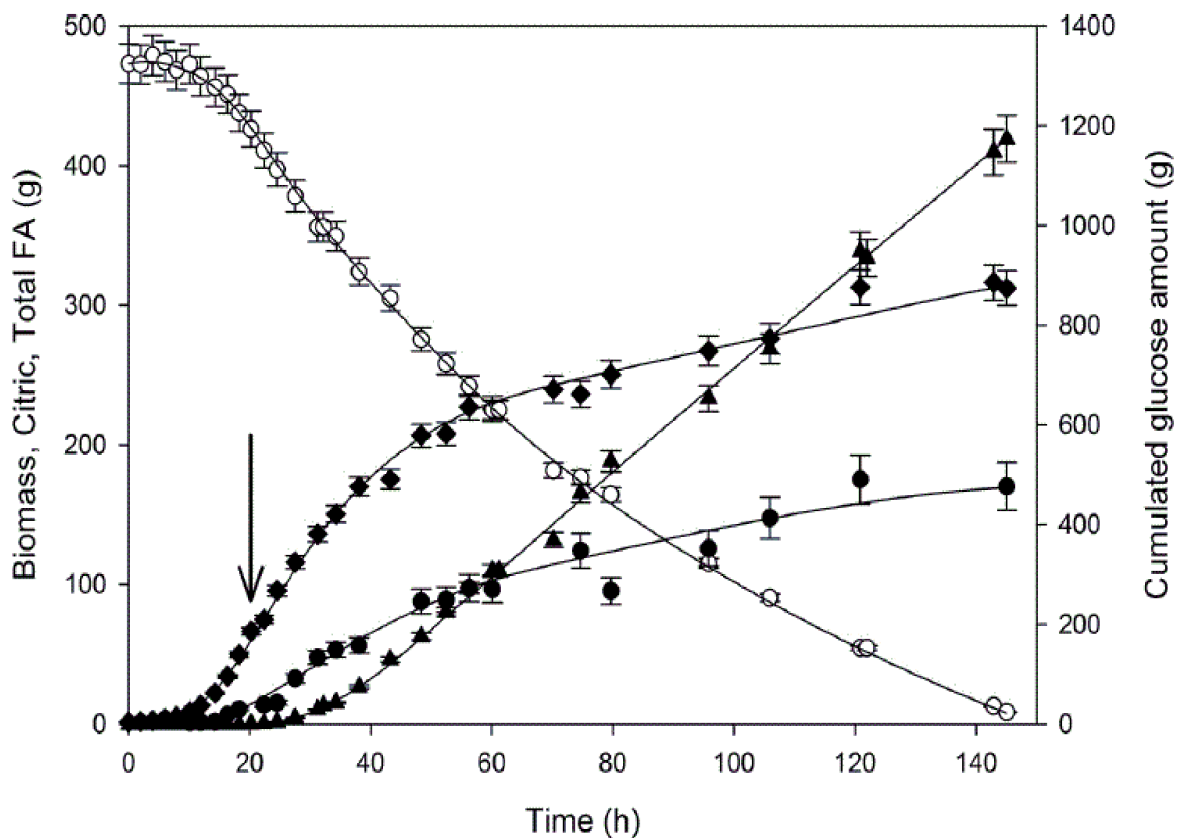
234 solution; 200  $\mu$ l of this cell suspension were placed in a 96-well Nuclon™ $\Delta$  surface Microplate  
235 and read at 528 nm with an excitation wavelength value of 428 nm. The measurements were  
236 repeated 5 times showing a standard deviation lower than 5%.

237 The quantification of residual ammonium in the medium was determined with an Orion  
238 ammonium probe (ORION Research Inc., Boston, USA) and voltmeter (ORION pH/ISE  
239 Meter, USA) as follows: 5 ml of culture broth were filtered on 0.45 $\mu$ m pore sized diameter  
240 polyamide membrane (Sartorius AG, Germany) and mixed with 200  $\mu$ l of ISA buffer solution  
241 (Ionic Strength Adjustor: NaOH, 5mol $^{-1}$ ; disodium EDTA, 0.05 mol $^{-1}$  and methanol 1 gl $^{-1}$ ).  
242 The concentration of NH<sub>4</sub> was determined with a calibration curve correlating the mV and the  
243 NH<sub>4</sub> concentration in a range of 10 $^{-1}$ -10 $^{-4}$  mol $^{-1}$  NH<sub>4</sub>Cl.

### 244 **3. Results and discussion**

#### 245 3.1. Impact of Nitrogen depleted condition on the lipid accumulation and citric acid production 246 in *Y. lipolytica* JMY3501 strain

247 The *Yarrowia lipolytica* JMY3501 strain was first evaluated in bioreactor under non nutrient  
248 limited conditions followed by a switch to Nitrogen depleted conditions in a mineral medium  
249 with glucose as the sole Carbon source (Figure 1). The first phase consisted in a batch  
250 phase under non nutrient limited conditions with an initial glucose concentration of 100g.L $^{-1}$ .  
251 The JMY3501 strain grew exponentially at a maximal specific growth ( $\mu_{max}$ ) rate of 0.24h $^{-1}$ . It  
252 was close to the  $\mu_{max}$  of the parent strain W29 grown under the same conditions ( $\mu_{max}$ =0.27h $^{-1}$ ;  
253 (Ochoa-Estopier and Guillouet, 2014). The global biomass yield on glucose was identical  
254 to the one of the parent strain at 0.49g<sub>DCW</sub>.g<sub>glucose</sub> $^{-1}$  (Ochoa-Estopier and Guillouet, 2014)  
255 pointing out no drastic impact of the engineering on the oxidative metabolism of the strain.



256

257 **Figure 1.** Fed-batch cultivation of the strain JMY3501 on mineral medium on glucose as the  
 258 sole carbon source. Evolution of masses of biomass (◆), citric acid (▲), total FA content (●)  
 259 and cumulated glucose consumed (○). Arrow indicated the time of Nitrogen depletion. Data  
 260 are presented as means ± standard deviation.

261

262 Once nitrogen was completely consumed after 20 hours of growth, metabolism switched

263 toward lipid accumulation and citric acid secretion. After 145 hours of cultivation, citric acid

264 concentration reached 70 g. L<sup>-1</sup> and the total lipid content 55 %. Comparatively, the parent

265 W29 strain cultivated under the same conditions accumulated lower lipid content of around

266 18% (Table1). Lipid content and yield on glucose were both higher in the engineered strain

267 concomitantly with a reduction in the Citric acid production yield by a factor of 1.3 and 4,

268 respectively. Lipid production yield reached a maximal value of 0.18 g g<sup>-1</sup> corresponding to

269 56% of the theoretical yield (0.32 g g<sup>-1</sup>). Improvement of lipid accumulation by the double pull

270 strategy was significant in our strain in the range of the one obtained by the push and pull

271 strategy through the overexpression of ACC1 and DGA1 (Tai and Stephanopoulos, 2013).

272 The authors reached 61% of lipid content and 0.19 g g<sup>-1</sup> of overall lipid yield (59 % of the

273 theoretical yield) with a peak at 0.27 g g<sup>-1</sup> during the highest oil production phase between 70

274 and 100h. However yields are not fully comparable due to the presence of yeast extract in  
 275 their medium. Supplementation of mineral medium with yeast extract has been reported to  
 276 slightly enhance lipid accumulation indeed (Bellou et al., 2016)

277 The increase in the lipid titer and yield observed in our engineered strain was concomitantly  
 278 accompanied with a 1.5 fold-decrease in the citric acid production in terms of overall yield  
 279 suggesting that the Carbon flow was further directed into lipid formation. The citric acid  
 280 production yield from glucose decreased from 0.68 to 0.4 g g<sup>-1</sup>. Comparatively, the ACC1-  
 281 DGA1 overexpressing strain had a citric acid yield of 0.25 g g<sup>-1</sup> during the highest lipid  
 282 production phase (Tai and Stephanopoulos, 2013).

283

284 Table1: Comparison of the strain performances under non limited and depleted Nitrogen  
 285 conditions.

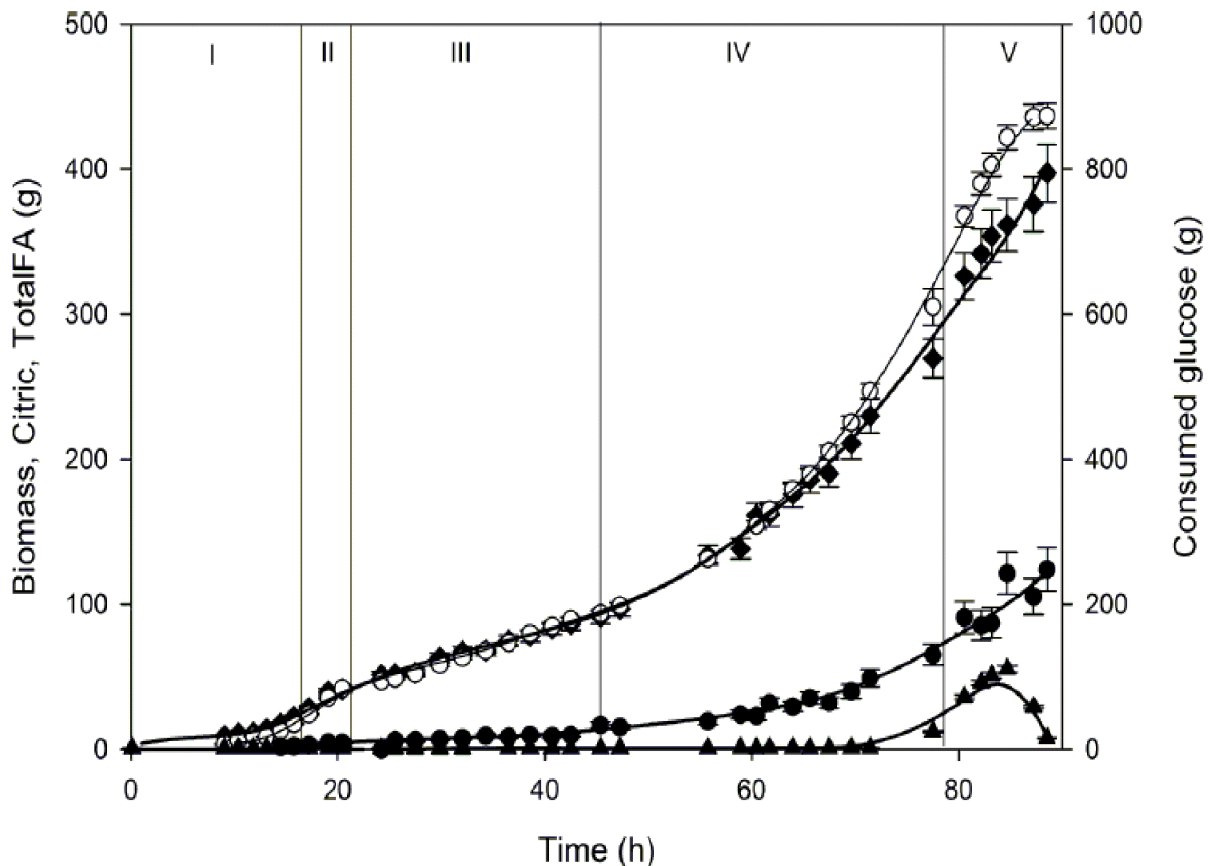
	Non limited phase		N depleted phase		
	$\mu_{\max}$ (h <sup>-1</sup> )	$Y_{\text{glc},x}$ (g g <sup>-1</sup> )	Total lipid (%)	$Y_{\text{glc},\text{lipid}}$ average/max (g g <sup>-1</sup> )	$Y_{\text{glc},\text{cit}}$ average/max (g g <sup>-1</sup> )
W29	0.27	0.49	18	0.035/0.058	0.68/0.74
JMY3501	0.24	0.49	55	0.14/0.18	0.40/0.49

286

### 287 3.2. Impact of the N/C ratio on the lipid accumulation and citric acid production in *Y. lipolytica* 288 JMY3501 from glucose as sole carbon source

289 In order to characterize the JMY3501 *Y. lipolytica* strain in terms of metabolic shift  
 290 modulation, the strain was cultivated in a 5 L bioreactor under fed-batch mode (Figure 2).  
 291 After 16 hours of controlled exponential growth phase at  $\mu=0.18$  h<sup>-1</sup>, the culture was switched  
 292 into N-limited phase at a specific C/N ratio below 33 Cmol.Nmol<sup>-1</sup> in order to induce lipid  
 293 accumulation without citric acid secretion. Ochoa-Estopier and Guillouet, 2014 previously  
 294 demonstrated under double N- and C-limitation in chemostat cultures at a dilution rate of  
 295 0.08 h<sup>-1</sup> that accumulation of lipids without secretion of citric acid was possible when C/N  
 296 ratio was maintained precisely below a critical value of 47.6 Cmol.Nmol<sup>-1</sup>. Identical critical  
 297 value was obtained in fed-batch culture as well (Morin et al., 2011).

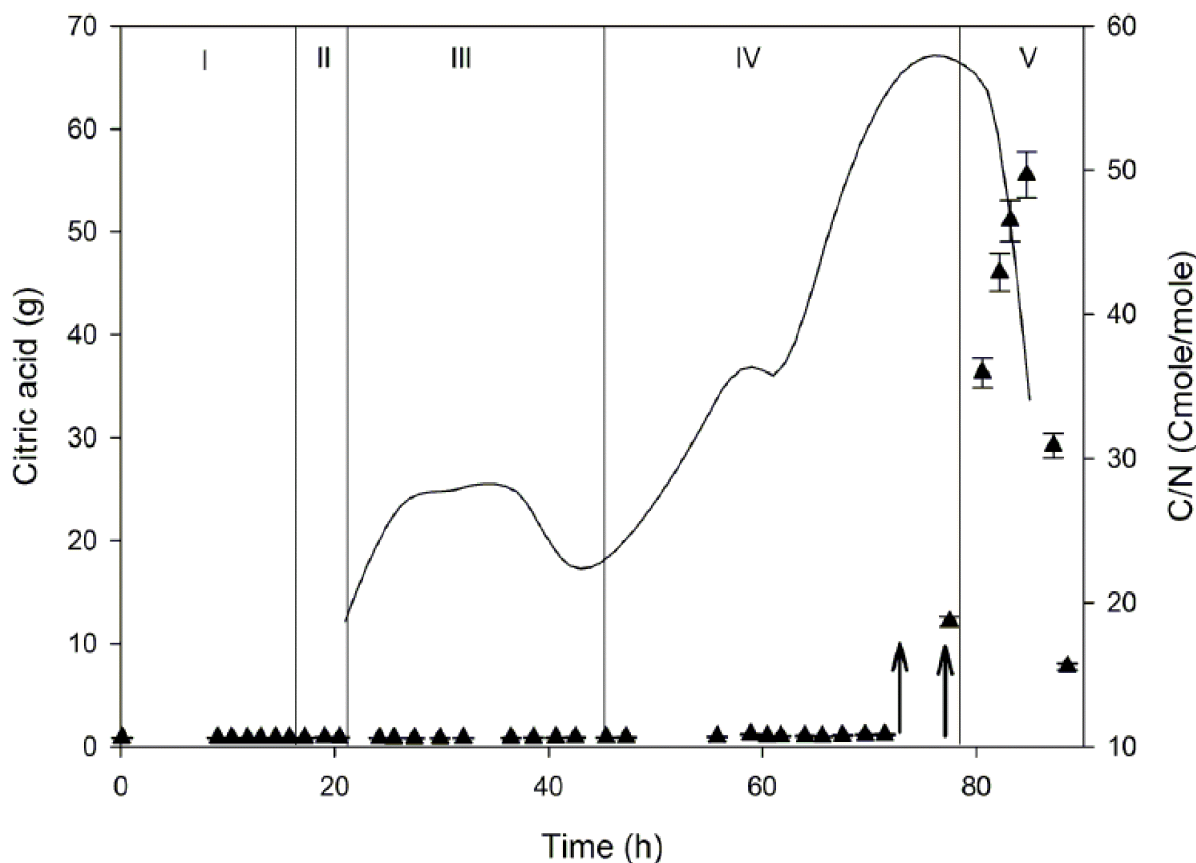
298 Therefore the C/N ratio was maintained below 33  $\text{Nmol.Cmol}^{-1}$  for around 24 hours and  
 299 confirmed lipid accumulation without any citric acid secretion. The total lipid content slightly  
 300 increased from 10 to 15 % of cell dry weight during this period. No citric acid was detected  
 301 (Fig.2).



302  
 303 **Figure 2:** Fed-batch cultivation of the strain JMY3501 on mineral medium on glucose as the  
 304 sole carbon source. Evolution of the masses of biomass ( $\blacklozenge$ ), citric acid ( $\blacktriangle$ ), total FA content  
 305 ( $\bullet$ ) and cumulated glucose consumed ( $\circ$ ). Phases: (I) Unlimited growth phase, (II) Transition  
 306 phase, (III) N- and C limited phase, (IV) C/N increasing phase, (V) C/N decreasing phase.  
 307 Data are presented as means  $\pm$  standard deviation.  
 308

309 After 45 hours of cultivation, the profile of glucose feeding rate was constantly increased  
 310 without changing the profile of ammonia feeding rate in order to decrease gradually the C/N  
 311 ratio without changing the specific growth rate that was maintained constant at  $0.04 \text{ h}^{-1}$ . The  
 312 total lipid content continuously increased during the whole period to finally reach a value of  
 313  $34 \pm 2 \%$ ; citric acid was detected in the medium at 71 h, at 77 h its concentration was at  $0.5$   
 314  $\text{g L}^{-1}$  and continued to increase to reach  $8 \text{ g L}^{-1}$  at 81 h. Between 71 and 77 h the C/N ratio

315 increased from 55.5 to 58.8 C mole Nmole<sup>-1</sup> (Fig.3). Once citric acid was detected, at 78h the  
 316 profile of glucose feeding rate was inverted and constantly decreased without changing the  
 317 profile of ammonia feeding rate in order to decrease gradually the C/N ratio. The  
 318 concentration of citric acid continued to increase until reaching 11.6 g L<sup>-1</sup> at 85 h and then  
 319 decreased with decreasing C/N ratio down to 1.6 g L<sup>-1</sup> at the end of the culture. It  
 320 demonstrated that based on the modulation profile of the N and C fluxes the yeast is able to  
 321 rapidly and reversibly excrete or consume citric acid during FA accumulation.



322  
 323 **Figure 3:** Fed-batch cultivation of the strain JMY3501 on mineral medium on glucose.  
 324 Evolution of the C/N ratio (line) and the mass of citric acid (triangles) versus time. Arrows  
 325 indicated the period of the citric acid excretion onset. Phases: (I) Un-limited growth phase,  
 326 (II) Transition phase, (III) N- and C-limited phase, (IV) C/N increasing phase, (V) C/N  
 327 decreasing phase. Data are presented as means  $\pm$  standard deviation.  
 328

329 Here the critical C/N ratio determined at the onset of the citric acid excretion was determined  
 330 at 55.5-58.8 Cmole.Nmole<sup>-1</sup> for the DAG2-GPD1 engineered strain. Ochoa-Estopier and  
 331 Guillouet (2014) previously determined the critical C/N ratio for the onset of citric acid

332 excretion in D-stat cultivation system with the parent strain at 47.6 C mol.Nmol<sup>-1</sup> and at 45.4  
333 C mol Nmol<sup>-1</sup> in fed-batch cultivation system under similar strategy (Ochoa Estopier, 2012).  
334 Therefore, the engineering of the strain led to a 15 % modulation of the critical C/N ratio,  
335 suggesting that the over-expression of DGA and GPD1 enabled to delay the onset of acid  
336 excretion. Further modulation of the critical C/N ratio would imply a much better robustness  
337 in terms of bioprocess design: as an example, comparatively to the wild type strain, using  
338 this engineered strain in fed-batch process could be performed for FA accumulation without  
339 citric acid excretion (i) at a C/N rate ratio higher (within the range 47.6 - 58.8 Cmol.Nmol<sup>-1</sup>)  
340 than the critical ratio determined for the WT strain (47.6 Cmol.Nmol<sup>-1</sup>) allowing a higher  
341 productivity or (ii) at the WT critical ratio of 47.6 Cmol.Nmol<sup>-1</sup> with less sensitivity to slight  
342 fluctuations of the feeding rates of nitrogen or carbon.

#### 343 **4. Conclusions**

344 Increasing the Glycerol Phosphate availability and its binding to fatty acids through over-  
345 expression of yIDGA2 and yIGPD1 led to a strong improvement of lipid content and yield of  
346 accumulation on glucose concomitantly to a reduction of the excretion of citric acid and an  
347 increase in the critical C/N ratio. It demonstrated an overall improvement of the lipid  
348 production performances of the engineering strain compared to the parent strain with and  
349 improvement of the robustness that could be beneficial to an industrial process.

#### 350 **Acknowledgments**

351 Financial support for this study was provided by Agence Nationale de la Recherche (ANR)  
352 and Commissariat aux Investissements d'Avenir via the project ProBio3 "Biocatalytic  
353 production of lipidic bioproducts from renewable resources and industrial by-products: BioJet  
354 Fuel Application" (ref. ANR-11-BTBT-0003). The authors have no conflict of interest to  
355 declare.

#### 356 **References**

357 The references cited in this article represented in Chapter 5.  
358 The journal format of the article represented in Annex.

### 3.2.2. Fed-batch culture of *Y. lipolytica* JMY3501 under nitrogen limitation with solvent pulses

The objective of the experiment was to study the impact of ethanol pulses for fed-batch culture of *Y. lipolytica* JMY3501 in terms of lipid accumulation, the fatty acid composition and citric acid secretion under nitrogen limitation conditions.

The fed-batch experiment was performed in two phases. During the growth phase the bioreactor was exponentially fed with glucose solution at a concentration of 215 g. L<sup>-1</sup> to control a constant specific growth rate of 0.18 h<sup>-1</sup> and during the nitrogen limitation phase 0.31 M NH<sub>4</sub>OH solution was exponentially fed in order to control a constant residual growth rate of 0.02 h<sup>-1</sup>. Furthermore the feeding of C and N-sources was performed in a way to keep the rN/rC constant within a range where cells accumulate lipids without citric acid as demonstrated by Ochoa-Estopier and Guillouet, 2014.

The first ethanol pulse was performed to the culture approximately 15 hours after the onset of lipid accumulation phase and each 6 hours a new pulse was applied as shown in Figure 3.12 with red arrows. The first solvent pulse amount was calculated according the equivalent ratio of 9 mg triclosan.g<sup>-1</sup><sub>DCW</sub>. In order to keep the pulse ratio constant over the yeast cells during the culture time, the following pulse ratios were calculated according the ratio of 9 mg triclosan. Δg<sup>-1</sup><sub>DCW</sub>. Figure 3.11 shows the ethanol additions to the culture with each pulse.

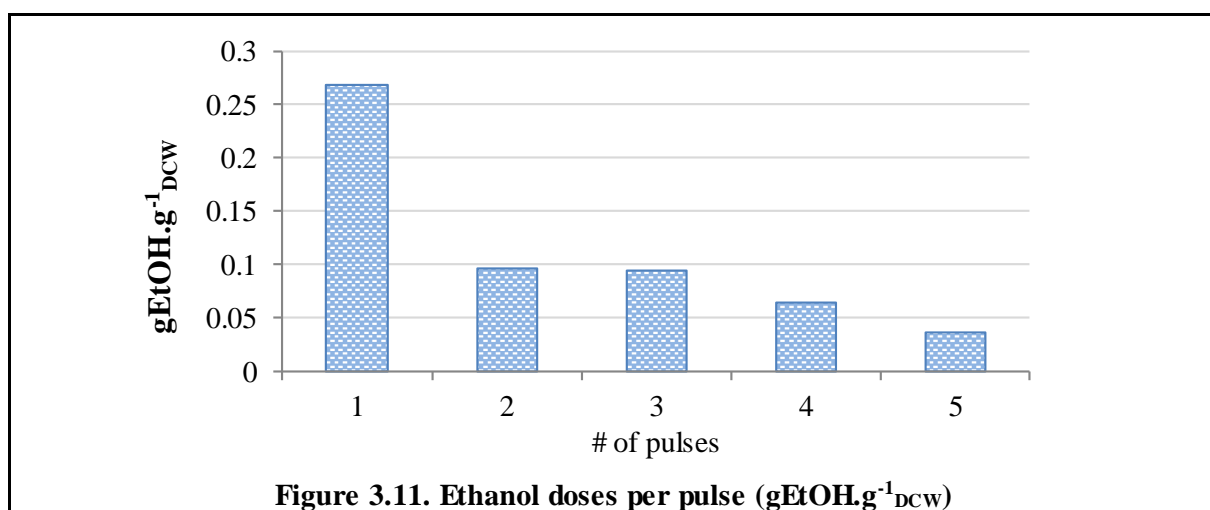


Figure 3.12 (A) showed the online acquisition of respiratory quotient (RQ) and the online measurement of rN/rC ratio. In the early stage of lipid accumulation phase the rN/rC ratio was increased quickly up to 0.010 and then was stable between 0.011 to 0.014 Nmol. Cmol<sup>-1</sup>. During the growth phase, RQ was constant at the value of 1.07 ± 0.092 which is characteristic

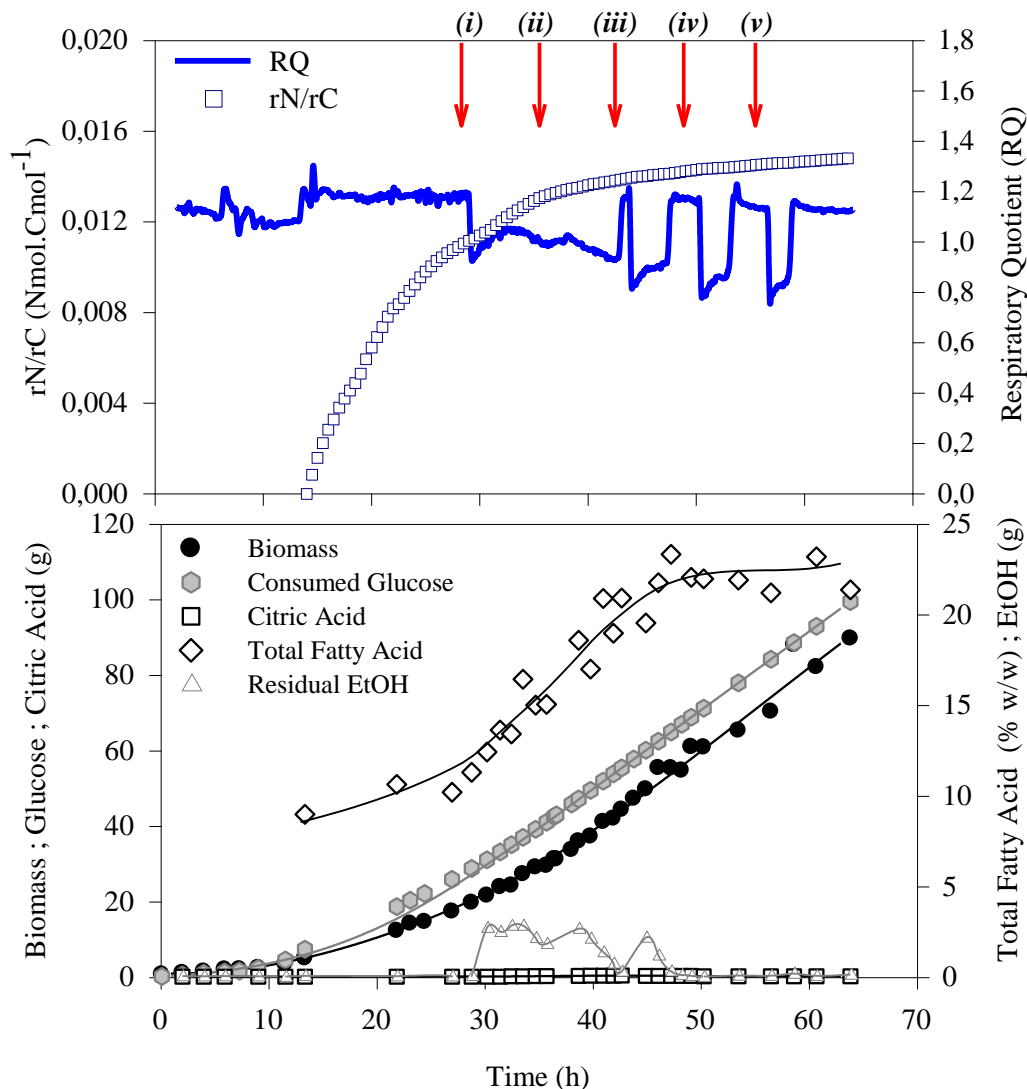


Figure 3.12. Fed-batch culture of *Y. lipolytica* JMY3501 under nitrogen limitation with solvent pulses.

(A) rN/rC ratio and Respiratory Quotient; (B) Variation of state variables.

The symbols represent experimental data and lines are the smoothed values. Ethanol pulses were shown in arrows (i)  $0.27 \text{ g}\cdot\text{g}^{-1}_{\text{DCW}}$ ; (ii)  $0.1 \text{ g}\cdot\Delta\text{g}^{-1}_{\text{DCW}}$ ; (iii)  $0.09 \text{ mg}\cdot\Delta\text{g}^{-1}_{\text{DCW}}$ ; (iv)  $0.06 \text{ g}\cdot\Delta\text{g}^{-1}_{\text{DCW}}$ ; (v)  $0.04 \text{ g}\cdot\Delta\text{g}^{-1}_{\text{DCW}}$

to a fully oxidative growth on glucose. During the nitrogen limitation phase the RQ was found constant at  $1.18 \pm 0.019$  characteristic for lipid accumulation phase on glucose. However with each solvent pulses the RQ value strongly decreased to a value of 0.8. These drastic decreases of RQ revealed that the metabolic activity of cells was impacted. This decrease in the RQ could be explained by the temporary production of a molecule with a degree of reduction lower than the glucose (citric acid for example) or by the consumption of the ethanol (degree of reduction higher than glucose). As seen in Figure 3.12 (B), with the solvent pulses 7.4 g of ethanol were fed to the culture and no citric acid secretion was detected throughout the time

course and residual ethanol was close to zero by 47 h which suggests that the decrease of RQ was due to the consumption of ethanol.

After more than 40 h of nitrogen limitation, 99.3 g of glucose were consumed and the final biomass concentration reached up to 89.5 g<sub>DCW</sub>. Before the solvent pulses the total fatty acid content was 10 % (w/w) and quickly increased up to 15 % with the first pulse and to 23 % at the end of the culture as seen in Figure 3.12 (B).

Figure 3.13 shows the impact of solvent pulses on the total fatty acid composition during lipid accumulation phase under nitrogen limitation, Figure 3.13 (A) for the long and medium chain length fatty acids from C16:0 to C18:2 and Figure 3.13 (B) for the short chain length fatty acids of C12:0 and C14:0 and for the very long chain fatty acids from C20:0 to C24:0.

Before the solvent pulses, the total fatty acid percentages (% (w/w)) of long chain fatty acids (LCFA) were  $49.6 \pm 0.2$  % for oleic (C18:1),  $17.7 \pm 0.1$  % for linoleic (C18:2). However oleic acid reached to  $53 \pm 0.1$  % with two solvent pulses but a decrease was observed with the following pulses and reached back to  $50.1 \pm 0.3$  % at the end of the culture. Moreover linoleic acid decreased to  $12 \pm 1.6$  % at the end of the pulses. Besides, slight increased was observed for stearic (C18:0) acid which was around  $6.3 \pm 0.12$  % before the pulses and was found  $7.6 \pm 1$  % at the end of five pulses.

On the contrary the total fatty acid percentage of (% (w/w)) medium chain length fatty acid (MCFA) palmitic acid (C16:0) increased from  $17 \pm 0.2$  % to  $21.8 \pm 2.4$  % at the end of the culture with five pulses. Besides, no strong modification was observed in palmitoleic (C16:1) and was found  $5.9 \pm 0.12$  % and  $5.5 \pm 1.8$  % before the pulses and at the end of five pulses, respectively.

During the early stage of lipid accumulation phase before the pulse injections, short chain length fatty acids (SCFA) were obtained at a percentage of (% (w/w))  $0.12 \pm 0.01$  % and  $0.34 \pm 0.05$  % for lauric (C12:0) and myristic (C14:0) acids, respectively. However after the third solvent pulse no more short chain fatty acids production was observed as shown in Figure 3.13 (B).

Before the pulse injections very long chain length fatty acids (VLCFA) were obtained at a percentage of (% (w/w))  $0.52 \pm 0.01$  % for arachidic (C20:0),  $0.47 \pm 0.03$  % for behenic (C22:0) and  $1.85 \pm 0.04$  % for lignoceric (C24:0) acids. The total fatty acid percentage of VLCFA had slight modifications after solvent pulses: arachidic acid reached to  $0.73 \pm 0.11$  % ,

behenic acid reached to  $0.54 \pm 0.05$  % and a decrease was observed in lignoceric acid from  $1.85 \pm 0.04$  % to  $1.62 \pm 0.19$  % as shown in Figure 3.13 (B).

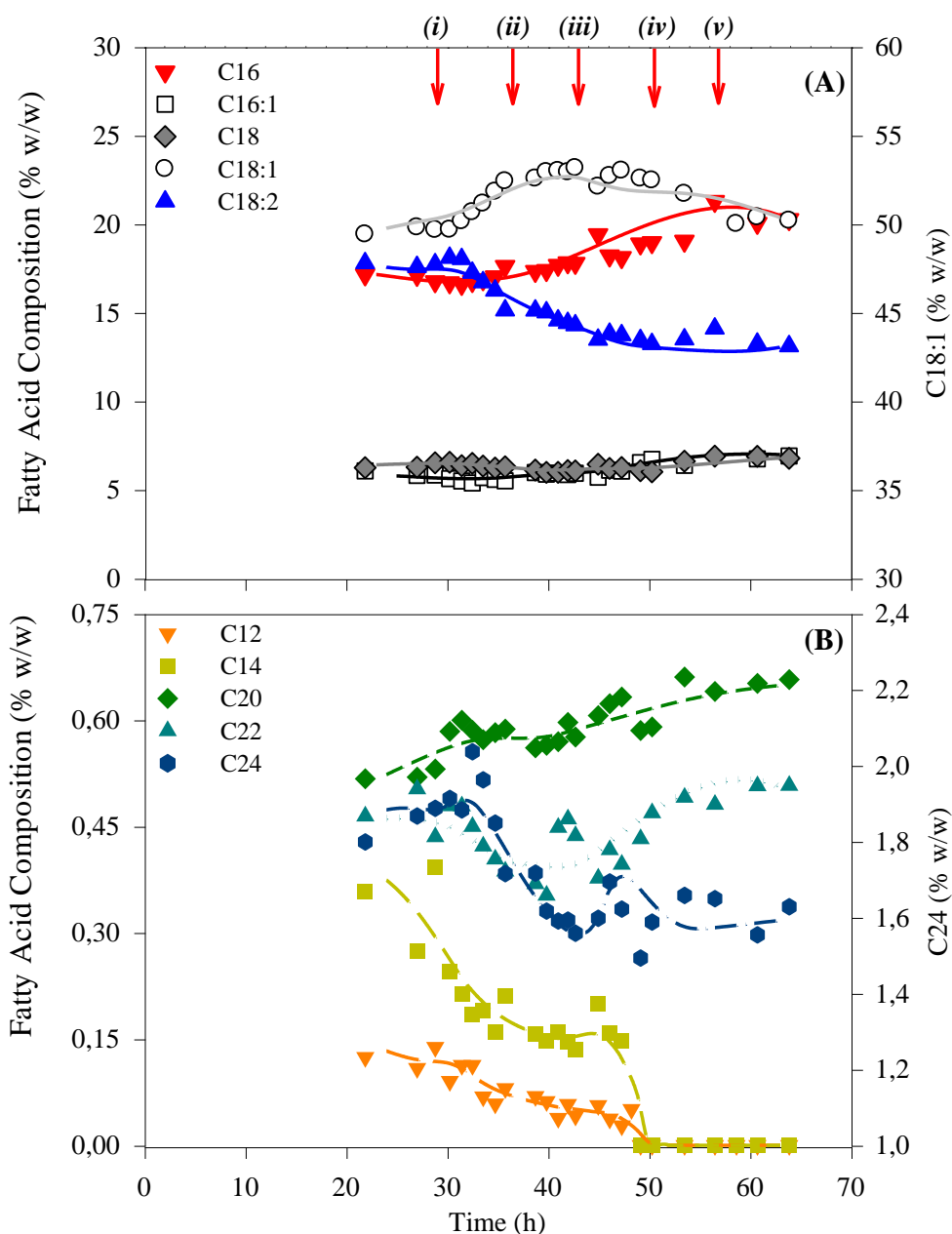


Figure 3.13. Impact of solvent pulses on fatty acid composition (% w/w) during lipid accumulation phase for fed-batch cultures of *Y. lipolytica* JMY3501 under nitrogen limitation.

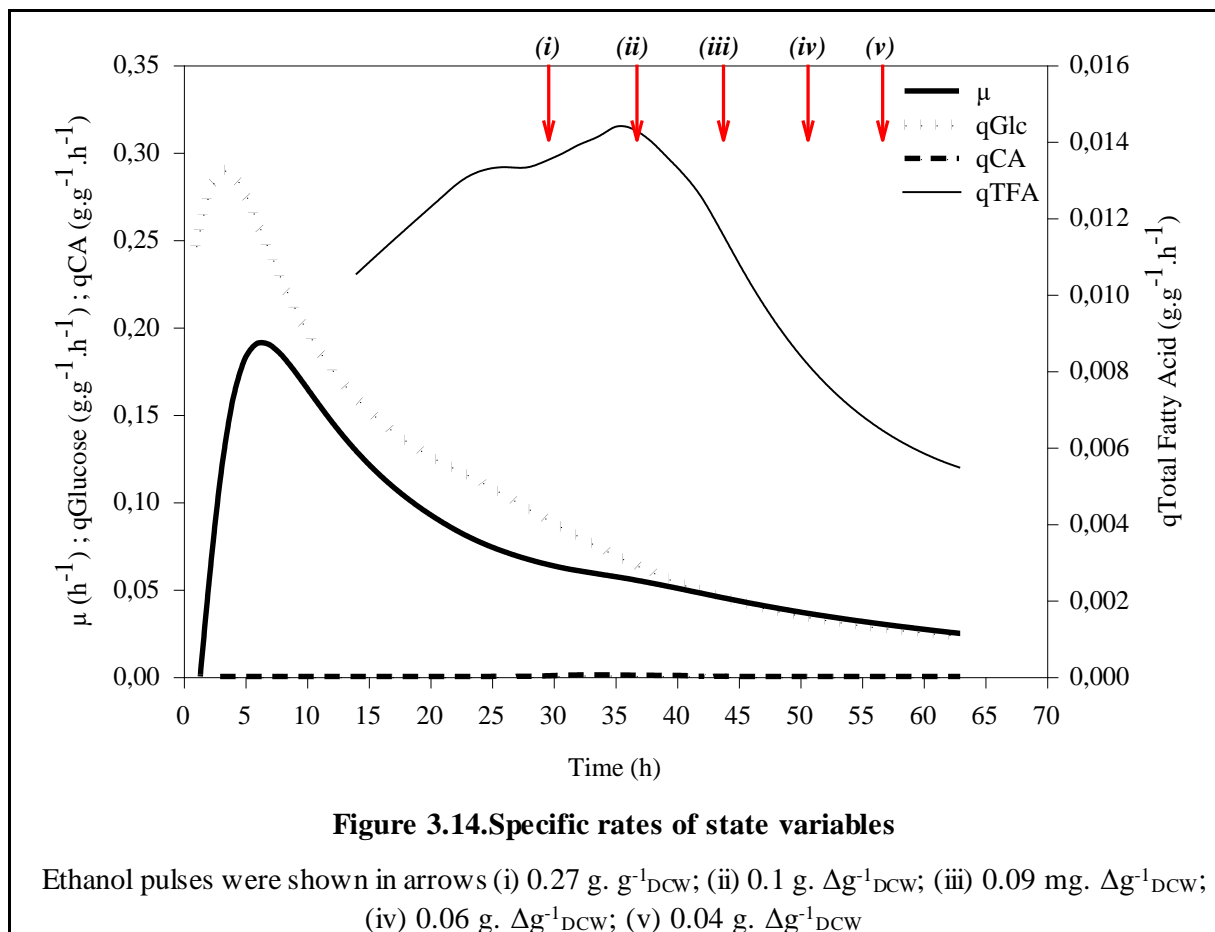
Fatty Acid Compositions (% w/w): Figure A ( $\blacktriangledown$  C16:0), ( $\square$  C16:1), ( $\blacklozenge$  C18:0), ( $\circ$  C18:1), ( $\blacktriangle$  C18:2) and Figure B ( $\blacktriangledown$  C12:0), ( $\blacksquare$  C14:0), ( $\blacklozenge$  C20:0), ( $\blacktriangle$  C22:0), ( $\bullet$  C24:0).

**The symbols represent experimental data and lines are smoothed values. Ethanol pulses were shown in arrows (i)  $0.27 \text{ g} \cdot \text{g}^{-1}_{\text{DCW}}$ ; (ii)  $0.1 \text{ g} \cdot \Delta \text{g}^{-1}_{\text{DCW}}$ ; (iii)  $0.09 \text{ mg} \cdot \Delta \text{g}^{-1}_{\text{DCW}}$ ; (iv)  $0.06 \text{ g} \cdot \Delta \text{g}^{-1}_{\text{DCW}}$ ; (v)  $0.04 \text{ g} \cdot \Delta \text{g}^{-1}_{\text{DCW}}$**

Figure 3.14 shows the specific rates as a function of time. During the growth phase, the maximum specific growth rate ( $\mu_{\text{max}}$ ) and the maximum specific glucose consumption rate

( $q_{\text{Glucose}}$ ) were  $0.19 \text{ h}^{-1}$  and  $0.29 \text{ g}_{\text{Glucose}} \cdot \text{g}^{-1}_{\text{DCW}} \cdot \text{h}^{-1}$ , respectively. During the nitrogen limitation phase between 14 h and 63 h, the specific growth rate ( $\mu$ ) and the specific glucose consumption rate ( $q_{\text{Glucose}}$ ) followed almost the same profile throughout the culture time.

After the onset of nitrogen limitation phase at around 14 h, the specific total fatty acid production rate ( $q_{\text{TFA}}$ ) increased from  $0.0105$  to  $0.0133 \text{ g}_{\text{TFA}} \cdot \text{g}^{-1}_{\text{DCW}} \cdot \text{h}^{-1}$  and kept constant at a value of  $0.0133 \text{ g}_{\text{TFA}} \cdot \text{g}^{-1}_{\text{DCW}} \cdot \text{h}^{-1}$  before the pulses. 6 h after the first solvent pulse, the maximum specific total fatty acid production rate was  $0.0144 \text{ g}_{\text{TFA}} \cdot \text{g}^{-1}_{\text{DCW}} \cdot \text{h}^{-1}$  and no increase was observed with the following pulses.



### 3.2.3. Conclusions

In this section the fed-batch culture of *Y. lipolytica* JMY3501 lipid metabolism and the possible impacts of the solvent additions during nitrogen limitation to the physiological state of the culture were investigated.

The results showed that the impact of ethanol pulses on the induction of lipid metabolism of *Y. lipolytica* in fed-batch culture was not the same as in the flask cultures due to the lack of control on the substrate feeding in batch cultures. First of all, it was possible to maintain lipid accumulation without producing citric acid; in addition, reduced metabolic activity -due to the consumption of ethanol- slightly alter the fatty acid compositions as seen in Table 3.3.

Table 3.3. Fatty acid composition of *Y. lipolytica* JMY3501 mutant strain with and without solvent pulses (*n. m. not measured*)

<i>Y. lipolytica</i> JMY3501	C16:0	C16:1	C18:0	C18:1	C18:2	others
without pulses	23.3	5.8	7.2	50.0	13.7	<i>n.m.</i>
with pulses	20.3	6.9	6.8	50.2	13.1	2.7

Moreover, contradictory to the flask conditions ethanol was consumed at the same time with glucose and improved accumulation of fatty acids from 15 % to 22 % (w/w), accelerated the specific production of fatty acids from 0.007 to 0.013 g. g<sup>-1</sup>. h<sup>-1</sup> and increased total fatty acid production yield on glucose from 0.14 to 0.21 g. g<sup>-1</sup> suggesting that somehow carbon sources were channeled more efficiently into fatty acid biosynthesis. However, if we consider ethanol was consumed as a co-substrate, the total fatty acid production yield was remained unaffected with and without solvent pulses 0.27 and 0.28 Cmol.Cmol<sup>-1</sup>, respectively as seen in Table 3.4.

Table 3.4. Comparison of *Y. lipolytica* JMY3501 mutant strain performances with and without solvent pulses

<i>Y. lipolytica</i> JMY3501	Total FA (%)	q <sub>TFA</sub> (g.g.h <sup>-1</sup> ) max	Y <sub>Glc, TFA</sub> (g.g <sup>-1</sup> ) average/max	Y <sub>S, TFA</sub> (Cmol.Cmol <sup>-1</sup> ) average/max
without pulses	15	0.007	0.14 / 0.18	0.28/0.36
with pulses	22	0.013	0.21 / 0.24	0.27/0.32

Hence, ethanol was used in the following studies for this strain in fed-batch cultures to dissolve the inhibitory molecules.

### **3.3. Fed-batch cultures of *Yarrowia lipolytica* under nitrogen limitation with cerulenin pulses**

#### **3.3.1. Fed-batch culture of *Yarrowia lipolytica* JMY3501 under nitrogen limitation with cerulenin pulses**

In this section fed-batch cultures of *Y. lipolytica* JMY3501 under nitrogen limitation were performed in order to study the effect of cerulenin pulses, a potent inhibitor of fatty acid synthase enzyme, to the lipid metabolism and to the physiology of yeast.

The fed-batch cultures were conducted with identical feeding strategies. The feeding of C and N-sources was performed in a way to maintain the rN/rC ratio within a range where cells accumulate lipids without citric acid as demonstrated by Ochoa-Estopier and Guillouet, 2014.

The main objective of this investigation was to assess the cerulenin effect on the accumulation of triglycerides and their composition in fatty acids. Moreover possible impacts associated with the cerulenin amounts per gram dry cell weight were investigated. Thus, after the onset of lipid accumulation phase induced by nitrogen limitation, cerulenin dose ratios ( $\text{mg}_{\text{Cerulenin}} \cdot \text{g}^{-1}_{\text{DCW}}$ ) were chosen based on two different objectives as outlined in the following steps:

1. To select the right dosage based on lipid accumulation
  - High dosage cerulenin pulses ( $7 \text{ mg}_{\text{Cerulenin}} \cdot \text{g}^{-1}_{\text{DCW}}$ ),
  - Middle dosage cerulenin pulses ( $[0.25-1.5] \text{ mg}_{\text{Cerulenin}} \cdot \text{g}^{-1}_{\text{DCW}}$ ),
2. A single cerulenin pulse at  $0.5 \text{ mg}_{\text{Cerulenin}} \cdot \text{g}^{-1}_{\text{DCW}}$  was chosen based on the former experiments' analysis on the fatty acid composition.

### 3.3.1.1. Fed-batch culture of *Yarrowia lipolytica* JMY3501 under nitrogen limitation with high dosage of cerulenin pulses

The fed-batch experiment was performed in two phases. During the growth phase, the bioreactor was exponentially fed with glucose solution at a concentration of 222 g. L<sup>-1</sup> to maintain constant the specific growth rate at 0.18 h<sup>-1</sup> and during the nitrogen limitation phase, 0.48 M NH<sub>4</sub>OH solution was exponentially fed in order to keep constant the specific growth rate at 0.02 h<sup>-1</sup>.

Preliminary studies in the laboratory showed that concentration of 10 mg<sub>Cerulenin</sub> · g<sup>-1</sup><sub>DCW</sub> or more had a strong inhibitory impact on the growth (unpublished data). Therefore for a high dosage of cerulenin less than 10 mg<sub>Cerulenin</sub> per gram of biomass was chosen to quantify the modulation of fatty acids.

The cerulenin pulses were performed every 6 hours and the first pulse was applied to the culture approximately 8 hours after the onset of lipid accumulation phase as shown in Figure 3.16 with red arrows. Cerulenin was dissolved in ethanol and the first cerulenin pulse was at a ratio of 7 mg. g<sup>-1</sup><sub>DCW</sub>. In order to expose constant quantity of cerulenin over the yeast cells, the consecutive cerulenin pulses were applied at a ratio of 7 mg. Δg<sup>-1</sup><sub>DCW</sub>. Consequently solvent additions were reduced as shown in Figure 3.15. Samples were taken regularly every hour after the pulse.

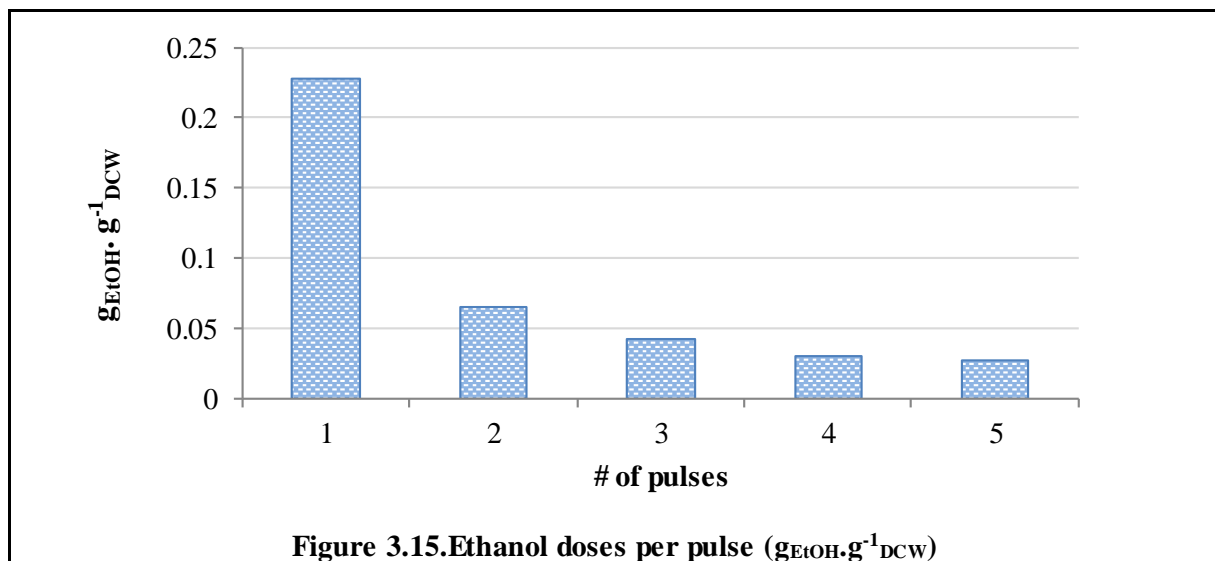
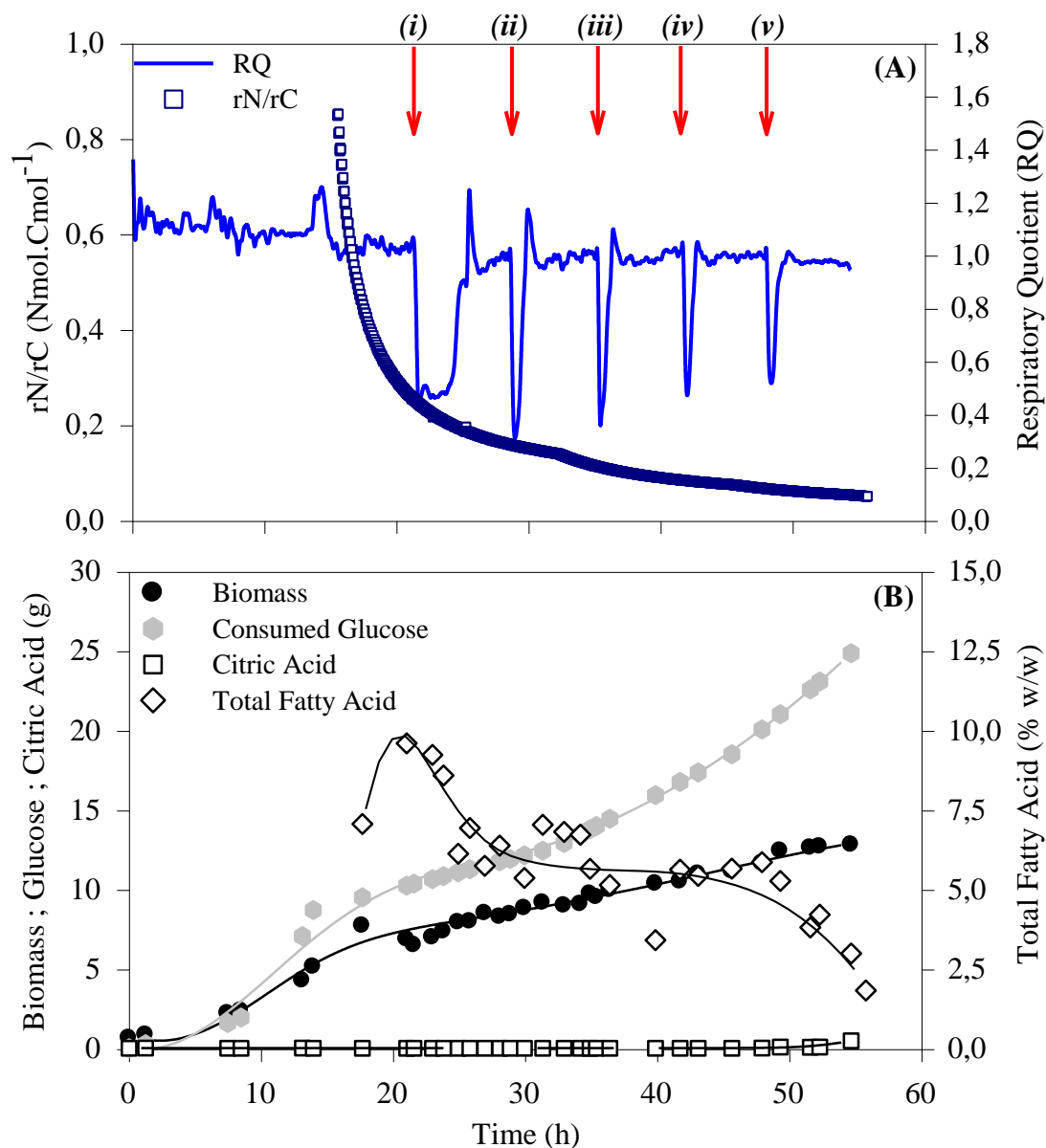


Figure 3.16 (A) shows the online acquisition of respiratory quotient (RQ) and the online measurement of rN/rC ratio. In the early stage of nitrogen limitation phase the rN/rC ratio quickly decreased to 0.24 Nmol<sup>-1</sup> · Cmol<sup>-1</sup> and reached to 0.04 Nmol<sup>-1</sup> · Cmol<sup>-1</sup> during the lipid accumulation phase. The respiratory quotient was found constant at 1.11 ± 0.09 in the

beginning of lipid accumulation phase but with each inhibitor pulses RQ strongly decreased down to 0.4 which suggested sudden metabolic shifts that could be explained by the consumption of ethanol by the cells.



**Figure 3.16. Fed-batch culture of *Y. lipolytica* JMY3501 for fed-batch cultures under nitrogen limitation with high dose of Cerulenin pulses.**

(A) rN/rC ratio and Respiratory Quotient; (B) Variation of state variables.

The symbols represent experimental data and lines are smoothed values. Cerulenin pulses were shown in arrows (i)  $7 \text{ mg. g}^{-1}\text{DCW}$ ; (ii, iii, iv, v)  $7 \text{ mg. } \Delta\text{g}^{-1}\text{DCW}$

Figure 3.16 (B) shows the biomass production, glucose consumption, citric acid production and total fatty acid percentage (TFA) as a function of time. After more than 40 h of lipid accumulation, total glucose consumption was 24.3 g. and the final dry cell weight reached to

12.7  $g_{DCW}$ . Even though strong decrease in respiratory quotient occurred with each inhibitor pulses, no citric acid production was obtained until the end of the fourth cerulenin pulse. With the fifth cerulenin pulse at 48 h, a very small amount of citric acid secretion (0.36 g.) was observed.

Before the inhibitor pulse total fatty acid percentage was at 9.6 % (w/w) but with the first and the second cerulenin pulses at a ratio of 7 mg.  $\Delta g^{-1}_{DCW}$ , total fatty acid was decreased down to 6 % (w/w). No decrease or increase were obtained and the TFA % was found stable at around 6 % with the third and the fourth cerulenin pulses at a constant ratio of 7 mg.  $\Delta g^{-1}_{DCW}$ . However at the end of the fifth cerulenin pulse, TFA % strongly decreased and was found below 5 % (w/w) as seen in Figure 3.16 (B).

These results indicate a drastic inhibition on the fatty acid synthesis occurred with constant ratio of 7 mg.  $\Delta g^{-1}_{DCW}$  cerulenin pulses. Considering that the constitutive FA content for membrane lipids is about 7 % of the dry cell weight, these results indicated that the cells did not accumulate FA during the cultivation. They even suggested a loss of total FA within the cells leading to potential membrane rearrangement.

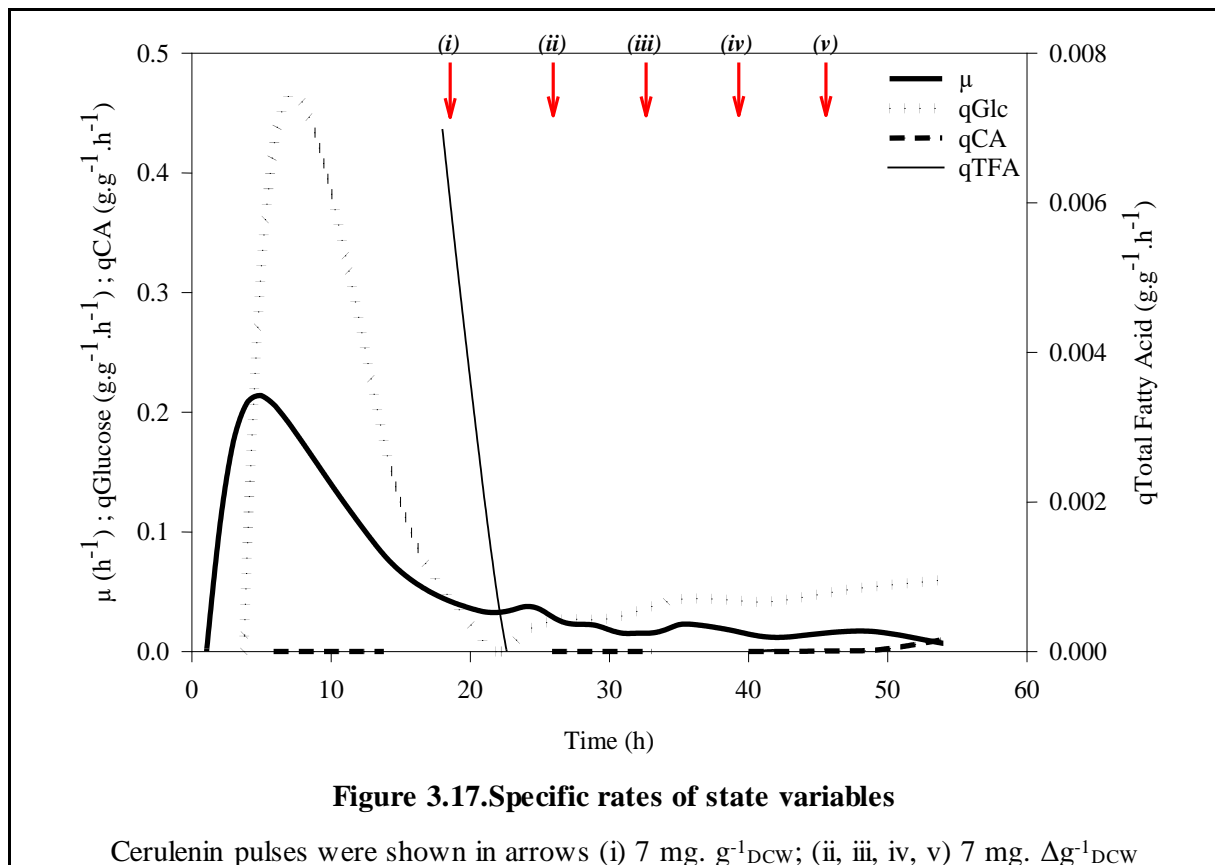


Figure 3.17 shows the specific growth, glucose consumption, citric acid production and total fatty acid production rates as a function of time. During the growth phase the maximum

specific growth rate ( $\mu_{\max}$ ) and the maximum specific glucose consumption rate ( $q_{\text{Glucose}}$ ) were found at a value of  $0.21 \text{ h}^{-1}$  and  $0.47 \text{ g}_{\text{Glucose}} \cdot \text{g}^{-1}_{\text{DCW}} \cdot \text{h}^{-1}$ , respectively. During the nitrogen limited phase, the specific total FA production rate dropped drastically to reach negative values. This confirms the fact that cerulenin pulses at high dosage stopped the overall FA synthesis and cells react by modifying their membrane lipid content.

### **3.3.1.2. Fed-batch culture of *Yarrowia lipolytica* JMY3501 under nitrogen limitation with middle dosage of cerulenin pulses**

The fed-batch experiment was carried out in two phases. During the growth phase the bioreactor was exponentially fed with glucose solution at a concentration of  $690 \text{ g} \cdot \text{L}^{-1}$  to maintain constant specific growth rate at  $0.18 \text{ h}^{-1}$  and during the nitrogen limitation phase  $3\text{M}$   $\text{NH}_4\text{OH}$  solution was exponentially fed in order to keep the growth rate constant at  $0.02 \text{ h}^{-1}$ .

Cerulenin was dissolved in ethanol and four consecutive pulses were performed at lower dosage at a ratio of 0.25, 0.5, 1 and  $1.5 \text{ mg} \cdot \text{g}^{-1}_{\text{DCW}}$ , respectively. In order to expose increased doses of cerulenin for all the yeast cells, cerulenin amounts were calculated for the cell production between the consecutive pulses and adjusted further by taking into account of previous pulse cell target. The first pulse was applied to the culture 24 hours after the onset of lipid accumulation phase as shown in Figure 3.18. The addition of ethanol with each pulse was at a ratio of  $0.007 \pm 0.001 \text{ g}_{\text{EtOH}} \cdot \text{g}^{-1}_{\text{DCW}}$ . Samples were withdrawn regularly every hour after the pulse.

The evolution of respiratory quotient (RQ) and the  $r\text{N}/r\text{C}$  ratio throughout the culture was shown in Figure 3.18 (A). After the onset of nitrogen limitation the  $r\text{N}/r\text{C}$  ratio was found constant at a value of  $0.022 \pm 0.012 \text{ Nmole} \cdot \text{Cmole}^{-1}$ . After the first cerulenin pulse the  $r\text{N}/r\text{C}$  ratio was found between 0.019 and  $0.025 \text{ Nmole} \cdot \text{Cmole}^{-1}$  until the end of the culture.

During the lipid accumulation phase up to 40 h, the respiratory quotient was constant at a value of  $1.2 \pm 0.04$ . The on-line determination of the respiratory quotient showed a decrease in its value with the first cerulenin pulse at a ratio of  $0.25 \text{ mg} \cdot \text{g}^{-1}_{\text{DCW}}$  to 0.95 and 2 h later possibly due to the end of ethanol consumption the value of RQ reached back to 1.05 as seen in Figure 3.18 (A).

However, surprisingly the respiratory quotient slowly decreased its value from 1.05 to 0.9. These observed decreases in RQ could be interpreted as being a result of a shift in the metabolism to citric acid production phase. The RQ further reduced to a value of 0.76 with

the second pulse of cerulenin at a ratio of  $0.5 \text{ mg. g}^{-1}_{\text{DCW}}$ . In a period of 8 h, the RQ value slowly increased first to 0.9 and later at 62 h up to 1.05. The third pulse of cerulenin at a ratio of  $1 \text{ mg. g}^{-1}_{\text{DCW}}$  was applied to the culture at 67 h, the RQ showed rather a slower response compared to previous pulses and decreased its value to 0.8 and until to the fourth pulse the value was constant at  $0.94 \pm 0.05$ . With the last pulse of cerulenin at a ratio of  $1.5 \text{ mg. g}^{-1}_{\text{DCW}}$  the RQ exhibited less decrease and reached to 0.85. Three hours later the RQ increased and stabilized at  $0.95 \pm 0.03$ .

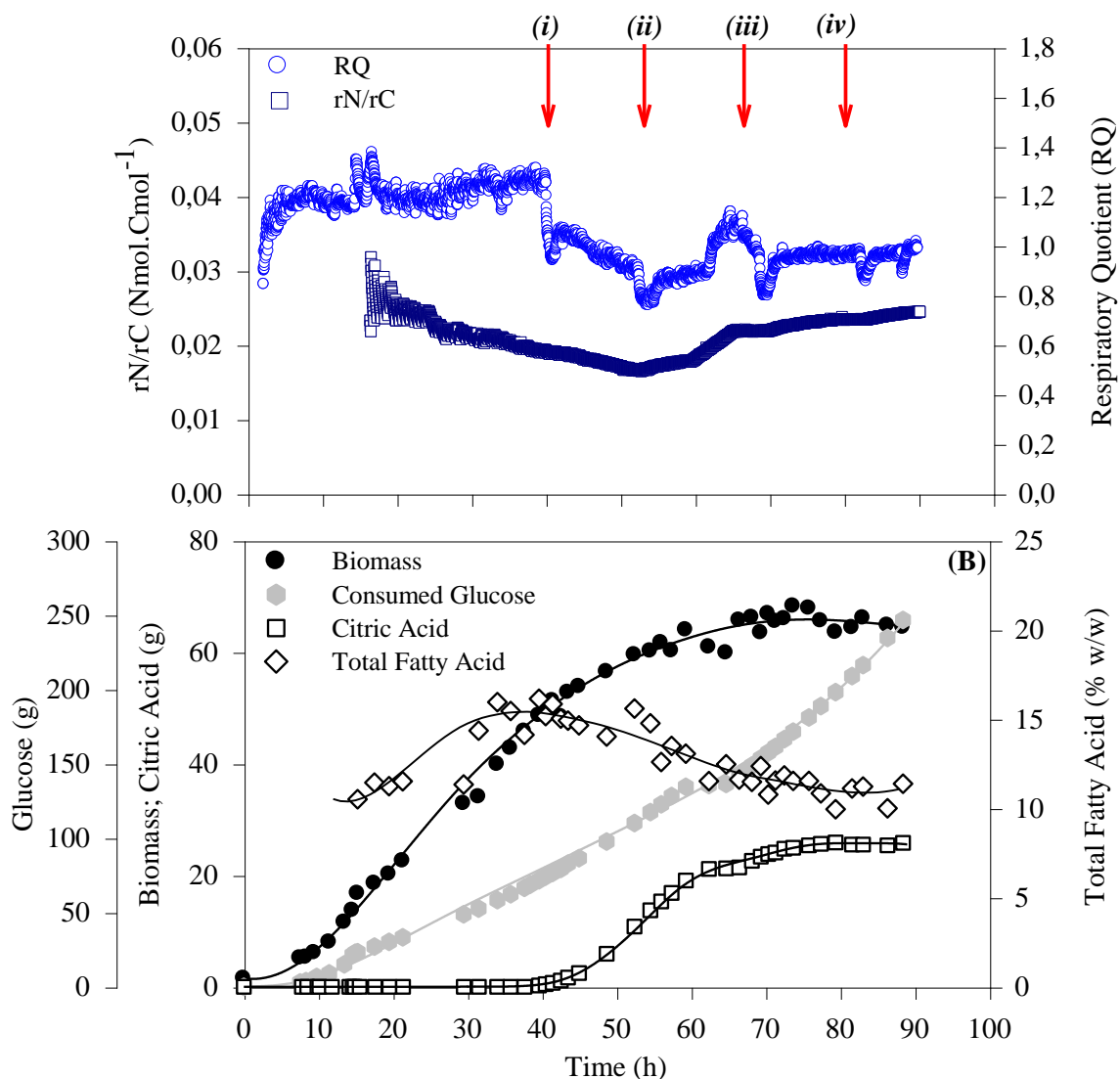


Figure 3.18. Fed-batch culture of *Y. lipolytica* JMY3501 for fed-batch cultures under nitrogen limitation with middle dose of Cerulenin pulses.

(A)  $rN/rC$  ratio and Respiratory Quotient; (B) Variation of state variables.

The symbols represent experimental data and lines are smoothed values. Cerulenin pulses were shown in arrows (i)  $0.25 \text{ mg. g}^{-1}_{\text{DCW}}$ ; (ii)  $0.5 \text{ mg. g}^{-1}_{\text{DCW}}$ ; (iii)  $1 \text{ mg. g}^{-1}_{\text{DCW}}$ ; (iv)  $1.5 \text{ mg. g}^{-1}_{\text{DCW}}$

The results on biomass production, glucose consumption, citric acid production and total fatty acid percentage (TFA) are presented in Figure 3.18 (B). At the end of 73 h of nitrogen limitation, the culture reached to 65 g dry cell weight with 240 g of total glucose consumption. At the beginning of the nitrogen limitation phase the total fatty acid was around 11 % and increased up to 15 % (w/w). In contrast to the results in the previous section with five consecutive cerulenin pulses at a constant ratio, the total fatty acid percentage slightly decreased with increased doses of four consecutive cerulenin pulses and at the end of the culture total fatty acids reached back to 11 %.

It is worthwhile noting that after the first cerulenin pulse at a ratio of 0.25 mg. g<sup>-1</sup>DCW, citric acid secretion occurred. This finding confirms the reason of observed decreases in RQ after the first cerulenin pulse. However the production of citric acid stabilized after the second pulse at a ratio of 0.5 mg. g<sup>-1</sup>DCW and reached to 25.6 g of citric acid at the end of culture.

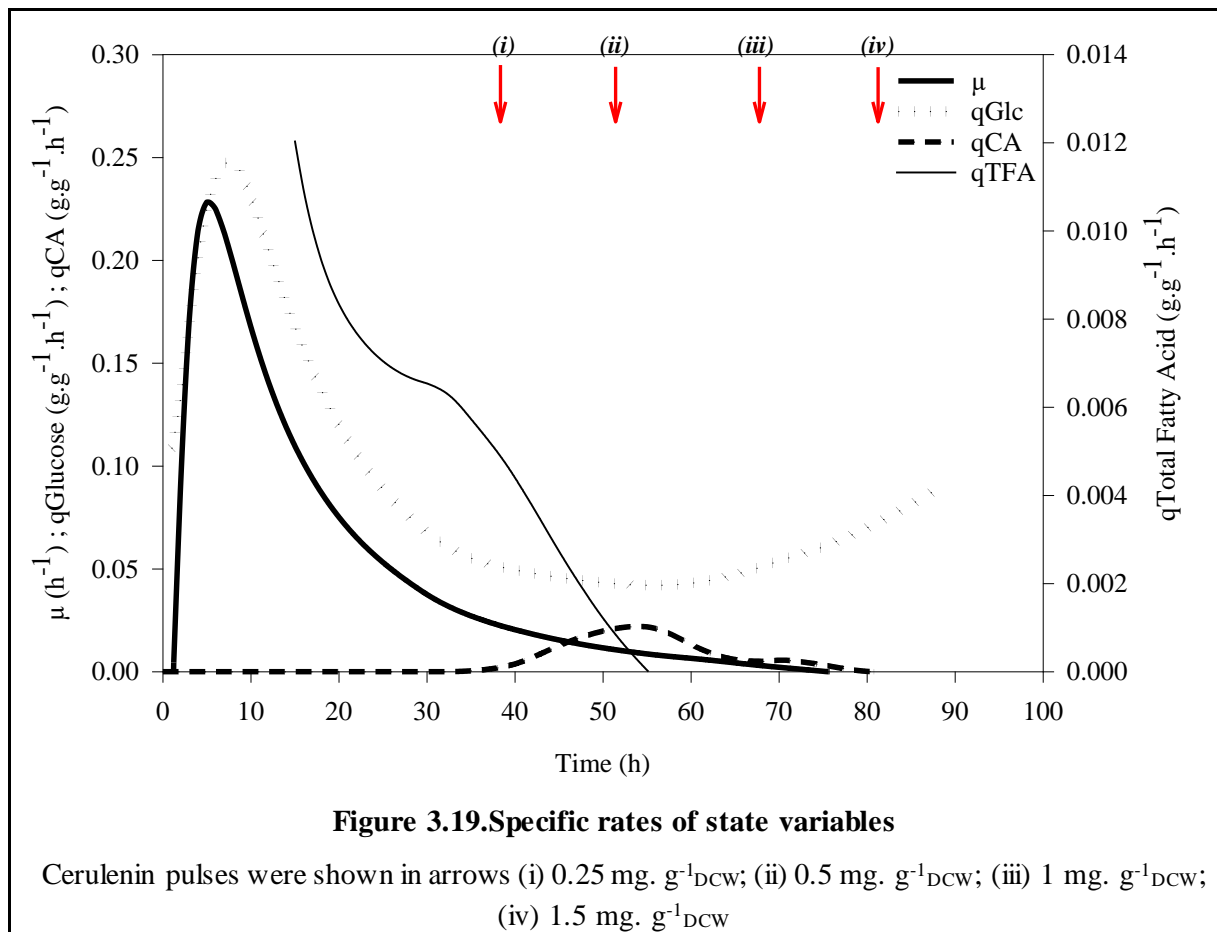


Figure 3.19 shows the specific rates as a function of time. During the growth phase the maximum specific growth rate ( $\mu_{max}$ ) and the maximum specific glucose consumption rate ( $q_{Glucose}$ ) were found at a value of 0.23 h<sup>-1</sup> and 0.25 g<sub>Glucose</sub>· g<sup>-1</sup>DCW· h<sup>-1</sup>, respectively. During the beginning of lipid accumulation phase glucose consumption rate was stable at 0.059

$\pm 0.005 \text{ g}_{\text{Glucose}} \cdot \text{g}^{-1}_{\text{DCW}} \cdot \text{h}^{-1}$ . After the onset of nitrogen limitation phase at around 15 h, the specific total fatty acid production rate ( $q_{\text{TFA}}$ ) decreased and kept a constant value of  $0.007 \text{ g}_{\text{TFA}} \cdot \text{g}^{-1}_{\text{DCW}} \cdot \text{h}^{-1}$  before the cerulenin pulses. However after the first cerulenin pulse,  $q_{\text{TFA}}$  decelerated to  $0.001 \text{ g}_{\text{TFA}} \cdot \text{g}^{-1}_{\text{DCW}} \cdot \text{h}^{-1}$ . After the second pulse, the FA specific production rates get negative suggesting again a rearrangement of FA as observed with high cerulenin dosage.

### **3.3.1.3. A single cerulenin pulse**

Based on the former experiments' analysis on the fatty acid composition, the cerulenin pulse was chosen at  $0.5 \text{ mg}_{\text{Cerulenin}} \cdot \text{g}^{-1}_{\text{DCW}}$  and applied to fed-batch culture of the overproducer strain *Y. lipolytica* JMY3501 under nitrogen limitation on glucose.

The study was presented as a journal article:

1 **Project of a paper**

2 **Title: Modulation of the carbon chain length profile of accumulated fatty acids in**  
3 ***Yarrowia lipolytica***

4

5

6 **Authors:**

7 Rana Sagnak, Coraline Rigouin, Carole Molina-Jouve, Alain Marty, Florence Bordes  
8 and Stéphane E. Guillouet

9 Université de Toulouse, INSA, UPS, INP, LISBP, 135 Av. de Rangueil F-31077 Toulouse France

10 INRA, UMR792 Ingénierie des Systèmes Biologiques et des Procédés, F-31400 Toulouse, France

11 CNRS, UMR5504, F-31400 Toulouse, France

12

13 **Corresponding author:**

14 S.E. Guillouet

15 e-mail: [stephane.guillouet@insa-toulouse.fr](mailto:stephane.guillouet@insa-toulouse.fr)

16 tel: (33)5 61 55 94 47

17 fax: (33)5 61 55 94 00

18

19 **Abstract**

20 Fatty acid synthase (FAS) is an essential enzymatic complex involved in lipid metabolism.  
21 Among the several catalytic domains in fungal FAS (FASI), the rate limiting step for the  
22 synthesis of fatty acids chain formation is considered to be the specificity of initial condensing  
23 enzyme. Therefore, the objective of this study is to investigate the *de novo* short chain fatty  
24 acid production in *Yarrowia lipolytica* with a particular interest in the role of ketoacyl synthase  
25 (KS) domain. For this purpose, elongation of fatty acids in the level of condensation step  
26 blocked with a specific inhibitor of KS domain in an overproducer mutant strain of *Y. lipolytica*  
27 JMY3501 during lipid accumulation phase. Moreover, FAS-KS mutant strain of *Y. lipolytica*  
28 CR62 was cultivated in fed-batch culture under nitrogen depletion on glucose to evaluate the  
29 strain performance on the production of short chain fatty acid.

30

## 31 **1. Introduction**

32 Microbial lipid production by oleaginous microorganisms have received great attention over  
33 the past several years for their high potential to produce lipid and oil contents (above 20 % of  
34 their cellular dry weight) with a similar fatty acid composition to those obtained from the plant  
35 derived oils and fats. Among all the oleaginous microorganisms, yeasts have been known as  
36 the best candidates for lipid production because of their ability to accumulate lipids mainly in  
37 the form of triacylglycerol (TAG) (Athenstaedt et al., 2006; Rattray et al., 1975). Moreover,  
38 they grow faster and are generally easy to cultivate in large scales compared to fungi and  
39 microalgae (Ratledge and Cohen, 2008; Thevenieau and Nicaud, 2013).

40 The oleaginous yeast *Yarrowia lipolytica*, classified as Generally Recognized As Safe  
41 (GRAS) by the Food and Drug Administration (FDA, USA) (Groenewald et al., 2014), is one  
42 of the most extensively studied "non-conventional" yeast. The ability of using wide range of  
43 cost-effective renewable carbon sources (Barth and Gaillardin, 1997), the availability of  
44 efficient genetic tools (Fickers et al., 2005a) and the versatility of its metabolism to produce  
45 high value metabolites such as heterologous proteins (Madzak et al., 2004; Nicaud et al.,  
46 2002), lipids (Bankar et al., 2009; Beopoulos et al., 2009a; Papanikolaou et al., 2003) or citric  
47 acid (Moeller et al., 2007; Papanikolaou et al., 2002; Rymowicz et al., 2007) have made *Y.*  
48 *lipolytica* of particular interest in the field of biotechnological industry.

49 The lipid biosynthesis in oleaginous yeast takes place under conditions of limitations caused  
50 by a nutrient in the culture medium other than carbon. Generally nitrogen limitation is used to  
51 trigger lipid accumulation, but different nutrients such as phosphorus, magnesium or sulfur  
52 have been also shown to induce lipid accumulation in oleaginous yeasts (Bellou et al., 2016;  
53 Gill et al., 1977; Wu et al., 2011, 2010). Nitrogen is necessary for the synthesis of  
54 nucleotides and proteins, thus upon the exhaustion of nitrogen in the culture medium results  
55 a rapid decrease in the intra-cellular concentration of adenosine monophosphate (AMP) to  
56 supply  $\text{NH}_4^+$  ions to the nitrogen-starved cells. The diminished content of AMP via increased  
57 AMP-deaminase activity inhibits the tricarboxylic acid cycle and causes the accumulation of  
58 citrate in the mitochondria. Then, in exchange of malate by a citrate/malate transporter, the

59 accumulated citrate enters to cytosol and ATP-citrate lyase (ACL), a key enzyme  
60 differentiates the oleaginous yeast from non-oleaginous yeast, links the glucose metabolism  
61 to lipid synthesis by cleaving the accumulated citrate into cytosolic acetyl-CoA and  
62 oxaloacetate (Boulton and Ratledge, 1981b; Holdsworth et al., 1988; Ratledge, 2004; Zhang  
63 et al., 2007). Then oxaloacetate is converted via cytosolic malate dehydrogenase to malate  
64 and transported back to mitochondria to complete the citrate/malate translocase system.

65 The *de novo* fatty acid synthesis in yeast occurred in the cytosol. Following the first  
66 committed step of carboxylation of cytosolic acetyl-CoA to malonyl-CoA by acetyl-CoA  
67 carboxylase (ACC), the fungal type I fatty acid synthase (FASI), a large multifunctional  
68 protein, catalyzes cycles of multistep enzymatic reactions involving condensation, reduction,  
69 dehydration and reduction of carbon-carbon bonds which are all essential for *de novo* fatty  
70 acid synthesis (Jenni et al., 2007; Tehlivets et al., 2007). Fatty acid chain elongation grows  
71 through the addition of Malonyl-CoA and Acetyl-CoA in each cycle and requires two  
72 molecules of NADPH for the two reductive enzymatic reactions in each cycle. The major  
73 source of NADPH generation is considered to be the pentose phosphate pathway (PPP) for  
74 *Y. lipolytica* (Dulermo et al., 2015; Tehlivets et al., 2007; Wasylenko et al., 2015). After the  
75 repetitive enzymatic reactions, the yeast FASI culminates C16 or C18 acyl-CoAs and further  
76 elongation or desaturation take place in the endoplasmic reticulum by respective elongases  
77 and desaturases.

78 The fungal type I fatty acid synthase (FASI) contains six copies of eight independent  
79 functional domains with a subunit sequence of acetyl transferase (AT), enoyl reductase (ER),  
80 dehydratase (DH), malonyl palmitoyl transferase (MPT) in  $\beta$  subunit (*FAS1*); acyl carrier  
81 protein (ACP), ketoacyl reductase (KR), ketoacyl synthase (KS) and phosphopantetheine  
82 transferase (PPT) in  $\alpha$  subunit (*FAS2*) (Lomakin et al., 2007; Schweizer et al., 1988). Of  
83 which, the KS domain in  $\beta$  subunits considered to be the most important catalytic domain  
84 since the reaction catalyzed by KS, covalently joining malonyl-ACP with the acetyl-ACP, is  
85 the first and key reaction step in the synthesis of fatty acids (Sangwallek et al., 2013). So far,  
86 a few inhibitors targeting KS domain have been reported (Kridel et al., 2007; Little et al.,

87 2007; Price et al., 2001). The most well known is cerulenin which is isolated from the culture  
88 broth of the fungus *Cephalosporium caerulens* and originally developed as an antifungal  
89 antibiotic (Omura, 1976). It was reported that the activity of condensation reaction by the  
90 enzyme ketoacyl synthase (KS) is irreversibly inhibited by this inhibitory molecule both for  
91 prokaryotes (type II FAS) and eukaryotes (type I FAS) (D'agnolo et al., 1973; Goldberg et al.,  
92 1973; Vance et al., 1972). Cerulenin was used for selection of high lipid producing mutants  
93 for the oleaginous yeast *Rhodotorula glutinis* and *Lipomyces starkeyi* (Tapia V et al., 2012;  
94 Wang et al., 2009). It was also shown that fatty acid composition was altered when cerulenin  
95 added in the culture medium both for oleaginous bacteria (Morita et al., 2005; Porrini et al.,  
96 2014) and oleaginous microalgae (Chaung et al., 2012; Hauvermale et al., 2006).

97 The TAG synthesis in *Y. lipolytica* follows the Kennedy pathway and requires acyl-CoA and  
98 glycerol-3-phosphate (G3P) as substrates. The second required precursor G3P, that  
99 provides the activated glycerol backbone for TAG synthesis, can be produced either from  
100 glycerol via glycerol kinase (*GUT1*) in the cytosol or can be synthesized from  
101 dihydroxyacetone phosphate (DHAP) by G3P-dehydrogenase (*GPD1*) which is a reversible  
102 reaction catalyzed by an isoform of G3P dehydrogenase (*GUT2*) (Dulermo and Nicaud,  
103 2011). It was reported that *GUT2* deactivation, *GPD1* over-expression or both mutations  
104 increased TAG accumulation (Dulermo and Nicaud, 2011). During the first step of TAG  
105 assembly, G3P is acylated by G3P acyltransferase to create lysophosphatidic acid (LPA) and  
106 further acylated by LPA acyltransferase to generate phosphatidic acid (PA). PA is  
107 dephosphorylated to form diacylglycerol (DAG) which is then acylated to synthesize TAG. In  
108 the final step, DAG is acylated either from acyl-CoA dependent reaction by DAG  
109 acyltransferases (*DGA1*, *DGA2*) or from glycerophospholipids as an acyl donor by  
110 phospholipid DAG acyltransferase (*LRO1*) (Beopoulos et al., 2012). It has been shown that  
111 over-expression of acyl-CoA dependent acyltransferases in *Y. lipolytica* enhanced lipid  
112 production (Beopoulos et al., 2012; Blazeck et al., 2014; Gajdoš et al., 2015).

113 Moreover, in order to increase lipid accumulation in *Y. lipolytica*, a pull and push strategy was  
114 applied by combining the over-expression of ACC to push the carbon flow (C-flow) into *de*

115 *novo* fatty acid synthesis pathway and the over-expression of DGA1 to pull the C-flow into  
116 the final product of TAG synthesis pathway. This strategy led to an increase of total lipid  
117 content from 18 to 61 % (Tai and Stephanopoulos, 2013). We recently demonstrated that a  
118 double-pull engineering strategy to increase the accumulation of lipids by pulling the C-flow  
119 into TAG synthesis pathway via over-expression of *GPD1* to increase the glycerol phosphate  
120 availability and its binding to fatty acids through the over-expression of *DGA2* in *Y. lipolytica*  
121 led to 3-fold improved TAG accumulation and 4-fold increase in lipid yield on glucose  
122 (Sagnak et al., 2017).

123 In addition to metabolic engineering efforts to redirect the metabolic flux towards lipid  
124 production, we, here, further studied two *Y. lipolytica* mutant strains JMY3501 and CR62 in  
125 fed-batch mode to alter the accumulation of fatty acids with a specific inhibitory molecule of  
126 KS domain and to investigate how the FASI-KS domain engineered strain regulates and  
127 controls the accumulation of fatty acids, respectively.

## 128 **2. Materials and Methods**

### 129 2.1. Microorganisms, media and growth conditions

130 The strains used in this study were *Y. lipolytica* JMY3501 obtained from the Laboratoire  
131 Microbiologie et Génétique Moléculaire, INRA, (Paris-Grignon., France) and *Y. lipolytica*  
132 CR62 obtained from the Laboratoire d'Ingénierie des Systèmes Biologiques et des Procédés  
133 (Toulouse, France). Their genotypes were as follows strain JMY 3501: MATa URA3-302  
134 Leu2-270 xpr2-322  $\Delta$ tg14  $\Delta$ pox1-6 + LEU2ex TEF-yIDGA2 + URA3ex TEF-GPD1 and for  
135 strain CR62: MATa URA3-302 Leu2-270 xpr2-322  $\Delta$ tg14  $\Delta$ phd1  $\Delta$ mfe1 +LEU2ex TEF-  
136 yIDGA2 + URA3ex-TEF-GPD1 + URA3ex- $\Delta$ FAS2 + LEU2ex TEF-yIFAS2 I1220F

137 The strains maintained on YPD/glucose agar medium containing 10 g.L<sup>-1</sup> Yeast Extract, 20  
138 g.L<sup>-1</sup> Bactopeptone, 20 g.L<sup>-1</sup> Glucose and 20 g.L<sup>-1</sup> agar and plates were stored at 4°C. For  
139 preparation of glycerol stocks (for cryopreservation of the cells), pure sterile glycerol was  
140 added to the culture broth to reach a final glycerol concentration of 30 % (v/v). This cell  
141 suspension (glycerol stocks) was then stored at -80°C.

142 Precultivations were carried out on a 5-ml tube of YPD medium at 28°C for 17 h at 100 rpm.  
143 The culture in growth phase was transferred into a 1-L Erlenmeyer flask containing 150 ml of  
144 mineral medium at pH 5.6 prepared as follows (all compounds are expressed in gL<sup>-1</sup>):  
145 (NH<sub>4</sub>)<sub>2</sub>SO<sub>4</sub> 3.5; KH<sub>2</sub>PO<sub>4</sub>, 6; MgSO<sub>4</sub>, 2; EDTA, 0.0375; ZnSO<sub>4</sub>·7H<sub>2</sub>O, 0.0281; MnCl<sub>2</sub>·4H<sub>2</sub>O,  
146 0.0025; CoCl<sub>2</sub>·6H<sub>2</sub>O, 0.00075; CuSO<sub>4</sub>·5H<sub>2</sub>O, 0.00075; Na<sub>2</sub>MoSO<sub>4</sub>·2H<sub>2</sub>O, 0.00005;  
147 CaCl<sub>2</sub>·2H<sub>2</sub>O, 0.0125; FeSO<sub>4</sub>·7H<sub>2</sub>O, 0.00875; H<sub>3</sub>BO<sub>3</sub>, 0.0025; D-biotin, 0.00025; D-L-  
148 panthotenic acid, 0.001; nicotinic acid, 0.001; myo-inositol, 0.00625; thiamin, 0.001;  
149 pyridoxine, 0.001; para-aminobenzoic acid, 0.0002. Glucose was added to a final  
150 concentration of 18 g.L<sup>-1</sup> with chloramphenicol at 10 mg. L<sup>-1</sup>. After 17 h of growth at 28°C and  
151 100 rpm, different pre-culture volumes were adjusted according to initial fermentation volume  
152 with the amount of 10% (v.v<sup>-1</sup>) inoculums in a 3-L or 5-L bioreactor.

## 153 2.2. Chemicals used

154 The chemicals glucose, salts, oligo-elements (Carb Erba), EDTA (Qbiogène),  
155 orthophosphoric acid were provided by VWR, the vitamins by Sigma. Cerulenin was  
156 purchased from EnzoLife Sciences and dimethyl sulfoxide (DMSO) from PanReac  
157 AppliChem. All products had the highest analytical grade available.

## 158 2.3. Fed-batch cultivation in bioreactor.

159 Fed-batch experiments were performed in either a 5-L stirred tank bioreactor with a working  
160 volume of 3 L or 3-L stirred tank bioreactor with a working volume of 1.5 L using the Biostat  
161 B-DCU Braun Biotech International (Sartorius AG, Germany) with the acquisition software  
162 MFCS/win 2.0.

163 The temperature was controlled at 28°C with water jacket. The pH was kept constant at 5.6  
164 with the automatic additions of acid/base solutions and monitored by a pH probe (Mettler-  
165 Toledo International Inc.). The relative pressure in the bioreactor was maintained at 300  
166 mbar. Foaming was prevented by addition of polypropylene glycol (PPG) antifoam agent. In  
167 order to avoid oxygen limitation, bioreactor was flushed with air and stirred with Rushton  
168 turbines to maintain dissolved oxygen above 20 % of saturation and measured with an  
169 autoclavable probe (InPro6000/Optical O<sub>2</sub> sensor Mettler-Toledo International Inc.). Inlet and

170 outlet air were passed through a 0.2 $\mu$ m sterile polyamide membrane filter and composition of  
171 inlet and outlet gas were analyzed with a mass spectrometer (Dycor Proline Process Mass  
172 Spectrometer, AMATEK Inc.).

173 The fed-batch cultures were supplied with sterile feeding solutions (glucose, ammonia,  
174 acid/base solutions) via pre-calibrated peristaltic pumps (Watson-Marlow). Concentration of  
175 glucose feeding solution was determined precisely from the density of solution (DE40  
176 Density Meter Mettler-Toledo International Inc.). The mass flow rates of all feeding solutions  
177 supplied to bioreactor during the experiment time were determined on-line with 0.1 to 0.01  
178 gram precision using digital scales (Sartorius AG) and generated data was obtained via Lab  
179 VIEW data acquisition software (International Instruments Cor.).

180 Fed-batch cultures were applied following two different procedures depending on the  
181 objective of the study: a procedure under Nitrogen depletion and a procedure under Nitrogen  
182 limitation.

### 183 2.3.1. Fed-batch cultivation under N depleted conditions

184 The fed-batch cultivation was divided into two phases:

185 *Growth batch phase:* After the inoculation of bioreactor, a batch phase was applied under  
186 non nutrient limited condition. Glucose and ammonium sulfate concentrations were set at  
187 100 g.L<sup>-1</sup> and 2.5 g.L<sup>-1</sup>, respectively. The nitrogen concentration was calculated in order to  
188 produce up to 15 g.L<sup>-1</sup> of biomass before reaching N-limited conditions. The pH was  
189 regulated with 5M KOH solution.

190 *N-depleted phase:* Growth phase switched naturally to N-depleted production phase when  
191 ammonium was completely exhausted. Glucose was fed by pulses of a 750 g.L<sup>-1</sup> sterile  
192 glucose solution when residual glucose concentration reached 20 g.L<sup>-1</sup> in the bioreactor.  
193 Pulse was applied in order to bring the residual glucose concentration back to 100 g.L<sup>-1</sup>.

### 194 2.3.2. Fed-batch cultivation under N-limitation conditions

195 The fed-batch culture was divided in three phases according to a feeding strategy.

196 *Growth phase:* After the inoculation of bioreactor, a sterile glucose solution with at a  
197 concentration of 205 g.L<sup>-1</sup> was exponentially fed with a peristaltic pump to maintain constant

198 the specific growth rate at  $0.18 \text{ h}^{-1}$ . The nitrogen source was supplied by sterile  $0.44 \text{ M}$   
199 ammonia solution which was also used for pH regulation.

200 *Transition phase:* When biomass concentration reached approximately  $2 \text{ g.L}^{-1}$ , the pH  
201 corrector solution was switched to a sterile  $2.5 \text{ M}$  potassium hydroxide (KOH) solution.

202 *N-limited phase:* When the nitrogen source was depleted in the culture medium,  $0.44 \text{ M}$   
203 sterile ammonia solution was exponentially fed to the reactor with a peristaltic pump in order  
204 to maintain a constant residual growth rate at  $0.02 \text{ h}^{-1}$ . Concomitantly the feeding profile of  
205 glucose was modified in order to maintain a constant N/C molar ratio above  $0.03 \text{ Nmol.Cmol}^{-1}$   
206 in order to induce lipid accumulation without citric acid secretion as demonstrated in Ochoa-  
207 Estopier and Guillouet, 2014.

## 208 2.5. Off gas analysis

209 The inlet and outlet gas composition in carbon dioxide ( $\text{CO}_2$ ) and oxygen ( $\text{O}_2$ ) were  
210 measured by a fermentation gas monitor system (LumaSense technologies Europe). The  
211 system combines a multipoint sampler 1309 with a gas analyzer (INNOVA1313). Gas  
212 analysis was performed every minute during the whole experiment.  $\text{CO}_2$  production rate  
213 ( $r_{\text{CO}_2}$ ) and  $\text{O}_2$  consumption rate ( $r_{\text{O}_2}$ ) were calculated as described by Poilpre et al., 2002.  
214 The Respiratory Quotient (RQ) was calculated as the molar ratio between  $r_{\text{CO}_2}$  and  $r_{\text{O}_2}$ .

## 215 2.6. Determination of biomass

216 Yeast growth was evaluated by a turbidimetric method using a spectrophotometer (Hach-  
217 Lange DR3900, UK) at  $620 \text{ nm}$  ( $\text{OD}_{620\text{nm}}$ ) with a  $2 \text{ mm}$  path length special optical glass  
218 cuvette (Hellma Analytics, Germany). The dry cell weight (DCW) measurement was  
219 determined by a gravimetric method by filtering an accurate volume of the culture on  $0.45 \mu\text{m}$   
220 pore-sized polyamide membranes (Sartorius AG, Göttingen, Germany) which were  
221 previously dried and weighed. After the filtration, the membranes were washed with  
222 deionized water to eliminate the culture medium and then dried at  $60^\circ\text{C}$  under partial vacuum  
223 of  $200 \text{ mmHg}$  (Heraeus, France) for 48 hours and weighed. The quantification of DCW was  
224 determined by the difference in membrane mass before and after the filtration and expressed  
225 in  $\text{g}_{\text{DCW}}.\text{L}^{-1}$ .

226 Growth rates were determined based on time-courses of optical density ( $OD_{620nm}$ ).  $OD_{620nm}$   
227 was calibrated against dry cell weight measurements. The biomass formula used to convert  
228 cell dry weight into molar carbon concentration was  $CH_{1.770}O_{0.440}N_{0.165}$  with a molecular  
229 weight of 26.33 g.Cmol<sup>-1</sup>.

## 230 2.7. Metabolite analysis

231 The culture supernatants were analyzed by High performance Liquid Chromatography  
232 (Alliance 2690, Waters, Massachusetts, US) using an Aminex HPX-87H<sup>+</sup> ion exchange  
233 column (Bio-Rad, US) coupled with a dual detection (IR and UV at 210 nm). The column was  
234 operated at 50 °C using a mobile phase of 5 mM H<sub>2</sub>SO<sub>4</sub> at a flow rate of 0.5 ml.min<sup>-1</sup>. Culture  
235 supernatant was obtained by centrifuging (MiniSpin Eppendorf, USA) the fermentation  
236 culture in Eppendorf tubes at 12000 g. for 4 min. The supernatant was filtered on Minisart  
237 filters 0.45 µm pore-sized diameter polyamide membranes (Sartorius AG, Germany). The  
238 metabolites searched for detections and quantification was glucose, citrate, isocitrate, alpha-  
239 ketoglutarate, pyruvate, malate, succinate, fumarate, lactate and acetate.

240 The quantification of lipids was carried out by digestion-methylation method based on  
241 Browse et al., 1986. 20 mg of lyophilized cells were suspended with 2 ml of methanol  
242 solution containing 25 ml. L<sup>-1</sup> of sulfuric acid (95 %), 1 mg.ml<sup>-1</sup> antioxidant (2,6-di-tert-butyl-  
243 4-methylphenol, (BHT)) and internal standard (C9:0). The mix in sealed Pyrex tubes was  
244 placed in an 85°C bath for 120 minutes. After cooling, 1.5 ml of 5 % NaCl (v/v) solution  
245 containing 1 mg.ml<sup>-1</sup> BHT and 2 ml of n-Hexane containing 1 mg.ml<sup>-1</sup> BHT were added and  
246 tubes were vortexed for 2 min (Multi Reax shaker, Heidolph, Germany) and centrifuged at  
247 790 g for 10 min at 4°C (Centrifuge 5810R, US). The lipidic phase was then collected and the  
248 composition was analyzed by Gas Chromatography as mentioned in (Cescut et al., 2011).  
249 Lipid quantification was also performed by epifluorescence after staining the cells with  
250 Bodipy 493/503 in a Microplate reader (Synergy HT, Biotek, USA) as follows: the pellets  
251 were washed 3 times with PBS buffer solution (in g.L<sup>-1</sup>, NaCl, 8; Na<sub>2</sub>HPO<sub>4</sub>, 1.15; KCl, 0.2;  
252 KH<sub>2</sub>PO<sub>4</sub>, 0.2; pH at 6.9-7.1) at 4 °C and resuspended in the same buffer solution to a  $OD_{620nm}$   
253 of 0.5; 1 ml of the cell suspension was mixed with 10µl of Bodipy 493/503 (100 µg.ml<sup>-1</sup> in

254 DMSO) and incubated 5 min at 4°C; the mixture was then centrifuged 3 min at 13,000 rpm  
255 and re-suspended into 1 ml PBS buffer solution; 200 µl of this cell suspension were placed in  
256 a 96-well Nuclon™Δ surface Microplate and read at 528 nm with an excitation wavelength  
257 value of 428 nm. The measurements were repeated 5 times showing a standard deviation  
258 lower than 5 %.

259 The quantification of residual ammonium in the medium was determined with an Orion  
260 ammonium probe (ORION Research Inc., Boston, USA) and voltmeter (ORION pH/ISE  
261 Meter, USA) as follows: 5 ml of culture broth were filtered on 0.45 µm pore sized diameter  
262 polyamide membrane (Sartorius AG, Germany) and mixed with 200 µl of ISA buffer solution  
263 (Ionic Strength Adjustor: NaOH, 5 mol L<sup>-1</sup>; disodium EDTA, 0.05 mol L<sup>-1</sup> and methanol 1 g L<sup>-1</sup>  
264 ). The concentration of NH<sub>4</sub> was determined with a calibration curve correlating the mV and  
265 the NH<sub>4</sub> concentration in a range of 10<sup>-1</sup>-10<sup>-5</sup>mol L<sup>-1</sup> NH<sub>4</sub>Cl.

### 266 **3. Results and Discussion**

#### 267 3.1. Impact of cerulenin on fatty acid accumulation and fatty acid profile

268 In order to assess the impact of a specific ketoacyl synthase inhibitor on the accumulation of  
269 triglycerides and fatty acid composition, the *Y. lipolytica* JMY3501 strain was performed in a  
270 3L bioreactor under nitrogen limited conditions for fed-batch mode (Fig.1). The fed-batch  
271 experiment was conducted in two phases: during the growth phase, glucose solution as the  
272 sole carbon source at a concentration of 210 ± 5g.L<sup>-1</sup> was exponentially fed at a specific  
273 growth rate of  $\mu=0.18\text{ h}^{-1}$ , the culture was switched into nitrogen limited phase after 12 h of  
274 growth phase.

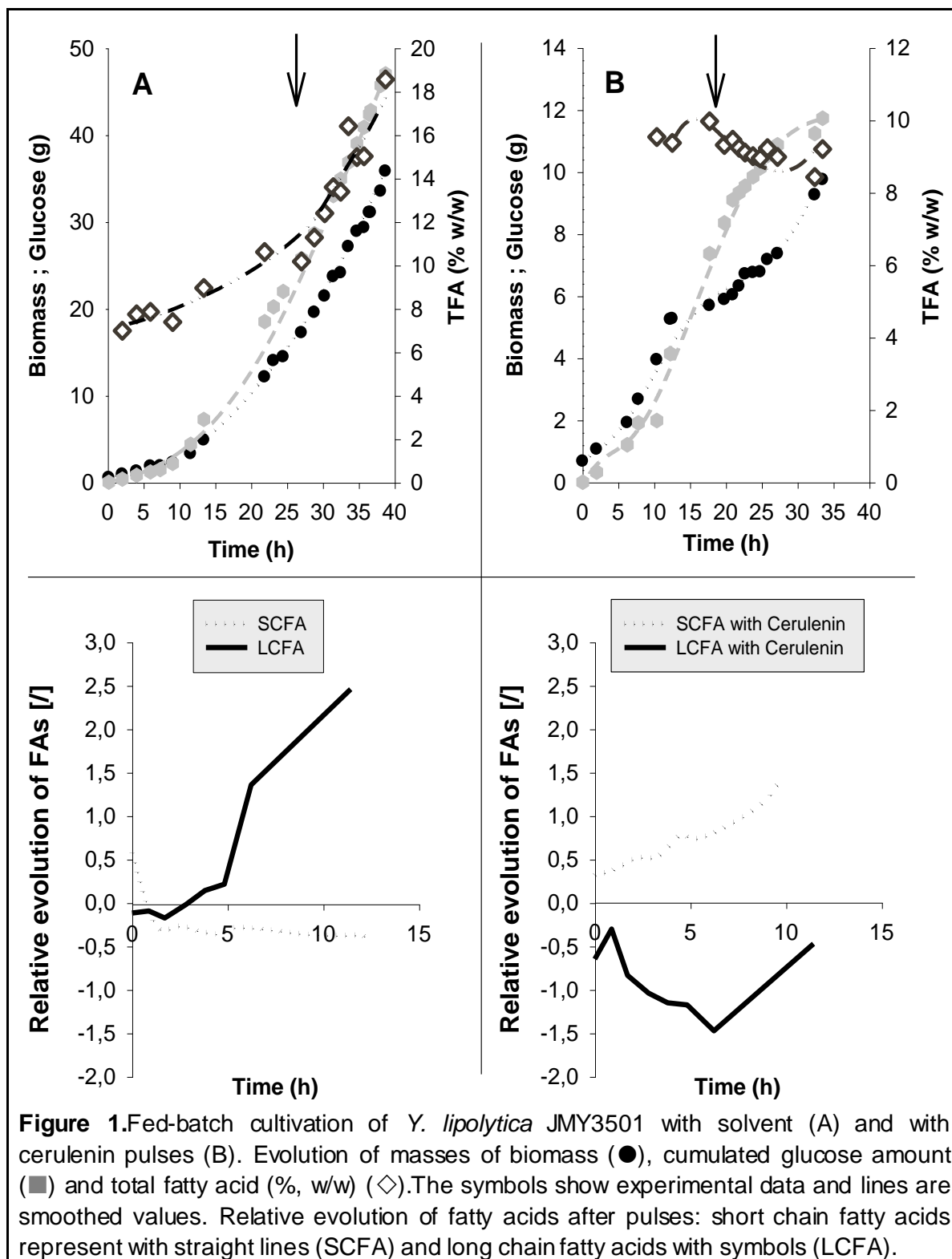
275 During the growth phase, the maximum specific growth rate ( $\mu_{\max}$ ) was found at a value of  
276 0.24 h<sup>-1</sup> with a global biomass yield on glucose at 0.50 g<sub>CDW</sub>.g<sub>glucose</sub><sup>-1</sup> which are the  
277 characteristics of this strain when grown on glucose (Sagnak et al., 2017). It is observed that  
278 when *Y. lipolytica* cultivated on glucose as the sole carbon source, upon nutrient limitation  
279 mainly citric acid production occurred over lipid accumulation only 5-10 % of TAG (wt.wt<sup>-1</sup>)  
280 (Papanikolaou et al., 2006). On the other hand, Ochoa-Estopier and Guillouet, (2014)  
281 demonstrated that accumulation of TAG without producing citric acid was possible under

282 nitrogen limited conditions on *Y. lipolytica* wild type strain W29 and suggested to control the  
283 N/C ratio above a critical value of 0.021 Nm<sup>ol</sup>.Cmol<sup>-1</sup>. Therefore, in order to induce lipid  
284 accumulation without citric acid secretion, the feeding rate of carbon and nitrogen source  
285 was performed to keep the N/C ratio above 33 Cmol.Nmol<sup>-1</sup>.

286 The fatty acid synthase inhibitor Cerulenin was pulsed to the culture 9 hours after the onset  
287 of the lipid accumulation phase at a ratio of 0.5 mg<sub>Cerulenin</sub>.g<sup>-1</sup>DCW as shown in (Figure 1B) with  
288 an arrow. The quantitative analysis of fatty acid composition was performed by GC to  
289 determine the Cerulenin impact on fatty acid synthesis. Cerulenin dissolved in ethanol, thus a  
290 reference culture of the strain was also performed with this solvent pulse after the onset of  
291 the lipid accumulation. Prior to solvent and cerulenin pulses total lipid contents were 10.2 ±  
292 0.8 % and 9.6 ± 0.3 % (w/w), respectively.

293 The principal fatty acids produced during the cultivation of the strain under nitrogen limitation  
294 composed of long chain length fatty acids (LCFA) for both cultures before pulses. Oleic acid  
295 (C18:1) was the major fatty acid together and followed by linoleic acid (C18:2) and palmitic  
296 acid (C16:0). These three fatty acids were accounted for both cultures at an average  
297 percentage of 93 ± 3.6 % of the total fatty acids. However, GC analysis showed that the fatty  
298 acids synthesized after the cerulenin pulse within 12 hours had a different chain length profile  
299 than those synthesized without cerulenin (Figure 1 C and D). Solvent pulse resulted an  
300 increase in LCFAs: obtained with an increase level of C18:1 and C16:1 (20 % and 3 %, respectively)  
301 and a decrease level of C18:2 and C16 (35 % and 4 %, respectively). On the  
302 contrary, cerulenin pulse significantly enhanced the abundance of short chain length fatty  
303 acids and slightly decreased the production of long chain length fatty acids (the maximum  
304 obtained with 14 % reduction on C18:2 level). The short chain length fatty acids represents  
305 11.5 % of total fatty acid content after cerulenin pulse and the highest increase obtained with  
306 capric acid (C10) at 87 % and followed by lauric acid (C12) and myristic acid (C14) at a  
307 percentage of 13 % and 11 %, respectively.

308 Following cerulenin pulse a decline was observed on lipid production yield on glucose which  
309 was found at an average value of 0.11 ± 0.03 g.g<sup>-1</sup> however no citric acid production was



311 detected throughout the culture. Moreover, lipid production yield reached a maximal value of  
 312 0.17 g. g<sup>-1</sup> which is consistent with our previous findings (Sagnak et al., 2017). Therefore, it  
 313 suggests that the engineered yeast was able to overcome this level of KS inhibition to  
 314

315 maintain cell survival by consuming citric acid and rearranging fatty acid composition. And as  
316 a result of unaffected cell viability, chemically disrupted FASII enzyme system in KS domain  
317 of the *Y. lipolytica* JMY3501 strain significantly enhanced the accumulation of short chain  
318 length fatty acids.

### 319 3.2. Fatty acid accumulation of *Y. lipolytica* CR62 engineered strain in the Ketoacyl Synthase 320 domain

321 In order to characterize fatty acid accumulation of *Y. lipolytica* CR62, the engineered strain  
322 was performed in 5L bioreactor under non nutrient limited conditions followed by a switch to  
323 nitrogen depleted conditions in a mineral medium with glucose as the sole carbon source  
324 (Fig.2). The fed-batch cultivation was divided into two phases. The batch growth phase was  
325 conducted under non nutrient limitation with an initial glucose concentration at 100 g. L<sup>-1</sup>. The  
326 strain grew exponentially at a maximal growth rate ( $\mu_{max}$  calculated by linearization of the  
327 data in the exponential growth phase) of 0.16 h<sup>-1</sup> with a global biomass yield on glucose at  
328 0.38 g<sub>CDW</sub> g<sub>glucose</sub><sup>-1</sup>. The obtained growth rate and the global biomass yield on glucose were  
329 lower compared to wild type strain ( $\mu_{max}=0.27$  h<sup>-1</sup> and 0.49 g<sub>CDW</sub> g<sub>glucose</sub><sup>-1</sup>) (Ochoa-Estopier  
330 and Guillouet, 2014)), which suggest a drastic impact of the engineered FAS on the growth.  
331 Once nitrogen was completely consumed after 23 h of growth phase, metabolism switched  
332 toward lipid accumulation and citric acid secretion. After 76 h of cultivation, citric acid  
333 concentration reached 59 g. L<sup>-1</sup> with a citric acid production yield on glucose at 0.52 g g<sup>-1</sup> and  
334 total lipid content 16 %. The lipid content was identical to the parent strain W29 of around 18  
335 % accompanied with a 1.3 fold-decrease in the citric acid production yield on glucose at 0.68  
336 g g<sup>-1</sup> (Ochoa-Estopier and Guillouet, 2014). On the other hand, CA production yield was 1.3  
337 fold higher compared to strain JMY3501 at 0.4 g.g<sup>-1</sup> (Sagnak et al., 2017) suggesting that the  
338 nature of nitrogen depletion in the culture medium favor the metabolic carbon flux towards  
339 citric acid formation instead of fatty acid production.

340

341

342

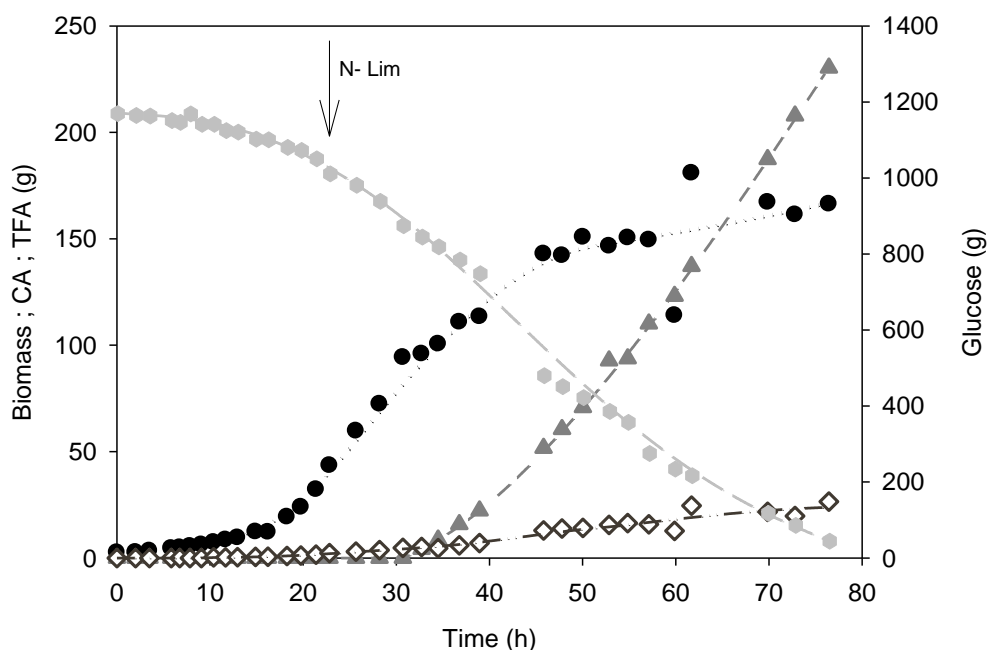


**Figure 2.** Fed-batch cultivation of *Y. lipolytica* CR62. Evolution of masses of biomass (●), citric acid (▲), cumulated glucose consumed (●) and total lipid content (◇). The symbols represent experimental data and lines are smoothed values. Arrow indicates the onset of nitrogen limitation phase.

344  
345  
346

**Table 1:** Fatty acid composition of *Y. lipolytica* strains during exponential growth (% w/w)

<i>Yarrowia lipolytica</i>	C16	C16:1	C18	C18:1	C18:2	Ref
<b>W29</b>	6.3 ±2.6	2.4 ±0.6	4.5 ±1.2	53.4 ±5.2	17.8 ±1.5	This study
<b>JMY 3501</b>	19.4 ±1.9	5.6 ±0.5	5.2 ±0.7	38.3 ±3.0	25 ±4.7	This study
<b>CR62</b>	13.7 ±0.5	16 ±1.3	0 ±0	15.8 ±0.9	54.5 ±2.4	This study

347  
348 The fatty acid composition of the FAS engineered strain of *Y. lipolytica* CR62 differ its fatty  
349 acid profile compared to wild type strain W29 and to engineered strain JMY 3501 during the  
350 growth phase (Table1). The FAS engineered strain CR62 composed of high level of C18:2  
351 and C16:1 at approximately 55 % and 16 %, respectively. Comparatively to wild type W29  
352 and to overproducer JMY3501 strains, CR62 contained very low level of C18:1 at  
353 approximately 16 % which was the major fatty acid for both strains at approximately 54 %  
354 and 38 % of the total fatty acids during the growth phase, respectively (Table1).

355  
356

**Table2:** Fatty acid composition of *Y. lipolytica* strains at the end of culture (% w/w).

<i>Yarrowia lipolytica</i>	C14	C16	C16:1	C18	C18:1	C18:2	Ref
<b>W29</b>	/	17.4	7.1	11.9	52.5	7.3	(Lazar et al., 2014)
<b>JMY 3501</b>	/	22.6 ±0.6	5.4 ±0.2	7.3 ±0.1	50.3 ±0.2	14.3 ±0.5	This study
<b>CR62</b>	10.4±0.9	31.3 ±0.2	11.1±0.1	5.2 ±0.1	22.1 ±0.2	19.9 ±0.5	This study

357  
358

After 76 h of cultivation, the CR62 strain mostly contained palmitic acid (C16:0) with a percentage of 31.3 ± 0.2 % of the total fatty acids, represented 37 % among the accumulated fatty acids in this strain (Table 2). The second most common fatty acid was oleic acid (C18:1) represents 25 % of accumulated fatty acids which was also the most reduced fatty acid between *Y. lipolytica* strains during lipid accumulation. Moreover, upon nitrogen depletion CR62 decrease the level of C18:2 and reached 19.9 ± 0.5 % of the total fatty acids which represents 8 % of accumulated fatty acids at the end of the culture.

365

Besides the improved level of medium chain fatty acids and reduced level of long chain fatty acids (oleic and linoleic acid), engineering the ketoacyl synthase domain to prevent long chain fatty acid synthesis, significantly enhanced the accumulation of short chain fatty acid. Myristic acid (C14:0) at 10.4±0.9 % (w/w) of total fatty acid at the end of the culture represented the third most accumulated fatty acid at 16 % after palmitic and oleic acids. These values correlate favorably with Rigouin *et al.* 2017 successfully demonstrated 5.8 % (w/w) myristic acid production with *Y. lipolytica* engineered in FAS-KS domain and corresponding to 18 fold increase compared to parental wild type strain.

373

Altogether these results support the role of engineering the FAS-KS domain to modify its substrate specificity promotes the accumulation of short chain length fatty acids however causes a decrease on their catalytic efficiency in order to compromise cell viability and membrane fluidity (Rigouin et al., 2017; Sangwallek et al., 2013).As indeed demonstrated with the deletion of elongase enzyme (elo1) in a mutant strain of *Y. lipolytica* that also engineered in FAS - KS domain and lacking the β- oxidation pathway required a

379 supplementation of essential fatty acids to allow the growth of that strain (Rigouin et al.,  
380 2018) suggesting that in FAS engineered strains, the elongation and desaturation enzymes  
381 play a critical role to support cell growth and cell viability.

#### 382 **4. Conclusions**

383 Regulation of fungal fatty acid synthase enzyme system in *Y. lipolytica* led to a strong  
384 modification in fatty acid profile. Targeted inhibition of FAS enzyme system in ketoacyl  
385 synthase domain with its specific inhibitor without affecting cell viability significantly  
386 enhanced the short chain length fatty acid production under nitrogen limitation without citric  
387 acid secretion. Similarly, FAS-KS domain engineered strain enhanced the short chain length  
388 fatty acids however; citric acid secretion occurred due to the nature of nitrogen depletion.  
389 The results provide further evidence for the importance of ketoacyl synthase domain on the  
390 fatty acid accumulation and chain length determination.

#### 391 **Acknowledgments**

392 Financial support for this study was provided by Agence Nationale de la Recherche (ANR)  
393 and Commissariat aux Investissements d'Avenir via the project ProBio3 "Biocatalytic  
394 production of lipidic bioproducts from renewable resources and industrial by-products: BioJet  
395 Fuel Application" (ref. ANR-11-BTBT-0003). The authors have no conflict of interest to  
396 declare.

#### 397 **References**

398 The references cited in this article represented in Chapter 5.

### **3.3.2. Cell Viability and Morphology**

In this section, the physiological and morphological state of yeast cells in response to solvent and cerulenin pulses were investigated. Assessment of metabolic activity, membrane integrity, cell viability, cell shape, cell size and the internal complexity of the strain *Y. lipolytica* JM3501 were determined by flow cytometry methods as explained in section 2.6.4.

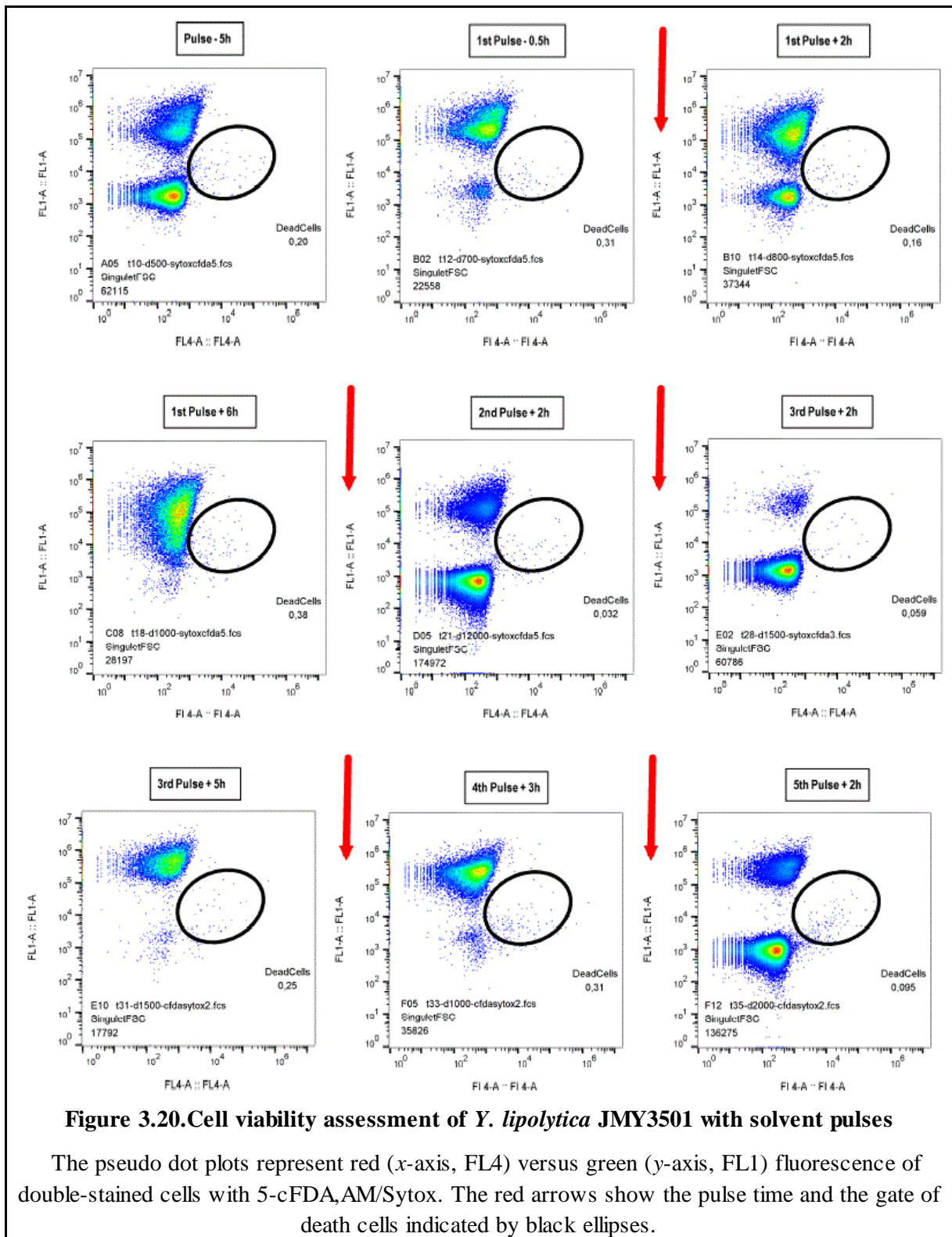
#### **3.3.2.1. Cell Viability**

##### **3.3.2.1.1. Reference Culture**

Figure 3.20 showed the flow cytometry analysis to assess the viability (based on esterase activity) of *Y. lipolytica* JMY3501 before and after the solvent pulses.

The cell viability assessment showed that more than 99 % cells were viable and the cells possessed intact membrane after the pulses. This suggests that cells were resistant to solvent pulses; indicates that solvent pulses do not have a toxic impact and additionally cellular morphology was not really affected.

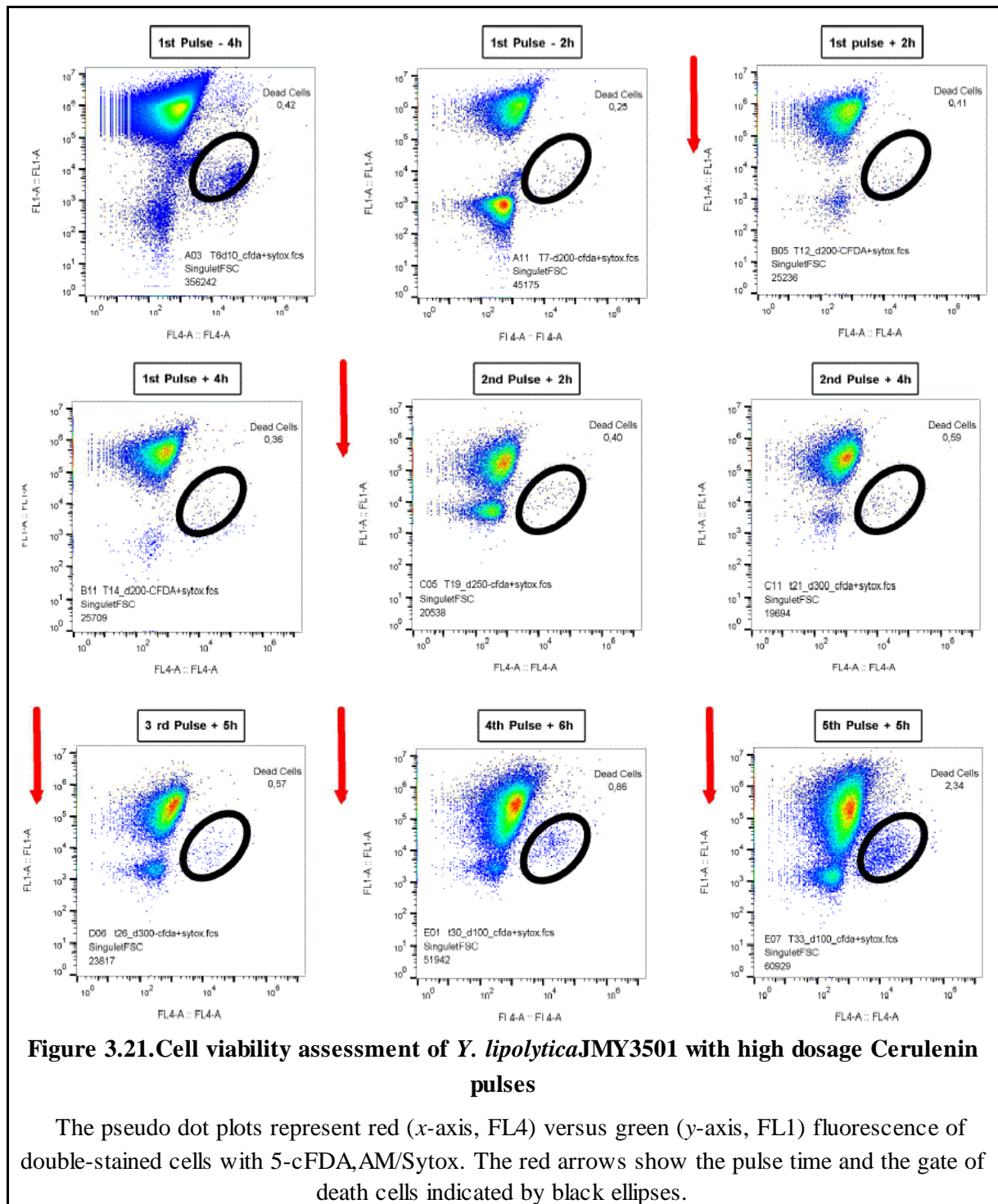
Even though cells still maintained intact membrane, their relocation through y-axis after two hours of pulse as seen in the Figure 3.20 for the 1<sup>st</sup>, 2<sup>nd</sup>, 3<sup>rd</sup> and 5<sup>th</sup> pulses indicates that the cells possessed low intracellular nonspecific esterase activity. However this decreased metabolic activity reverted after the pulses as seen in the sample of 4th Pulse + 3 hours and completely recovered more than 3 hours later as seen in the sample of 1<sup>st</sup> Pulse + 6 h and 3<sup>rd</sup> Pulse + 5 h (Figure 3.20).



### 3.3.2.1.2. High dosage of cerulenin pulses

Due to the drastic rearrangement of lipid cell content after high dose of cerulenin pulses, membrane integrity and the cell viability of *Y. lipolytica* JMY3501 was analyzed and the responses of yeast cells shown in Figure 3.21.

The results revealed the fact that the cells sustained intact membrane with high dosage of cerulenin pulses with a constant ratio. The dead cell percentage was found always lower than 1 %. The only exception was observed 5 hours after the fifth cerulenin pulse as seen in the Figure 3.21 where the dead cell percentage increased to 2.34 %. Then the strong inhibition on FA composition upon cerulenin pulses at high dosage did not translate to loss of membrane integrity.



### 3.3.2.1.3. Middle dosage of cerulenin pulses

Figure 3.22 shows the flow cytometry analysis to assess the viability of *Y. lipolytica* JMY3501 with middle dosage of cerulenin pulses. The results revealed that almost 97.5 % of cells maintained intact membrane throughout the culture with middle dose of cerulenin pulses.

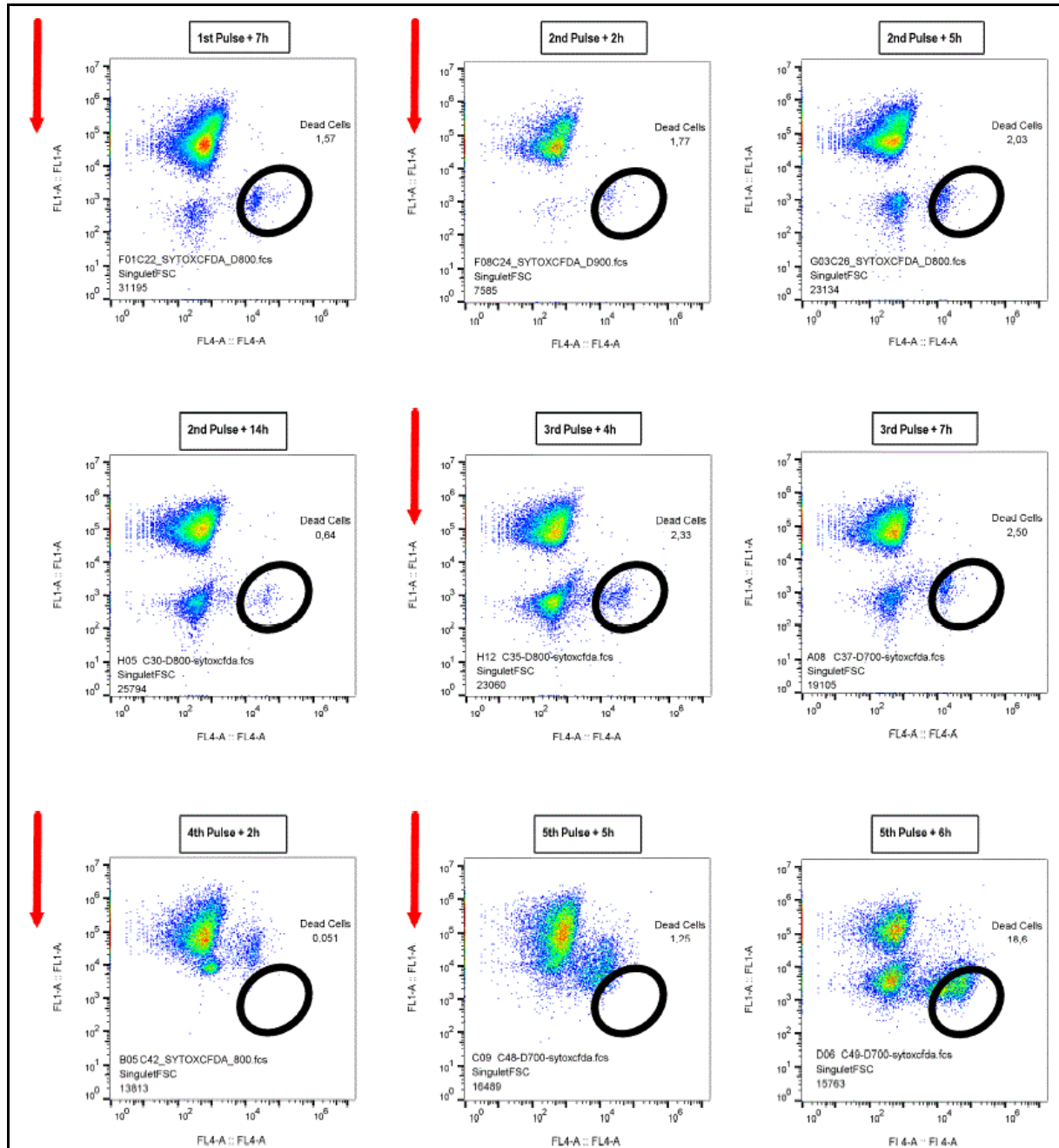


**Figure 3.22. Cell viability assessment of *Y. lipolytica* JMY3501 with middle dosage cerulenin pulses**

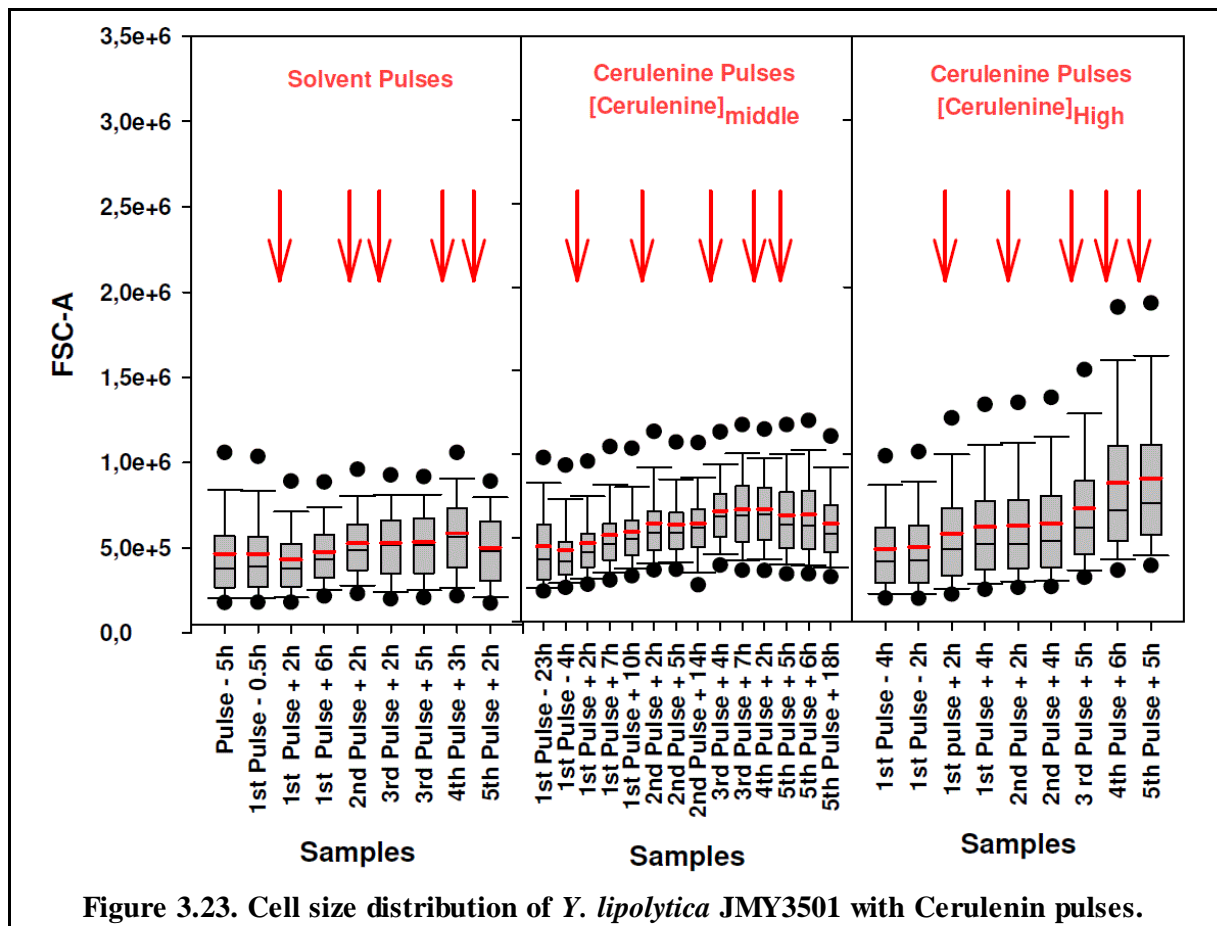
The pseudo dot plots represent red ( $x$ -axis, FL4) versus green ( $y$ -axis, FL1) fluorescence of double-stained cells with 5-cFDA,AM/Sytox. The red arrows show the pulse time and the gate of death cells indicated by black ellipses.

### 3.3.2.2. Cell Morphology

The distribution of cell population in terms of morphological features of yeast cells such as cell size, cell length and cell granularity in response to cerulenin pulses were shown in Figure 3.23, Figure 3.24 and Figure 3.25, respectively.

The forward scatter (FSC) signal is the amount of light diffracted in the forward direction ( $0^\circ \pm 13^\circ$ ) and used proportionally to the size of the cells which means that the magnitude of FSC signal increases with cell size (Díaz et al., 2010; Hyka et al., 2013).

Distribution of cell size in reference culture with solvent pulses did not show significant variations. On the contrary, cerulenin pulses were significantly induced the cell size distribution: compared to the middle dosage of cerulenin pulses, the high dosage of cerulenin pulses were strongly influenced the cell size distribution as seen in Figure 3.23.



As the cell passes through the laser beam, it generates a signal pulse. The width of the pulse generated from FSC signal is proportional to the time that the cell spends in the laser beam and can be used to distribute yeast cell length (Timoumi et al., 2017a, 2017b).

The mean and the median values of the reference culture were found almost equal throughout the culture suggesting that Gaussian distribution was observed (mean = median) and solvent pulses did not significantly affect the homogeneity of the yeast cells as seen in Figure 3.24.

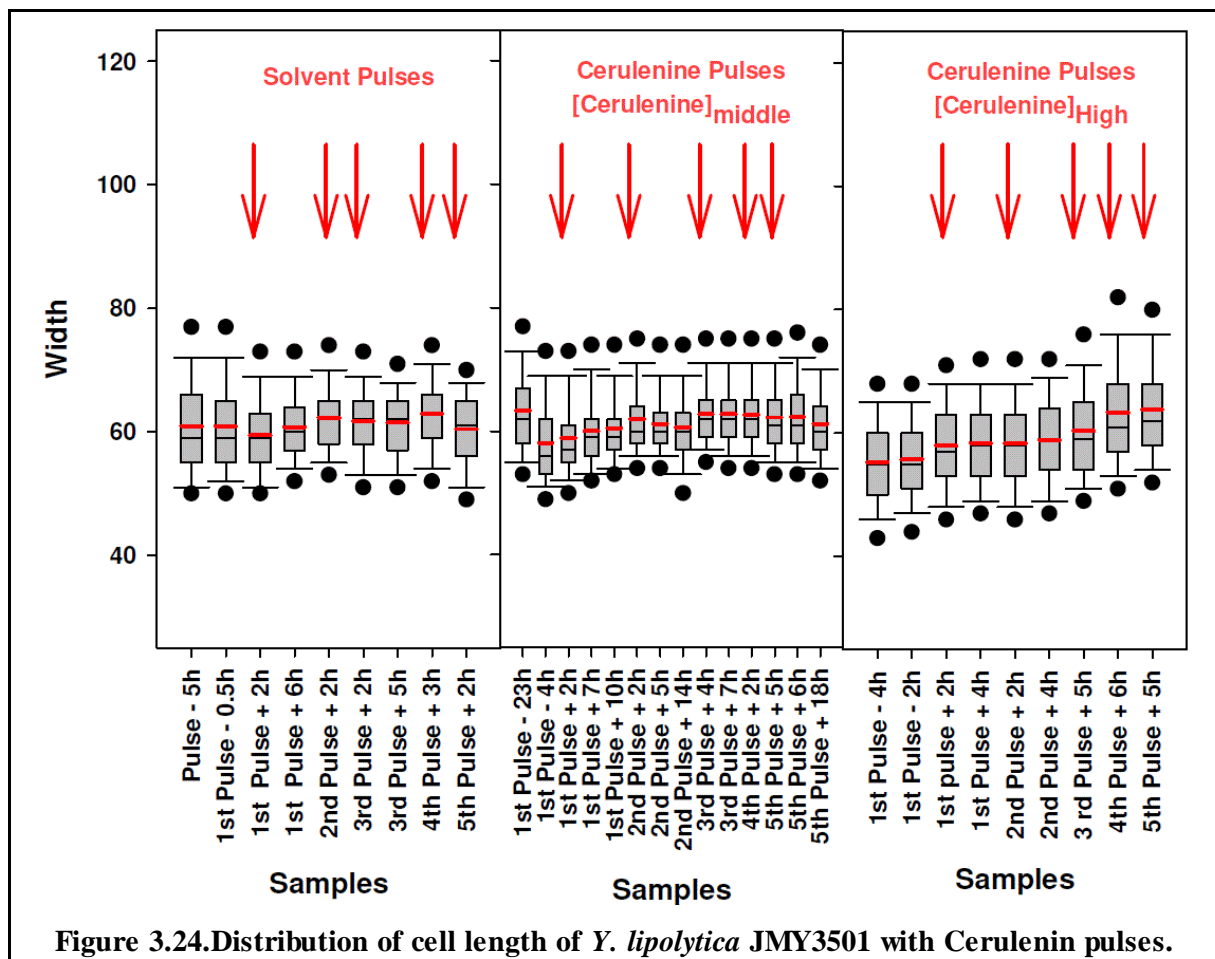


Figure 3.24. Distribution of cell length of *Y. lipolytica* JMY3501 with Cerulenin pulses.

By contrast, the yeast cell length distribution was found asymmetrical with cerulenin pulses suggesting that the distribution of yeast cell population was not anymore Gaussian as seen Figure 3.24. The cell length distribution gradually increased with high dose of cerulenin pulses while no strong impact was observed with the middle dosages.

The side scatter (SSC) signal is the amount of light reflected and/or refracted at large angle ( $90^\circ \pm 13$ ) when cells pass through the laser beam and can be used to provide information about the intracellular structures of the cell. A higher SSC signal intensity is usually obtained from cells that contain higher volume of cellular components such as storage compounds (Davey and Kell, 1996; Silva et al., 2012).

The internal complexity of yeast cells with cerulenin pulses showed a significant variation compared to the solvent pulse culture. The mean and median values were significantly

increased with cerulenin pulses. Moreover the SSC signal intensity was found higher with high dosage of cerulenin pulses compared to the middle dosage of cerulenin pulses. Furthermore the length of box plots and the upper whiskers from 75<sup>th</sup> percentile to 90<sup>th</sup> percentile were found longer compared to the middle dosage of cerulenin pulses suggesting a strong increase occurred in the intracellular structures of the cells as seen in Figure 3.25.

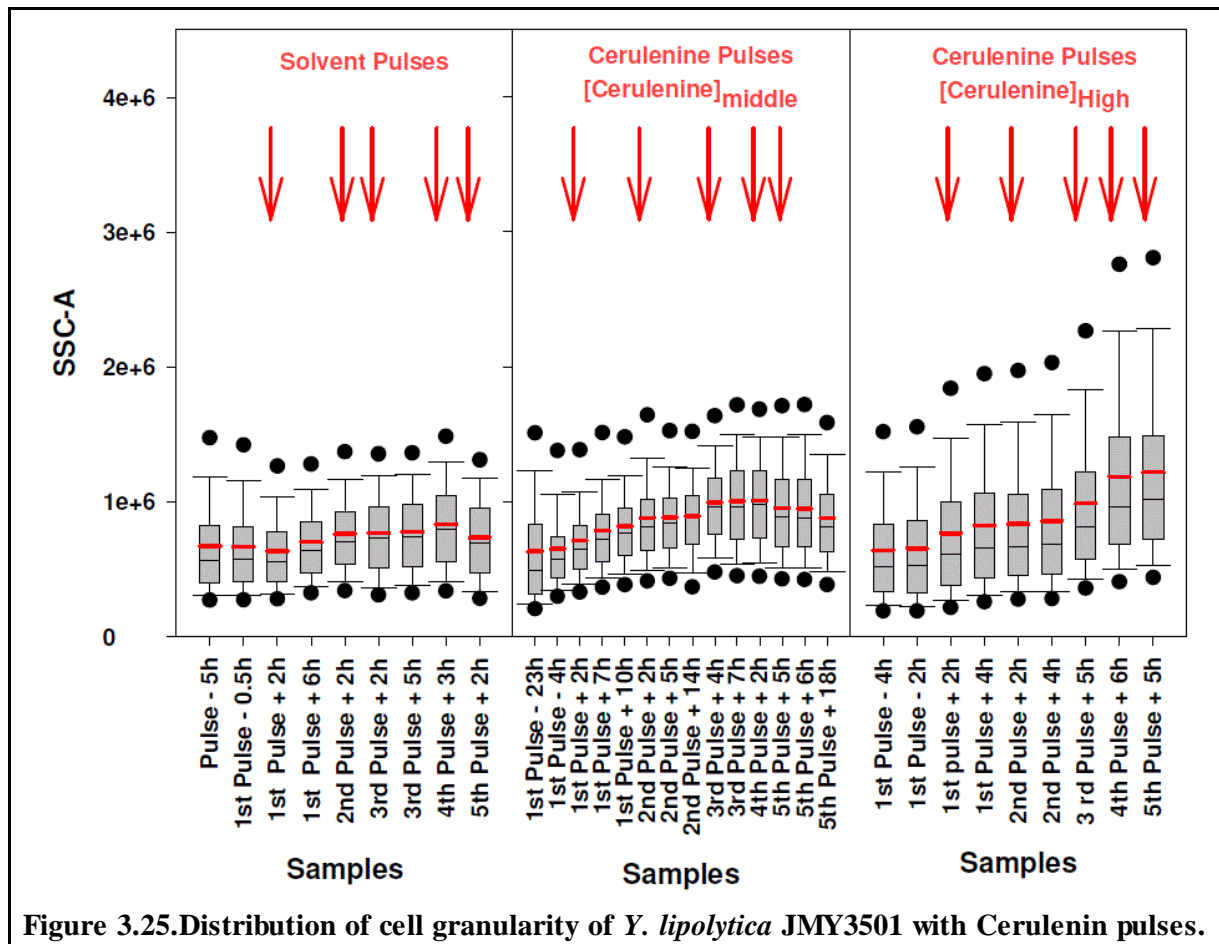


Figure 3.25. Distribution of cell granularity of *Y. lipolytica* JMY3501 with Cerulenin pulses.

## 3.4. Fed-batch culture of *Yarrowia lipolytica* JMY3501 under nitrogen limitation with Orlistat

### 3.4.1. Orlistat pulses

In this section the fed-batch culture of *Y. lipolytica* JMY3501 under nitrogen limitation were performed in order to study the effect of orlistat pulses, a potent inhibitor of fatty acid synthase enzyme, to the lipid metabolism and to the physiology of yeast. Orlistat is known to be an inhibitor of the thioesterase responsible for the termination of the FA elongation pathway. However its role is controversial in the yeast *Yarrowia lipolytica*, as some authors suggest that thioesterase is not involved in the termination but malonyl/palmitoyl-transacylase. In our strategy, orlistat would allow us to investigate the impact of the termination on the composition of the synthesized FAs.

The fed-batch experiment was performed in two phases. During the growth phase the bioreactor was exponentially fed with glucose solution at a concentration of 683 g. L<sup>-1</sup> to maintain constant the specific growth rate at 0.18 h<sup>-1</sup> and during the nitrogen limitation phase 3 M NH<sub>4</sub>OH solution was exponentially fed in order to maintain constant the specific growth rate at 0.02 h<sup>-1</sup>. The feeding of C and N-sources was performed in a way to maintain the rN/rC ratio within a range where cells accumulate lipids without citric acid as demonstrated by Ochoa-Estopier and Guillouet, 2014.

Orlistat pulses were applied after the onset of lipid accumulation phase induced by nitrogen limitation in order to assess the effect on the accumulation of triglycerides and their composition in fatty acids. Orlistat was dissolved in ethanol and four consecutive pulses were performed at a ratio of 0.5, 0.5, 1 and 2 mg<sub>Orlistat</sub>. g<sup>-1</sup><sub>DCW</sub>, respectively. The first orlistat pulse were applied 24h after the onset of nitrogen limited phase as shown in Figure 3.26. Orlistat amounts were calculated for the cell production between the consecutive pulses and adjusted further by taking into account of previous pulse cell target. The addition of ethanol with each pulse was at a ratio of 0.011 ± 0.006 g<sub>EIOH</sub>. g<sup>-1</sup><sub>DCW</sub>. Samples were withdrawn regularly every hour after the pulse.

The evolution of respiratory quotient (RQ) and the rN/rC ratio throughout the culture was shown in Figure 3.26 (A). At the beginning of nitrogen limitation the rN/rC ratio was found constant at a value of 0.011 ± 0.005 Nm<sub>ol</sub>.Cm<sub>ol</sub><sup>-1</sup>. After the first orlistat pulses the rN/rC ratio

increased to 0.014 and during the consecutive orlistat pulses the rN/rC ratio was found constant at  $0.02 \pm 0.009 \text{ Nmol.Cmol}^{-1}$ .

The RQ was at  $1.09 \pm 0.1$  and  $1.2 \pm 0.05$  during the growth and nitrogen limitation phase, respectively. The first orlistat pulse decreased the RQ from 1.2 to 1.08 and 3 h after the value reached back to 1.2. With the second pulse of orlistat at the same ratio ( $0.5 \text{ mg}_{\text{Orlistat}} \cdot \text{g}^{-1}_{\text{DCW}}$ ) the RQ value decreased from to 1.22 to 1.07 and again 3 h after the RQ reached back to 1.21.

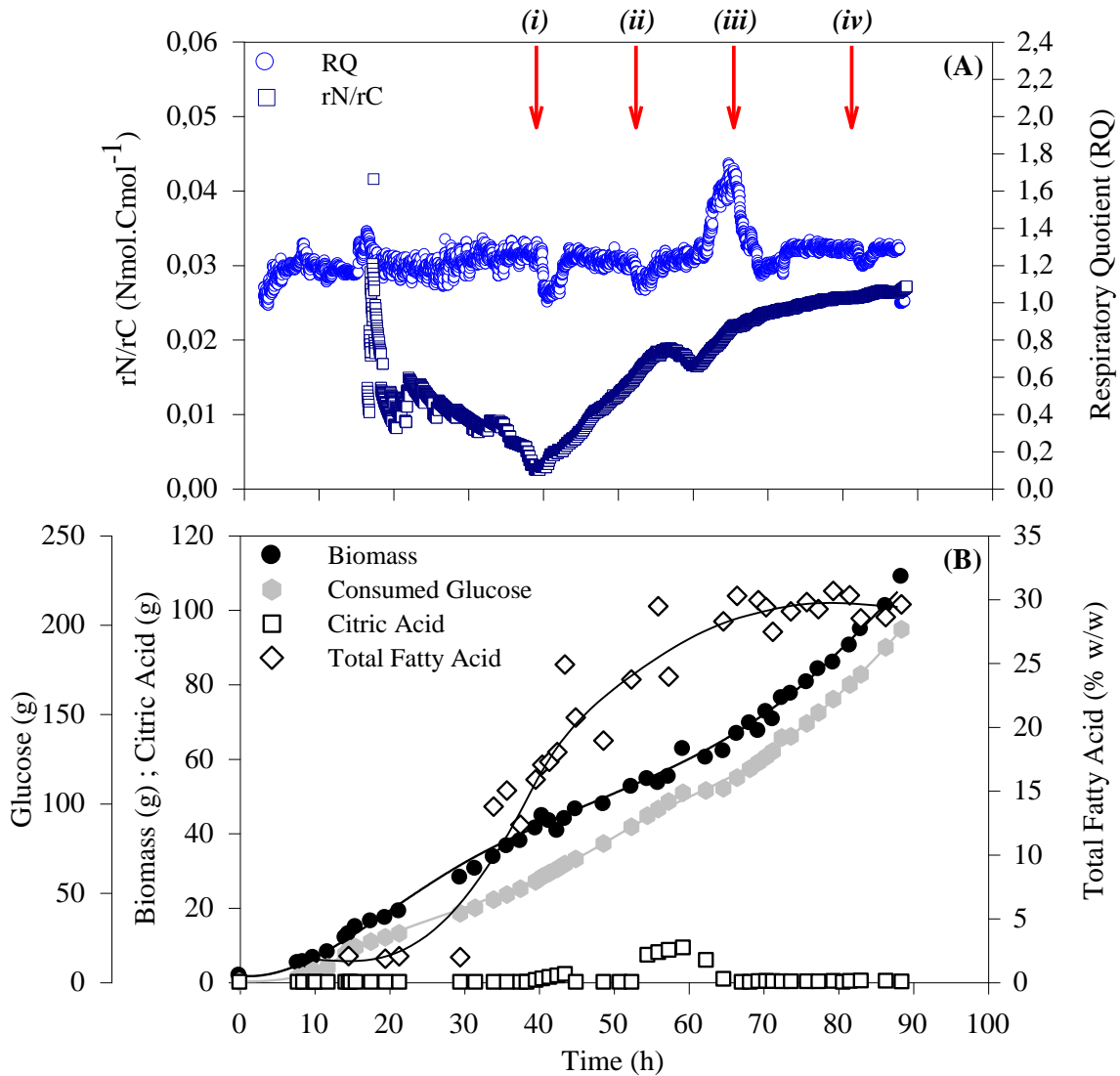


**Figure 3.26. Fed-batch culture of *Y. lipolytica* JMY3501 for fed-batch cultures under nitrogen limitation with Orlistat pulses.**

(A) rN/rC ratio and Respiratory Quotient, (B) Variation of state variables.

The symbols represent experimental data and lines are smoothed values. Orlistat pulses were shown in arrows (i)  $0.5 \text{ mg} \cdot \text{g}^{-1}_{\text{DCW}}$ ; (ii)  $0.5 \text{ mg} \cdot \Delta \text{g}^{-1}_{\text{DCW}}$ ; (iii)  $1 \text{ mg} \cdot \Delta \text{g}^{-1}_{\text{DCW}}$ ; (iv)  $2 \text{ mg} \cdot \Delta \text{g}^{-1}_{\text{DCW}}$

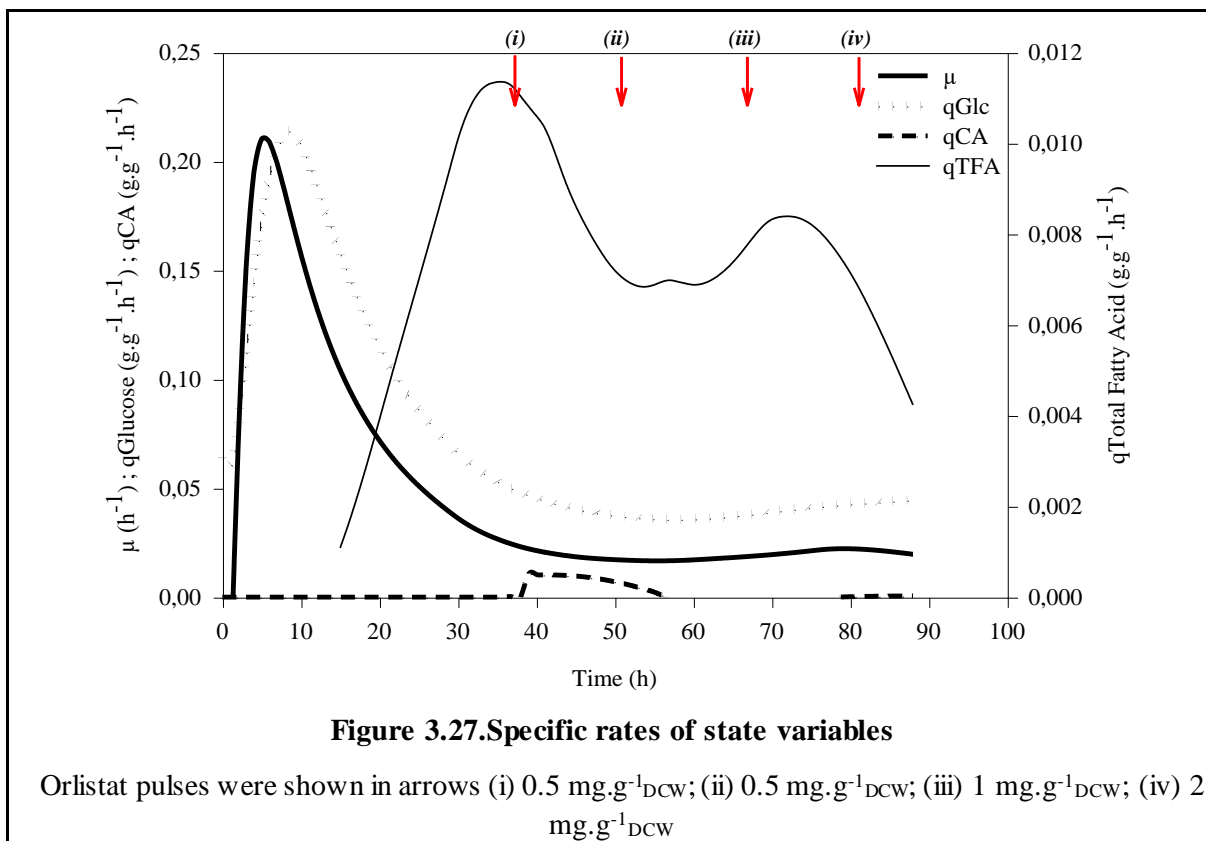
However 10 h after the second orlistat pulse, the RQ strongly increased up to 1.7. After the third orlistat pulse at a ratio of  $1 \text{ mg}_{\text{Orlistat}} \cdot \text{g}^{-1}_{\text{DCW}}$  the RQ strongly decreased to 1.3. Before the

fourth orlistat pulse at a ratio of  $2 \text{ mg}_{\text{Orlistat}} \cdot \text{g}^{-1}_{\text{DCW}}$  the RQ was found constant at  $1.28 \pm 0.013$  and decreased to 1.18 with the fourth orlistat pulse and reached back to 1.28 at the end of the culture.

Figure 3.26(B) shows the biomass production, glucose consumption, citric acid production and total fatty acid percentage (TFA) as a function of time. After more than 70 h of lipid accumulation, total glucose consumption was 195.3 g. and the final dry cell weight reached to  $104.7 \text{ g}_{\text{DCW}}$  at the end of the culture. At the beginning of the nitrogen limitation phase the total fatty acid was around 15 % (w/w). After the first orlistat pulse, the TFA reached to 21 % and 4h after the second orlistat pulse with the same ratio the TFA reached to 31 % but no more increase was obtained with the increased ratio of consecutive orlistat pulses. After the first and the second orlistat pulses at the ratio of  $0.5 \text{ mg}_{\text{Orlistat}} \cdot \text{g}^{-1}_{\text{DCW}}$ , citric acid secretion was observed maximum at the value of 2.1 g. and 9.2 g., respectively, but with consecutive orlistat pulses no more secretion was detected.

Figure 3.27 shows the specific rates as a function of time. During the growth phase the maximum specific growth rate ( $\mu_{\text{max}}$ ) and the maximum specific glucose consumption rate ( $q_{\text{Glucose}}$ ) were found at a value of  $0.21 \text{ h}^{-1}$  and  $0.21 \text{ g}_{\text{Glucose}} \cdot \text{g}^{-1}_{\text{DCW}} \cdot \text{h}^{-1}$ , respectively. After the onset of nitrogen limitation phase, growth rate and glucose consumption rate decelerated and during the consecutive orlistat pulses were found stable at  $0.022 \pm 0.002 \text{ h}^{-1}$  and  $0.047 \pm 0.003 \text{ g}_{\text{Glucose}} \cdot \text{g}^{-1}_{\text{DCW}} \cdot \text{h}^{-1}$ , respectively.

After the onset of nitrogen limitation phase at around 15 h, the specific total fatty acid production rate ( $q_{\text{TFA}}$ ) was accelerated and reached to  $0.011 \text{ g}_{\text{TFA}} \cdot \text{g}^{-1}_{\text{DCW}} \cdot \text{h}^{-1}$ . However after the first orlistat pulse,  $q_{\text{TFA}}$  decelerated down to  $0.007 \text{ g}_{\text{TFA}} \cdot \text{g}^{-1}_{\text{DCW}} \cdot \text{h}^{-1}$  and was found stable after the second orlistat pulse at the same ratio. The  $q_{\text{TFA}}$  reaccelerated up to 0.008 with the third orlistat pulse at a ratio of  $1 \text{ mg} \cdot \text{g}^{-1}_{\text{DCW}}$  but no more increase was observed with the final orlistat pulse at a ratio of  $2 \text{ mg} \cdot \text{g}^{-1}_{\text{DCW}}$ .



The impact of consecutive orlistat pulses during lipid accumulation phase under nitrogen limitation on the total fatty acid composition of *Y. lipolytica* JMY3501 is presented in Figure 3.28 (A) and (B). Figure 3.28 (A) shows the medium and long chain length fatty acids from C16:0 to C18:2 and the short and the very long chain length fatty acids of C14:0 and C20:0 to C24:0 shown in Figure 3.28(B), respectively.

Before the first orlistat pulses, the medium chain length fatty acids were at a percentage of (% w/w)  $14.4 \pm 9.7 \%$  for palmitic (C16:0) and  $7.63 \pm 0.97 \%$  for palmitoleic (C16:1) acids. The long chain length fatty acids were at a percentage of (% w/w)  $7 \pm 0.86\%$  for stearic (C18:0),  $47.6 \pm 5.7 \%$  for oleic (C18:1) and  $19.4 \pm 1.7 \%$  for linoleic (C18:2) acids (Figure 3.28 (A)).

The medium chain length fatty acids were increased with consecutive orlistat pulses: palmitic acid from  $14.4 \pm 9.7 \%$  to  $27.4 \pm 0.05 \%$  and palmitoleic acid increased from  $7.63 \pm 0.97 \%$  to  $8.47 \pm 0.07 \%$  while the long chain length fatty acids were decreased: stearic acid from  $7 \pm 0.86 \%$  to  $6.32 \pm 0.03 \%$ , oleic acid from  $47.6 \pm 5.7 \%$  to  $43.3 \pm 0.12 \%$  and linoleic acid from  $19.4 \pm 1.7 \%$  to  $12 \pm 0.09 \%$  (w/w) as shown in Figure 3.28 (A).

Before the orlistat pulses the short and the very long chain length fatty acids were at a percentage of (% w/w)  $0.18 \pm 0.04 \%$  for myristic acid (C14:0) and  $0.73 \pm 0.1 \%$  for arachidic

acid (C20:0),  $0.53 \pm 0.04$  % for behenic acid (C22:0) and  $2.45 \pm 0.24$  % for lignoceric acid (Figure 3.28 (B)).

With the first orlistat pulse, myristic acid increased from  $0.18 \pm 0.04$  % to  $0.32 \pm 0.09$  % (w/w) and was found constant at  $0.30 \pm 0.01$  % with the consecutive orlistat pulses as shown in Figure 3.28 (B).

With the first orlistat pulse all the very long chain length fatty acids were decreased to  $0.63 \pm 0.02$  %,  $0.42 \pm 0.03$  % and  $1.82 \pm 0.26$  % for arachidic (C20:0), behenic (C22:0) and lignoceric (C24:0) acids, respectively. With the consecutive orlistat pulses no increase were observed and the arachidic, behenic and lignoceric acids were at a percentage of (% w/w)  $0.58 \pm 0.01$  %,  $0.34 \pm 0.01$  % and  $1.27 \pm 0.04$  % at the end of the culture, respectively as shown in Figure 3.28 (B).

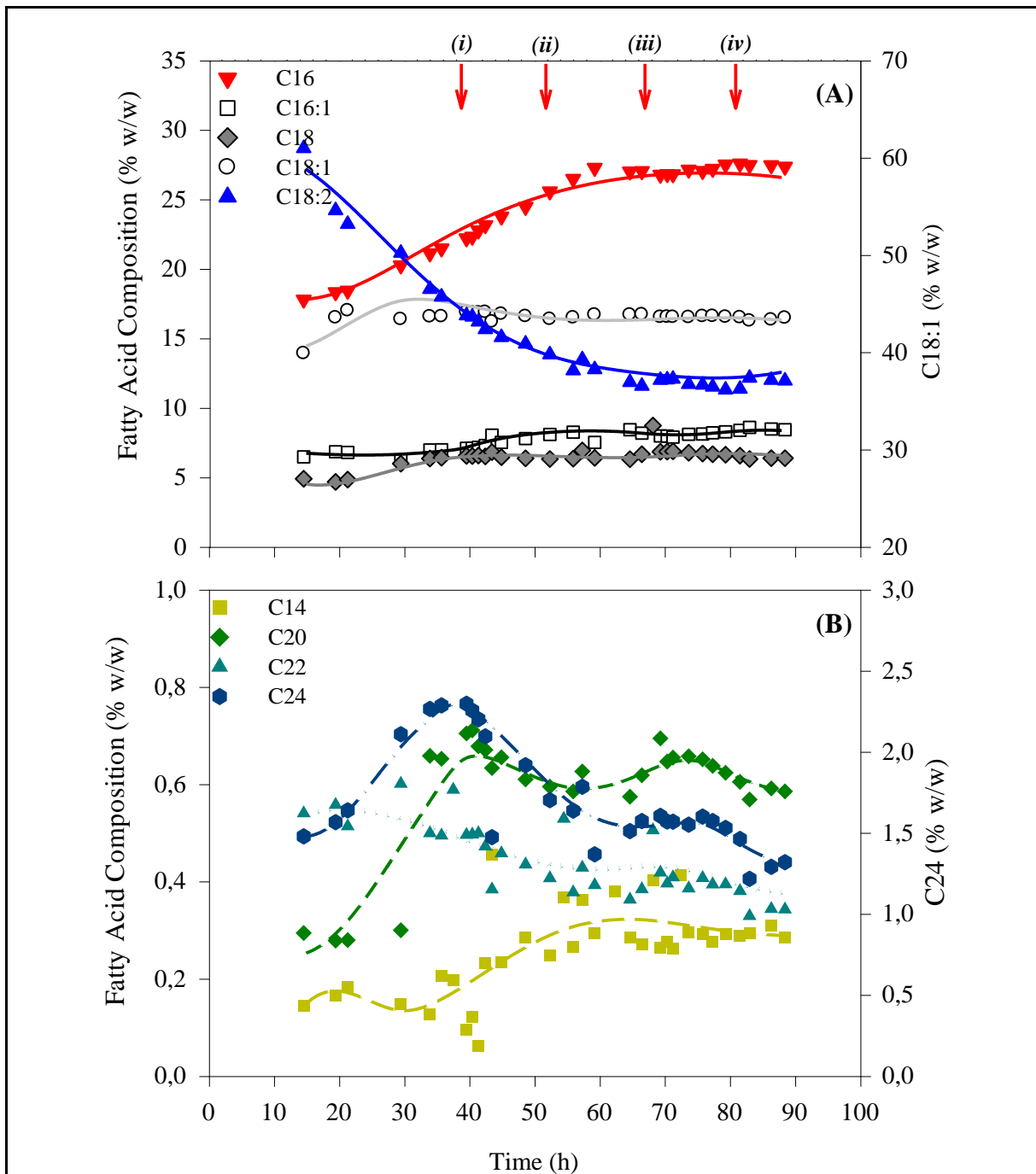


**Figure 3.28. Impact of Orlistat pulses on fatty acid composition (% w/w) during lipid accumulation phase for fed-batch cultures of *Y. lipolytica* JMY3501 under nitrogen limitation.**

Fatty Acid Compositions (% w/w): (Figure A (▼C16:0), (□C16:1), (◆C18:0), (○C18:1), (▲C18:2)). (Figure B (■C14:0), (◆C20:0), (▲C22:0), (●C24:0)).

The symbols represent experimental data and lines are smoothed values. Orlistat pulses were shown in arrows (i)  $0.5 \text{ mg} \cdot \text{g}^{-1}_{\text{DCW}}$ ; (ii)  $0.5 \text{ mg} \cdot \text{g}^{-1}_{\text{DCW}}$ ; (iii)  $1 \text{ mg} \cdot \text{g}^{-1}_{\text{DCW}}$ ; (iv)  $2 \text{ mg} \cdot \text{g}^{-1}_{\text{DCW}}$

### 3.4.2. Cell Viability and Cell Morphology

In this section, the physiological and morphological state of yeast cells in response to orlistat pulses was investigated. Assessment of metabolic activity, membrane integrity, cell viability, cell shape, cell size and the internal complexity of the strain *Y. lipolytica* JM3501 were determined by flow cytometry methods as explained in section 2.6.4.

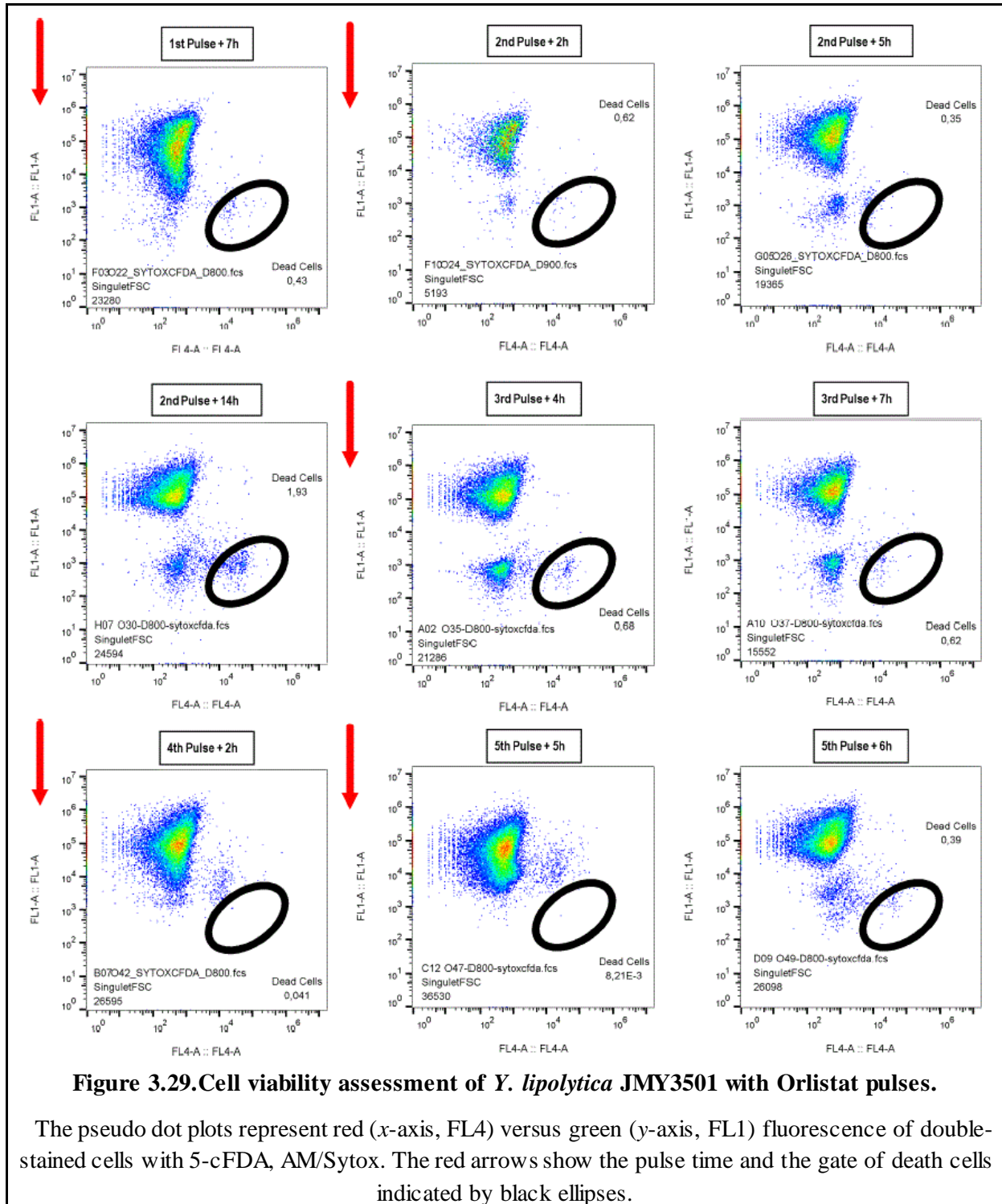
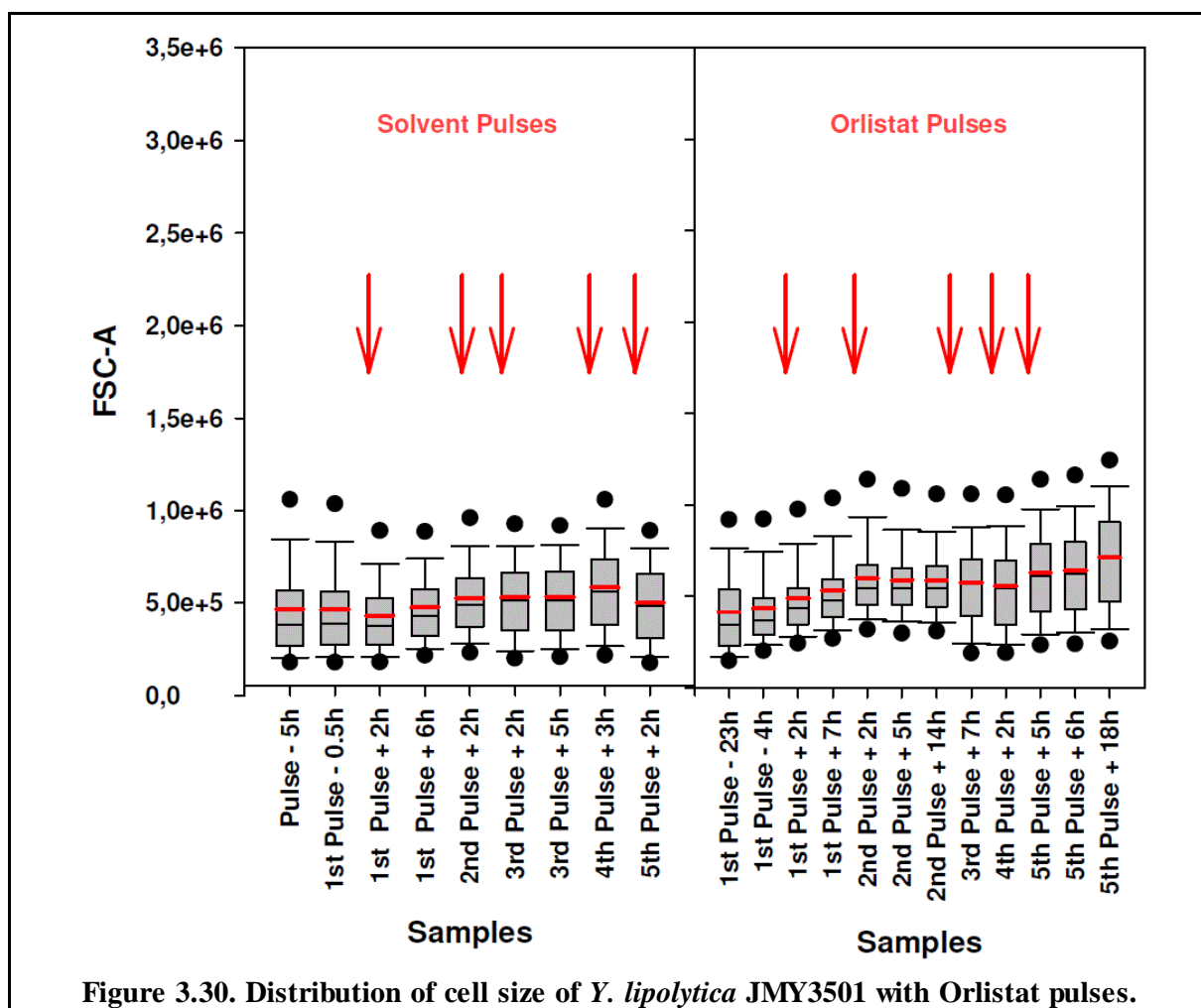


Figure 3.29 shows the flow cytometry analysis to assess the viability of *Y. lipolytica* JMY3501 with consecutive orlistat pulses. The assessment revealed that more than 98 % of cells were viable and the cells maintained membrane integrity with the modification of FA composition throughout the culture with consecutive orlistat pulses.

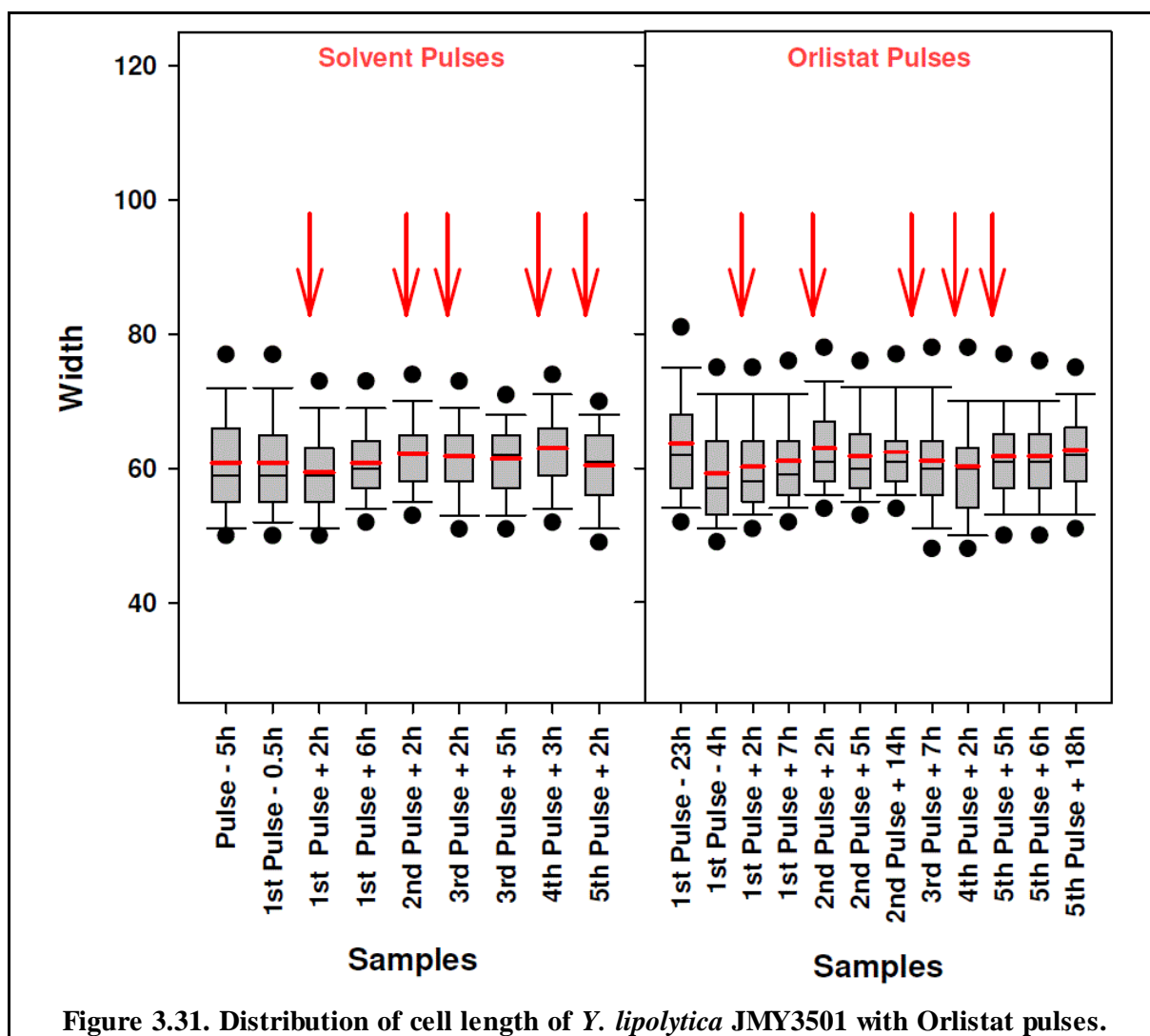
The distribution of cell population in terms of morphological features of yeast cells such as cell size, cell length and cell granularity in response to orlistat pulses were shown in Figure 3.30, Figure 3.31, Figure 3.32, respectively. The red and black vertical lines inside the box plots represent the mean and the median values, respectively. The pulses were shown by red arrows.

As explained in sections 2.6.4 and 3.3.2.2, the FSC signal is used proportionally to the size of the cells. Distribution of cell size in reference culture did not show significant variations with solvent pulses as seen in Figure 3.30. By contrast, the first orlistat pulse slightly increased the cell size distribution but no more increase was observed after the second orlistat pulse that the mean and median values of the cell size population were found constant until

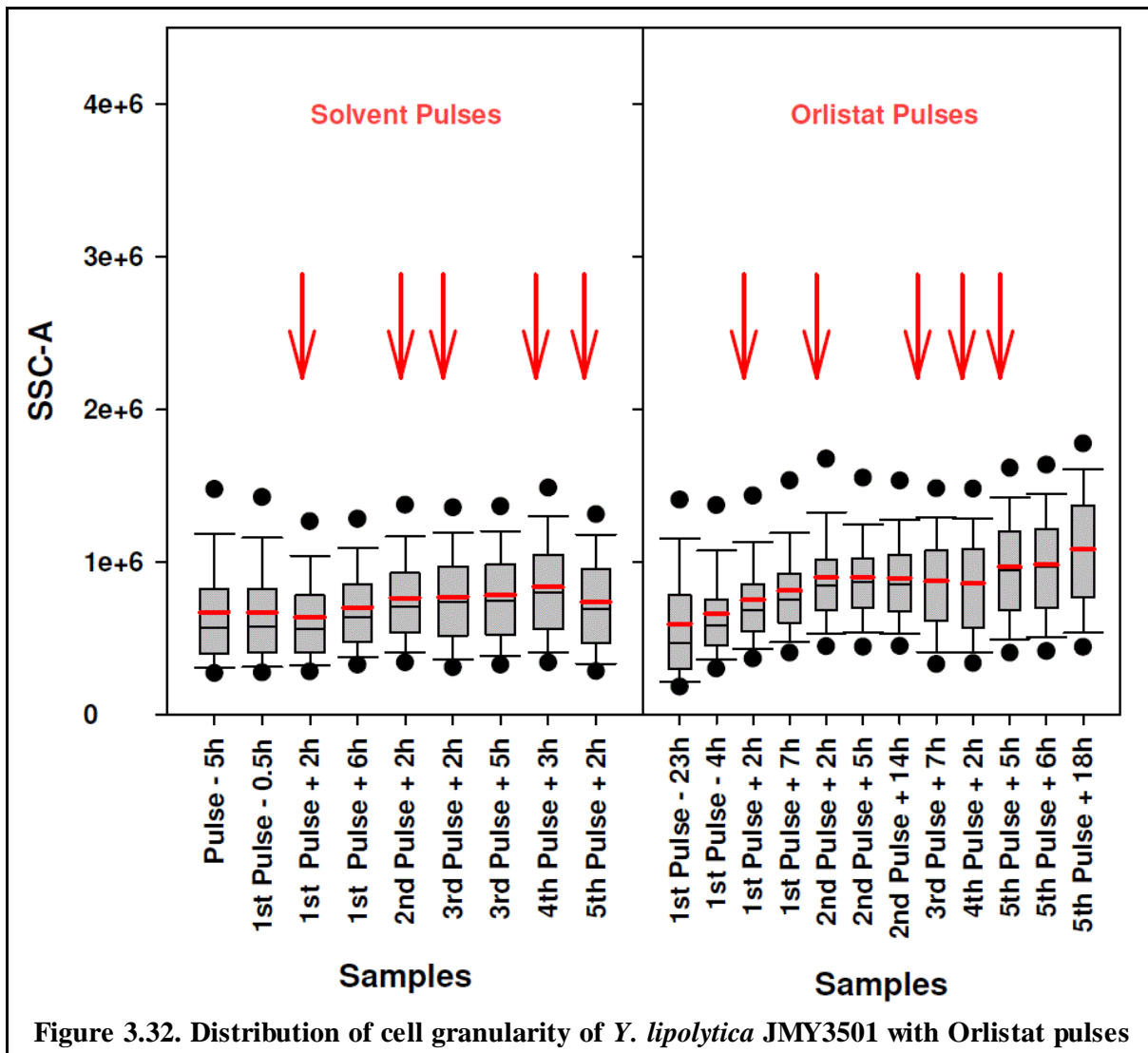


the end of the culture. However, 14 h later than the second pulse, the cell size distribution was more spread out on the lower half of the box plots compared to the previous pulses suggesting a decrease occurred in the yeast cell size (Figure 3.30).

As explained in sections 2.6.4 and 3.3.2.2, the width of the FSC signal provides information about cell length. Solvent pulses slightly reduced the cell length as seen in Figure 3.31. In contrast to solvent pulses, the cell length distribution increased with orlistat pulses. However, more than 75<sup>th</sup> percentile of the cell population was still in the range of reference culture.



As explained in sections 2.6.4 and 3.3.2.2, SSC provides helpful information about the internal complexity of a cell. The cell granularity of the reference culture showed no significant variations as seen in Figure 3.32. However, the mean and median values of the SSC signal slightly increased with orlistat pulses suggesting an increase occurred in cellular granularity (Figure 3.32).



## CHAPTER 4. CONCLUSION AND PERSPECTIVES

---

This research work focuses on the modulation of the lipid content and its fatty acid (FA) profile in the oleaginous yeast *Yarrowia lipolytica* together with biochemical and metabolic engineering strategies. The objectives of these works were:

- to investigate the dynamics of the metabolic shifts of *Yarrowia lipolytica* towards the lipid metabolism
- to modulate the FA profile through the modulation of the carbon fluxes up - and downward of fatty acid synthesis pathway via C/N feeding strategies and addition of specific inhibitors of the FAS system

The literature review reported main works on *de novo* fatty acid synthesis pathway, the key enzymes involved in fatty acid synthesis of the oleaginous microorganism and their regulation. Inhibitors of these key enzymes have been identified and previous works investigated their impact on the enzyme activity, on the lipid metabolism and on the fatty acid content and composition; their influence to target the specific domain of fatty acid enzyme system (FAS), specifically used in medical sciences, suggested to be very interesting regarding the objectives of the present research works.

The molecular structure of fatty acid synthase (FAS) enzyme system is diverse among the biological systems; however, the enzymatic reaction mechanism of FAS is conserved for all eukaryotic cells and it is the only *de novo* pathway for fatty acid synthesis. Therefore we have hypothesized that if the use of inhibitors on this essential cytosolic enzyme system would lead to fatty acid release before the complete synthesis of C16 or C18 fatty acids from Acetyl-CoA and thus yields shorter chain length fatty acids.

Three inhibitory molecules, cerulenin, triclosan and orlistat, were then selected to study in order to target different catalytic domains of FAS enzyme system aiming to modify the synthesis of fatty acids for the oleaginous yeast *Y. lipolytica*. The iterative elongation of fatty acid chains through reaction cycle of FAS was focused to control on different catalytic domains:

- (i) on the condensation step by ketoacyl synthase (KS) with the inhibitory molecule cerulenin,
- (ii) on the second reduction step by enoyl reductase (ER) with inhibitory molecule triclosan,

(iii) on the termination step by thioesterase with the inhibitory molecule orlistat.

The challenge was to adjust the amount of these inhibitors in order to identify enzymatic reactions within the FAS that control the elongation of fatty acids and the carbon chain length, without affecting the cell's viability of *Y. lipolytica*.

Preliminary cultures were carried out in the laboratory in shake flask with *Y. lipolytica* wild type strain to elucidate the influence of different dissolving agents of the inhibitor drugs on the dynamics of lipid metabolism of *Y. lipolytica*; ethanol was identified as the best solvent for further experiments regarding to the influence of inhibitors on the lipid accumulation and on the synthesis of fatty acids.

We first characterized the modulation of the metabolic shift from oxidative metabolism to lipid accumulation and citric acid production of a mutant strain of *Y. lipolytica* JMY3501 on glucose. This engineered strain has the ability to pull the carbon flow into triacylglycerol (TAG) synthesis, prevents both mobilization and degradation of fatty acids from its lipid stores. This investigation with the mutant strain demonstrated an overall improvement of lipid production performances with an increase lipid yield and content on glucose, and concomitantly decreased citric acid formation yield compared to parent strain. Furthermore, we demonstrated based on the modulation profile of nitrogen and carbon fluxes the yeast was able to rapidly and reversibly excrete or consume citric acid during fatty acid accumulation and led to a 15 % increase in the critical carbon/nitrogen ratio compared to parent strain. It demonstrated a higher robustness of the strain towards fluctuations in the C and N-content. It also set the cultivation conditions for the investigation of the effect of inhibitors on the accumulation of FA and their composition.

This metabolically engineered strain was next exposed to inhibitors of FAS enzyme system with pulses in fed-batch culture during lipid accumulation phase under nitrogen limitation.

The results obtained with targeted inhibition on the ketoacyl synthase (KS) domain of the FAS enzyme system with the inhibitor cerulenin were the most promising but were dose-dependent:

The lipid metabolism of the strain *Y. lipolytica* JMY3501 was dramatically affected with high dose of cerulenin pulses; FA synthesis strongly inhibited thus cells prevented TAG formation. On the other hand, carbon flow was directed into the formation of citric acid with the middle doses. However, at a lower dose of cerulenin pulse the strain *Y. lipolytica* JMY3501 without slowing the overall rate of fatty acid synthesis significantly enhanced accumulation of short

(87 % increase in C10) and medium (13 % and 11% increase in C12 and C14) chain length fatty acid without producing citric acid.

On the other hand, the targeted inhibition on the termination step of FAS enzyme system with middle dose of orlistat pulses enhanced TAG synthesis up to 31 % and favored the accumulation of medium chain length fatty acids (71 % increase in C14).

Finally Triclosan addition in flask cultures did not show any changes in FA profiles and was then abandoned for further experiments in bioreactor. However the data suggested that inhibiting the middle part of the FA elongation process (enoyl reductase) may not be interesting for FA profile modulation.

Moreover, to ensure that inhibitor amounts do not lead to cell death, cell viability analysis was performed with flow cytometry. There was no significant difference related to the inhibitors and the amount of the inhibitor in terms of cell survival that inhibition on FAS activity did not affect cell viability. However, further flow cytometry analyses revealed that the yeast cells displayed significant morphological alterations in a dose-dependent manner. The changes in morphological features, particularly the length, the shape and the internal granularity of yeast cells were more pronounced with high dose of cerulenin pulses that did not occur with orlistat pulses.

Therefore, these results indicate that reducing the activity of FAS enzyme system significantly modified the chain length of fatty acids and leads to the accumulation of short and medium chain length fatty acids. However, dose related inhibition on KS domain of FAS tightly controlled the metabolic flux of FA into TAG synthesis. A possible explanation of this is that since cerulenin is the inhibitor of ketoacyl synthase domain which initiates fatty acid synthesis, it may control iterative chain elongation within the FAS enzyme system. On the other hand, orlistat is the inhibitor of the termination of FA synthesis, it does not limit the incorporation of malonyl-ACP and Acetyl-ACP for further iterative chain reactions thus does not limit the synthesis of fatty acids. Moreover, this mutant strain is unable to degrade FA via  $\beta$ -oxidation to provide the metabolic energy for cellular maintenance from its stored lipids. Therefore high dose of cerulenin pulses caused toxicity therefore cells may have channeled the flux of FA towards membrane lipid synthesis rather than to store them as storage lipids in the form of TAG.

Consequently, we studied the *Y. lipolytica* CR62, which had the same genetic background as the strain JMY3501 but further engineered on KS domain of FAS to modify the fatty acid

chain length. This strain promoted the accumulation of medium chain length fatty acids; 11 % for C14 and 31 % for C16, however, simultaneously produced citric acid with a low total lipid content of 16 % that was identical to the wild type strain of *Y. lipolytica* W29. Both strategies applied on the initial step of FAS enzyme lead more short chain length fatty acids and low total lipid content.

The evidence from this study suggests that it is possible to modulate the synthesized fatty acid chain length of the oleaginous yeast *Y. lipolytica* by using specific inhibitors as a way to identify interesting genetic targets and then by targeting a catalytic domain of FAS enzyme system with mutation. Therefore, it is possible to state that engineering the FAS termination domain of this oleaginous yeast might also be a promising approach to modify FA chain length with high lipid content. Besides, obtaining such a mutant strain could eventually alter the FA profile without byproduct formation, without affecting membrane lipid homeostasis and cell survival.

These research works demonstrated that oleaginous yeast *Yarrowia lipolytica* with combined engineering efforts presented novel opportunities for the production of designed and/or high value fatty acids.

The future follow-up studies could also include:

- The *Y. lipolytica* CR62 engineered strain could be optimized for substrate feeding rate strategies (rN/rC ratio) for fed-batch culture mode under nitrogen limitation. Such strain optimization should improve lipid accumulation performances due to the efficient direction of carbon fluxes towards lipid accumulation instead of citric acid secretion.
- Identification of mechanism of action of FAS inhibitors with the catalytic domains of FAS enzyme system for the yeast *Y. lipolytica* -specifically with the inhibitor Orlistat and MPT domain of FAS- remains to be determined. Such studies might provide further support for the actual studies.
- Even though the inhibitors are required in relatively small amounts during these research studies, engineered strains would overcome the cost of inhibitors particularly in large-scale systems. However, before the construction of a new strain, the following suggestion should be considered: instead of using constitutive promoter to express the engineered FAS2 gene (such as for the FAS2 gene: TEF-yIFAS2 I1220F) it could be replaced by an inducible promoter. This would eliminate the necessity to delete the native FAS2 gene. Such genetic replacements would promote FA modification by only modifying the chain

length of accumulated FAs during lipid accumulation phase without affecting membrane phospholipid synthesis; thus, the viability of the cells should remain unaffected.

## CHAPTER 5. REFERENCES

---

- Adams, I.P., Dack, S., Dickinson, F.M., Ratledge, C., 2002. The distinctiveness of ATP:citrate lyase from *Aspergillus nidulans*. *Biochim. Biophys. Acta - Protein Struct. Mol. Enzymol.* 1597, 36–41. doi:10.1016/S0167-4838(02)00276-5
- Ageitos, J.M., Vallejo, J.A., Veiga-Crespo, P., Villa, T.G., 2011. Oily yeasts as oleaginous cell factories. *Appl. Microbiol. Biotechnol.* 90, 1219–1227. doi:10.1007/s00253-011-3200-z
- Aggelis, G., Sourdis, J., 1997. Prediction of lipid accumulation-degradation in oleaginous micro-organisms growing on vegetable oils. *Antonie van Leeuwenhoek, Int. J. Gen. Mol. Microbiol.* 72, 159–165. doi:10.1023/A:1000364402110
- Anastassiadis, S., Aivasidis, A., Wandrey, C., 2003. Citric acid production by *Candida* strains under intracellular nitrogen limitation. *Appl. Microbiol. Biotechnol.* 60, 81–87. doi:10.1007/s00253-002-1098-1
- Anastassiadis, S., Wandrey, C., Rehm, H.J., 2005. Continuous citric acid fermentation by *Candida oleophila* under nitrogen limitation at constant C/N ratio. *World J. Microbiol. Biotechnol.* 21, 695–705. doi:10.1007/s11274-004-3850-4
- Athenstaedt, K., Daum, G., 2006. The life cycle of neutral lipids: Synthesis, storage and degradation. *Cell. Mol. Life Sci.* 63, 1355–1369. doi:10.1007/s00018-006-6016-8
- Athenstaedt, K., Jolivet, P., Boulard, C., Zivy, M., Negroni, L., Nicaud, J.M., Chardot, T., 2006. Lipid particle composition of the yeast *Yarrowia lipolytica* depends on the carbon source. *Proteomics* 6, 1450–1459. doi:10.1002/pmic.200500339
- Bankar, A. V., Kumar, A.R., Zinjarde, S.S., 2009. Environmental and industrial applications of *Yarrowia lipolytica*. *Appl. Microbiol. Biotechnol.* 84, 847–865. doi:10.1007/s00253-009-2156-8
- Barth, G., Gaillardin, C., 1997. Physiology and genetics of the dimorphic fungus *Yarrowia lipolytica*. *FEMS Microbiol. Rev.* 19, 219–237.
- Bellou, S., Triantaphyllidou, I.E., Mizerakis, P., Aggelis, G., 2016. High lipid accumulation in *Yarrowia lipolytica* cultivated under double limitation of nitrogen and magnesium. *J. Biotechnol.* 234, 116–126. doi:10.1016/j.jbiotec.2016.08.001
- Beopoulos, A., Cescut, J., Haddouche, R., Uribelarrea, J.L., Molina-Jouve, C., Nicaud, J.M., 2009a. *Yarrowia lipolytica* as a model for bio-oil production. *Prog. Lipid Res.* 48, 375–387. doi:10.1016/j.plipres.2009.08.005
- Beopoulos, A., Chardot, T., Nicaud, J.M., 2009b. *Yarrowia lipolytica*: A model and a tool to understand the mechanisms implicated in lipid accumulation. *Biochimie* 91, 692–696. doi:10.1016/j.biochi.2009.02.004
- Beopoulos, A., Haddouche, R., Kabran, P., Dulermo, T., Chardot, T., Nicaud, J.M., 2012. Identification and characterization of DGA2, an acyltransferase of the DGAT1 acyl-CoA:diacylglycerol acyltransferase family in the oleaginous yeast *Yarrowia lipolytica*. New insights into the storage lipid metabolism of oleaginous yeasts. *Appl. Microbiol. Biotechnol.* 93, 1523–1537. doi:10.1007/s00253-011-3506-x
- Beopoulos, A., Mrozova, Z., Thevenieau, F., Le Dall, M.-T., Hapala, I., Papanikolaou, S., Chardot, T., Nicaud, J.-M., 2008. Control of lipid accumulation in the yeast *Yarrowia lipolytica*. *Appl. Environ. Microbiol.* 74, 7779–89. doi:10.1128/AEM.01412-08

- Beopoulos, A., Nicaud, J.M., 2012. Yeast: A new oil producer? OCL - Ol. Corps Gras Lipides 19, 22–28. doi:10.1684/oc1.2012.0426
- Beopoulos, A., Nicaud, J.M., Gaillardin, C., 2011. An overview of lipid metabolism in yeasts and its impact on biotechnological processes. Appl. Microbiol. Biotechnol. 90, 1193–1206. doi:10.1007/s00253-011-3212-8
- Blazeck, J., Hill, A., Liu, L., Knight, R., Miller, J., Pan, A., Otoupal, P., Alper, H.S., 2014. Harnessing *Yarrowia lipolytica* lipogenesis to create a platform for lipid and biofuel production. Nat. Commun. 5, 3131. doi:10.1038/ncomms4131
- Botham, P.A., Ratledge, C., 1979. A Biochemical Explanation for Lipid Accumulation in *Candida* 107 and Other Oleaginous Micro-organisms. J. Gen. Microbiol. 114, 361–375.
- Boulton, C.A., Ratledge, C., 1983. Use of Transition Studies in Continuous Cultures of *Lipomyces starkeyi*, an oleaginous yeast, to Investigate the Physiology of Lipid Accumulation. J. Gen. Microbiol. 129, 2871–2876. doi:10.1099/00221287-129-9-2871
- Boulton, C.A., Ratledge, C., 1981a. ATP: Citrate Lyase - The Regulatory Enzyme for Lipid Biosynthesis in *Lipomyces starkeyi*? Microbiology 127, 423–426. doi:10.1099/00221287-127-2-423
- Boulton, C.A., Ratledge, C., 1981b. Correlation of Lipid Accumulation in Yeasts with Possession of ATP: Citrate Lyase. Microbiology 127, 169–176. doi:10.1099/00221287-127-1-169
- Browse, J., Mccourt, P.J., Sommerville, C.R., 1986. Fatty Acid Composition of Leaf Lipids Determined after Combined Digestion and Fatty Acid Methyl Ester Formation from Fresh Tissue. Anal. Biochem. 152, 141–145.
- Browse, J., Warwick, N., Somerville, C.R., Slack, C.R., 1986. Fluxes through the prokaryotic and eukaryotic pathways of lipid synthesis in the “16:3” plant *Arabidopsis thaliana*. Biochem. J. 235, 25–31.
- Carsanba, E., Papanikolaou, S., Erten, H., 2018. Production of oils and fats by oleaginous microorganisms with an emphasis given to the potential of the nonconventional yeast *Yarrowia lipolytica*. Crit. Rev. Biotechnol. 38, 1230–1243. doi:10.1080/07388551.2018.1472065
- Cescut, J., 2009. Accumulation d’acylglycérols par des espèces levuriennes à usage carburant aéronautique : physiologie et performances de procédés. Institut National des Sciences Appliquées de Toulouse.
- Cescut, J., Severac, E., Molina-Jouve, C., Uribelarrea, J.L., 2011. Optimizing pressurized liquid extraction of microbial lipids using the response surface method. J. Chromatogr. A 1218, 373–379. doi:10.1016/j.chroma.2010.12.003
- Chang, G.G., Tong, L., 2003. Structure and Function of Malic Enzymes, A New Class of Oxidative Decarboxylases. Biochemistry 42, 12721–12733. doi:10.1021/bi035251+
- Chang, K.-C., Chu, C.-Y., Su, Y.-M., Chen, Y.-M., 2012. Effect of culture conditions on growth, lipid content, and fatty acid composition of *Aurantiochytrium mangrovei* strain BL10. AMB Express 2, 42. doi:10.1186/2191-0855-2-42
- Cronan, J.E., Waldrop, G.L., 2002. Multi-subunit acetyl-CoA carboxylases. Prog. Lipid Res. 41, 407–435. doi:10.1016/S0163-7827(02)00007-3
- Czabany, T., Athenstaedt, K., Daum, G., 2007. Synthesis, storage and degradation of neutral lipids in yeast. Biochim. Biophys. Acta - Mol. Cell Biol. Lipids 1771, 299–309.

doi:10.1016/j.bbalip.2006.07.001

- D'agnolo, G., Rosenfeld, I.S., Awaya, J., Omura, S., Vagelos, P.R., 1973. Inhibition of Fatty Acid Synthesis by the Antibiotic Cerulenin. Specific Inactivation of Beta-Ketoacyl-acyl Carrier Protein Synthetase. *Biochim. Biophys. Acta* 326, 155–166.
- Daum, G., Lees, N.D., Bard, M., Dickson, R., 1998. Biochemistry, cell biology and molecular biology of lipids of *Saccharomyces cerevisiae*. *Yeast* 14, 1471–510. doi:10.1002/(SICI)1097-0061(199812)14:16<1471::AID-YEA353>3.0.CO;2-Y
- Davey, H.M., Kell, D.B., 1996. Flow cytometry and cell sorting of heterogeneous microbial populations: the importance of single-cell analyses. *Microbiol. Rev.* 60, 641–96. doi:10.1016/j.mimet.2004.10.020
- Davis, M.S., Solbiati, J., Cronan, J.E., 2000. Overproduction of acetyl-CoA carboxylase activity increases the rate of fatty acid biosynthesis in *Escherichia coli*. *J. Biol. Chem.* 275, 28593–28598. doi:10.1074/jbc.M004756200
- Deak, T., 2001. Identification of yeasts isolated from poultry meat. *Acta Biol. Hung.* 52, 195–200.
- Díaz, M., Herrero, M., García, L.A., Quirós, C., 2010. Application of flow cytometry to industrial microbial bioprocesses. *Biochem. Eng. J.* 48, 385–407. doi:10.1016/j.bej.2009.07.013
- Dulermo, T., Lazar, Z., Dulermo, R., Rakicka, M., Haddouche, R., Nicaud, J.M., 2015. Analysis of ATP-citrate lyase and malic enzyme mutants of *Yarrowia lipolytica* points out the importance of mannitol metabolism in fatty acid synthesis. *Biochim. Biophys. Acta - Mol. Cell Biol. Lipids* 1851, 1107–1117. doi:10.1016/j.bbalip.2015.04.007
- Dulermo, T., Nicaud, J.M., 2011. Involvement of the G3P shuttle and B-oxidation pathway in the control of TAG synthesis and lipid accumulation in *Yarrowia lipolytica*. *Metab. Eng.* 13, 482–491. doi:10.1016/j.ymben.2011.05.002
- Dulermo, T., Tréton, B., Beopoulos, A., Gnankon, A.P.K., Haddouche, R., Nicaud, J.M., 2013. Characterization of the two intracellular lipases of *Y. lipolytica* encoded by TGL3 and TGL4 genes: New insights into the role of intracellular lipases and lipid body organisation. *Biochim. Biophys. Acta - Mol. Cell Biol. Lipids* 1831, 1486–1495. doi:10.1016/j.bbalip.2013.07.001
- Estopier, A.O., 2012. Analyses systématique des bascules métaboliques chez les levures d'intérêt industriel. Institut National des Sciences Appliquées de Toulouse.
- Evans, C.T., Ratledge, C., 1985. The Physiological Significance of Citric acid in the Control of Metabolism in Lipid-accumulating Yeasts. *Biotechnol. Genet. Eng. Rev.* 3, 349–375.
- Evans, C.T., Ratledge, C., 1983. A comparison of the oleaginous yeast, *Candida curvata*, grown on different carbon sources in continuous and batch culture. *Lipids* 18, 623–629. doi:10.1007/BF02534673
- Evans, C.T., Scragg, A.H., Ratledge, C., Candida, D., 1983. A Comparative Study of Citrate Efflux from Mitochondria of Oleaginous and Non-oleaginous Yeasts. *Eur. J. Biochem.* 130, 195–204.
- Evans, C.T., Scragg, a H., Ratledge, C., 1981. Regulation of citrate efflux from mitochondria of oleaginous and non-oleaginous yeasts by long-chain fatty acyl-CoA esters. *Eur. J. Biochem.* 132, 617–622. doi:10.1111/j.1432-1033.1983.tb07136.x
- Fahy, E., Dawn, C., Manish, S., Subramaniam, S., 2011. Lipid classification, structure and

- tools. *Biochim Biophys Acta*. 1811, 637–647. doi:10.1016/j.bbailip.2011.06.009.Lipid
- Fahy, E., Subramaniam, S., Brown, H.A., Glass, C.K., Merrill, A.H., Murphy, R.C., Raetz, C.R.H., Russell, D.W., Seyama, Y., Shaw, W., Shimizu, T., Spener, F., van Meer, G., VanNieuwenhze, M.S., White, S.H., Witztum, J.L., Dennis, E. a, 2005. A comprehensive classification system for lipids. *J. Lipid Res.* 46, 839–861. doi:10.1194/jlr.E400004-JLR200
- Fako, V.E., Zhang, J.T., Liu, J.Y., 2014. Mechanism of orlistat hydrolysis by the thioesterase of human fatty acid synthase. *ACS Catal.* 4, 3444–3453. doi:10.1021/cs500956m
- Fickers, P., Benetti, P.H., Waché, Y., Marty, A., Mauersberger, S., Smit, M.S., Nicaud, J.M., 2005a. Hydrophobic substrate utilisation by the yeast *Yarrowia lipolytica*, and its potential applications. *FEMS Yeast Res.* 5, 527–543. doi:10.1016/j.femsyr.2004.09.004
- Fickers, P., Fudalej, F., Le Dall, M.T., Casaregola, S., Gaillardin, C., Thonart, P., Nicaud, J.M., 2005b. Identification and characterisation of LIP7 and LIP8 genes encoding two extracellular triacylglycerol lipases in the yeast *Yarrowia lipolytica*. *Fungal Genet. Biol.* 42, 264–274. doi:10.1016/j.fgb.2004.12.003
- Fickers, P., Marty, A., Nicaud, J.M., 2011. The lipases from *Yarrowia lipolytica*: Genetics, production, regulation, biochemical characterization and biotechnological applications. *Biotechnol. Adv.* 29, 632–644. doi:10.1016/j.biotechadv.2011.04.005
- Finogenova, T. V, Kamzolova, S. V, Shishkanova, N. V, Ilchenko, A.P., Dedyukhina, E.G., 1996. Influence of the specific growth rate and zinc ions on the synthesis of citric and isocitric acids and on the biomass composition of *Yarrowia lipolytica* N 1 yeast. *Appl. Biochem. Microbiol.* 32, 30–34.
- Flavin, R., Peluso, S., Nguyen, P., Loda, M., 2010. Fatty acid synthase as a potential therapeutic target in cancer. *Futur. Oncol.* 6, 551–562. doi:10.2217/fon.10.11.Fatty
- Fontanille, P., Kumar, V., Christophe, G., Nouaille, R., Larroche, C., 2012. Bioconversion of volatile fatty acids into lipids by the oleaginous yeast *Yarrowia lipolytica*. *Bioresour. Technol.* 114, 443–449. doi:10.1016/j.biortech.2012.02.091
- Funabashi, H., Kawaguchi, A., Tomoda, H., Omura, S., Okuda, S., Iwasaki, S., 1989. Binding site of cerulenin in fatty acid synthetase. *J. Biochem.* 105, 751–755.
- Gajdoš, P., Nicaud, J.M., Rossignol, T., Čertík, M., 2015. Single cell oil production on molasses by *Yarrowia lipolytica* strains overexpressing DGA2 in multicopy. *Appl. Microbiol. Biotechnol.* 99, 8065–8074. doi:10.1007/s00253-015-6733-8
- Gelpi, J.L.I., Dordal, A., Mazo, A., Cortes, A., 1992. Kinetic studies of the regulation of mitochondrial malate dehydrogenase by citrate. *Biochem. J.* 283, 289–297.
- Gill, C.O., Hall, M.J., Ratledge, C., 1977. Lipid Accumulation in an Oleaginous Yeast (*Candida 107*) Growing on Glucose Under Various Conditions in a One-and Two-Stage Continuous Culture. *Appl. Environ. Microbiol.* 33, 231–239.
- Gill, C.O., Ratledge, C., 1973. Regulation of de novo fatty acid biosynthesis in the n-alkane-utilizing yeast, *Candida 107*. *J. Gen. Microbiol.* 78, 337–347. doi:10.1099/00221287-78-2-337
- Goldberg, I., Walker, J.R., Bloch, K., 1973. Inhibition of Lipid Synthesis in *Escherichia coli* Cells by the Antibiotic Cerulenin. *Antimicrob. Agents Chemother.* 3, 549–554. doi:10.1128/aac.
- Gonçalves, F. a. G., Colen, G., Takahashi, J. a, 2013. *Yarrowia lipolytica* and its multiple

- applications in the biotechnological industry. *Sci. World J.* 2014. doi:in press
- Granger, L.M., Perlot, P., Goma, G., Pareilleux, A., 1993. Effect of various nutrient limitations on fatty acid production by *Rhodotorula glutinis*. *Appl. Microbiol. Biotechnol.* 38, 784–789. doi:10.1007/BF00167145
- Groenewald, M., Boekhout, T., Neuvéglise, C., Gaillardin, C., van Dijck, P.W.M., Wyss, M., 2014. *Yarrowia lipolytica*: safety assessment of an oleaginous yeast with a great industrial potential. *Crit. Rev. Microbiol.* 40, 187–206. doi:10.3109/1040841X.2013.770386
- Harvey R. A.; Ferrier D. R., 2011. *Lippincott's Illustrated Reviews: Biochemistry*, Fifth Edit. ed, Lippincott Williams & Wilkins, a Wolters Kluwer business. Lippincott Williams & Wilkins. doi:10.1016/0307-4412(87)90018-5
- Harzevili, F.D., 2014. *Yarrowia lipolytica* in Biotechnological Applications, *Biotechnological Applications of the Yeast Yarrowia lipolytica*. doi:10.1007/978-3-319-06437-6
- Hasslacher, M., Ivessa, A.S., Paltauf, F., Kohlwein, S.D., 1993. Acetyl-CoA carboxylase from yeast is an essential enzyme and is regulated by factors that control phospholipid metabolism. *J. Biol. Chem.* 268, 10946–10952. doi:10.1074/jbc.M802685200
- Hauvermale, A., Kuner, J., Rosenzweig, B., Guerra, D., Diltz, S., Metz, J.G., 2006. Fatty acid production in *Schizochytrium* sp.: Involvement of a polyunsaturated fatty acid synthase and a type I fatty acid synthase. *Lipids* 41, 739–747. doi:10.1007/s11745-006-5025-6
- Heath, R.J., White, S.W., Rock, C.O., 2001. Lipid biosynthesis as a target for antibacterial agents. *Prog. Lipid Res.* 40, 467–497. doi:10.1016/S0163-7827(01)00012-1
- Heath, R.J., Yu, Y.T., Shapiro, M.A., Olson, E., Rock, C.O., 1998. Broad spectrum antimicrobial biocides target the FabI component of fatty acid synthesis. *J. Biol. Chem.* 273, 30316–30320. doi:10.1074/jbc.273.46.30316
- Holdsworth, J.E., Veenhuis, M., Ratledge, C., 1988. Enzyme activities in oleaginous yeasts accumulating and utilizing exogenous or endogenous lipids. *J. Gen. Microbiol.* 134, 2907–2915. doi:10.1099/00221287-134-11-2907
- Huang, C., Chen, X. fang, Xiong, L., Chen, X. de, Ma, L. long, Chen, Y., 2013. Single cell oil production from low-cost substrates: The possibility and potential of its industrialization. *Biotechnol. Adv.* 31, 129–139. doi:10.1016/j.biotechadv.2012.08.010
- Hyka, P., Lickova, S., Přibyl, P., Melzoch, K., Kovar, K., 2013. Flow cytometry for the development of biotechnological processes with microalgae. *Biotechnol. Adv.* 31, 2–16. doi:10.1016/j.biotechadv.2012.04.007
- Iassonova, D.R., Hammond, E.G., Beattie, S.E., 2008. Oxidative stability of polyunsaturated triacylglycerols encapsulated in oleaginous yeast. *JAOCS, J. Am. Oil Chem. Soc.* 85, 711–716. doi:10.1007/s11746-008-1255-5
- Il'chenko, A., Shishkanova, N., Chernyavskaya, O., Finogenova, T., 1998. Oxygen concentration as a factor controlling central metabolism and citric acid biosynthesis in the yeast *Yarrowia lipolytica* grown on ethanol. *Microbiology* 67, 241–244.
- Jenni, S., Leibundgut, M., Boehringer, D., Frick, C., Mikolasek, B., Ban, N., 2007. Structure of fungal fatty acid synthase and implications for iterative substrate shuttling. *Science* (80-. ). 316, 254–261. doi:10.1126/science.1138248
- Jenni, S., Leibundgut, M., Maier, T., Ban, N., 2006. Architecture of a fungal fatty acid synthase at 5 Å resolution. *Science* 311, 1263–1267. doi:10.1126/science.1123251

- Johansson, P., Mulinacci, B., Koestler, C., Vollrath, R., Oesterhelt, D., Grininger, M., 2009. Multimeric Options for the Auto-Activation of the *Saccharomyces cerevisiae* FAS Type I Megasyntase. *Structure* 17, 1063–1074. doi:10.1016/j.str.2009.06.014
- Kabani, M., Boisramé, A., Beckerich, J.M., Gaillardin, C., 2000. A highly representative two-hybrid genomic library for the yeast *Yarrowia lipolytica*. *Gene* 241, 309–315. doi:10.1016/S0378-1119(99)00476-X
- Kabran, P., Rossignol, T., Gaillardin, C., Nicaud, J.M., Neuvéglise, C., 2012. Alternative Splicing Regulates Targeting of Malate Dehydrogenase in *Yarrowia lipolytica*. *DNA Res.* 19, 231–244. doi:10.1093/dnares/dss007
- Kamiryo, T., Nishikawa, Y., Mishina, M., Terao, M., Numa, S., 1979. Involvement of long-chain acyl coenzyme A for lipid synthesis in repression of acetyl-coenzyme A carboxylase in *Candida lipolytica*. *Proc. Natl. Acad. Sci. U. S. A.* 76, 4390–4394. doi:10.1073/pnas.76.9.4390
- Kamzolova, S. V., Shishkanova, N. V., Morgunov, I.G., Finogenova, T. V., 2003. Oxygen requirements for growth and citric acid production of *Yarrowia lipolytica*. *FEMS Yeast Res.* 3, 217–222. doi:10.1016/S1567-1356(02)00188-5
- Kawaguchi, A., Tomoda, H., Nozoe, S., Omura, S., Okuda, S., 1982. Mechanism of Action of Cerulenin on Fatty Acid Synthetase. Effect of Cerulenin on Iodoacetamide-Induced Malonyl-CoA Decarboxylase Activity. *J. Biochem.* 92, 7–12.
- Kawasse, F.M., Amaral, P.F., Rocha-Leão, M.H.M., Amaral, A.L., Ferreira, E.C., Coelho, M.A.Z., 2003. Morphological analysis of *Yarrowia lipolytica* under stress conditions through image processing. *Bioprocess Biosyst. Eng.* 25, 371–375. doi:10.1007/s00449-003-0319-z
- Klug, L., Daum, G., 2014. Yeast lipid metabolism at a glance. *FEMS Yeast Res.* 14, 369–388. doi:10.1111/1567-1364.12141
- Kosa, M., Ragauskas, A.J., 2011. Lipids from heterotrophic microbes: Advances in metabolism research. *Trends Biotechnol.* 29, 53–61. doi:10.1016/j.tibtech.2010.11.002
- Kridel, S.J., Axelrod, F., Rozenkrantz, N., Smith, J.W., 2004. Orlistat Is a Novel Inhibitor of Fatty Acid Synthase with Antitumor Activity. *Cancer Res.* 64, 2070–2075. doi:10.1158/0008-5472.CAN-03-3645
- Kridel, S.J., Lowther, W.T., Pemble IV, C.W., 2007. Fatty acid synthase inhibitors: new directions for oncology. *J. Expert Opin. Investig. Drugs* 16, 1817–1829.
- Kurita, O., 2003. Overexpression of peroxisomal malate dehydrogenase MDH3 gene enhances cell death on H<sub>2</sub>O<sub>2</sub> stress in the *ald5* mutant of *Saccharomyces cerevisiae*. *Curr. Microbiol.* 47, 192–197. doi:10.1007/s00284-002-3979-z
- Kurosawa, K., Wewetzer, S.J., Sinskey, A.J., 2013. Engineering xylose metabolism in triacylglycerol-producing *Rhodococcus opacus* for lignocellulosic fuel production. *Biotechnol. Biofuels* 6, 134. doi:10.1186/1754-6834-6-134
- Lanciotti, R., Gianotti, A., Baldi, D., Angrisani, R., Suzzi, G., Mastrocola, D., Guerzoni, M.E., 2005. Use of *Yarrowia lipolytica* strains for the treatment of olive mill wastewater. *Bioresour. Technol.* 96, 317–322. doi:10.1016/j.biortech.2004.04.009
- Lazar, Z., Dulermo, T., Neuvéglise, C., Crutz-Le Coq, A.M., Nicaud, J.M., 2014. Hexokinase-A limiting factor in lipid production from fructose in *Yarrowia lipolytica*. *Metab. Eng.* 26, 89–99. doi:10.1016/j.ymben.2014.09.008

- Ledesma-Amaro, R., Dulermo, R., Niehus, X., Nicaud, J.-M., 2016. Combining metabolic engineering and process optimization to improve production and secretion of fatty acids. *Metab. Eng.* 38, 38–46. doi:10.1016/j.ymben.2016.06.004
- Ledesma-Amaro, R., Dulermo, T., Nicaud, J.M., 2015. Engineering *Yarrowia lipolytica* to produce biodiesel from raw starch. *Biotechnol. Biofuels* 8, 148. doi:10.1186/s13068-015-0335-7
- Leibundgut, M., Maier, T., Jenni, S., Ban, N., 2008. The multienzyme architecture of eukaryotic fatty acid synthases. *Curr. Opin. Struct. Biol.* 18, 714–725. doi:10.1016/j.sbi.2008.09.008
- Lentini A, Rogers P, Higgins V, Dawes I, Chandler M, S.G.& C.P., 2003. The impact of ethanol stress on yeast physiology., in: *Brewing Yeast Fermentation Performance*. Blackwell Science, Oxford, UK., p. 25 – 38.
- Li, Q., Du, W., Liu, D., 2008. Perspectives of microbial oils for biodiesel production. *Appl. Microbiol. Biotechnol.* 80, 749–756. doi:10.1007/s00253-008-1625-9
- Liang, M.H., Jiang, J.G., 2013. Advancing oleaginous microorganisms to produce lipid via metabolic engineering technology. *Prog. Lipid Res.* 52, 395–408. doi:10.1016/j.plipres.2013.05.002
- Little, J.L., Wheeler, F.B., Fels, D.R., Koumenis, C., Kridel, S.J., 2007. Inhibition of fatty acid synthase induces endoplasmic reticulum stress in tumor cells. *Cancer Res.* 67, 1262–1269. doi:10.1158/0008-5472.CAN-06-1794
- Liu, H.-H., Ji, X.-J., Huang, H., 2015. Biotechnological applications of *Yarrowia lipolytica*: Past, present and future. *Biotechnol. Adv.* 33, 1522–1546. doi:10.1016/j.biotechadv.2015.07.010
- Liu, X.Y., Chi, Z., Liu, G.L., Madzak, C., Chi, Z.M., 2013. Both Decrease in ACL1 Gene Expression and Increase in ICL1 Gene Expression in Marine-Derived Yeast *Yarrowia lipolytica* Expressing INU1 Gene Enhance Citric Acid Production from Inulin. *Mar. Biotechnol.* 15, 26–36. doi:10.1007/s10126-012-9452-5
- Liu, Z., Gao, Y., Chen, J., Imanaka, T., Bao, J., Hua, Q., 2013. Analysis of metabolic fluxes for better understanding of mechanisms related to lipid accumulation in oleaginous yeast *Trichosporon cutaneum*. *Bioresour. Technol.* 130, 144–151. doi:10.1016/j.biortech.2012.12.072
- Lomakin, I.B., Xiong, Y., Steitz, T.A., 2007. The Crystal Structure of Yeast Fatty Acid Synthase, a Cellular Machine with Eight Active Sites Working Together. *Cell* 129, 319–332. doi:10.1016/j.cell.2007.03.013
- Lu, X., Vora, H., Khosla, C., 2008. Overproduction of free fatty acids in *E. coli*: Implications for biodiesel production. *Metab. Eng.* 10, 333–339. doi:10.1016/j.ymben.2008.08.006
- Lupu, R., Menendez, J. a, 2006. Pharmacological inhibitors of Fatty Acid Synthase (FASN)--catalyzed endogenous fatty acid biogenesis: a new family of anti-cancer agents? *Curr. Pharm. Biotechnol.* 7, 483–493. doi:10.2174/138920106779116928
- Madzak, C., 2018. Engineering *Yarrowia lipolytica* for Use in Biotechnological Applications: A Review of Major Achievements and Recent Innovations. *Mol. Biotechnol.* 60, 621–635. doi:10.1007/s12033-018-0093-4
- Madzak, C., 2015. *Yarrowia lipolytica*: recent achievements in heterologous protein expression and pathway engineering. *Appl. Microbiol. Biotechnol.* 99, 4559–4577.

doi:10.1007/s00253-015-6624-z

- Madzak, C., Beckerich, J.-M., 2013. Heterologous Protein Expression and Secretion in *Yarrowia lipolytica*, in: Barth, G. (Ed.), *Yarrowia Lipolytica: Biotechnological Applications*. Springer Berlin Heidelberg, Berlin, Heidelberg, pp. 1–76. doi:10.1007/978-3-642-38583-4\_1
- Madzak, C., Gaillardin, C., Beckerich, J.M., 2004. Heterologous protein expression and secretion in the non-conventional yeast *Yarrowia lipolytica*: A review. *J. Biotechnol.* 109, 63–81. doi:10.1016/j.jbiotec.2003.10.027
- Madzak C., B.J. (2013), 2013. *Heterologous Protein Expression and Secretion in Yarrowia lipolytica*. Springer, Berlin, Heidelberg.
- McIlvaine, T.C., 1921. A Buffer Solution for Colorimetric Comparison. *J. Biol. Chem.* 49, 183–186.
- McMurry, L.M., Oethinger, M., Levy, S.B., 1998. Triclosan targets lipid synthesis. *Nature* 394, 531–532. doi:10.1038/28970
- Meng, X., Yang, J., Cao, Y., Li, L., Jiang, X., Xu, X., Liu, W., Xian, M., Zhang, Y., 2011. Increasing fatty acid production in *E. Coli* by simulating the lipid accumulation of oleaginous microorganisms. *J. Ind. Microbiol. Biotechnol.* 38, 919–925. doi:10.1007/s10295-010-0861-z
- Meng, X., Yang, J., Xu, X., Zhang, L., Nie, Q., Xian, M., 2009. Biodiesel production from oleaginous microorganisms. *Renew. Energy* 34, 1–5. doi:10.1016/j.renene.2008.04.014
- Metzger, J.O., Bornscheuer, U., 2006. Lipids as renewable resources: Current state of chemical and biotechnological conversion and diversification. *Appl. Microbiol. Biotechnol.* 71, 13–22. doi:10.1007/s00253-006-0335-4
- Minárik, P., Tomaásková, N., Kollárová, M., Antalík, M., 2002. Malate Dehydrogenases - Structure and function. *Gen. Physiol. Biophys.* 21, 257–265.
- Mlícková, K., Roux, E., Athenstaedt, K., Andrea, S., Daum, G., Chardot, T., Nicaud, J., 2004a. Lipid Accumulation, Lipid Body Formation, and Acyl Coenzyme A Oxidases of the Yeast *Yarrowia lipolytica*. *Appl. Environ. Microbiol.* 70, 3918–3924. doi:10.1128/AEM.70.7.3918
- Mlícková, K., Roux, E., Athenstaedt, K., Andrea, S., Daum, G., Chardot, T., Nicaud, J., 2004b. Lipid Accumulation, Lipid Body Formation, and Acyl Coenzyme A Oxidases of the Yeast *Yarrowia lipolytica*. *Appl. Environ. Microbiol.* 70, 3918–3924. doi:10.1128/AEM.70.7.3918
- Moeller, L., Strehlitz, B., Aurich, A., Zehnsdort, A., Bley, T., 2007. Optimization of citric acid production from glucose by *Yarrowia lipolytica*. *Eng. Life Sci.* 7, 504–511. doi:10.1002/elsc.200620207
- Monthéard, J., Garcier, S., Lombard, E., Cameleyre, X., Guillouet, S., Molina-Jouve, C., Alfenore, S., 2012. Assessment of *Candida shehatae* viability by flow cytometry and fluorescent probes. *J. Microbiol. Methods* 91, 8–13. doi:10.1016/j.mimet.2012.07.002
- Morales-Vargas, A.T., Domínguez, A., Ruiz-Herrera, J., 2012. Identification of dimorphism-involved genes of *Yarrowia lipolytica* by means of microarray analysis. *Res. Microbiol.* 163, 378–387. doi:10.1016/j.resmic.2012.03.002
- Morin, N., Cescut, J., Beopoulos, A., Lelandais, G., Le Berre, V., Uribelarrea, J.L., Molina-

- Jouve, C., Nicaud, J.M., 2011. Transcriptomic analyses during the transition from biomass production to lipid accumulation in the oleaginous yeast *Yarrowia lipolytica*. *PLoS One* 6. doi:10.1371/journal.pone.0027966
- Morita, N., Nishida, T., Tanaka, M., Yano, Y., Okuyama, H., 2005. Enhancement of polyunsaturated fatty acid production by cerulenin treatment in polyunsaturated fatty acid-producing bacteria. *Biotechnol. Lett.* 27, 389–393. doi:10.1007/s10529-005-1532-4
- Morrice, J., Mackenzie, D. a, Parr, a J., Archer, D.B., 1998. Isolation and characterisation of the acetyl-CoA carboxylase gene from *Aspergillus nidulans*. *Curr.Genet.* 34, 379–385. doi:10.1007/s002940050410
- Mullinax, T.R., Mock, J.N., Mcevely, A.J., Harrison, J.H., 1982. Regulation of Mitochondrial Malate Dehydrogenase. *J. Biol. Chem.* 257, 13233–13239.
- Muniraj, I.K., Xiao, L., Hu, Z., Zhan, X., Shi, J., 2013. Microbial lipid production from potato processing wastewater using oleaginous filamentous fungi *Aspergillus oryzae*. *Water Res.* 47, 3477–3483. doi:10.1016/j.watres.2013.03.046
- Nicaud, J.-M., 2012. *Yarrowia lipolytica*. *Yeast* 29, 409–418. doi:10.1002/yea
- Nicaud, J.-M., Madzak, C., van den Broek, P., Gysler, C., Duboc, P., Niederberger, P., Gaillardin, C., Broek, P. Van Den, Gysler, C., Duboc, P., Niederberger, P., Gaillardin, C., 2002. Protein expression and secretion in the yeast *Yarrowia lipolytica*. *FEMS Yeast Res.* 2, 371–9. doi:10.1111/j.1567-1364.2002.tb00106.x
- Ochoa Estopier, A., 2012. Analyse systématique des bascules métaboliques chez les levures d'intérêt industriel : application aux bascules du métabolisme lipidique chez *Yarrowia lipolytica* (phdthesis).
- Ochoa-Estopier, A., Guillouet, S.E., 2014. D-stat culture for studying the metabolic shifts from oxidative metabolism to lipid accumulation and citric acid production in *Yarrowia lipolytica*. *J. Biotechnol.* 170, 35–41. doi:10.1016/j.jbiotec.2013.11.008
- Omura, S., 1976. The antibiotic cerulenin, a novel tool for biochemistry as an inhibitor of fatty acid synthesis. *Bacteriol. Rev.* 40, 681–697.
- Papanikolaou, S., Aggelis, G., 2011a. Lipids of oleaginous yeasts. Part I: Biochemistry of single cell oil production. *Eur. J. Lipid Sci. Technol.* 113, 1031–1051. doi:10.1002/ejlt.201100014
- Papanikolaou, S., Aggelis, G., 2011b. Lipids of oleaginous yeasts. Part II: Technology and potential applications. *Eur. J. Lipid Sci. Technol.* 113, 1052–1073. doi:10.1002/ejlt.201100015
- Papanikolaou, S., Aggelis, G., 2010. *Yarrowia lipolytica*: A model microorganism used for the production of tailor-made lipids. *Eur. J. Lipid Sci. Technol.* 112, 639–654. doi:10.1002/ejlt.200900197
- Papanikolaou, S., Aggelis, G., 2002. Lipid production by *Yarrowia lipolytica* growing on industrial glycerol in a single stage continuous culture. *Bioresour. Technol.* 82, 43–49. doi:10.1186/s13068-015-0286-z
- Papanikolaou, S., Beopoulos, A., Koletti, A., Thevenieau, F., Koutinas, A.A., Nicaud, J.M., Aggelis, G., 2013. Importance of the methyl-citrate cycle on glycerol metabolism in the yeast *Yarrowia lipolytica*. *J. Biotechnol.* 168, 303–314. doi:10.1016/j.jbiotec.2013.10.025
- Papanikolaou, S., Galiotou-Panayotou, M., Chevalot, I., Komaitis, M., Marc, I., Aggelis, G.,

2006. Influence of glucose and saturated free-fatty acid mixtures on citric acid and lipid production by *Yarrowia lipolytica*. *Curr. Microbiol.* 52, 134–142. doi:10.1007/s00284-005-0223-7
- Papanikolaou, S., Muniglia, L., Chevalot, I., Aggelis, G., Marc, I., 2003. Accumulation of a cocoa-butter-like lipid by *Yarrowia lipolytica* cultivated on agro-industrial residues. *Curr. Microbiol.* 46, 124–130. doi:10.1007/s00284-002-3833-3
- Papanikolaou, S., Muniglia, L., Chevalot, I., Aggelis, G., Marc, I., 2002. *Yarrowia lipolytica* as a potential producer of citric acid from raw glycerol. *J. Appl. Microbiol.* 92, 737–744. doi:10.1046/j.1365-2672.2002.01577.x
- Pemble, C.W., Johnson, L.C., Kridel, S.J., Lowther, W.T., 2007. Crystal structure of the thioesterase domain of human fatty acid synthase inhibited by Orlistat. *Nat. Struct. Mol. Biol.* 14, 704–709. doi:10.1038/nsmb1265
- Perez-Campo, F.M., Dominguez, A., 2001. Factors affecting the morphogenetic switch in *Yarrowia lipolytica*. *Curr. Microbiol.* 43, 429–433. doi:10.1007/s002840010333
- Pfützner, A., Kubicek, C.P., Röhr, M., 1987. Presence and regulation of ATP:citrate lyase from the citric acid producing fungus *Aspergillus niger*. *Arch. Microbiol.* 147, 88–91.
- Poilpre, E., Tronquit, D., Goma, G., Guillou, V., 2002. On-line estimation of biomass concentration during transient growth on yeast chemostat culture using light reflectance. *Biotechnol. Lett.* 24, 2075–2081. doi:10.1023/A:1021389827244
- Porrini, L., Cybulski, L.E., Altabe, S.G., Mansilla, M.C., de Mendoza, D., 2014. Cerulenin inhibits unsaturated fatty acids synthesis in *Bacillus subtilis* by modifying the input signal of DesK thermosensor. *Microbiologyopen* 3, 213–224. doi:10.1002/mbo3.154
- Price, A.C., Choi, K.H., Heath, R.J., Li, Z., White, S.W., Rock, C.O., 2001. Inhibition of  $\beta$ -ketoacyl-acyl carrier protein synthases by thiolactomycin and cerulenin: Structure and mechanism. *J. Biol. Chem.* 276, 6551–6559. doi:10.1074/jbc.M007101200
- Rajakumari, S., Grillitsch, K., Daum, G., 2008. Synthesis and turnover of non-polar lipids in yeast. *Prog. Lipid Res.* 47, 157–171. doi:10.1016/j.plipres.2008.01.001
- Ratledge, C., 2004. Fatty acid biosynthesis in microorganisms being used for Single Cell Oil production. *Biochimie* 86, 807–815. doi:10.1016/j.biochi.2004.09.017
- Ratledge, C., 2002. Regulation of lipid accumulation in oleaginous micro-organisms. *Biochem. Soc. Trans.* 30, 1047–1050. doi:10.1042/
- Ratledge, C., Cohen, Z., 2008. Microbial and algal oils: Do they have a future for biodiesel or as commodity oils? *Lipid Technol.* 20, 155–160. doi:10.1002/lite.200800044
- Ratledge, C., Wynn, J.P., 2002. The Biochemistry and Molecular Biology of Lipid Accumulation in Oleaginous Microorganisms. *Adv. Appl. Microbiol.* 51, 1–51.
- Rattray, J.B.M., Schibeci, A., Kidby, D.K., 1975. Lipids of Yeasts. *Bacteriol. Rev.* 39, 197–231.
- Rigouin, C., Croux, C., Borsenberger, V., Ben Khaled, M., Chardot, T., Marty, A., Bordes, F., 2018. Increasing medium chain fatty acids production in *Yarrowia lipolytica* by metabolic engineering. *Microb. Cell Fact.* 17, 142. doi:10.1186/s12934-018-0989-5
- Rigouin, C., Gueroult, M., Croux, C., Dubois, G., Borsenberger, V., Barbe, S., Marty, A., Daboussi, F., André, I., Bordes, F., 2017. Production of Medium Chain Fatty Acids by *Yarrowia lipolytica*: Combining Molecular Design and TALEN to Engineer the Fatty

- Acid Synthase. *ACS Synth. Biol.* 6, 1870–1879. doi:10.1021/acssynbio.7b00034
- Rodríguez-Frómata, R.A., Gutiérrez, A., Torres-Martínez, S., Garre, V., 2013. Malic enzyme activity is not the only bottleneck for lipid accumulation in the oleaginous fungus *Mucor circinelloides*. *Appl. Microbiol. Biotechnol.* 97, 3063–3072. doi:10.1007/s00253-012-4432-2
- Rossi, M., Amaretti, A., Raimondi, S., Leonardi, A., 2011. Getting Lipids for Biodiesel Production from Oleaginous Fungi. *Biodiesel – Feed. Process. Technol.* 71–92. doi:10.5772/25864
- Rossi, M., Amaretti, A., Raimondi, S., Leonardi, A., 2010. Getting Lipids for Biodiesel Production from Oleaginous Fungi. *Biodiesel – Feed. Process. Technol.* 71–92. doi:10.5772/25864
- Ruenwai, R., Cheevadhanarak, S., Laoteng, K., 2009. Overexpression of Acetyl-CoA carboxylase gene of *Mucor rouxii* enhanced fatty acid content in *Hansenula polymorpha*. *Mol. Biotechnol.* 42, 327–332. doi:10.1007/s12033-009-9155-y
- Ruiz-Herrera, J., Sentandreu, R., 2002. Different effectors of dimorphism in *Yarrowia lipolytica*. *Arch. Microbiol.* 178, 477–483. doi:10.1007/s00203-002-0478-3
- Runguphan, W., Keasling, J.D., 2014. Metabolic engineering of *Saccharomyces cerevisiae* for production of fatty acid-derived biofuels and chemicals. *Metab. Eng.* 21, 103–113. doi:10.1016/j.ymben.2013.07.003
- Rymowicz, W., Rywinska, A., Zarowska, B., 2007. Biosynthesis of citric acid from crude glycerol by *Yarrowia lipolytica* in repeated-batch cultivations. *J. Biotechnol.* 131, 148–149. doi:10.1016/j.jbiotec.2007.07.862
- Sagnak, R., Cochet, S., Molina-Jouve, C., Nicaud, J.-M., Guillouet, S.E., 2017. Modulation of the Glycerol Phosphate availability led to concomitant reduction in the citric acid excretion and increase in lipid content and yield in *Yarrowia lipolytica*. *J. Biotechnol.* 265, 40–45. doi:10.1016/j.jbiotec.2017.11.001
- Sangwallek, J., Kaneko, Y., Sugiyama, M., Ono, H., Bamba, T., Fukusaki, E., Harashima, S., 2013. Ketoacyl synthase domain is a major determinant for fatty acyl chain length in *Saccharomyces cerevisiae*. *Arch. Microbiol.* 195, 843–852. doi:10.1007/s00203-013-0933-3
- Sattur, A.P., Karanth, N.G., 1989. Production of microbial lipids: III. Influence of C/N ratio - experimental observations. *Biotechnol. Bioeng.* 34, 872–874.
- Savitha, J., Wynn, J.P., Ratledge, C., 1997. Malic enzyme: Its purification and characterization from *mucor circinelloides* and occurrence in other oleaginous fungi. *World J. Microbiol. Biotechnol.* 13, 7–9. doi:10.1007/Bf02770799
- Sawangkeaw, R., Ngamprasertsith, S., 2013. A review of lipid-based biomasses as feedstocks for biofuels production. *Renew. Sustain. Energy Rev.* 25, 97–108. doi:10.1016/j.rser.2013.04.007
- Schweizer, E., Hofmann, J., 2004. Microbial Type I Fatty Acid Synthases ( FAS ): Major Players in a Network of Cellular FAS Systems. *Microbiol. Mol. Biol. Rev.* 68, 501–517. doi:10.1128/MMBR.68.3.501
- Schweizer, E., Köttig, H., Regler, R., Rottner, G., 1988. Genetic control of *Yarrowia lipolytica* fatty acid synthetase biosynthesis and function. *J. Basic Microbiol.* 28, 283–92.
- Shi, K., Gao, Z., Shi, T.Q., Song, P., Ren, L.J., Huang, H., Ji, X.J., 2017. Reactive oxygen

- species-mediated cellular stress response and lipid accumulation in oleaginous microorganisms: The state of the art and future perspectives. *Front. Microbiol.* 8, 1–9. doi:10.3389/fmicb.2017.00793
- Silva, T.L. da, Roseiro, J.C.J.C., Reis, A., da Silva, T.L., 2012. Applications and perspectives of multi-parameter flow cytometry to microbial biofuels production processes. *Trends Biotechnol.* 30, 225–232. doi:10.1016/j.tibtech.2011.11.005
- Sinigaglia, M., Lanciotti, R., Guerzoni, M.E., 1994. Biochemical and physiological characteristics of *Yarrowia lipolytica* strains in relation to isolation source. *Can. J. Microbiol.* 40, 54–59. doi:10.1139/m94-008
- Song, Y., Wynn, J.P., Li, Y., Grantham, D., Ratledge, C., 2001. A pre-genetic study of the isoforms of malic enzyme associated with lipid accumulation in *Mucor circinelloides*. *Microbiology* 147, 1507–1515.
- Sorger, D., Daum, G., 2003. Triacylglycerol biosynthesis in yeast. *Appl. Microbiol. Biotechnol.* 61, 289–299. doi:10.1007/s00253-002-1212-4
- Soriano, A., Radice, A.D., Herbitter, A.H., Langsdorf, E.F., Stafford, J.M., Chan, S., Wang, S., Liu, Y.H., Black, T.A., 2006. *Escherichia coli* acetyl-coenzyme A carboxylase: Characterization and development of a high-throughput assay. *Anal. Biochem.* 349, 268–276. doi:10.1016/j.ab.2005.10.044
- Tai, M., Stephanopoulos, G., 2013. Engineering the push and pull of lipid biosynthesis in oleaginous yeast *Yarrowia lipolytica* for biofuel production. *Metab. Eng.* 15, 1–9. doi:10.1016/j.ymben.2012.08.007
- Tamano, K., Bruno, K.S., Karagiosis, S.A., Culley, D.E., Deng, S., Collett, J.R., Umemura, M., Koike, H., Baker, S.E., Machida, M., 2013. Increased production of fatty acids and triglycerides in *Aspergillus oryzae* by enhancing expressions of fatty acid synthesis-related genes. *Appl. Microbiol. Biotechnol.* 97, 269–281. doi:10.1007/s00253-012-4193-y
- Tang, X., Feng, H., Chen, W.N., 2013. Metabolic engineering for enhanced fatty acids synthesis in *Saccharomyces cerevisiae*. *Metab. Eng.* 16, 95–102. doi:10.1016/j.ymben.2013.01.003
- Tapia V, E., Anschau, A., Coradini, A.L., T Franco, T., Deckmann, A.C., 2012. Optimization of lipid production by the oleaginous yeast *Lipomyces starkeyi* by random mutagenesis coupled to cerulenin screening. *AMB Express* 2, 64. doi:10.1186/2191-0855-2-64
- Tehlivets, O., Scheuringer, K., Kohlwein, S.D., 2007. Fatty acid synthesis and elongation in yeast. *Biochim. Biophys. Acta - Mol. Cell Biol. Lipids* 1771, 255–270. doi:10.1016/j.bbalip.2006.07.004
- Thevenieau, F., Le Dall, M.T., Nthangeni, B., Mauersberger, S., Marchal, R., Nicaud, J.M., 2007. Characterization of *Yarrowia lipolytica* mutants affected in hydrophobic substrate utilization. *Fungal Genet. Biol.* 44, 531–542. doi:10.1016/j.fgb.2006.09.001
- Thevenieau, F., Nicaud, J.-M., 2013. Microorganisms as sources of oils. *Ocl* 20, D603. doi:10.1051/ocl/2013034
- Timoumi, A., Bideaux, C., Guillouet, S.E., Allouche, Y., Molina-Jouve, C., Fillaudeau, L., Gorret, N., 2017a. Influence of oxygen availability on the metabolism and morphology of *Yarrowia lipolytica*: insights into the impact of glucose levels on dimorphism. *Appl. Microbiol. Biotechnol.* 101, 7317–7333. doi:10.1007/s00253-017-8446-7

- Timoumi, A., Cléret, M., Bideaux, C., Guillouet, S.E., Allouche, Y., 2016. Dynamics of metabolic and physiological responses of *Yarrowia lipolytica* to pH perturbations under well-controlled conditions in batch and continuous modes of culture. pp. 1–56.
- Timoumi, A., Cléret, M., Bideaux, C., Guillouet, S.E., Allouche, Y., Molina-Jouve, C., Fillaudeau, L., Gorret, N., 2017b. Dynamic behavior of *Yarrowia lipolytica* in response to pH perturbations: dependence of the stress response on the culture mode. *Appl. Microbiol. Biotechnol.* 101, 351–366. doi:10.1007/s00253-016-7856-2
- Timoumi, A., Guillouet, S.E., Molina-Jouve, C., Fillaudeau, L., Gorret, N., 2018. Impacts of environmental conditions on product formation and morphology of *Yarrowia lipolytica*. *Appl. Microbiol. Biotechnol.* 102, 3831–3848. doi:10.1007/s00253-018-8870-3
- Vance, D., Goldberg, I., Mitsuhashi, O., Bloch, K., Omura, S., Nomura, S., 1972. Inhibition of fatty acid synthetases by the antibiotic cerulenin. *Biochem. Biophys. Res. Commun.* 48, 649–656. doi:10.1016/0006-291X(72)90397-X
- Vandermies, M., Fickers, P., 2019. Bioreactor-Scale Strategies for the Production of Recombinant Protein in the Yeast *Yarrowia lipolytica*. *Microorganisms* 7, 40. doi:10.3390/microorganisms7020040
- Waite, M., Wakil, S.J., 1962. Studies on the mechanism of fatty acid synthesis. XII. Acetyl Coenzyme A Carboxylase. *J. Biol. Chem.* 237, 2750–2757.
- Wang, J., Li, R., Lu, D., Ma, S., Yan, Y., Li, W., 2009. A quick isolation method for mutants with high lipid yield in oleaginous yeast. *World J. Microbiol. Biotechnol.* 25, 921–925. doi:10.1007/s11274-009-9960-2
- Wasylenko, T.M., Ahn, W.S., Stephanopoulos, G., 2015. The oxidative pentose phosphate pathway is the primary source of NADPH for lipid overproduction from glucose in *Yarrowia lipolytica*. *Metab. Eng.* 30, 27–39. doi:10.1016/j.ymben.2015.02.007
- Weibel, E.K., Hadvary, P., Hochuli, E., Kupfer, E., Lengsfeld, H., 1987. Lipstatin, an inhibitor of pancreatic lipase, produced by *Streptomyces toxytricini*. I. Producing organism, fermentation, isolation and biological activity. *J. Antibiot. (Tokyo)*. 40, 1081–1085. doi:10.7164/antibiotics.40.1081
- Wright, H.T., Reynolds, K.A., 2007. Antibacterial targets in fatty acid biosynthesis. *Curr. Opin. Microbiol.* 10, 447–453. doi:10.1016/j.mib.2007.07.001
- Wu, S., Hu, C., Jin, G., Zhao, X., Zhao, Z.K., 2010. Phosphate-limitation mediated lipid production by *Rhodospiridium toruloides*. *Bioresour. Technol.* 101, 6124–6129. doi:10.1016/j.biortech.2010.02.111
- Wu, S., Zhao, X., Shen, H., Wang, Q., Zhao, Z.K., 2011. Microbial lipid production by *Rhodospiridium toruloides* under sulfate-limited conditions. *Bioresour. Technol.* 102, 1803–1807. doi:10.1016/j.biortech.2010.09.033
- Wynn, J.P., Hamid, A.A., Ratledge, C., 1999. The role of malic enzyme in the regulation of lipid accumulation in filamentous fungi. *Microbiology* 145, 1911–1917. doi:10.1099/13500872-145-8-1911
- Wynn, J.P., Kendrick, A., Ratledge, C., 1997. Sesamol as an inhibitor of growth and lipid metabolism in *Mucor circinelloides* via its action on malic enzyme. *Lipids* 32, 605–610. doi:10.1007/s11745-997-0077-1
- Wynn, J.P., Ratledge, C., 1997. Malic enzyme is a major source of NADPH for lipid accumulation by *Aspergillus nidulans*. *Microbiology* 143, 253–257.

doi:10.1099/00221287-143-1-253

- Xie, D., 2017. Integrating Cellular and Bioprocess Engineering in the Non-Conventional Yeast *Yarrowia lipolytica* for Biodiesel Production: A Review. *Front. Bioeng. Biotechnol.* 5. doi:10.3389/fbioe.2017.00065
- Yalcin, H.T., Ucar, F.B., 2009. Isolation and characterization of cheese spoiler yeast isolated from Turkish white cheeses. *Ann. Microbiol.* 59, 477–483. doi:10.1007/BF03175134
- Zha, W., Rubin-Pitel, S.B., Shao, Z., Zhao, H., 2009. Improving cellular malonyl-CoA level in *Escherichia coli* via metabolic engineering. *Metab. Eng.* 11, 192–198. doi:10.1016/j.ymben.2009.01.005
- Zhang, H., Zhang, L., Chen, H., Chen, Y.Q., Ratledge, C., Song, Y., Chen, W., 2013. Regulatory properties of malic enzyme in the oleaginous yeast, *Yarrowia lipolytica*, and its non-involvement in lipid accumulation. *Biotechnol. Lett.* 35, 2091–2098. doi:10.1007/s10529-013-1302-7
- Zhang, S., Skerker, J.M., Rutter, C.D., Maurer, M.J., Arkin, A.P., Rao, C. V., 2016. Engineering *Rhodospiridium toruloides* for increased lipid production. *Biotechnol. Bioeng.* 113, 1056–1066. doi:10.1002/bit.25864
- Zhang, Y., Adams, I.P., Ratledge, C., 2007. Malic enzyme: The controlling activity for lipid production? Overexpression of malic enzyme in *Mucor circinelloides* leads to a 2.5-fold increase in lipid accumulation. *Microbiology* 153, 2013–2025. doi:10.1099/mic.0.2006/002683-0
- Zhang, Y., Ratledge, C., 2008. Multiple isoforms of malic enzyme in the oleaginous fungus, *Mortierella alpina*. *Mycol. Res.* 112, 725–730. doi:10.1016/j.mycres.2008.01.003
- Zhu, L.Y., Zong, M.H., Wu, H., 2008. Efficient lipid production with *Trichosporon fermentans* and its use for biodiesel preparation. *Bioresour. Technol.* 99, 7881–7885. doi:10.1016/j.biortech.2008.02.033
- Zweytick, D., Athenstaedt, K., Daum, G., 2000. Intracellular lipid particles of eukaryotic cells. *Biochim. Biophys. Acta - Rev. Biomembr.* 1469, 101–120. doi:10.1016/S0005-2736(00)00294-7



Contents lists available at ScienceDirect

Journal of Biotechnology

journal homepage: [www.elsevier.com/locate/jbiotec](http://www.elsevier.com/locate/jbiotec)

## Modulation of the Glycerol Phosphate availability led to concomitant reduction in the citric acid excretion and increase in lipid content and yield in *Yarrowia lipolytica*



Rana Sagnak<sup>a</sup>, Sandrine Cochot<sup>a</sup>, Carole Molina-Jouve<sup>a</sup>, Jean-Marc Nicaud<sup>b</sup>, Stéphane E. Guillouet<sup>a,\*</sup>

<sup>a</sup> LISBP, Université de Toulouse, CNRS, INRA, INSA, 135 avenue de Rangueil, 31077 Toulouse CEDEX 04, France

<sup>b</sup> Micalis Institute, INRA, AgroParisTech, Université Paris-Saclay, 78350 Jouy-en-Josas, France

### ARTICLE INFO

#### Keywords:

*Yarrowia lipolytica*  
Lipid accumulation  
Fed-batch  
Nitrogen limitation  
Citric acid production  
DGA2

### ABSTRACT

In order to improve TriAcylGlycerol (TAG) lipids accumulation in the yeast *Yarrowia lipolytica* on glucose, double over-expression of the major acyl-CoA:diacylglycerol acyltransferase encoding gene (*yIDGA2*) and of the glycerol-phosphate dehydrogenase encoding gene (*yIGPD1*) was carried out. The genes were over-expressed in a strain impaired for the mobilization of the accumulated lipids, through the deletion of the genes encoding acyl-coenzyme A oxidases (*POX1-6* genes) and the deletion of the very efficient lipase attached to the lipid bodies, encoded by *yITGL4*. This metabolic engineering strategy had the objective of pulling the C-flow into the TAG synthesis by increasing the availability of glycerol-3-phosphate and its binding to fatty acids for the TAG synthesis.

This strain showed a strong improvement in production performances on glucose in terms of lipid content (increase from 18 to 55%), lipid yield (increase from 0.035 to 0.14 g g<sup>-1</sup>) and by-product formation (decrease in citric acid yield from 0.68 to 0.4 g g<sup>-1</sup>).

For developing bioprocess for the production of triacylglycerol from renewable carbon sources as glucose it is of first importance to control the C/N ratio in order to avoid citric acid excretion during lipid accumulation. Our engineered strain showed a delay in the onset of citric acid excretion as suggested by the 15% modulation of the critical C/N ratio.

### 1. Introduction

*Yarrowia lipolytica* is one of the most studied “non-conventional” yeasts isolated from oily environments such as polluted soils, raw poultry or dairy products (Sinigaglia et al., 1994; Deak, 2001; Lanciotti et al., 2005; Yalcin and Ucar, 2009), classified as generally recognized as safe (GRAS) by the Food and Drug Administration (FDA, USA). It has become an important industrial microorganism due to the versatility of its metabolism to produce metabolites such as heterologous proteins (Nicaud et al., 2002; Madzak et al., 2004; Madzak, 2015; Madzak and Beckerich, 2015), lipids (Papanikolaou et al., 2003; Bankar et al., 2009; Beopoulos et al., 2009) or citric acid (Papanikolaou et al., 2002; Moeller et al., 2007; Rymowicz et al., 2007).

*Y. lipolytica* belongs to the so-called oleaginous yeasts due to its ability to accumulate high amounts of lipid mainly in the form of triacylglycerol (TAG) (Ratray et al., 1975). *Y. lipolytica* is indeed able to accumulate lipids up to 43% of its dry mass on glycerol

(Papanikolaou and Aggelis, 2002) and over 50% w.w<sup>-1</sup> of total lipids, on fatty acids (Papanikolaou et al., 2003).

*De novo* lipid accumulation in oleaginous yeasts from osidic substrates is triggered by nutrient imbalance in the culture medium between the carbon source (in excess) and the nitrogen source in limiting concentration (although other nutrients can be identically made limiting, such as phosphorus, zinc, iron) (Granger et al., 1993; Ratledge and Wynn, 2002; Fontanille et al., 2012). Lately, it was demonstrated that double limitation of nitrogen and magnesium was essential to reach high lipid titres in wild type *Yarrowia* strain (Bellou et al., 2016). Contrarily *ex-novo* lipid accumulation (i.e. from oily substrates) approximates to a bioconversion process and therefore is independent to any nutrient imbalance (Papanikolaou and Aggelis, 2011).

Ratledge and Wynn (2002) proposed a general pattern of succession of the metabolic events that take place upon a N-limitation in oleaginous microorganisms (*Candida 107* and *C. utilis*, *Rhodotorula glutinis*, *Mucor circinelloides*) leading to lipid accumulation as follows: drop in

\* Corresponding author at: LISBP, Université de Toulouse, CNRS, INRA, INSA, 135 avenue de Rangueil, 31077 Toulouse CEDEX 04, France.  
E-mail address: [stephane.guillouet@insa-toulouse.fr](mailto:stephane.guillouet@insa-toulouse.fr) (S.E. Guillouet).

<https://doi.org/10.1016/j.jbiotec.2017.11.001>

Received 30 August 2017; Received in revised form 24 October 2017; Accepted 1 November 2017

Available online 02 November 2017

0168-1656/ © 2017 Elsevier B.V. All rights reserved.

the adenosine monophosphate (AMP) concentration due to the activation of the AMP deaminase, inhibition of the isocitrate dehydrogenase (ICDH) by the low AMP content leading to the accumulation of isocitrate and citrate and then citrate that can be exported from the mitochondrion by a citrate/malate transporter, citrate is cleaved by the ATP-citrate lyase (ACL) into acetyl coenzyme A and oxaloacetate, the acetyl-CoA is used for fatty acid synthesis by the acetyl-CoA carboxylase (ACC). One characteristic that differentiates oleaginous yeasts from non-oleaginous yeasts is the presence of ATP citrate lyase (ACL) (Holdsworth et al., 1988; Zhang et al., 2007); several authors have also considered that Acetyl CoA carboxylase (ACC) (Waite and Wakil, 1962; Hasslacher et al., 1993) and malic enzyme (Zhang et al., 2007) are essential for lipid accumulation. However, over-expression of ME gene in *Y. lipolytica* did not result in increased lipid accumulation (Beopoulos et al., 2009). Tai and Stephanopoulos (2012) reported that *Y. lipolytica* lacks cyto-plasmatic ME and therefore PPP is the sole source of NADPH as recently verified by Dulermo et al. (2013).

Several studies have shown that the metabolic shift in *Y. lipolytica* is related to a nutrient-limited medium such as nitrogen, phosphorus or magnesium (Gill et al., 1977; Anastassiadis et al., 2002; Bellou et al., 2016) or to the cultivation conditions such as growth rate, oxygen availability, pH or temperature (Finogenova et al., 1996; Il'chenko et al., 1998; Kamzolova et al., 2003; Moeller et al., 2007). One of the parameters that influences the metabolic shift on glucose is the C/N ratio (Sattur and Karanth, 1989; Anastassiadis et al., 2005). It is commonly observed in oleaginous yeasts a transient citrate excretion during the first steps of lipogenesis (Boulton and Ratledge, 1983; Evans and Ratledge, 1983). However, *Y. lipolytica* when cultivated on glucose as the sole carbon source, mainly produces citric acid upon nutrient limitation over lipid accumulation only 5–10% (wt.wt<sup>-1</sup>) of TAG (Papanikolaou et al., 2006). We previously demonstrated that an accumulation of lipids without citric acid secretion was possible in *Y. lipolytica* wild type strain W29 as long as the C/N rate ratio was controlled below a value of 47.6 Cmole/Nmole under chemostat conditions (Morin et al., 2011; Ochoa-Estopier and Guillouet, 2014).

In order to improve lipid accumulation in *Yarrowia lipolytica*, a pull and push strategy was previously tested by overexpressing the acetyl-CoA carboxylase (ACC1) to push the C-flow into the FA biosynthetic pathway in combination with the over-expression of the diacylglycerol acyltransferase (DGA1), the final step of the triglyceride (TAG) synthesis pathway to pull the C-flow into the final product (Tai and Stephanopoulos, 2012). This strategy led to an increase of the total lipid content from 18 to 61%.

We here used a slightly different engineering strategy named as double-pull strategy. In order to increase the accumulation of lipids by pulling the C-flow into the TAG synthesis, the major acyl-CoA:diacylglycerol acyltransferase encoding gene (yIDGA2) was over-expressed (Beopoulos et al., 2012) in combination with the over-expression of yIGPD1 to increase the availability of glycerol-3-phosphate for the TAG synthesis. The genes were overexpressed in a strain impaired for the mobilization of the accumulated lipids, through the deletion of the genes encoding acyl-coenzyme A oxidases (POX1-6 genes) (Beopoulos et al., 2008) and the deletion of the very efficient lipase attached to the lipid bodies, encoded by yITGL4 (Dulermo et al., 2013). Lately, Lazar et al. (2014) improved the lipid content to 30% (w/w) in a *Yarrowia lipolytica* on sucrose by combining this design with expression of invertase and hexokinase.

We, here, further evaluated the strain on glucose as the sole Carbon source in terms of the dynamics of lipid accumulation and modulation of a metabolic shift towards citric acid in fed-batch cultivations on glucose as the sole carbon source. This study aimed at evaluating the gain of such a strain in terms of process robustness.

## 2. Materials and methods

### 2.1. Microorganism, media and growth conditions

The strain used in this study *Y. lipolytica* JMY3501 was engineered in the Laboratoire Microbiologie et Génétique Moléculaire, INRA, (Paris-Grignon, France) in the frame of the project common "ProBio3". Its genotype was as follows: MATa ura3-302 leu2-270 xpr2-322 Δtgl4 Apox1-6 + LEU2ex Tef-yIDGA2 + URA3ex Tef-GPD1 (Lazar et al., 2014).

The strain was maintained on YPD/glucose agar medium containing 10 g L<sup>-1</sup> Yeast Extract, 20 g L<sup>-1</sup> Bactopeptone, 20 g L<sup>-1</sup> Glucose and 20 g L<sup>-1</sup> agar. Plates were stored at 4 °C. For preparation of glycerol stocks (for cryopreservation of the cells), pure sterile glycerol was added to the culture broth to reach a final glycerol concentration of 30% (v/v). This cell suspension (glycerol stocks) was then stored at -80 °C.

Precultivations were carried out on a 5-ml tube of YPD medium at 28 °C for 16 h at 100 rpm. The culture in growth phase was transferred into a 1-L Erlenmeyer flask containing 170 mL of mineral medium at pH 5.6 prepared as follows (all compounds are expressed in g L<sup>-1</sup>): (NH<sub>4</sub>)<sub>2</sub>SO<sub>4</sub>, 3.5; KH<sub>2</sub>PO<sub>4</sub>, 6; MgSO<sub>4</sub>, 2; EDTA, 0.0375; ZnSO<sub>4</sub>·7H<sub>2</sub>O, 0.0281; MnCl<sub>2</sub>·4H<sub>2</sub>O, 0.0025; CoCl<sub>2</sub>·6H<sub>2</sub>O, 0.00075; CuSO<sub>4</sub>·5H<sub>2</sub>O, 0.00075; Na<sub>2</sub>MoSO<sub>4</sub>·2H<sub>2</sub>O, 0.00005; CaCl<sub>2</sub>·2H<sub>2</sub>O, 0.0125; FeSO<sub>4</sub>·7H<sub>2</sub>O, 0.00875; H<sub>3</sub>BO<sub>3</sub>, 0.0025; D-biotin, 0.00025; D-*l*-panthothenic acid, 0.001; nicotinic acid, 0.001; myo-inositol, 0.00625; thiamin, 0.001; pyridoxine, 0.001; para-aminobenzoic acid, 0.0002. Glucose was added to a final concentration of 18 g L<sup>-1</sup> with chloramphenicol at 10 mg L<sup>-1</sup>. After 16 h of growth at 28 °C and 100 rpm, 170 mL of the broth were used to inoculate 1.7 L of the same mineral medium in a 3-L bioreactor.

### 2.2. Chemicals used

The chemicals glucose, salts, oligo-elements (Carlo Erba) and EDTA (Qbigoène), orthophosphoric acid were provided by VWR, the vitamins by Sigma. All products had the highest analytical grade available.

### 2.3. Fed-batch cultivation in bioreactor

Fed-batch experiments were performed in a 5-L stirred tank bioreactor with a working volume of 3 L using the Biostat B-DCU. Braun Biotech International (Sartorius AG, Germany) with the acquisition software MFCS/win 2.0.

The temperature was controlled at 28 °C with a water-jacket. The pH was kept constant at 5.6 with the automatic additions of acid/base solutions and monitored by a pH probe (Mettler-Toledo International Inc.). The relative pressure in the bioreactor was maintained at 300 mbar. Foaming was prevented by the addition of polypropylene glycol (PPG) antifoam agent. In order to avoid the oxygen limitation, bioreactor was flushed with air and stirred with Rushton turbines to maintain dissolved oxygen above 20% of saturation and measured with an autoclavable probe (InPro 6000/Optical O<sub>2</sub> sensor Mettler-Toledo International Inc.). Inlet and outlet air were passed through a 0.2 μm sterile polyamide membrane filter and compositions of inlet and outlet gas were analyzed with a mass spectrometer.

The fed-batch cultures were supplied with sterile feeding solutions (glucose, ammonia, acid/base solutions) via pre-calibrated peristaltic pumps (Watson-Marlow). The concentration of glucose feeding solution was determined precisely from the density of the solution (DE40 Density Meter Mettler-Toledo International Inc.). The mass flow rates of all feeding solutions supplied to bioreactor during the experiment time were determined on-line with 0.1–0.01 g precision using digital scales (Sartorius AG) and generated data was obtained via LabVIEW data acquisition software (International Instruments Cor.).

Fed-batch cultures were applied following two different procedures

depending on the objective of the strain evaluation: a procedure under Nitrogen depletion and a procedure under Nitrogen limitation.

### 2.3.1. Fed-batch cultivation under N depleted conditions

The fed-batch cultivation was divided in two phases

**2.3.1.1. Growth batch phase.** After the inoculation of bioreactor, a batch phase was applied without any nutrient limitation. Initial glucose and ammonium sulfate concentrations were set at  $100 \text{ g L}^{-1}$  and  $5 \text{ g L}^{-1}$ , respectively. The nitrogen concentration was calculated in order to produce up to  $15 \text{ g L}^{-1}$  of biomass before reaching N-limited conditions. pH was regulated with 9 M KOH solution.

**2.3.1.2. N-depleted phase.** Growth phase switched naturally to N-depleted production phase when ammonium was completely exhausted. Glucose was fed by pulses of a  $750 \text{ g L}^{-1}$  sterile glucose solution when residual glucose concentration reached  $20 \text{ g L}^{-1}$  in the bioreactor. Pulses were applied in order to bring the residual glucose concentration back to  $100 \text{ g L}^{-1}$ .

### 2.3.2. Fed-batch cultivation under N-limitation conditions

The fed-batch culture was divided into five phases according to a feeding strategy.

**2.3.2.1. Growth phase.** After the inoculation of bioreactor, a sterile glucose solution at a concentration of  $200 \text{ g L}^{-1}$  was exponentially fed by a peristaltic pump to maintain constant the specific growth rate at  $0.18 \text{ h}^{-1}$ . The nitrogen source was supplied with sterile 2.5 M ammonia solution which was also used for pH regulation.

**2.3.2.2. Transition phase.** When biomass concentration reached approximately  $10 \text{ g L}^{-1}$ , the pH corrector solution was switched to a sterile 2.5 M potassium hydroxide (KOH) solution. This second phase can be considered as an adaptation period, corresponding to the time required for the biomass to use all the nitrogen present in the medium.

**2.3.2.3. Set-up of N- and C-limited phase.** When the nitrogen source was depleted in the culture medium, 0.3 M sterile ammonia solution was fed exponentially to the reactor with a peristaltic pump in order to maintain a constant residual growth rate at  $0.04 \text{ h}^{-1}$ . Concomitantly the feeding profile of glucose was modified in order to maintain a constant C/N molar rate ratio below  $33 \text{ Cmol Nmol}^{-1}$  in order to induce lipid accumulation without citric acid secretion as demonstrated in Ochoa-Estopier and Guillouet (2014).

**2.3.2.4. C/N-increasing phase.** After 24 h under N- and C-limited phase (45 h), the glucose feeding rate was accelerated without changing the ammonia feeding profile. Therefore, N-limited condition and constant specific growth rate were maintained, but the C/N was gradually increased.

**2.3.2.5. C/N-decreasing phase.** Once citric acid was detected in the fermentation broth and the critical C/N ratio determined, the feeding strategy was reversed. The glucose feeding rate was decelerated without changing the ammonia feeding profile. Therefore, the C/N was gradually decreased without changing the specific growth rate.

## 2.4. Off gas analysis

The inlet and outlet gas compositions in carbon dioxide ( $\text{CO}_2$ ) and oxygen ( $\text{O}_2$ ) were measured by a fermentation gas monitor system (LumaSense Technologies Europe). The system combines a multipoint sampler 1309 with a gas analyzer (INNOVA 1313). Gas analysis was performed every minute during the whole experiment.  $\text{CO}_2$  production rate ( $r_{\text{CO}_2}$ ) and  $\text{O}_2$  consumption rate ( $r_{\text{O}_2}$ ) were calculated as described by Poilpre et al. (2002). The Respiratory Quotient (RQ) was calculated

as the molar ratio between  $r_{\text{CO}_2}$  and  $r_{\text{O}_2}$ .

## 2.5. Determination of biomass

Yeast growth was evaluated by spectrophotometric measurements at 620 nm in a spectrophotometer (Biochrom Libra S4, UK). Growth rates were determined based on time-courses of optical density ( $\text{OD}_{620\text{nm}}$ ).  $\text{OD}_{620\text{nm}}$  was calibrated against dry cell weight measurements. The biomass formula used to convert cell dry weight into molar carbon concentration was  $\text{CH}_{1.744}\text{O}_{0.451}\text{N}_{0.132}$  for a molecular weight of  $24.67 \text{ g Cmol}^{-1}$  (Ochoa-Estopier and Guillouet, 2014).

## 2.6. Metabolite analysis

The culture supernatants were analyzed by High Performance Liquid Chromatography (DIONEX Ultimate 3000, USA) using an Aminex HPLC-87H<sup>+</sup> column (Bio-Rad, US) and the following conditions: a temperature of  $50 \text{ }^\circ\text{C}$  with  $5 \text{ mM H}_2\text{SO}_4$  as eluant (flow rate of  $0.5 \text{ mL min}^{-1}$ ) and a dual detection (IR and UV at 210 nm). Culture supernatant was obtained by centrifuging (MiniSpin ependorf, USA) the fermentation culture in Eppendorf tubes at 13,000 rpm for 3 min. The supernatant was filtered on Minisart filters  $0.45 \mu\text{m}$  pore-size diameter polyamide membranes (Sartorius AG, Germany). The metabolites searched for detections and quantification were glucose, citrate, isocitrate, alpha-ketoglutarate, pyruvate, malate, succinate, fumarate, lactate and acetate.

The quantification of lipids was carried out as described by Browne et al. (1986) 20 mg of lyophilized cells were added to 1 mL of methanol solution containing  $25 \text{ mL L}^{-1}$  of sulfuric acid (95%) and internal standard (C9:0). The mix in sealed tubes was placed in a  $80 \text{ }^\circ\text{C}$  bath for 90 min. After cooling,  $450 \mu\text{L}$  hexane and 1.5 mL water were added and vortexed. The lipidic phase was then sampled and the composition was analysed by Gas Chromatography as mentioned in Cescut et al. (2011). Lipid quantification was also performed by epifluorescence after staining the cells with Bodipy 493/503 in a Microplate reader (Synergy HT, Biotek, USA) as follows: the pellets were washed 3 times with PBS buffer solution (in  $\text{g L}^{-1}$ , NaCl, 8;  $\text{Na}_2\text{HPO}_4$ , 1.15; KCl, 0.2;  $\text{KH}_2\text{PO}_4$ , 0.2; pH at 6.9–7.1) at  $4 \text{ }^\circ\text{C}$  and resuspended in the same buffer solution to a  $\text{OD}_{620\text{nm}}$  of 0.5; 1 mL of the cell suspension was mixed with  $200 \mu\text{L}$  of Bodipy 493/503 ( $100 \mu\text{g mL}^{-1}$  in DMSO) and incubated 5 min at  $4 \text{ }^\circ\text{C}$ ; the mixture was then centrifuged 3 min at 13,000 rpm and resuspended into 1 mL of PBS buffer solution;  $200 \mu\text{L}$  of this cell suspension were placed in a 96-well Nunclon™D surface Microplate and read at 528 nm with an excitation wavelength value of 428 nm. The measurements were repeated 5 times showing a standard deviation lower than 5%.

The quantification of residual ammonium in the medium was determined with an Orion ammonium probe (ORION research INC., Boston, USA) and a voltmeter (ORION pH/ISE Meter, USA) as follows: 5 mL of culture broth were filtered on  $0.45 \mu\text{m}$  pore-size diameter polyamide membrane (Sartorius AG, Germany) and mixed with  $200 \mu\text{L}$  of ISA buffer solution (Ionic Strength Adjustor: NaOH,  $5 \text{ mol L}^{-1}$ ; disodium EDTA,  $0.05 \text{ mol L}^{-1}$  and methanol  $1 \text{ g L}^{-1}$ ). The concentration of  $\text{NH}_4$  was determined with a calibration curve correlating the mV and the  $\text{NH}_4$  concentration in a range of  $10^{-1}$ – $10^{-4} \text{ mol L}^{-1} \text{ NH}_4\text{Cl}$ .

## 3. Results and discussion

### 3.1. Impact of nitrogen depleted condition on the lipid accumulation and citric acid production in *Y. lipolytica* JMY3501 strain

The *Yarrowia lipolytica* JMY3501 strain was first evaluated in bioreactor under non nutrient limited conditions followed by a switch to Nitrogen depleted conditions in a mineral medium with glucose as the sole Carbon source (Fig. 1). The first phase consisted in a batch phase under non nutrient limited conditions with an initial glucose

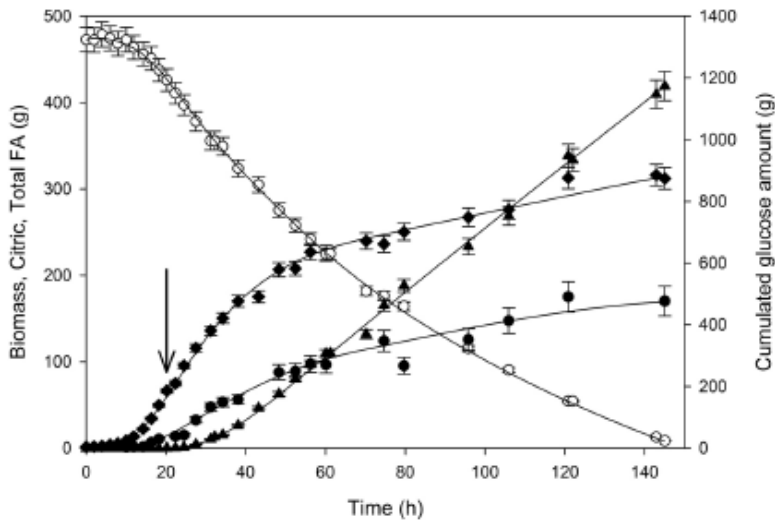


Fig. 1. Fed-batch cultivation of the strain JMY3501 on mineral medium on glucose as the sole carbon source. Evolution of masses of biomass (◆), citric acid (▲), total FA content (●) and cumulated glucose consumed (○). Arrow indicated the time of Nitrogen depletion. Data are presented as means  $\pm$  standard deviation.

concentration of  $100 \text{ g L}^{-1}$ . The JMY3501 strain grew exponentially at a maximal specific growth ( $\mu_{\max}$ ) rate of  $0.24 \text{ h}^{-1}$ . It was close to the  $\mu_{\max}$  of the parent strain W29 grown under the same conditions ( $\mu_{\max} = 0.27 \text{ h}^{-1}$ ; Ochoa-Estropier and Guillouet (2014)). The global biomass yield on glucose was identical to the one of the parent strain at  $0.49 \text{ g}_{\text{CDW}} \text{ g}_{\text{glucose}}^{-1}$  (Ochoa-Estropier and Guillouet, 2014) pointing out no drastic impact of the engineering on the oxidative metabolism of the strain.

Once nitrogen was completely consumed after 20 h of growth, metabolism switched toward lipid accumulation and citric acid secretion. After 145 h of cultivation, citric acid concentration reached  $70 \text{ g L}^{-1}$  and total lipid content 55%. Comparatively, the parent W29 strain cultivated under the same conditions accumulated lower lipid content of around 18% (Table 1). Lipid content and yield on glucose were both higher in the engineered strain concomitantly with a reduction in the Citric acid production yield by a factor of 1.3 and 4, respectively. Lipid production yield reached a maximal value of  $0.18 \text{ g g}^{-1}$  corresponding to 56% of the theoretical yield ( $0.32 \text{ g g}^{-1}$ ). Improvement of lipid accumulation by the double pull strategy was significant in our strain in the range of the one obtained by the push and pull strategy through the over-expression of ACC1 and DGA1 (Tai and Stephanopoulos, 2012). The authors reached 61% of lipid content and  $0.19 \text{ g g}^{-1}$  of overall lipid yield (59% of the theoretical yield) with a peak at  $0.27 \text{ g g}^{-1}$  during the highest oil production phase between 70 and 100 h. However, yields are not fully comparable due to the presence of yeast extract in their medium. Supplementation of mineral medium with yeast extract has been reported to slightly enhance lipid accumulation indeed (Bellou et al., 2016).

The increase in the lipid titer and yield observed in our engineered strain was concomitantly accompanied with a 1.5 fold-decrease in the citric acid production in terms of overall yield suggesting that the

Carbon flow was further directed into lipid formation. The citric acid production yield from glucose decreased from  $0.68$  to  $0.4 \text{ g g}^{-1}$ . Comparatively, the ACC1-DGA1 overexpressing strain had a citric acid yield of  $0.25 \text{ g g}^{-1}$  during the highest lipid production phase (Tai and Stephanopoulos, 2012).

### 3.2. Impact of the C/N ratio on the lipid accumulation and citric acid production in *Y. lipolytica* JMY3501 from glucose as sole carbon source

In order to characterize the JMY3501 *Y. lipolytica* strain in terms of metabolic shift modulation, the strain was cultivated in a 5 L bioreactor under fed-batch mode (Fig. 2). After 16 h of controlled exponential growth phase at  $\mu 0.18 \text{ h}^{-1}$ , the culture was switched into  $\text{N}_2$  limited phase at a specific C/N rate ratio below  $33 \text{ Cmol Nmol}^{-1}$  in order to induce lipid accumulation without citric acid secretion. Ochoa-Estropier and Guillouet (2014) previously demonstrated under double N- and C-limitation in chemostat cultures at a dilution rate of  $0.08 \text{ h}^{-1}$  that accumulation of lipids without secretion of citric acid was possible when C/N ratio was maintained precisely below a critical value of  $47.6 \text{ Cmol Nmol}^{-1}$ . Identical critical value was obtained in fed-batch culture as well (Morin et al., 2011).

Therefore, the C/N ratio was maintained below  $33 \text{ Nmol Cmol}^{-1}$  for around 24 h and confirmed lipid accumulation without any citric acid secretion. The total lipid content slightly increased from 10 to 15% of cell dry weight during this period. No citric acid was detected (Fig. 2).

After 45 h of cultivation, the profile of glucose feeding rate was constantly increased without changing the profile of ammonia feeding rate in order to increase gradually the C/N ratio without changing the specific growth rate that was maintained constant at  $0.04 \text{ h}^{-1}$ . The total lipid content continuously increased during the whole period to finally reach a value of  $34 \pm 2\%$ ; citric acid was detected in the medium until 71 h, at 77 h its concentration was at  $0.5 \text{ g L}^{-1}$  and continued to increase to reach  $8 \text{ g L}^{-1}$  at 81 h. Between 71 and 77 h the C/N ratio increased from  $55.5$  to  $58.8 \text{ Cmol Nmol}^{-1}$  (Fig. 3). Once citric acid was detected, at 78 h the profile of glucose feeding rate was inverted and constantly decreased without changing the profile of ammonia feeding rate in order to decrease gradually the C/N ratio. The concentration of citric acid continued to increase until reaching  $11.6 \text{ g L}^{-1}$  at 85 h and then decreased with decreasing C/N ratio down to  $1.6 \text{ g L}^{-1}$  at the end of the culture. It demonstrated that based on the modulation profile of the N and C fluxes the yeast is able to rapidly and reversibly excrete or consume citric acid during FA accumulation.

Table 1

Comparison of the strain performances under non limited and depleted Nitrogen conditions.

	Non limited phase		N depleted phase		
	$\mu_{\max} (\text{h}^{-1})$	$Y_{\text{glc}} (\text{g g}^{-1})$	Total lipid (%)	$Y_{\text{glc,lipid}}$ Average/max ( $\text{g g}^{-1}$ )	$Y_{\text{glc,cit}}$ Average/max ( $\text{g g}^{-1}$ )
W29	$0.27 \pm 0.01$	$0.49 \pm 0.012$	18	$0.035/0.058$	$0.68/0.74$
JMY3501	$0.24 \pm 0.01$	$0.49 \pm 0.01$	55	$0.14/0.18$	$0.40/0.49$

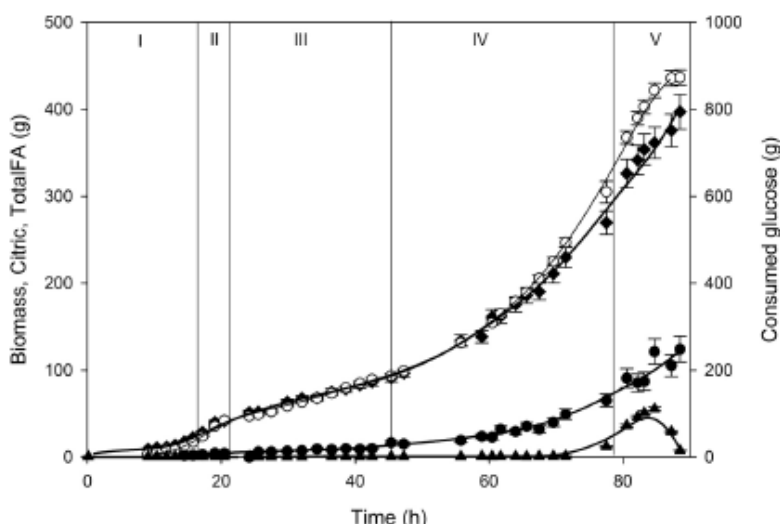


Fig. 2. Fed-batch cultivation of the strain JMY3501 on mineral medium on glucose as the sole carbon source. Evolution of the masses of biomass (●), citric acid (▲), total FA content (●) and cumulated glucose consumed (○). Phases: (I) Unlimited growth phase, (II) Transition phase, (III) N- and C-limited phase, (IV) C/N increasing phase, (V) C/N decreasing phase. Data are presented as means  $\pm$  standard deviation.

Here the critical C/N ratio determined at the onset of the citric acid excretion was determined at 55.5–58.8 Cmol Nmol<sup>-1</sup> for the DAG2-GPD1 engineered strain. Ochoa-estopier and Guillouet (2014) previously determined the critical C/N ratio for the onset of citric acid excretion in D-stat cultivation system with the parent strain at 47.6 Cmol Nmol<sup>-1</sup> and at 45.4 Cmol Nmol<sup>-1</sup> in fed-batch cultivation system under similar strategy (Ochoa-Estopier (2012)). Therefore, the engineering of the strain led to a 15% modulation of the critical C/N ratio, suggesting that the over-expression of DGA2 and GPD1 enabled to delay the onset of citric acid excretion. Further modulation of the critical C/N ratio would imply a much better robustness in terms of bio-process design: as an example, comparatively to the wild type strain, using this engineered strain in fed-batch process could be performed for FA accumulation without citric acid excretion (i) at a C/N rate ratio higher (within the range 47.6–58.8 Cmol Nmol<sup>-1</sup>) than the critical ratio determined for the WT strain (47.6 Cmol Nmol<sup>-1</sup>) allowing a higher productivity or (ii) at the WT critical C/N ratio of 47.6 Cmol Nmol<sup>-1</sup> with less sensitivity to slight fluctuations of the

feeding rates of nitrogen or carbon.

#### 4. Conclusions

Increasing the Glycerol Phosphate availability and its binding to fatty acids through over-expression of yLDGA2 and yLGPD1 led to a strong improvement of lipid content and yield of accumulation on glucose concomitantly to a reduction of the excretion of citric acid and an increase in the critical C/N ratio. It demonstrated an overall improvement of the lipid production performances of the engineering strain compared to the parent strain with an improvement of the robustness that could be beneficial to an industrial process.

#### Acknowledgments

Financial support for this study was provided by Agence Nationale de la Recherche (ANR) and Commissariat aux Investissements d'Avenir via the project ProBio3 "Biocatalytic production of lipidic bioproducts

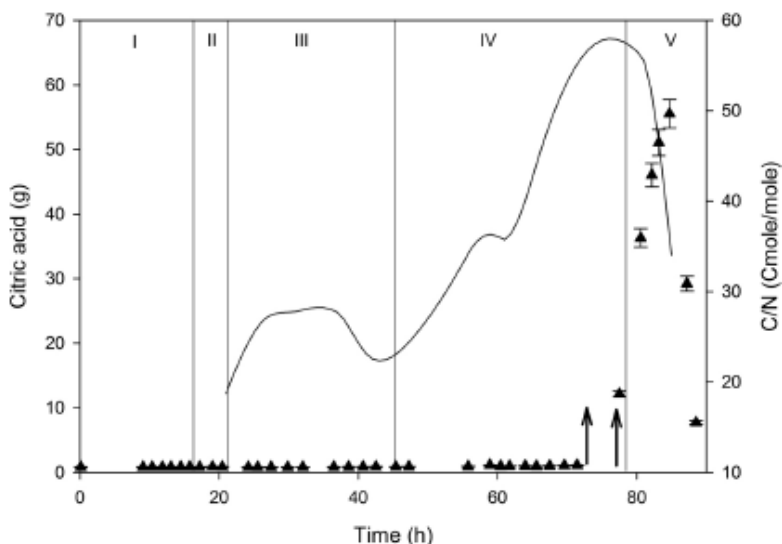


Fig. 3. Fed-batch cultivation of the strain JMY3501 on mineral medium on glucose. Evolution of the C/N ratio (line) and the mass of citric acid (▲) versus time. Arrows indicated the period of the citric acid excretion onset. Phases: (I) Unlimited growth phase, (II) Transition phase, (III) N- and C-limited phase, (IV) C/N increasing phase, (V) C/N decreasing phase. Data are presented as means  $\pm$  standard deviation.

from renewable resources and industrial by-products: BioJet Fuel Application" (ref. ANR-11-BTBT-0003). The authors have no conflict of interest to declare.

## References

- Anastasiadis, S., Aivasidis, A., Wandrey, C., 2002. Citric acid production by *Candida* strains under intracellular nitrogen limitation. *Appl. Microbiol. Biotechnol.* 60 (1–2), 81–87.
- Anastasiadis, S., Wandrey, C., Rehm, H.J., 2005. Continuous citric acid fermentation by *Candida oleophila* under nitrogen limitation at constant C/N ratio. *World J. Microbiol. Biotechnol.* 21 (5), 695–705.
- Bankar, A.V., Kumar, A.R., Zinjarde, S.S., 2009. Environmental and industrial applications of *Yarrowia lipolytica*. *Appl. Microbiol. Biotechnol.* 84 (5), 847–865.
- Bellou, S., Triantaphyllidou, L.E., Mizerakis, P., Aggelis, G., 2016. High lipid accumulation in *Yarrowia lipolytica* cultivated under double limitation of nitrogen and magnesium. *J. Biotechnol.* 234, 116–126.
- Beopoulos, A., Mroczka, Z., Theveniau, F., Le Dall, M.T., Hapala, I., Papanikolaou, S., Chardot, T., Nicaud, J.M., 2008. Control of lipid accumulation in the yeast *Yarrowia lipolytica*. *Appl. Environ. Microbiol.* 74, 7779–7789.
- Beopoulos, A., Cescut, J., Haddouche, R., Uribebarrena, J.L., Molina-Jouve, C., Nicaud, J.M., 2009. *Yarrowia lipolytica* as a model for bio-oil production. *Prog. Lipid Res.* 48 (6), 375–387.
- Beopoulos, A., Haddouche, R., Kabran, P., Dulermo, T., Chardot, T., Nicaud, J.M., 2012. Identification and characterization of DGA2, an acyltransferase of the DGAT1 acyl-CoA: diacylglycerol acyltransferase family in the oleaginous yeast *Yarrowia lipolytica*. New insights into the storage lipid metabolism of oleaginous yeasts. *Appl. Microbiol. Biotechnol.* 93, 1523–1537.
- Boulton, C.A., Ratledge, C., 1983. Use of transition studies in continuous cultures of *Lipomyces starkeyi*, an oleaginous yeast, to investigate the physiology of lipid accumulation. *Microbiology* 129 (9), 2871–2876.
- Browse, J., Warwick, N., Somerville, C.R., Slack, C.R., 1986. Fluxes through the prokaryotic and eukaryotic pathways of lipid-synthesis in the 16:3 plant *Arabidopsis-thaliana*. *Biochem. J.* 235 (1), 25–31.
- Cescut, J., Severac, E., Molina-Jouve, C., Uribebarrena, J.L., 2011. Optimizing pressurized liquid extraction of microbial lipids using the response surface method. *J. Chromatogr. A* 1218 (3), 373–379.
- Deak, T., 2001. Identification of yeasts isolated from poultry meat. *Acta Biol. Hung.* 52 (2–3), 195–200.
- Dulermo, T., Treton, B., Beopoulos, A., Kabran Gnanon, A.P., Haddouche, R., Nicaud, J.M., 2013. Characterization of the two intracellular lipases of *Y. lipolytica* encoded by TGL3 and TGL4 genes: new insights into the role of intracellular lipases and lipid body organization. *Biochim. Biophys. Acta* 1831, 1486–1495.
- Evans, C.T., Ratledge, C., 1983. A comparison of the oleaginous yeast, *Candida curvata*, grown on different carbon sources in continuous and batch culture. *Lipids* 18 (9), 623–629.
- Finogenova, T.V., Kamzolova, S.V., Shishkanova, N.V., Ilchenko, A.P., Dedyukhina, E.G., 1996. Influence of the specific growth rate and zinc ions on the synthesis of citric and isocitric acids and on the biomass composition of *Yarrowia lipolytica* N1 yeast. *Appl. Biochem. Microbiol.* 32 (1), 30–34.
- Fontanille, P., Kumar, V., Christophe, G., Nouaille, R., Larroche, C., 2012. Bioconversion of volatile fatty acids into lipids by the oleaginous yeast *Yarrowia lipolytica*. *Biores. Technol.* 114, 443–449.
- Gill, C.O., Hill, M.J., Ratledge, C., 1977. Lipid accumulation in an oleaginous yeast (*Candida* 107) growing on glucose in single-stage continuous culture. *Appl. Environ. Microbiol.* 33 (2), 231–239.
- Granger, L.M., Perlot, P., Goma, G., Pareilleux, A., 1993. Effect of various nutrient limitations on fatty-acid production by *Rhodotorula glutinis*. *Appl. Microbiol. Biotechnol.* 38 (6), 784–789.
- Haselbacher, M., Ivessa, A.S., Paltauf, F., Kohlwein, S.D., 1993. Acetyl-coA carboxylase from yeast is an essential enzyme and is regulated by factors that control phospholipid metabolism. *J. Biol. Chem.* 268 (15), 10946–10952.
- Holdsworth, J.E., Veenhuis, M., Ratledge, C., 1988. Enzyme-activities in oleaginous yeasts accumulating and utilizing exogenous or endogenous lipids. *J. Gen. Microbiol.* 134, 2907–2915.
- Ilchenko, A.P., Shishkanova, N.V., Chernyavskaya, O.G., Finogenova, T.V., 1998. Oxygen concentration as a factor controlling central metabolism and citric acid biosynthesis in the yeast *Yarrowia lipolytica* grown on ethanol. *Microbiology* 67 (3), 241–244.
- Kamzolova, S.V., Shishkanova, N.V., Morgunov, I.G., Finogenova, T.V., 2003. Oxygen requirements for growth and citric acid production of *Yarrowia lipolytica*. *FEMS Yeast Res.* 3 (2), 217–222.
- Lancioti, R., Gianotti, A., Baldi, D., Angrisani, R., Suzzi, G., Mastrocola, D., Guernoni, M.E., 2005. Use of *Yarrowia lipolytica* strains for the treatment of olive mill wastewater. *Biores. Technol.* 96 (3), 317–322.
- Lazar, Z., Dulermo, T., Neugebelle, C., Cruz-Le Coq, A.M., Nicaud, J.M., 2014. Hexokinase – a limiting factor in lipid production from fructose in *Yarrowia lipolytica*. *Metab. Eng.* 26, 89–99.
- Madzak, C., Beckerich, J.M., 2015. Heterologous protein expression and secretion in *Yarrowia lipolytica*. In: Barth, G. (Ed.), *Yarrowia Lipolytica*. Springer, Berlin Heidelberg 2013, pp. 1–76.
- Madzak, C., Gaillardin, C., Beckerich, J.M., 2004. Heterologous protein expression and secretion in the non-conventional yeast *Yarrowia lipolytica*: a review. *J. Biotechnol.* 109 (1–2), 63–81.
- Madzak, C., 2015. *Yarrowia lipolytica*: recent achievements in heterologous protein expression and pathway engineering. *Appl. Microbiol. Biotechnol.* 99, 4559–4577.
- Moeller, L., Strähle, B., Aurich, A., Zehndorf, A., Bley, T., 2007. Optimization of citric acid production from glucose by *Yarrowia lipolytica*. *Eng. Life Sci.* 7 (5), 504–511.
- Morin, N., Cescut, J., Beopoulos, A., Lelandais, G., Le Berre, V., Uribebarrena, J.L., Molina-Jouve, C., Nicaud, J.M., 2011. Transcriptomic analyses during the transition from biomass production to lipid accumulation in the oleaginous yeast *Yarrowia lipolytica*. *PLoS One* 6 (11), e27966.
- Nicaud, J.M., Madzak, C., van den Broek, P., Gysler, C., Duboc, P., Niederberger, P., Gaillardin, C., 2002. Protein expression and secretion in the yeast *Yarrowia lipolytica*. *FEMS Yeast Res.* 2 (3), 371–379.
- Ochoa-Bustier, A., Guillolet, S.E., 2014. D-stat culture for studying the metabolic shifts from oxidative metabolism to lipid accumulation and citric acid production in *Yarrowia lipolytica*. *J. Biotechnol.* 170, 35–41.
- Ochoa-Bustier, A., 2012. *Analyses systématique des bascules métaboliques chez les levures d'intérêt industriel: application aux bascules du métabolisme lipidique chez Yarrowia lipolytica*. Available: <http://www.theses.fr/2012ISAT0056> Accessed June 29 2012. PhD Thesis. University of Toulouse, France.
- Papanikolaou, S., Aggelis, G., 2002. Lipid production by *Yarrowia lipolytica* growing on industrial glycerol in a single-stage continuous culture. *Biores. Technol.* 82 (1), 43–49.
- Papanikolaou, S., Aggelis, G., 2011. Lipids of oleaginous yeasts. Part II: technology and potential applications. *Eur. J. Lipid Sci. Technol.* 113, 1052–1073.
- Papanikolaou, S., Muniña, L., Chevalot, L., Aggelis, G., Marc, I., 2002. *Yarrowia lipolytica* as a potential producer of citric acid from raw glycerol. *J. Appl. Microbiol.* 92 (4), 737–744.
- Papanikolaou, S., Muniña, L., Chevalot, L., Aggelis, G., Marc, I., 2003. Accumulation of a coxa-butter-like lipid by *Yarrowia lipolytica* cultivated on agro-industrial residues. *Curr. Microbiol.* 46 (2), 124–130.
- Papanikolaou, S., Gallotou-Panayotou, M., Chevalot, L., Komaitis, M., Marc, I., Aggelis, G., 2006. Influence of glucose and saturated free-fatty acid mixtures on citric acid and lipid production by *Yarrowia lipolytica*. *Curr. Microbiol.* 52 (2), 134–142.
- Poilpre, E., Tronquit, D., Goma, G., Guillolet, V., 2002. On-line estimation of biomass concentration during transient growth on yeast chemostat culture using light reflectance. *Biotechnol. Lett.* 24, 2075–2081.
- Ratledge, C., Wynn, J.P., 2002. The biochemistry and molecular biology of lipid accumulation in oleaginous microorganisms. *Adv. Appl. Microbiol.* 51, 1–51.
- Rattray, J.B.M., Schibed, A., Kidby, D.K., 1975. Lipids of yeasts. *Bacteriol. Rev.* 39 (3), 197–231.
- Rymowicz, W., Rywinska, A., Zarowska, B., 2007. Biosynthesis of citric acid from crude glycerol by *Yarrowia lipolytica* in repeated-batch cultivations. *J. Biotechnol.* 131 (2), 149–150.
- Sattur, A.P., Karanth, N.G., 1989. Production of microbial lipids. 3. Influence of c/n ratio – experimental observations. *Biotechnol. Bioeng.* 34 (6), 872–874.
- Singhla, M., Lancioti, R., Guernoni, M.E., 1994. Biochemical and physiological characteristics of *Yarrowia lipolytica* strains in relation to isolation source. *Can. J. Microbiol.* 40 (1), 54–59.
- Tai, M., Stephanopoulos, G., 2012. Engineering the push and pull of lipid biosynthesis in oleaginous yeast *Yarrowia lipolytica* for biofuel production. *Metab. Eng.* 15, 1–9.
- Waite, M., Wakil, S.J., 1962. Studies on mechanism of fatty acid synthesis. 12. acetyl coenzyme A carboxylase. *J. Biol. Chem.* 237 (9), 2750–2757.
- Yalcin, H.T., Ucar, F.B., 2009. Isolation and characterization of cheese spoiler yeast isolated from Turkish white cheeses. *Ann. Microbiol.* 59 (3), 477–483.
- Zhang, Y., Adams, I.P., Ratledge, C., 2007. Malic enzyme: the controlling activity for lipid production? Over-expression of malic enzyme in *Mucor circinelloides* leads to a 2.5-fold increase in lipid accumulation. *Microbiology* 153, 2013–2025.

## ANNEX-2. RESUME EN FRANÇAIS

---

### CONTENTS

RESUME .....	157
INTRODUCTION.....	157
CHAPITRE 1 - SYNTHÈSE BIBLIOGRAPHIQUE.....	157
CHAPITRE 2 - FICHES TECHNIQUES ET STRATÉGIE EXPERIMENTALE .....	159
2.1. Microorganisme, milieux et conditions de croissance .....	159
2.2. Produits chimiques utilisés .....	160
2.3. Culture Fed-batch en bioréacteur.....	160
2.3.1. Culture Fed-batch dans des conditions appauvries en N.....	161
2.3.2. Culture Fed-batch dans des conditions de limitation N.....	161
2.4. Analyse des gaz d'échappement .....	161
2.5. Détermination de la biomasse .....	162
2.6. Analyse des métabolites.....	162
2.7. Évaluations de la viabilité cellulaire et de la morphologie cellulaire par cytomètre en flux.....	162
CHAPITRE 3 - RESULTATS ET DISCUSSIONS .....	164
CHAPITRE 4 - CONCLUSION ET PERSPECTIVES .....	166

## RESUME

Ces travaux de recherche se focalisent sur l'amélioration du contenu lipidique et la modification du profil des acides gras d'une levure oléagineuse *Yarrowia lipolytica* selon des approches d'ingénierie biochimique et métabolique. La stratégie expérimentale est basée sur la modulation des flux de carbone en amont et en aval de la voie de synthèse des acides gras, et examine les réponses de la levure *Y. lipolytica* à ces modulations en termes d'accumulation de lipides, de profil des acides gras, et de formation d'acide citrique.

Les résultats ont montré que le métabolisme des lipides et la formation de produits de la souche *Y. lipolytica* JMY3501 peuvent être altérés de manière significative en ciblant l'activité de l'enzyme FAS : lors des ajouts séquencés de composés inhibiteurs, le profil des acides gras a été modifié et l'accumulation d'acides gras à chaîne courte et moyenne a été favorisée sans affecter la survie cellulaire.

Enfin, la souche mutante de *Y. lipolytica* CR62 présentant une mutation sur le domaine KS de FAS a permis l'obtention d'une amélioration significative de la production d'acides gras de longueur de chaîne moyenne. Ce travail de recherche a démontré que la levure oléagineuse *Y. lipolytica* offre de nouvelles opportunités pour la production d'acides gras spécifiques lorsque les ingénieries biochimique et métabolique se combinent.

## INTRODUCTION

Ces travaux se sont concentrés sur l'étude du métabolisme lipidique de *Y. lipolytica* visant à déterminer si la dynamique des flux métaboliques de carbone vers le haut et vers le bas de la voie de synthèse des acides gras contrôle le déplacement métabolique du métabolisme lipidique et dans quelle mesure l'accumulation de lipides, la composition en acides gras et la formation d'acide citrique sont affectées.

Pour atteindre cet objectif, la stratégie est développée pour la modulation d'enzymes spécifiques impliquées dans le métabolisme lipidique en utilisant des inhibiteurs spécifiques à concentration modérée. L'idée derrière cette stratégie est d'identifier quelles sont les cibles génétiques ou les enzymes clés qui devraient être ciblées afin de construire une souche mutante conduisant potentiellement à l'accumulation d'acides gras à chaîne courte.

À cet égard, ce document a été organisé de la manière suivante.

Le premier chapitre consacré au métabolisme lipidique de la levure oléagineuse *Y. lipolytica* s'intéresse particulièrement à la voie de synthèse des acides gras de novo.

Le deuxième chapitre décrit les souches et les conditions de croissance, la conception de la culture et la stratégie des expériences, et détaille les instruments analytiques et les logiciels utilisés dans cette thèse.

Dans le troisième chapitre, les résultats sont rapportés dans des sections basées sur la stratégie de criblage des molécules inhibitrices, la caractérisation des souches de *Y. lipolytica* et les investigations des deux molécules inhibitrices impactant le métabolisme lipidique et la physiologie de cette levure.

Enfin, le dernier chapitre tire une conclusion à partir des résultats obtenus et propose des études de suivi potentielles.

## CHAPITRE 1 - SYNTHÈSE BIBLIOGRAPHIQUE

Les graisses (solides à température ambiante) et les huiles (liquides à température ambiante) sont principalement constituées de triacylglycérol qui se compose de trois acides gras à longue chaîne estérifiés en molécule de glycérol. Les acides gras et leurs dérivés sont des molécules qui présentent un intérêt majeur dans de nombreux secteurs industriels tels que l'agroalimentaire, la pharmacie, l'oléochimie et les biocarburants. Outre

l'origine animale et végétale de ces molécules (Metzger et Bomscheuer, 2006), la production microbienne a été au centre des efforts de recherche actuels dans le secteur universitaire et privé, en raison de la demande croissante des marchés sur des produits à faible coût, respectueux de l'environnement, durables, à savoir des alternatives de qualité.

La production de graisses et d'huiles avec des microorganismes pour des applications industrielles et nutritionnelles présente plusieurs avantages par rapport à la production mécanique et chimique à partir de sources comestibles et non comestibles telles que le palme, le soja, la noix physique, le ricin, le colza etc. Ils ne sont pas compétitifs avec les aliments, nécessitent une surface de production beaucoup plus petite, sont faciles à mettre à l'échelle et sont également indépendants des conditions saisonnières et climatiques (Sawangkeaw et Ngamprasertsith, 2013; Thevenieau et Nicaud, 2013).

Il a été rapporté par C. Ratledge (Ratledge, 2004) que la capacité d'un organisme à accumuler une quantité significative de lipides, c'est-à-dire la raison du caractère oléagineux, est basée sur :

- (i) La capacité à produire un apport continu d'acétyl-CoA directement dans le cytosol de la cellule en tant que précurseur nécessaire de l'acide gras synthase (FAS),
- (ii) La capacité à produire une quantité suffisante de NADPH en tant que cofacteur réduit essentiel utilisé dans la biosynthèse des acides gras.

La majorité de ces lipides sont généralement des triacylglycérols (TAG) et des esters de stérols (SE). Selon les espèces de levures, le mode de culture ainsi que les conditions environnementales influencent la teneur en lipides.

Une nomenclature simplifiée de ces composés de lipides définie par leur nombre total d'atomes de carbone et le nombre d'éventuelles doubles liaisons. Par exemple, la notation C16:0 désigne un 16 atomes de carbone sans aucune double liaison, alors que C18:2 signifie qu'il y a deux doubles liaisons. Les acides gras pourraient être classés en fonction de leur longueur de chaîne carbonée, comme :

- ◆ Acides gras à chaîne courte (SCFA): contiennent moins de 12 atomes de carbone tels que C8:0 et C10:0,
- ◆ Acides gras à chaîne moyenne (MCFA): contiennent moins de 16 atomes de carbone tels que C12:0 et C14:0,
- ◆ Acides gras à longue chaîne (LCFA): contiennent 16 ou 18 atomes de carbone tels que C16:1, C18:0 et C18:2,
- ◆ Acides gras à très longue chaîne (VLCFA): contiennent plus de 18 atomes de carbone tels que C20:0 et C24:0

*Yarrowia lipolytica*, avec des caractéristiques physiologiques spéciales et l'acceptation de son statut généralement reconnu comme sûr, est un excellent exemple de micro-organisme aux multiples applications biotechnologiques (Bankar et al., 2009; Gonçalves et al., 2013; Harzevili, 2014; Liu et al., 2015).

De plus, grâce au développement de divers outils moléculaires et génétiques (Barth et Gaillardin, 1997; Madzak, 2018), *Y. lipolytica* est reconnu comme un organisme modèle pour de nombreuses études académiques telles que la dégradation des hydrocarbures (Fickers et al., 2005a; Thevenieau et al., 2007), la sécrétion de protéines (protéases, lipases) (Fickers et al., 2011; Madzak, 2015; Madzak C., 2013; Vandermies et Fickers, 2019), la sécrétion d'acides organiques (isocitriques,  $\alpha$ -cétoglutarique, acide citrique) (Moeller et al., 2007; Papanikolaou et al., 2002), et la réponse au stress et dimorphisme (Morales-Vargas et al., 2012; Ruiz-Herrera et Sentandreu, 2002; Shi et al., 2017; Timoumi et al., 2018).

En outre, *Y. lipolytica* est considéré comme un hôte avantageux pour le développement de plates-formes de production de produits chimiques à base de lipides en raison de sa capacité à synthétiser et accumuler des lipides à plus de 20% de son poids de cellules sèches (Beopoulos et al., 2009a; Carsanba et al., 2018; Xie, 2017).

Les efforts de recherche sont présentés pour améliorer la production de lipides des levures oléagineuses, y compris les surexpressions génétiques et les suppressions d'enzymes clés qui entraînent le flux de carbone du métabolisme central du carbone vers la synthèse des acides gras. L'accumulation de lipides dans un microorganisme oléagineux comme *Y. lipolytica* sur le glucose commence lorsqu'un nutriment minéral devient limitant dans le milieu de culture avec un excès de carbone. De plus, pour la synthèse d'acides gras, un complexe enzymatique essentiel, l'acide gras synthase (FAS), et ses inhibiteurs connus de ce système enzymatique, sont passés en revue.

Chez les levures oléagineuses, le FAS est un membre de la famille FAS de type I. La levure à structure en forme de tonneau FAS contient six copies de huit domaines fonctionnels indépendants avec une séquence de AT-ER-DH-MPT / ACP-KR-KS-PPT dans un  $\alpha 6\beta 6$  complexe dodécamère de 2,6 MDa (Tehlivets et al., 2007).

Des inhibiteurs de ces enzymes clés ont été identifiés et des travaux antérieurs ont étudié leur impact sur l'activité enzymatique, sur le métabolisme des lipides et sur la teneur et la composition en acides gras ; leur influence pour cibler le domaine spécifique du système enzymatique des acides gras (FAS), spécifiquement utilisé en sciences médicales, semble être très intéressante au regard des objectifs des présents travaux de recherche. La structure moléculaire du système enzymatique de l'acide gras synthase (FAS) est diversifiée parmi les systèmes biologiques ; cependant, le mécanisme de réaction enzymatique du FAS est conservé pour toutes les cellules eucaryotes et c'est la seule voie de novo pour la synthèse des acides gras.

Par conséquent, nous avons émis l'hypothèse que si l'utilisation d'inhibiteurs sur ce système enzymatique cytosolique essentiel conduisait à la libération d'acides gras avant la synthèse complète des acides gras en C16 ou C18 à partir de l'acétyl-CoA, cela mènerait à produire des acides gras de longueur de chaîne plus courte. Trois molécules inhibitrices, la cérolénine, le triclosan et l'orlistat, ont donc été sélectionnées pour être étudiées afin de cibler différents domaines catalytiques du système enzymatique FAS visant à modifier la synthèse des acides gras pour la levure oléagineuse *Y. lipolytica*.

## CHAPITRE 2 - FICHES TECHNIQUES ET STRATEGIE EXPERIMENTALE

La stratégie expérimentale est développée sur la base de la modulation dirigée des flux de carbone vers le haut et vers le bas de la voie de synthèse de l'AF grâce à des approches d'ingénierie biochimique et d'ingénierie métabolique.

### 2.1. Microorganisme, milieux et conditions de croissance

La souche utilisée dans cette étude était *Y. lipolytica* JMY3501 obtenue par le Laboratoire Microbiologie et Génétique Moléculaire, INRA, (Paris-Grignon., France) dans le cadre du projet commun "ProBio3". Son génotype était le suivant :

MA Ta ura3-302 leu2-270 xpr2-322  $\Delta$ tg14  $\Delta$ pox1-6 + LEU2ex Tef-yIDGA2 + URA3ex Tef-GPD1 (Lazar et al., 2014).

La souche a été maintenue sur un milieu d'agar YPD / glucose contenant 10 gL<sup>-1</sup> d'extrait de levure, 20 gL<sup>-1</sup> de bactopeptone, 20 gL<sup>-1</sup> de glucose et 20 gL<sup>-1</sup> de gélose. Les plaques ont été conservées à 4 ° C. Pour la

préparation de stocks de glycérol (pour la cryoconservation des cellules), du glycérol stérile pur a été ajouté au bouillon de culture pour atteindre une concentration finale de glycérol de 30% (v / v). Cette suspension cellulaire (stocks de glycérol) a ensuite été stockée à -80 ° C.

Des pré-cultivations ont été effectuées sur un tube de 5 ml de milieu YPD à 28 ° C pendant 16 h à 100 rp. La culture en phase de croissance a été transférée dans un Erlenmeyer de 1 L contenant 170 ml de milieu minéral à pH 5,6, préparé comme suit (tous les composés sont exprimés en g<sup>-1</sup>): (NH<sub>4</sub>)<sub>2</sub>SO<sub>4</sub> 3,5; KH<sub>2</sub>PO<sub>4</sub>, 6; MgSO<sub>4</sub>, 2; EDTA, 0,0375; ZnSO<sub>4</sub>·7H<sub>2</sub>O, 0,0281; MnCl<sub>2</sub>·4H<sub>2</sub>O, 0,0025; CoCl<sub>2</sub>·6H<sub>2</sub>O, 0,00075; CuSO<sub>4</sub>·5H<sub>2</sub>O, 0,00075; Na<sub>2</sub>MoSO<sub>4</sub>·2H<sub>2</sub>O, 0,00005; CaCl<sub>2</sub>·2H<sub>2</sub>O, 0,0125; FeSO<sub>4</sub>·7H<sub>2</sub>O, 0,00875; H<sub>3</sub>BO<sub>3</sub>, 0,0025; D-biotine, 0,00025; Acide D-L-panthoténique, 0,001; acide nicotinique, 0,001; myo-inositol, 0,00625; thiamine, 0,001; pyridoxine, 0,001; acide para-aminobenzoïque, 0,0002. Du glucose a été ajouté à une concentration finale de 18 g de L<sup>-1</sup> avec du chloramphénicol à 10 mg de L<sup>-1</sup>. Après 16 h de croissance à 28 ° C et 100 rpm, 170 ml du bouillon ont été utilisés pour ensemencer 1,7 L du même milieu minéral dans un bioréacteur de 3 L.

## 2.2. Produits chimiques utilisés

Les produits chimiques glucose, sels, oligo-éléments (Carlo Erba), EDTA (Qbiogène), et acide orthophosphérique ont été fournis par VWR, les vitamines par Sigma. Tous les produits avaient la plus haute qualité analytique disponible.

## 2.3. Culture Fed-batch en bioréacteur.

Des expériences Fed-batch ont été réalisées dans un bioréacteur à cuve agitée de 5 L avec un volume de travail de 3 L en utilisant le Biostat B-DCU. Braun Biotech International (Sartorius AG, Allemagne) avec le logiciel d'acquisition MFCS / win 2.0.

La température a été contrôlée à 28 ° C avec une chemise d'eau. Le pH a été maintenu constant à 5,6 avec les ajouts automatiques de solutions acide / base et surveillé par une sonde de pH (Mettler-Toledo International Inc.). La pression relative dans le bioréacteur a été maintenue à 300 mbar. La formation de mousse a été empêchée par l'ajout d'un agent antimousse de polypropylène glycol (PPG). Afin d'éviter la limitation de l'oxygène, le bioréacteur a été rincé à l'air et agité avec des turbines Rushton pour maintenir l'oxygène dissous au-dessus de 20% de la saturation et mesuré avec une sonde autoclavable (InPro 6000 / Optical O<sub>2</sub> sensor Mettler-Toledo International Inc.). L'air d'entrée et de sortie a été passé à travers un filtre à membrane en polyamide stérile de 0,2 µm et la composition du gaz d'entrée et de sortie a été analysée avec un spectromètre de masse.

Les cultures alimentées en lots ont été nourries en solutions d'alimentation stériles (glucose, ammoniacale, solutions acide / base) via des pompes péristaltiques pré-étalonnées (Watson-Marlow). La concentration de la solution d'alimentation en glucose a été déterminée précisément à partir de la densité de la solution (DE40 Density Meter Mettler-Toledo International Inc.). Les débits massiques de toutes les solutions d'alimentation fournies au bioréacteur pendant la durée de l'expérience ont été déterminés en ligne avec une précision de 0,1 à 0,01 gramme à l'aide de balances numériques (Sartorius AG) et les données générées ont été obtenues via le logiciel d'acquisition de données Lab VIEW (International Instruments Cor.).

Les cultures Fed-batch ont été appliquées suivant deux procédures différentes en fonction de l'objectif de l'évaluation de la souche : une procédure sous appauvrissement en azote et une procédure sous limitation en azote.

### 2.3.1. Culture Fed-batch dans des conditions appauvries en N

La culture fed-batch a été divisée en deux phases :

Phase de lot de croissance : Après l'inoculation du bioréacteur, une phase de lot a été appliquée sous limitation non nutritionnelle limitée. Les concentrations de glucose et de sulfate d'ammonium ont été fixées à  $100 \text{ gL}^{-1}$  et  $5 \text{ gL}^{-1}$ , respectivement. La concentration d'azote a été calculée afin de produire jusqu'à  $15 \text{ gL}^{-1}$  de biomasse avant d'atteindre des conditions limitées en N. Le pH a été régulé avec une solution de KOH 9 M.

Phase appauvrie en N : La phase de croissance est passée naturellement à la phase de production appauvrie en N lorsque l'ammonium a été complètement épuisé. Le glucose a été alimenté par impulsions d'une solution de glucose stérile  $750 \text{ gL}^{-1}$  lorsque la concentration résiduelle de glucose a atteint  $20 \text{ gL}^{-1}$  dans le bioréacteur. Une impulsion a été appliquée afin de ramener la concentration résiduelle de glucose à  $100 \text{ gL}^{-1}$ .

### 2.3.2. Culture Fed-batch dans des conditions de limitation N

La culture fed-batch a été divisée en cinq phases selon une stratégie d'alimentation.

Phase de croissance : Après l'inoculation du bioréacteur, une solution de glucose stérile à une concentration de  $200 \text{ gL}^{-1}$  a été alimentée de manière exponentielle avec une pompe péristaltique pour maintenir constant le taux de croissance spécifique à  $0,18 \text{ h}^{-1}$ . La source d'azote a été fournie par une solution d'ammoniaque stérile 2,5 M qui a également été utilisée pour la régulation du pH.

Phase de transition : lorsque la concentration de la biomasse a atteint environ  $10 \text{ gL}^{-1}$ , la solution correcteur de pH a été remplacée par une solution stérile d'hydroxyde de potassium 2,5 M (KOH).

Phase limitée en N : lorsque la source d'azote a été épuisée dans le milieu de culture, une solution d'ammoniac stérile 0,3 M a été introduite de manière exponentielle dans le réacteur avec une pompe péristaltique afin de maintenir un taux de croissance résiduel constant à  $0,04 \text{ h}^{-1}$ . Parallèlement, le profil d'alimentation du glucose a été modifié afin de maintenir un rapport molaire N / C constant supérieur à  $0,03 \text{ Nmol.Cmol}^{-1}$  afin d'induire une accumulation de lipides sans sécrétion d'acide citrique comme démontré dans Ochoa-Estopier et Guillouet, 2014.

Phase de diminution du N / C : Après 24 heures sous la phase limitée en N, la vitesse d'alimentation en glucose a été accélérée sans changer le profil d'alimentation en ammoniac. Par conséquent, la condition limitée en N et le taux de croissance spécifique constant ont été maintenus, mais le N / C a été progressivement diminué.

Phase d'augmentation de N / C : Une fois l'acide citrique détecté dans le bouillon de fermentation et le rapport N / C critique déterminé, la stratégie d'alimentation a été inversée. Le taux d'alimentation en glucose a été ralenti sans modifier le profil d'alimentation en ammoniac. Par conséquent, le N / C a été progressivement augmenté sans modifier le taux de croissance spécifique.

## 2.4. Analyse des gaz d'échappement

La composition des gaz d'entrée et de sortie en dioxyde de carbone ( $\text{CO}_2$ ) et en oxygène ( $\text{O}_2$ ) a été mesurée par un système de surveillance des gaz de fermentation (LumaSense technologies Europe). Le système combine un échantillonneur multipoint 1309 avec un analyseur de gaz (INNOVA 1313). L'analyse des gaz a été effectuée toutes les minutes pendant toute l'expérience. Le taux de production de  $\text{CO}_2$  ( $r\text{CO}_2$ ) et le taux de consommation d' $\text{O}_2$  ( $r\text{O}_2$ ) ont été calculés comme décrit par Poilpre et al., 2002. Le quotient respiratoire (QR) a été calculé comme le rapport molaire entre  $r\text{CO}_2$  et  $r\text{O}_2$ .

## 2.5. Détermination de la biomasse

La croissance des levures a été évaluée par des mesures spectrophotométriques à 620 nm dans un spectrophotomètre (Biochrom Libra S4, Royaume-Uni). Les taux de croissance ont été déterminés sur la base de l'évolution dans le temps de la densité optique (OD 620 nm). Le OD 620 nm a été étalonné par rapport aux mesures du poids des cellules sèches. La formule de la biomasse utilisée pour convertir le poids sec des cellules en concentration molaire de carbone était  $\text{CH}_{1,744}\text{O}_{0,451}\text{N}_{0,132}$  pour un poids moléculaire de 24,67 g  $\text{Cmol}^{-1}$  (Ochoa-Estopier et Guillouet, 2014).

## 2.6. Analyse des métabolites

Les surnageants de culture ont été analysés par chromatographie liquide haute performance (DIONEX Ultimate 3000, USA) en utilisant une colonne Aminex HPX-87H<sup>+</sup> (Bio-Rad, US) et les conditions suivantes : une température de 50 ° C avec 5 mM H<sub>2</sub>SO<sub>4</sub> comme éluant (débit de 0,5 ml min<sup>-1</sup>) et une double détection (IR et UV à 210 nm). Le surnageant de culture a été obtenu par centrifugation (MiniSpin Eppendorf, USA) de la culture de fermentation dans des tubes Eppendorf à 13 000 tr / min pendant 3 min. Le surnageant a été filtré sur des filtres Minisart sur des membranes en polyamide de diamètre de pores de 0,45 µm (Sartorius AG, Allemagne). Les métabolites recherchés pour les détections et la quantification étaient le glucose, le citrate, l'isocitrate, l'alpha-cétoglutarate, le pyruvate, le malate, le succinate, le fumarate, le lactate et l'acétate.

La quantification des lipides a été réalisée par digestion comme décrit par Browse et al., 1986. 20 mg de cellules lyophilisées ont été ajoutés à 1 ml de solution méthanolique contenant 25 mL<sup>-1</sup> d'acide sulfurique (95 %) et étalon interne (C9:0). Le mélange dans des tubes scellés a été placé dans un lot à 80 ° C pendant 90 minutes. Après refroidissement, 450 µl d'hexane et 1,5 ml d'eau ont été ajoutés et vortexés. La phase lipidique a ensuite été prélevée et la composition a été analysée par chromatographie en phase gazeuse comme mentionné dans Cescut et al., 2011. La quantification des lipides a également été réalisée par épifluorescence après coloration des cellules avec Bodipy 493/503 dans un lecteur de microplaques (Synergy HT, Biotek, USA) comme suit: les culots ont été lavés 3 fois avec une solution tampon PBS (dans gL<sup>-1</sup>, NaCl, 8; Na<sub>2</sub>HPO<sub>4</sub>, 1,15; KCl, 0,2; KH<sub>2</sub>PO<sub>4</sub>, 0,2; pH à 6,9-7,1) à 4 ° C, et remis en suspension dans la même solution tampon à une DO620 nm de 0,5. 1 ml de la suspension cellulaire a été mélangé avec 10 µl de Bodipy 493/503 (100 µg.ml<sup>-1</sup> dans du DMSO) et incubé 5 min à 4 °. Le mélange a ensuite été centrifugé 3 min à 13 000 tr / min et remis en suspension dans 1 ml de solution tampon PBS. 200 µl de cette suspension cellulaire ont été placés dans une microplaque de surface Nuclon™ A à 96 puits et lus à 528 nm avec une valeur de longueur d'onde d'excitation de 428 nm. Les mesures ont été répétées 5 fois montrant un écart type inférieur à 5 %.

La quantification de l'ammonium résiduel dans le milieu a été déterminée avec une sonde Orion ammonium (ORION Research Inc., Boston, USA) et un voltmètre (ORION pH / ISE Meter, USA) comme suit: 5 ml de bouillon de culture ont été filtrés sur une membrane de polyamide de diamètre de pore 0,45 µm (Sartorius AG, Allemagne) et mélangé avec 200 µl de solution tampon ISA (Ionic Strength Adjustor: NaOH, 5 molL<sup>-1</sup>; disodium EDTA, 0,05 molL<sup>-1</sup> and methanol 1 gL<sup>-1</sup>). La concentration de NH<sub>4</sub> a été déterminée avec une courbe d'étalonnage corrélant la concentration en mV et NH<sub>4</sub> dans une gamme de 10<sup>-1</sup>-10<sup>-4</sup> molL<sup>-1</sup> NH<sub>4</sub>Cl.

## 2.7. Évaluations de la viabilité cellulaire et de la morphologie cellulaire par cytomètre en flux

La cytométrie en flux permet une analyse rapide de plusieurs caractéristiques au niveau d'une seule cellule. Les caractéristiques qui peuvent être mesurées par cytométrie en flux comprennent la forme et la taille des

cellules, et la complexité cytoplasmique, et, par un marquage avec un fluorochrome approprié, les propriétés physiologiques des cellules telles que l'activité métabolique, l'intégrité de la membrane et la viabilité cellulaire peuvent être évaluées. Le cytomètre en flux est composé de trois parties principales : la fluidique, l'optique et les systèmes électroniques. Le système fluidique du cytomètre en flux délivre une seule cellule dans un flux de fluide au faisceau laser pour interrogation. Par l'effet de la focalisation hydrodynamique, lorsqu'une seule cellule traverse le faisceau laser, le système de détection optique recueille la lumière diffusée et la fluorescence émise. La lumière diffusée et l'intensité de fluorescence obtenues par le système optique sont converties en signaux de tension par un système électronique. Les signaux de tension peuvent en outre être analysés en fonction du temps pour la caractérisation morphologique des cellules, y compris la taille et la granularité des cellules dans deux directions de signal. Le signal de diffusion vers l'avant (FSC) correspond à la quantité de lumière diffusée dans la direction vers l'avant avec un petit angle ( $0^\circ \pm 13$ ) qui est proportionnel à la taille de la cellule (forme de la cellule). Le signal de diffusion latérale (SSC) correspond à la lumière collectée à un grand angle ( $90^\circ \pm 13$ ) qui est proportionnel à la granularité de la cellule. La durée des signaux (temps de vol) générés par le FSC peut également être corrélée à la largeur de la cellule (longueur). L'analyse par cytométrie en flux a été réalisée sur un BD Accuri™ C6 (BD Biosciences) équipé de doubles excitations laser ; 488 nm à 20 mW et 640 nm 14,7 mW. Deux filtres optiques standards ont été utilisés pour détecter l'émission de fluorescence : FL1 (530/30 nm  $\pm$  15) pour une émission de lumière verte à 517 nm, et FL4 ( $> 670$  nm) pour une émission de lumière rouge à 660 nm. Un débit lent ( $14 \mu\text{l} \cdot \text{min}^{-1}$ ) a été appliqué pour effectuer l'analyse avec de l'eau MiliQ comme fluide de gaine avec une taille de noyau de 10  $\mu\text{m}$ . Le volume de l'échantillon a été réglé à 20  $\mu\text{l}$  et analysé pour 1000 cellules  $\cdot \mu\text{l}^{-1}$ . La valeur seuil a été définie à 80000 sur FSC pour éliminer les débris et les événements de bruit de fond. Le kit d'étalonnage de taille de cytométrie en flux (F-13838; Molecular probes, Inc.) a été utilisé selon les instructions du fabricant pour optimiser les signaux FSC en fonction de la taille des cellules. Des échantillons de données ont été générés en utilisant CFlow® (Accuri Cytomètres, Inc.) et une analyse supplémentaire des données a été réalisée avec les logiciels FlowJo (Tree Star, Inc.) et Sigma Plot (Systat Software Inc.).

Les échantillons de culture ont été collectés pendant le temps expérimental et centrifugés à 12 000 g pendant 4 min à  $4^\circ \text{C}$  pour culotter les cellules. Les culots de cellules récoltées ont été lavés deux fois dans une solution tampon McIlvain (McIlvaine, 1921) à pH 4 pour éliminer les traces de composants du milieu interférant de la suspension de levure et centrifugés à 12 000 g pendant 4 min. et à  $4^\circ \text{C}$  et remis en suspension dans 1 ml de solution tampon. La solution tampon McIlvain a été préparée en mélangeant de l'acide citrique 100 mM ( $\text{C}_6\text{H}_8\text{O}_7$ ,  $\text{H}_2\text{O}$ ) et du phosphate disodique 200 mM ( $\text{Na}_2\text{HPO}_4$ ,  $12\text{H}_2\text{O}$ ) et stockée à  $4^\circ \text{C}$  après stérilisation avec un filtre à membrane de 0,2  $\mu\text{m}$ . Une dilution en série a été appliquée avec une solution tampon pour atteindre une suspension cellulaire relative de  $10^6$  cellules  $\cdot \text{ml}^{-1}$ . D'autres suspensions de cellules diluées ont été préparées pour des échantillons témoins non traités, traités thermiquement et colorés par fluorescence. Deux colorants de fluorescence ont été utilisés pour les évaluations de la viabilité cellulaire par double protocole de coloration basé sur Monthéard et al., (2012). Le 5-cFDA, AM (5-Carboxyfluorescein diacetate, Acetoxymethyl ester) (Molecular probes, Inc.) est un substrat fluorogène estérifié perméable à la membrane qui, une fois à l'intérieur de la cellule, subit une hydrolyse des groupes diacétate en carboxyfluoresceine fluorescente par des estérases intracellulaires non spécifiques qui indiquent l'activité et l'intégrité de la membrane cellulaire des cellules de levure. Sytox® Red Dead Stain (Molecular probes, Inc.) est un colorant d'acide nucléique de haute affinité qui pénètre facilement dans les cellules dont les membranes plasmiques sont endommagées mais ne traversera pas les

membranes cellulaires intactes. Une solution mère de cFDA a été préparée en dissolvant 5 mg de cFDA dans 500 µl de diméthylsulfoxyde (DMSO) et 1 ml de réactif Pluronic® F-127 (solution à 20% (p / v) dans du DMSO anhydre) (Molecular probes, Inc.) et conservé dans l'obscurité à température ambiante. La concentration finale de colorants dans 10<sup>6</sup> cellules.ml<sup>-1</sup> de suspension cellulaire était de 3,3 µg.ml<sup>-1</sup> et 5 µM pour cFDA et Sytox, respectivement. Les suspensions cellulaires colorées incubées dans l'obscurité pendant 10 minutes à 37 °C et après le temps d'incubation, les échantillons ont été vortexés vigoureusement pendant 5 à 10 secondes et immédiatement analysés par cytomètre en flux. En tant que témoin à 100 % de cellules mortes, un échantillon de culture a été collecté et soumis à un choc thermique pendant 20 minutes à 70 °C. Après incubation, les cellules récoltées ont été lavées deux fois dans du tampon McIlvain et mises en culot à 12 000 g pendant 4 min. Les culots cellulaires ont été remis en suspension dans une solution tampon et encore dilués pour obtenir 10<sup>6</sup> cellules.ml<sup>-1</sup>. La suspension cellulaire a été colorée deux fois avec du cFDA et du Sytox® Red et réincubée dans l'obscurité pendant 10 minutes à 37 °C. Après le temps d'incubation, l'échantillon analysé dans un cytomètre en flux.

### CHAPITRE 3 - RESULTATS ET DISCUSSIONS

L'allongement itératif des chaînes d'acides gras à travers le cycle de réaction du FAS a été concentré pour contrôler trois domaines catalytiques différents :

- (i) lors de l'étape de condensation par la cétoacyl synthase (KS) avec la molécule inhibitrice Céruléine,
- (ii) lors de la deuxième étape de réduction par l'énoyl réductase (ER) avec la molécule inhibitrice Triclosan,
- (iii) sur l'étape de terminaison avec la molécule inhibitrice Orlistat.

L'idée était d'utiliser peu de ces inhibiteurs sans affecter la viabilité cellulaire de la levure *Y. lipolytica* afin d'identifier les réactions enzymatiques au sein de la voie de biosynthèse des FA qui contrôlent l'allongement des acides gras et la longueur de la chaîne carbonée.

Des cultures préliminaires ont été réalisées en laboratoire dans un flacon agité avec la souche de type sauvage *Y. lipolytica* W29 pour élucider l'influence de différents agents de dissolution des médicaments inhibiteurs sur la dynamique du métabolisme lipidique de *Y. lipolytica*; l'éthanol a été identifié comme le meilleur solvant pour d'autres expériences concernant l'influence des inhibiteurs sur l'accumulation des lipides et sur la synthèse des acides gras. Nous avons d'abord caractérisé la modulation du passage métabolique du métabolisme oxydatif à l'accumulation de lipides et à la production d'acide citrique d'une souche mutante de *Y. lipolytica* JMY3501 sur le glucose. Cette souche d'ingénierie a la capacité de tirer le flux de carbone dans la synthèse du triacylglycérol (TAG), et empêche à la fois la mobilisation et la dégradation des acides gras de ses réserves de lipides.

Cette étude avec la souche mutante a démontré une amélioration globale des performances de production de lipides avec une augmentation du rendement lipidique et de la teneur en glucose, et une diminution concomitante du rendement de formation d'acide citrique par rapport à la souche sauvage. En outre, nous avons démontré sur la base du profil de modulation des flux d'azote et de carbone que la levure était capable d'excréter ou de consommer rapidement et de manière réversible de l'acide citrique lors de l'accumulation d'acides gras et a conduit à une augmentation de 15 % du rapport critique carbone / azote par rapport à la souche sauvage. Il a démontré une plus grande robustesse de la souche vis-à-vis des fluctuations de la teneur en C et en N. Il a également établi les conditions de culture pour l'étude de l'effet des inhibiteurs sur l'accumulation de FA et leur

composition. Cette souche métaboliquement modifiée a ensuite été exposée à des inhibiteurs du système enzymatique FAS avec des pulses en culture fed-batch pendant la phase d'accumulation de lipides sous limitation d'azote. Les résultats obtenus avec l'inhibition ciblée du domaine de la cétoacyl synthase (KS) du système enzymatique FAS avec l'inhibiteur de la céruléine étaient les plus prometteurs mais étaient dose-dépendants :

Le métabolisme lipidique de la souche *Y. lipolytica* JMY3501 a été considérablement affecté par des doses élevées de d'impulsions à la céruléine; La synthèse d'acides gras a fortement été inhibée ainsi les cellules ont empêché la formation de TAG. D'autre part, le flux de carbone était dirigé vers la formation d'acide citrique avec les doses moyennes. Cependant, à une dose plus faible de céruléine, la souche *Y. lipolytica* JMY3501, sans ralentir le taux global de synthèse des acides gras, a considérablement amélioré l'accumulation de chaînes courtes (augmentation de 87 % en C10) et moyennes (augmentation de 13 % et 11 % en C12 et C14 respectivement) d'acide gras sans production d'acide citrique.

D'autre part, l'inhibition ciblée de l'étape de terminaison du système enzymatique FAS avec une dose moyenne des pulses d'orlistat a amélioré la synthèse de TAG jusqu'à 31 % et favorisé l'accumulation d'acides gras de longueur de chaîne moyenne (augmentation de 71 % du C14). Enfin, l'ajout de triclosan dans des cultures en flacon n'a montré aucun changement dans les profils de FA et a ensuite été abandonné pour d'autres expériences en bioréacteur.

La voie synthèse des acides gras de novo et les enzymes clés impliquées dans la synthèse des acides gras du microorganisme oléagineux ont été examinées. Grâce à la recherche documentaire, la régulation des enzymes clés impliquées dans la synthèse de novo des acides gras au niveau des expressions et des délétions génétiques et l'impact de ces réglementations sur le métabolisme des acides gras et l'accumulation de lipides pour les levures oléagineuses ont été rapportées.

Les données suggèrent que l'inhibition de la partie médiane du processus d'élongation FA (énoyl réductase) peut ne pas être intéressante pour la modulation du profil FA. De plus, pour s'assurer que les quantités d'inhibiteurs n'entraînent pas la mort cellulaire, une analyse de la viabilité cellulaire a été réalisée par cytométrie en flux. Il n'y avait pas de différence significative liée aux inhibiteurs et à la quantité de l'inhibiteur en termes de survie cellulaire, cette inhibition de l'activité du FAS n'affectant pas la viabilité cellulaire. Cependant, d'autres analyses de cytométrie en flux ont révélé que les cellules de levure présentaient des altérations morphologiques significatives d'une manière dose-dépendante. Les changements dans les caractéristiques morphologiques, en particulier la longueur, la forme et la granularité interne des cellules de levure, étaient plus prononcés avec des doses élevées d'impulsions à la céruléine qui ne se produisaient pas avec des pulses d'orlistat.

Par conséquent, ces résultats indiquent que la réduction de l'activité du système enzymatique FAS a modifié de manière significative la longueur de chaîne des acides gras et a conduit à l'accumulation d'acides gras de longueur de chaîne courte et moyenne. Cependant, l'inhibition liée à la dose sur le domaine KS du FAS a étroitement contrôlé le flux métabolique de l'AF dans la synthèse du TAG. Une explication possible de ceci est que, puisque la céruléine est l'inhibiteur du domaine de la cétoacyl synthase qui initie la synthèse des acides gras, elle peut contrôler l'allongement itératif de la chaîne dans le système enzymatique FAS. D'autre part, l'orlistat est l'inhibiteur de la terminaison de la synthèse de FA, il ne limite pas l'incorporation de malonyl-ACP et d'acétyl-ACP pour d'autres réactions itératives en chaîne donc ne limite pas la synthèse d'acides gras. De plus, la souche mutante JMY3501 est incapable de dégrader l'AF via la  $\beta$ -oxydation pour fournir l'énergie métabolique

nécessaire au maintien cellulaire à partir de ses lipides stockés. Par conséquent, des doses élevées d'impulsions de céruléine ont provoqué une toxicité et par conséquent, les cellules peuvent avoir canalisé le flux d'AF vers la synthèse des lipides membranaires plutôt que de les stocker comme lipides de stockage sous forme de TAG.

Pour cette raison, nous avons étudié le *Y. lipolytica* CR62, qui avait le même arrière-plan génétique que la souche JMY3501, mais modifié sur le domaine KS du FAS pour modifier la longueur de la chaîne des acides gras. Cette souche a favorisé l'accumulation d'acides gras à chaîne moyenne (11 % pour C14 et 31 % pour C16), produisant cependant simultanément de l'acide citrique avec une faible teneur totale en lipides de 16 % qui était identique à la souche de type sauvage de *Y. lipolytica* W29. Les deux stratégies appliquées à l'étape initiale de l'enzyme FAS conduisent à plus d'acides gras à chaîne courte et à une faible teneur totale en lipides.

## CHAPITRE 4 - CONCLUSION ET PERSPECTIVES

Ce travail de recherche porte sur la modulation de la teneur en lipides et de son profil en acides gras (AG) dans la levure oléagineuse *Yarrowia lipolytica* ainsi que sur des stratégies d'ingénierie biochimique et métabolique. Les objectifs de ces travaux étaient :

- d'étudier la dynamique des déplacements métaboliques de *Y. lipolytica* vers le métabolisme lipidique,
- de moduler le profil FA par la modulation des flux de carbone vers le haut et vers le bas de la voie de synthèse des acides gras via des stratégies d'alimentation C / N et l'ajout d'inhibiteurs spécifiques du système FAS

Le défi était d'ajuster la quantité de ces inhibiteurs afin d'identifier les réactions enzymatiques au sein du FAS qui contrôlent l'élongation des acides gras et la longueur de la chaîne carbonée, sans affecter la viabilité cellulaire de *Y. lipolytica*.

Les preuves de cette étude suggèrent qu'il est possible de moduler la longueur de la chaîne des acides gras synthétisés de la levure oléagineuse *Y. lipolytica*, en utilisant des inhibiteurs spécifiques comme moyen d'identifier des cibles génétiques intéressantes, puis en ciblant un domaine catalytique du système enzymatique FAS avec mutation. Par conséquent, il est possible d'affirmer que l'ingénierie du domaine de terminaison FAS de cette levure oléagineuse pourrait également être une approche prometteuse pour modifier la longueur de la chaîne FA avec une teneur élevée en lipides. En outre, l'obtention d'une telle souche mutante pourrait éventuellement modifier le profil FA sans formation de sous-produits, sans affecter l'homéostasie lipidique membranaire et la survie cellulaire.

Ces travaux de recherche ont démontré que la levure oléagineuse *Yarrowia lipolytica*, associée à des efforts d'ingénierie combinés, présentent de nouvelles opportunités pour la production d'acides gras conçus et / ou de haute valeur.

Les futures études de suivi pourraient également inclure les axes suivants :

- La souche d'ingénierie *Y. lipolytica* CR62 qui pourrait être optimisée pour les stratégies de taux d'alimentation du substrat (rapport rN / rC) pour le mode de culture fed-batch sous limitation d'azote. Une telle optimisation de la déformation devrait améliorer les performances d'accumulation de lipides en raison de la direction efficace des flux de carbone vers l'accumulation de lipides au lieu de la sécrétion d'acide citrique.

- L'identification du mécanisme d'action des inhibiteurs du FAS avec les domaines catalytiques du système enzymatique FAS pour la levure *Y. lipolytica* (en particulier avec l'inhibiteur Orlistat et le domaine MPT du

FAS) restant à déterminer. De telles études pourraient apporter un soutien supplémentaire aux études proprement dites.

- Et, même si les inhibiteurs sont requis en quantités relativement faibles au cours de ces études de recherche, les souches modifiées permettraient de surmonter le coût des inhibiteurs, en particulier dans les systèmes à grande échelle. Cependant, avant la construction d'une nouvelle souche, la suggestion suivante doit être envisagée : au lieu d'utiliser un promoteur constitutif pour exprimer le gène FAS2 modifié (comme pour le gène FAS2: TEF-yIFAS2 I1220F), il pourrait être remplacé par un promoteur inductible. Cela éliminerait la nécessité de supprimer le gène FAS2 natif. De tels remplacements génétiques favoriseraient la modification des FA en ne modifiant que la longueur de la chaîne des AG accumulés pendant la phase d'accumulation des lipides sans affecter la synthèse des phospholipides membranaires; ainsi, la viabilité des cellules ne devrait pas être affectée.